Synthesis and Bioactivity Studies of Harmonine – the Defense Alkaloid of the Asian Lady Beetle *Harmonia axyridis*

Dissertation

zur Erlangung des akademischen Grades doctor rerum naturalium
(Dr. rer. nat.)

vorgelegt dem Rat der Chemisch-Geowissenschaftlichen Fakultät der
Friedrich-Schiller-Universität Jena

von Master of Science (Natur- und Wirkstoffchemie)

Nadja Nagel

geboren am 05.02.1987 in Kronach (Oberfranken)

Gutachter:

1. Prof. Dr. Wilhelm Boland, Max-Planck-Institut für chemische Ökologie, Jena

2. Universitätsprofessor Dr. Rainer Beckert, Friedrich-Schiller-Universität Jena, Jena

Tag der öffentlichen Verteidigung: 22.06.2016

“Progress is made by trial and failure; the failures are generally a hundred times more numerous than the successes; yet they are usually left unchronicled.”

Sir William Ramsay (1852 – 1916, chemist)

Table of Contents

List of Abbreviations

abs.	absorbance
ACh(E)	acetylcholine(esterase)
AcN-CI-MS/MS	acetonitrile chemical ionization tandem mass spectrometry
amu	atomic mass unit
APCI	atmospheric pressure chemical ionization
APT	attached proton test
aq.	aqueous
AV	Annexin V
BLAST	basic local alignment search tool
BMDM	bone marrow derived macrophages
n-BuLi	*n*-butyllithium
calcd.	calculated
CI	chemical ionization
(M)CL	(muco)cutaneous leishmaniasis
COSY	correlated spectroscopy
m-CPBA	*meta*-chloroperoxybenzoic acid
d	day(s)
ddH_2O	double-distilled water
der.	derivatized
DIAD	diisopropyl azodicarboxylate
DiBAL-H	diisobutylaluminum hydride
DIPA	diisopropylamine
dist.	distilled
DMAP	4-dimethylaminopyridine
DMSO	dimethyl sulfoxide
DPPA	diphenyl phosphorazidate
DTNB	5,5′-dithiobis-2-nitrobenzoic acid
Ebc	European biocontrol strain
ee	enantiomeric excess
EI	electron impact
ESI	electrospray ionization
FAME	fatty acid methyl ester
FGI	functional group interconversion
Fig.	figure
FTIR	Fourier transform infrared spectroscopy
GC-MS	gas chromatography – mass spectrometry
h	hour(s)
HLE	horse liver esterase
HMBC	heteronuclear multiple bond correlation
HMDS	hexamethyldisilazide (bis(trimethylsilyl)amide)
HPLC-MS	high performance liquid chromatography – mass spectrometry

HR-MS	high resolution – mass spectrometry
HSQC	heteronuclear single-quantum correlation
IC_{50}	half maximal inhibitory concentration
LAH	$LiAlH_4$
LB	lysogeny broth
Luc-tg.	Luciferase-transgenic
MBTFA	*N*-methyl-bis(trifluoroacetamide)
MeI	methyl iodide
MIE	1-(methyleneimino)-1-ethenylium
min	minute(s)
MNBA	2-methyl-6-nitrobenzoic anhydride
MSTFA	*N*-trimethylsilyl-*N*-methyl trifluoroacetamide
MTBE	2-methoxy-2-methylpropane; methyl *tert*-butyl ether
MTPA	α-methoxy-α-trifluoromethylphenylacetic acid
m/*z*	mass-to-charge ratio
NMR	nuclear magnetic resonance
OD_{600}	optical density at λ = 600 nm
OPA	oxaphosphetane
PI	propidium iodide
PPh_3	triphenylphosphane
PS	phosphatidylserine
quant.	quantitative
rac	racemic
RP	reversed phase
rpm	revolutions per minute
rt	room temperature
RT	retention time
SAMP	(*S*)-l-amino-2-(methoxymethyl)pyrrolidine
SEM	standard error of the mean
SI	selectivity index
T	temperature
TBDMS	*tert*-butyldimethylsilyl
TCBC	2,4,6-trichlorobenzoyl chloride
TIC	total ion current
TLC	thin layer chromatography
TMS	trimethylsilyl
p-TsOH	*p*-toluenesulfonic acid
U	unit (amount of enzyme which converts 1 µmol min^{-1} substrate)
VL	visceral leishmaniasis
WHO	World Health Organization
w/w	weight/weight

1 Introduction

Among the order Coleoptera a very beloved, popular, and diverse group of beetles can be found: the lady beetle family (Coccinellidae). Members of this huge family are present worldwide, exhibit vivid and colorful elytra and are very well-known to each and every child. In the vernacular they are among others called "ladybugs", "ladyclocks", "ladycows", "ladyflies" or even “Bishop Barnabee”.[1] A testimony to the continuous adoration for this beetle family is given in a lot of nursery rhymes and myths. Lady beetles are said to bring the sun, bring good luck and predict the harvest or one’s fortune of love:[1]

> “Bishop, Bishop Barnabee, tell me when my wedding be;
> If it be tomorrow day, take your wings and fly away!
> Fly to the east, fly to the west, fly to him that I love best.”[1]

Despite the fact that most of the myths refer specifically to the seven spotted lady beetle (*Coccinella septempunctata*),[1] the family Coccinellidae comprises around 6000 species.[2] Lady beetles are in general 0.8 - 18 mm long and their body is shaped ovally. The dorsal surface is convex and the elytra show characteristic color patterns – the spots – which vary between species. The darker regions of the elytra consist of melanin and the lighter regions contain carotenoid derivatives, which are partly synthesized *de novo* and partly taken up from the food source.[3, 4] Many species are stenotopic and occupy only a very specific habitat. *Coccinula sinuatomarginata*, for example, can be found in dry meadows and steppes while *Anisosticta novemdecimpunctata* prefers marshes and moist meadows. However, very common species like *C. septempunctata* are eurytopic and can be found nearly everywhere.[5]

Within the Coccinellidae phytophagous, mycophagous, and carnivorous species are known. The accepted food range of predaceous coccinellids is rather broad. They prey not only on phytophagous mites, aphids, hoppers, and cycadas (Homoptera) but have also been observed consuming younger instars of beetles (Coleoptera), bees, ants, wasps (Hymenoptera), and moths and butterflies (Lepidoptera) as well as small flies (Diptera) and thrips (Thysanoptera).[6] Despite the former opinion that no real food specificity exists in coccinellids, specialists and generalists can be found as well as a sort of “mixed feeding” behavior to select a balanced diet.[6, 7] Other food sources which are often used during the absence of alternative prey are eggs or young larvae of conspecific or heterospecific

coccinellids classifying lady beetles as cannibals and intraguild predators. To prevent non-sibling cannibalism of newly laid eggs lady beetle females are able to identify larval tracks and to choose oviposition sites near aphid colonies but away from conspecific predators.[8] Furthermore, larvae are able to detect con- and heterospecific larval tracks to prevent frequent encounters. However, studies including the two generalist species *C. septempunctata* and *Harmonia axyridis* confirm that larval responses to these tracks differ between species. While *C. septempunctata* generally avoids larval tracks, *H. axyridis* only avoids conspecific tracks.[9] This asymmetric behavior of larvae suggests different levels of aggressiveness as intraguild predator between species.[9, 10]

Additionally, various other predators and parasites may threaten the coccinellids.[11] Among others, predaceous bugs (*Podisus maculiventris*)[12] and crab spiders (*Misumenops tricuspidatus*)[13] are natural enemies of some lady beetle species. Parasitoids like the braconid wasp (*Dinocampus coccinellae*)[14] or entomopathogenic nematodes (*Heterorhabditis bacteriophora* and *Steinernema carpocapsae*)[15] as well as entomopathogenic fungi (*Beauveria bassiana*)[16, 17] are also known to attack/infect lady beetles.

To defend themselves from the threats mentioned above, lady beetles developed various strategies. If a beetle is disturbed, it falls into thanatosis, death feigning, by keeping legs and antenna closely pressed to the body.[18, 19] Additionally, it releases droplets of hemolymph from the tibio-femoral joints of its legs. The hemolymph does not only contain repellent volatiles but also exhibits deterrent and sometimes toxic properties.[20-22] The toxic character of the hemolymph derives from contained alkaloids which are considered to be mostly synthesized autogenous by the beetles.[22]

In 1971, the first defense alkaloids of *C. septempunctata* were identified to be coccinelline (**1**) and precoccinelline (**2**) (**Fig. 1.1**) and their repellent activity against ants, as well as their bitter taste, was proven. Further studies at this time already confirmed that *C. undecimpunctata* also carried these alkaloids in its hemolymph.[23] Only two years later adaline (**3**) was found to be the defense compound of *Adalia bipunctata*.[24] With ongoing research more and more Coccinellidae alkaloids were discovered, like hippocasine (**4**) – the defense compound of *Hippodamia caseyi*[25] – or harmonine ((*R*)-**5**). The latter was at first found to be present in *Adonia variegata*, *H. quadripunctata*, *Semiadalia undecimnotata*, *Hippodamia convergens*, and *H. leis conformis*.[26] Recently it was also reported to be the major defense compound of *H. axyridis*.[27, 28] In the pupal secretion of *Subcoccinella vigintiquatuorpunctata*, dimeric polyazamacrolides, for example structure **6**, were found as main components, however, also isomeric forms or trimeric polyazamacrolides **7** could be detected.[29]

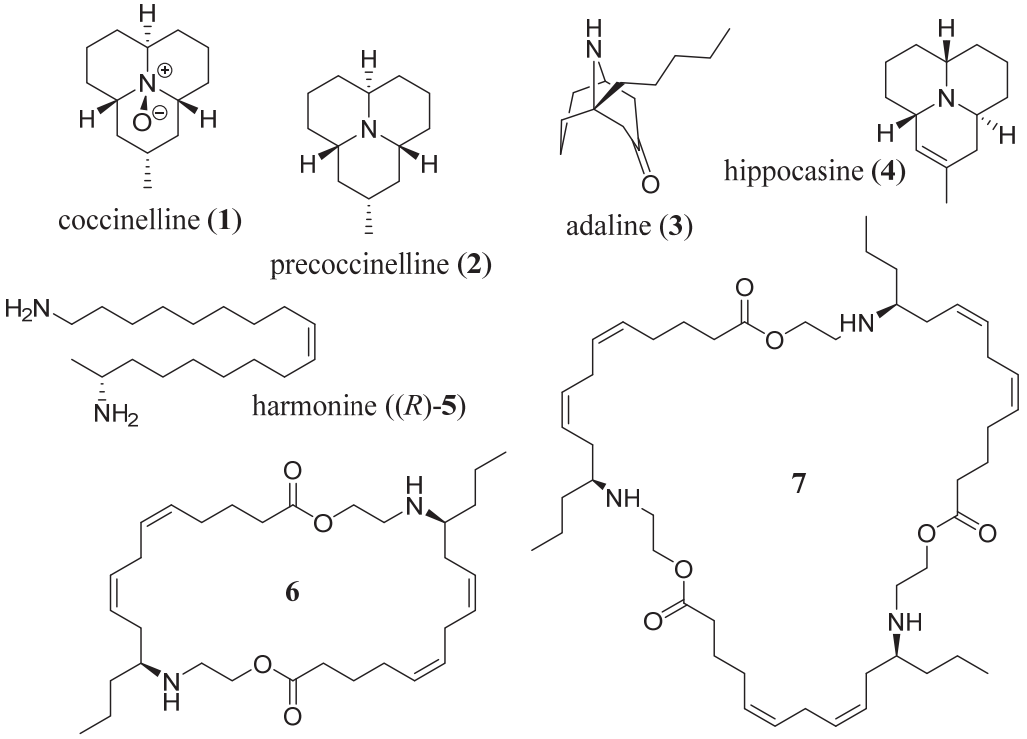

Figure 1.1: Some examples of alkaloids from popular lady beetle species.

Out of these entire lady beetle species one species as well as its defense alkaloid gained enormous attention during the last years:[27, 30, 31] the Asian lady beetle *H. axyridis* and harmonine ((*R*)-**5**) ((17*R*,9*Z*)-octadec-9-ene-1,17-diamine).

1.1 The Asian Lady Beetle *Harmonia axyridis*

The Asian lady beetle *H. axyridis* displays a rather complicated taxonomic history which was reviewed, among other topics, in 2003 by R. L. Koch.[31] Briefly worded, this species had eight synonyms proposed as names, *Harmonia* was raised to generic status twice (1912, 1943) and also various subspecies and aberrations have been characterized so far.[31] The latest taxonomic classification can be outlined as follows:[32]

Order: Coleoptera
Family: Coccinellidae
Subfamily: Coccinellinae
Tribe: Coccinellini
Genus: *Harmonia*
Species: *axyridis*

1.1.1 General Biology of *H. axyridis*

The disagreement regarding the taxonomy of *H. axyridis* might have derived from the enormous amount of colorful variations and maculations that coexist in this species. The phenotypic color forms are divided into two groups: the light succinea type with reddish or brownish ground color and the melanic type, which shows dark elytra (**Fig. 1.2 E**).[33, 34] The appearance of different color forms was studied intensively, suggesting that it might derive from genetic polymorphism, different geographic ranges of the beetles or differences in the absorption of solar energy between different elytra colors.[33-35]

Despite the unusual coloration of *H. axyridis*, its development and life cycle is similar to that of other coccinellids: it proceeds from the eggs through four larval instars, a prepupa and a pupa stage, to an adult stage (**Fig. 1.2**). The yellow eggs are laid in clusters and attached to the surface. Shortly before hatching their color changes to grey. The larvae remain on the eggs for approximately one day and consume unfertilized eggs or younger larvae. After three moulting processes the fourth instar is reached. The larvae stop eating and attach themselves with their anal discs, head down, to a surface. This prepupal stage can last up to several days before the moulting to the pupa is completed. Freshly hatched beetles are soft and exhibit a light, yellow color which changes only gradually to the common bright color with patterns.[36]

Figure 1.2: Developmental stages of *H. axyridis*. **A**) freshly laid eggs, **B**) fourth instar larva, **C**) pupa on a leaf, **D**) *H. axyridis* adult feeding on aphids, **E**) *H. axyridis* adults with different coloration and maculation. (All photos were taken at the MPI-CE, Jena with help of A.-K. Dietel)

The Asian lady beetle is natively distributed from southern Siberia to the South of China and from the Altai Mountains to the Pacific Coast. It can also be found on Formosa and Japan as well as on the Japanese Ryukyu Islands and the Bonin Islands.[31, 37]

Like most predaceous lady beetles *H. axyridis* is able to consume a broad spectrum of prey including, among others, various aphid species (Aphididae), spider mites (Tetranychidae), larval stages of leaf beetles (Chrysomelidae), moths and butterflies (Lepidoptera), and also pollen and nectar.[31, 38, 39] Lucas *et al*. studied the feeding behavior of *H. axyridis* compared to another coccinellid species (*C. septempunctata*) and clearly demonstrated the enormous amounts of prey consumed by *H. axyridis* and its voracity.[39]

1.1.2 Biological Control and Invasive Outbreak

The voracious feeding behavior qualified the Asian lady beetle as an ideal biological control agent. First releases of *H. axyridis* were recorded in California, USA in 1916 and later on in 1964 and 1965. They were followed by several introductions from 1978 to 1982 into various states of the USA like Georgia, Louisiana, Maine, Maryland, Mississippi, and Washington.[37] In Europe initial releases took place in the East – for example in the Ukraine (1964) and Belarus (1968) – followed by introductions into France (1982). *H. axyridis* was brought to the market as a biological control agent in 1995 and later on sold by various companies.[40]

However, after a while populations began to establish in their non-native range and first "wild" *H. axyridis* specimens were recorded in Lousiana and Mississippi in 1988.[37] With this event, the unstoppable radiation of the Asian lady beetles started and soon they became the most common lady beetles in various parts of the USA,[38] were observed in South America,[41] introduced into Egypt[42] and discovered in South Africa[43]. In 2004, *H. axyridis* beetles arrived in the UK from the European mainland and began to spread.[44] Since 1988 Asian lady beetle populations have established in more than 38 countries. Their estimated rate of spreading is between 100 and 500 km per year.[45]

The routes of the spreading of *H. axyridis* were examined by Lombaert *et al*.[46] and are illustrated in **Figure 1.3 A** (Europe: **Fig. 1.3 B**[45]). They used the analysis of population genetics and historical data of first observations as a basis and quantitatively compared invasion scenarios by applying approximate Bayesian computation methods. Their unexpected result is that only the populations in eastern and western North America originated from introductions from the native range. The South American and the African population are most likely to originate from North America. Genetic analysis of European *H. axyridis* populations revealed, however, that these beetles are a genetic mixture of beetles from

eastern North America and from the European biocontrol strain, which was introduced from the native range. These findings clearly indicate that first an "evolutionary shift triggering invasion occurred in eastern North America"[46] and that the worldwide invasion of *H. axyridis* descends from this successful invasive population.[46]

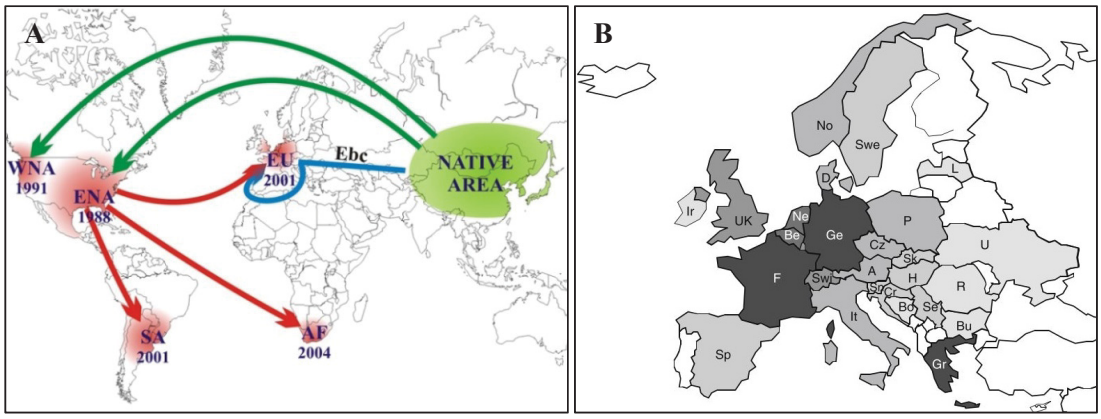

Figure 1.3: Worldwide distribution of *H. axyridis*. **A**) *H. axyridis*' route of invasion. Likeliest ways of invasion are depicted by arrows and the years of the first observations are noted. (modified from Lombaert *et al.*[46]) **B**) Distribution of *H. axyridis* in Europe. First reported presence: ☐ not reported, ☐ 2010-2009, ☐ 2008-2007, ☐ 2006-2005, ☐ 2004-2003, ☐ 2002-2001, ☐ to 2000. (modified from Brown *et al.*[45])

Wherever *H. axyridis* occurred and established not only positive effects like the biological control of pests were visible but also a lot of adverse effects could be observed. The Asian lady beetles can be associated with the decline of native coccinellid species. They are a pest to fruit and wine production as well as a household pest and an allergen.[44, 47] The direct negative effect on human health mostly derives from *H. axyridis'* preference to gather at objects with sharp linear contrasts to find overwintering sites. These contrasts can mostly be found at buildings, which leads to massive congregations of beetles in homes, dirty curtains and furniture, and allergic reactions of the inhabitants.[48]

Recently a methodology for risk assessment was developed to estimate the risks of a potential biological control agent to establish and to rate its effects on the non-target native species. *H. axyridis* was categorized to have a high-risk potential because it is not specific to any host.[49] Furthermore, the Asian lady beetle is nowadays seen as one of the most invasive species on earth showing unquestionably negative impact on native species.[44, 50]

With all these developments the question arises: Why is *H. axyridis* such a successful invader? The effective performance of the Asian lady beetle is certainly due to a variety of factors. First off all lady beetles are cannibals and predators. Studies have proven that *H. axyridis*, especially third and fourth instar larvae, acts as an aggressive intraguild predator, which dominates and thus decimates other lady beetle species.[10] Furthermore, *H. axyridis* larvae are less likely to be eaten by predatory crab spiders (*Misumenops tricuspidatus*) suggesting that the spiders are deterred by the larvae.[13] Last but not least *H. axyridis* is also more resistant to the entomopathogenic fungus *Beauveria bassiana* than other species.[17] This resistance against various pathogens is believed to be derived from harmonine ((*R*)-**5**), the defense compound of the Asian lady beetle.[27]

1.1.3 Harmonine - the Defense Alkaloid of *H. axyridis*

The aliphatic, long-chain diamine harmonine ((*R*)-**5**) was first found in five lady beetle species[26] and only in 2002 discovered to also be the major defense compound of *H. axyridis*[28]. The first material which was also used for initial structural elucidation was isolated from *H. leis conformis* of which 500 individuals were crushed. An acid-base extraction yielded a basic compound, which was acetylated and purified using column chromatography.[26, 51] To clarify the structure of the acetylated alkaloid HR-MS, IR and NMR techniques were applied. The position of the double bond was determined by epoxidation and also by oxidative cleavage followed by MS-analysis.[26] The complete structural confirmation and thereby the first racemic synthesis of *rac*-**5** was reported by Braconnier *et al*.[52] Starting from 1,6-hexanediol and 1,8-octanediol, they achieved the total synthesis of harmonine (*rac*-**5**) in 15 steps with an overall yield of 6.5%. Since first analyses have already proven that harmonine (**5**) is an optically active molecule, Braconnier *et al*. also determined the absolute configuration of the alkaloid **5** exploiting the lanthanide-induced shifts of diastereomeric Mosher-amides (MTPA-amides) in ^{1}H-NMR. With an empirical comparison of ^{1}H-NMR shifts of amines of known absolute configuration in the presence of europium and of the shifts of harmonine under the same conditions, it was possible to assign the (*R*)-configuration for harmonine ((*R*)-**5**).[52]

The first enantioselective synthesis of harmonine ((*R*)-**5**) was reported in 1991 by Enders *et al*.[53] and is outlined in **Scheme 1.1**. They developed a convergent synthesis starting from

diol **8** and ω-hydroxy chloride **11**. The latter was converted into the α,ω-disubstituted halide **12**.

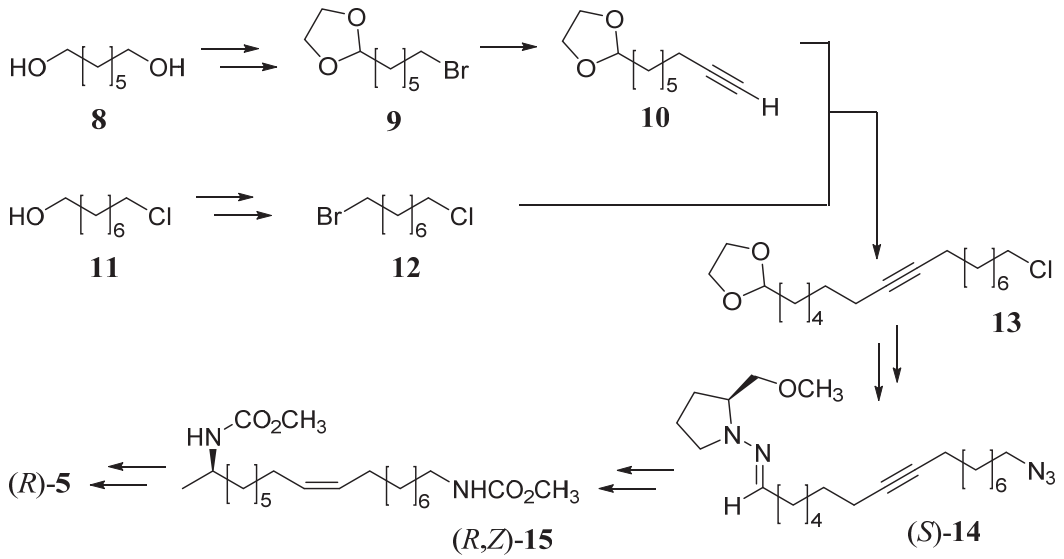

Scheme 1.1: Simplified representation of the enantioselective synthesis of harmonine ((*R*)-**5**) by Enders *et al*.[53]

To build up the alkyne moiety a five step sequence was employed. First, the diol **8** was heated with hydrobromic acid to give the mono-halide, which was oxidized and directly protected with 1,2-ethanediol to yield **9**. Finally, coupling with lithium acetylide-ethylenediamine complex introduced the alkyne residue. Then **10** and **12** were coupled in the presence of *n*-BuLi at -20 °C to give the skeleton **13** in 58 % yield. Next, the chloride at C-1 was transferred into a primary azide. At C-17 deprotection of the aldehyde was directly followed by its conversion into the SAMP hydrazone. (*S*)-**14** was then hydrogenated over Lindlar's palladium catalyst to yield selectively the (9*Z*)-double bond (4% *E*-isomer) and the primary amino group. Methyllithium was employed for the nucleophilic addition to the carbon atom of the C=N-bond and the reaction was quenched with methyl chloroformate to give the protected hydrazino amine. Finally, an excess of lithium in liquid ammonia removed the chiral auxiliary and a subsequent deprotection of the resulting (*R*,*Z*)-**15** yielded harmonine ((*R*)-**5**) in 13 steps and an overall yield of 5% (*ee* ≥ 97%).[53]

This long and costly synthesis has been the only source of synthetic harmonine ((*R*)-**5**) for years. However, during the completion of this thesis another synthesis was developed. In this synthesis, a *Z*-selective cross metathesis (*Z*/*E* > 90%) or a Wittig reaction was used as key

step to build up the carbon chain and the chiral center was introduced by use of *D*-alanine.[54] After the successful outcome and publication[55] of the synthetic procedure detailed in this thesis (see chapter 3.2.1 and 3.2.2), the next synthesis of harmonine ((*R*)-**5**) using a cross-metathesis reaction was reported. Abel *et al*. managed to exclusively form the *Z*-isomer employing a *Z*-selective Grubbs catalyst with low catalyst loading (2.6% of catalyst).[56]

Although a lot of research has been carried out on lady beetle defense systems in general, the biosynthesis of various alkaloids including harmonine ((*R*)-**5**) is not yet completely elucidated. The structural diversity of coccinellid alkaloids might be misleading though since most of them are simply build up from a chain of carbon atoms including one or more nitrogen atoms. This fact suggests a common biosynthetic origin related to a polyacetate pathway.[57, 58] To prove this hypothesis feeding experiments with *C. septempunctata*[59] and *A. bipunctata*[60] using $CH_3{}^{14}COONa$/$^{14}CH_3COONa$ were conducted, that showed incorporation of the precursors into the alkaloids, strongly suggesting a polyacetate origin. In general, however, these feeding experiments showed poor incorporation rates. Therefore, already established *in vitro* incubation assays[61] were modified to allow further biosynthetic studies of lady beetle alkaloids,[62] which revealed that glutamine is the most efficient nitrogen donor, the biosynthesis takes place in the fat body of the lady beetles, and that a fatty acid pathway is involved in the biosynthesis of lady beetle alkaloids.[62]
To study the biosynthesis of harmonine ((*R*)-**5**) *in vitro* incorporation experiments with labeled [$^3H_3$] myristic acid, [$^3H_3$] stearic acid and [$^2H_{17}$] stearic acid were conducted by Haulotte *et al*.[57] They showed that stearic acid (**16**) could be incorporated at a much higher rate indicating that it is the biosynthetic precursor of harmonine ((*R*)-**5**). The 17-fold deuterated stearic acid delivered a closer insight into the formation of the amine at C-17. Since 3 deuterium atoms were lost during the incorporation process the biosynthesis of ((*R*)-**5**) was outlined as shown in **Scheme 1.2**.[57]

Haulotte *et al*. proposed that at first stearic acid (**16**) is converted into oleic acid (**17**). The latter is oxidized at C-17 (loss of two deuterium atoms) and transformed into an imine **19** which can undergo imine-enamine tautomerism (loss of a third deuterium atom). The enamine is finally stereospecifically reduced to give harmonine ((*R*)-**5**).[57]

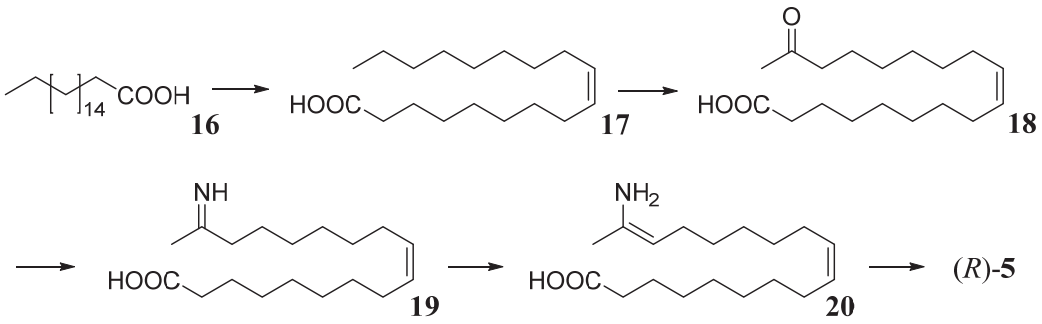

Scheme 1.2: Biosynthesis of harmonine ((*R*)-**5**) proposed by Haulotte *et al*.[57]

The ecological function, properties, and biological activities of harmonine ((*R*)-**5**) have been repeatedly studied over the past years. The bitter tasting alkaloid was found to be a feeding deterrent for ants (*Myrmica rubra*) at concentrations of 10^{-4} M indicating that ((*R*)-**5**) functions as protection against possible predators.[52] Recently, parasitic microsporidia related to *Nosema thompsoni* have been reported to be present in the hemolymph of *H. axyridis*. While these microsporidia are harmful to other coccinellid species and might be another aspect which contributes to the dominance of *H. axyridis* over native species, *H. axyridis* is not infected by the microsporidia.[30] In this context ((*R*)-**5**) was proposed to protect the Asian lady beetle from self-infection.[63]

However, ((*R*)-**5**) seems to be even more potent than these findings suggest: it demonstrates activity against 12 bacterial strains, it is active against the yeast *Candida albicans* and against four different fast-growing mycobacteria strains including *Mycobacterium tuberculosis*. Furthermore, harmonine ((*R*)-**5**) demonstrates multi-stage antimalarial activity by inhibiting the growth of the protozoan parasite *Plasmodium falciparum* (IC_{50} values of 4.8 and 7.6 mM).[27] ((*R*)-**5**) is also cytotoxic to five human tumor cell lines and displays inhibitory activity against acetylcholinesterase, neuraminidase, and prolylendopeptidase suggesting that it might be used as anti-Alzheimer medication.[28] Regarding all of these recent developments harmonine ((*R*)-**5**) is considered as a promising lead in drug development and for agricultural use (yellow biotechnology).[64]

1.2 Bioactivity Studies

As already outlined above, harmonine ((*R*)-**5**) displays an enormous range of different biological activities worth further evaluation. The assay-systems applied during the implementation of this thesis are introduced hereafter.

1.2.1 Acetylcholinesterase – Catalytic Function and Importance

Alam *et al*. described inhibitory activity of harmonine ((*R*)-**5**) on acetylcholinesterase (AChE).[28] This finding prompted the establishment of an assay system for further studies.

The neurotransmitter acetylcholine (**21**) (ACh; structure shown in **Scheme 1.3**) is responsible for various physiological processes in the peripheral and central nervous system. Among others, it controls sensory perception, sleep/wake cycles and arousal. In the periphery ACh (**21**) regulates the heart rate, smooth muscle activity and the motility of the gastrointestinal tract.[65, 66] These effects are mediated through activation of two different families of cell-surface receptors; the muscarinic receptor subtypes (mAChR, **Fig. 1.4 A** red) and the nicotinic receptor subtypes (nAChR, **Fig. 1.4 A** blue). The nAChRs are part of the ligand-gated ion channel superfamily and mediate fast neurotransmission. mAChRs are G-protein-coupled receptors and react slower through second messenger systems. Both receptor types exist in various subtypes that can be found in the synaptic cleft bound to the pre- and postsynaptic membrane.[66] Along with the vital enzyme AChE they are responsible for the transmission of action potentials across the synaptic cleft.[67]

The functioning of a cholinergic synapse is illustrated in **Figure 1.4 A**: In the presynaptic, cholinergic neuron choline-acetyltransferases (ChAT) catalyze the production of ACh (**21**) from choline (**22**) and acetyl-coenzyme A. Then vesicular ACh transporters (vAChT) pack ACh (**21**) into synaptic vesicles, which are releasing **21** into the synaptic cleft when triggered by action potentials.[66, 68] The released ACh (**21**) can now bind to pre- or postsynaptic receptors and control various processes through inhibition of adenylate cyclase (AC), activation of the inositol-1,4,5-trisphosphate (IP3) pathway[66] or through higher permeability of Na^+, K^+, and Ca^{2+}.[66] To terminate the transmission of action potentials AChE hydrolyzes the neurotransmitter **21**. The resulting choline (**22**) is taken back up by the presynaptic neuron through high-affinity choline transporters (ChT).[66, 68]

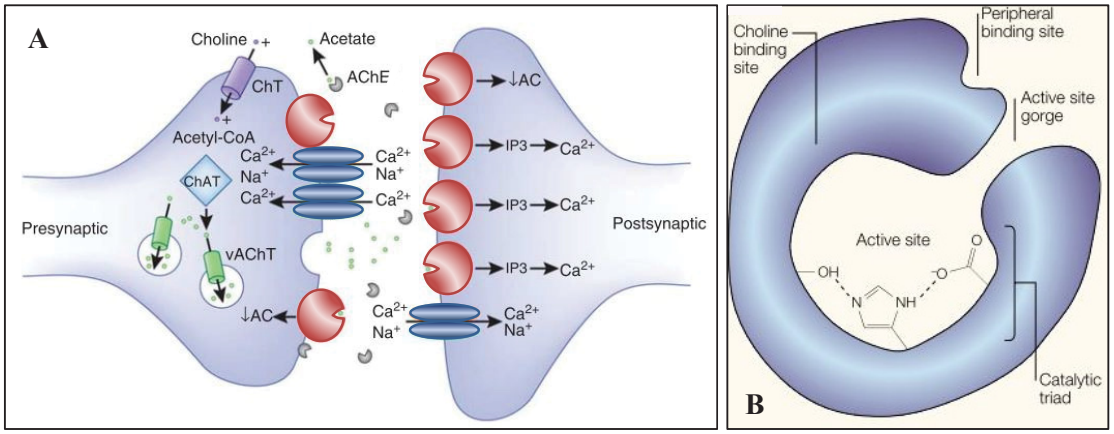

Figure 1.4: Acetylcholinesterase. **A**) Representation of a cholinergic synapse and the synaptic cleft with the biochemical processes taking place therein. (modified from Jones *et al.*[66]) **B**) Schematic representation of the binding sites and the active site of AChE. (reproduced from Soreq *et al.*[68]) **C**) Diagram of the catalytic subunit of the AChE from the pacific electric ray (*Torpedo californica*) with ACh (**21**) in the active site. (reproduced from Silmann et al.[69])

Purified AChEs from the electric organs of electric fish (*Electrophorus* and *Torpedo*) are structurally comparable to those present in vertebrates[70, 71] and allowed various studies of the arrangement of subunits and the mode of action of these enzymes.[71] A model of the catalytic subunit of an AChE from *Torpedo californica* is shown in **Figure 1.4 C**. Early studies pointed out that two subsites – the esteratic or catalytic site and the anionic or choline binding site – build up the active site of AChE (**Fig. 1.4 B**).[68, 72] The active site is located in a narrow and deep gorge which is lined by 14 conserved aromatic residues. This residues contribute to the choline binding site and to the peripheral binding site.[69] The esteratic site provides the catalytic triad which consists of serine, histidine and glutamate and lies at the bottom of the gorge.[73] This triad classifies AChEs as serine hydrolases, however, with a gluatamate residue instead of the usual aspartate residue.[68, 72]

The main function of AChE is the termination of receptor-mediated neurotransmission at cholinergic synapses by hydrolyzing ACh (**21**) (**Scheme 1.3**).[67] To fulfill this task, AChE functions with a very high activity and a turnover number $>10^4$ s^{-1},[67, 74] which is close to the rate of diffusion-controlled reactions.[71]

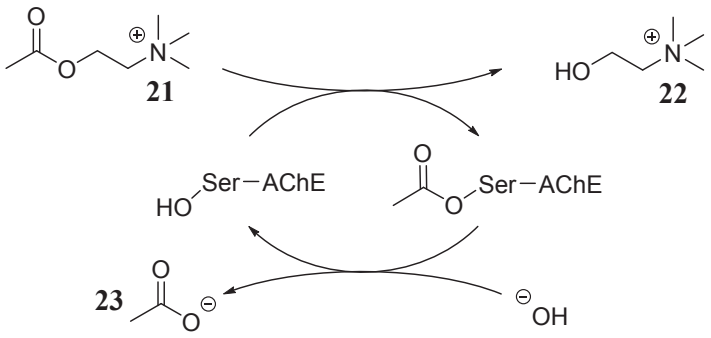

Scheme 1.3: AChE mediated hydrolysis of ACh. (modified from Soreq *et al*.[68])

The quarternary ammonium group of ACh (**21**) interacts with the choline binding site of the enzyme while the acetate-group is transferred to the hydroxyl group of serine (stabilized by the histidine and glutamate residue of the triad) at the eseratic site of the enzyme. Choline (**22**) is released from the newly formed acetyl-enzyme intermediate and through a subsequent hydrolysis the initial state of the AChE is recreated (**Scheme 1.3**).[68]

This important role of AChE made the enzyme an attractive target for drug development. Already in the early 1970s *post-mortem* studies of the brains of Alzheimer's disease patients revealed that these patients showed among others reduced choline (**22**) uptake and reduced ACh (**21**) release.[75] The resulting "cholinergic deficit hypothesis" explained many appearing symptoms by a general lack of neuronal ACh (**21**) and suggested drug development based on an inhibition of AChE to restore higher levels of the neurotransmitter **21**.[76] Nowadays it is understood that many other processes are contributing to the disorder[77] but AChE inhibition still plays a major role in drug development.[78]

1.2.2 Leishmaniasis and the *Leishmania* Parasites

The antiparasitic activity of (*R*)-**5** against *P. falciparum* has been reported[27] and initiated the evaluation of its activity against *L. major*, one of the causative agents of leishmaniasis.

Leishmaniasis can be described as a complex and diverse disease caused by more than 20 species of the protozoan genus *Leishmania*, which are transmitted to the human host during the bite of female sandflies (Phlebotominae). Depending on the transmitted parasite various forms of the disease can occur.[79, 80] The three major clinical forms are cutaneous (CL),

mucocutaneous (MCL), and visceral leishmaniasis (VL)[81] that can be found in at least 98 countries worldwide[82] with 350 million people at risk of infection.[83, 84]

CL is nonfatal but patients show skin lesions at the site of the sandfly bite,[81, 85] which may become large and permanent but are usually painless.[86] MCL can be characterized by the development of metastatic lesions leading to the destruction of mucous membranes.[87] The severest and frequently fatal form VL is accompanied by fever, anemia, weight loss, splenomegaly, and hepatomegaly.[81, 85]

The life cycle of the protozoan parasites exhibits two principal stages and is retained through transmission between sandflies and human hosts (detailed in **Fig. 1.5**).

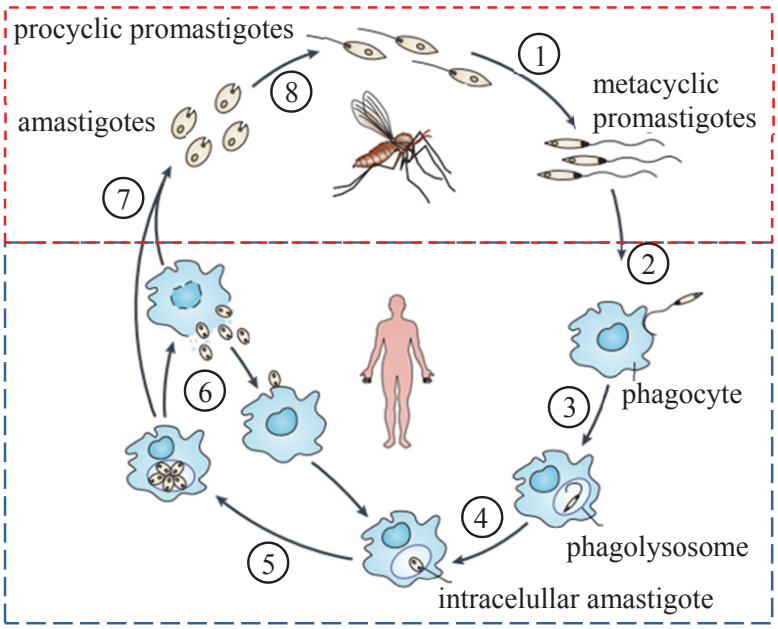

Figure 1.5: Life cycle of *Leishmania* parasites. 1) Procyclic promastigotes differentiate into infective metacyclic promastigotes in the sandfly gut. 2) During blood meal, promastigotes are regurgitated and enter the mammal body. 3) Phagocytes take up the promastigotes, which 4) differentiate into amastigotes. 5) Amastigotes proliferate, 6) rupture the host cell and infect other phagocytes. 7) When a sandfly is sucking blood from an infected host, it takes up infected phagocytes. The amastigotes develop into promastigotes in the midgut of the sandfly and the cycle starts anew. (modified from Kaye *et al.*[88])

In the gut of the sandfly, mobile and flagellated promastigotes process through various distinct stages (metacyclogenesis) until the noninfective, procyclic form is transformed into an infective, nondividing, metacyclic form with virulence capabilities. These metacyclic promastigotes migrate to the stomodeal valve - ready for transmission to the human host

during the blood meal. As soon as human macrophages phagocytize the promastigotes, they start to transform into immobile, nonflagellated amastigotes. These live as intracellular parasites in the human macrophages until a sandfly takes up and digests infected macrophages. The released amastigotes develop again into procyclic promastigotes in the sandfly midgut.[81, 88]

With over 50 000 deaths recorded annually,[83] leishmaniasis was estimated to have the second highest mortality of tropical, infectious diseases.[79, 89] Poverty, ecological factors associated with poverty[90, 91] and poor nutrition increase the risk of disease progression and mortality.[90, 92]

The medical treatments obtainable to this day were reviewed among others by Hussain *et al*.[93] and Sangshetti *et al*.[94] They demonstrate that very few drugs are available, which exhibit severe to life-threatening side effects. Furthermore, first resistances have been reported in these reviews. The mechanism of action of the approved antileishmanial drugs is still under investigation and not completely clarified yet.[93]

One of the most convenient treatments of leishmaniasis is miltefosine (**24**). This alkylphosphocholine drug is still the only orally available treatment.[95, 96] The main organ targeted by side effects is the gastrointestinal tract, however, in animal studies **24** revealed embryotoxic and fetotoxic properties and is therefore not recommended for use during pregnancy.[97] Another drug in use, the aminoglycoside antibiotic paromomycin (**25**) needs to be injected intramuscular,[98] which results in injection-site pain as the principal adverse effect.[99] Ototoxicity and nephrotoxicity are known to occur occasionally.[96]

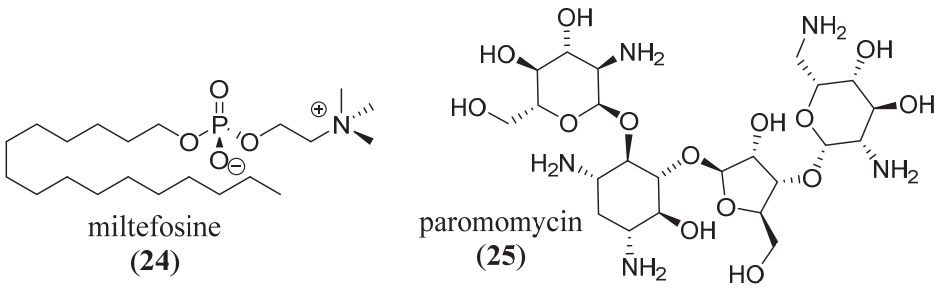

Figure 1.6: Two examples of approved drugs against leishmaniasis.

Since severe side effects and extremely high treatment costs are common among antileishmanial drugs[98, 99] and resistant *Leishmania* strains have been reported, the search for new and safer lead compounds continues.[96, 100]

2 Objectives and Scope of this Thesis

The Asian lady beetle *H. axyridis* attracted much attention over the past decades. As an invasive species, the beetles began to establish and to spread worldwide threatening the native lady beetles wherever they occur. The enormous invasive success derives from various factors, among others from their chemical protection against pathogens[17] and predators[13]. Their defense compound, which is synthesized *de novo*, is harmonine ((*R*)-**5**). (*R*)-**5** displays not only interesting ecological functions but also several biological activities worth testing.
The purpose of this thesis was to contribute to the still incomplete body of knowledge of harmonine ((*R*)-**5**) by analytical, chemical and biological means. In detail this thesis had the following scope and specific aims that should be addressed:

- As a prerequisite for further studies "beetle material" was needed. Since *H. axyridis* is an invasive species and is no longer commercially available, the first aim of this thesis was to build up a reliable beetle rearing. Therefore, a cultivation of bean plants and a breeding of *Acyrthosiphon pisum* as food source should be established.

- After the successful establishment of the beetle rearing, a fast and sensitive method to examine the composition of the hemolymph should be developed. Previously unknown compounds should be identified and characterized using GC-MS (EI) and AcN-CI-MS/MS techniques.

- Harmonine ((*R*)-**5**) displays promising biological activities which evoke a constant need of (*R*)-**5**. To satisfy this demand, a short, flexible and reasonable synthesis should be developed. This synthesis should be designed to deliver not only the racemic form of harmonine (*rac*-**5**) but also both enantiomers – the natural occurring (*R*)-harmonine ((*R*)-**5**) and the non-natural (*S*)-harmonine (*ent*-(*S*)-**5**) – as well as possible biosynthetic precursors and related derivatives.

- The efficiently synthesized compounds should be subsequently tested in different biological assays to identify new biological activities. Furthermore, the importance of the different functional groups and the stereochemistry for the biological activity of harmonine ((*R*)-**5**) should be examined. As assay systems microbial growth inhibition

assays, AChE inhibition assays and antileishmanial assays were chosen. The biological results should be complemented with docking studies and modeling.

Hence, this thesis should be conducive to the knowledge of the defense alkaloid harmonine ((*R*)-**5**) by not only providing synthetic access to all enantiomers of (*R*)-**5** and derivatives but also by delivering new insights into biological activities and structure-activity relationships.

3 Results and Discussion

To expand the knowledge regarding *H. axyridis* and harmonine ((*R*)-**5**) various measures were adopted during the implementation of this thesis. In general they can be differentiated into analysis, synthesis, and bioactivity studies. Hereafter, the results are discussed in previously stated order.

3.1 Hemolymph Analysis of *H. axyridis*

3.1.1 Beetle Rearing: the Prerequisite

As a prerequisite for the analysis of *H. axyridis*' hemolymph an adequate beetle rearing had to be established. The body of literature about beetle rearing is rather diverse and sometimes under-reported. To establish a successful long-term breeding the procedure described by Krengel *et al*.[101] was modified. Since *H. axyridis* is invasive and not marketed anymore, a stock of 250 - 300 adult beetles was permanently maintained (exact rearing conditions see chapter 6.3). The starting point were field collected fourth instar larvae reared on moth eggs (Lepidoptera: Gelechiidae: *Sitotroga*). The cannibalistic behavior of higher instars is relatively pronounced. Therefore, less than 15 larvae were kept in a box and food and water was constantly supplied to reduce cannibalistic incidents. After pupation, the newly hatched beetles were promptly separated into two different groups:

- Around 80% of the beetles were fed with *Sitotroga* eggs and kept in groups of around 30 individuals (group-S).
- The other 20% were kept in groups of up to 20 individuals and fed with pea aphids (*A. pisum*) sitting on bean plants three times a week. Old plant material was removed regularly to avoid mould and infection of the beetles (group-A).

Except for the different food, both beetle groups were treated equally and eggs were collected three times a week. Newly hatched larvae were kept in bigger groups, fed with *Sitotroga* eggs and only split up into groups of less than 15 when they reached the third instar. After pupation and hatching, the beetles were separated again into group-S or -A (ratio 80/20) and the cycle started anew.

The two different rearing groups were kept to allow a comparative study of *H. axyridis'* hemolymph composition and to identify feed-dependent differences if existing.

3.1.2 GC-MS Analysis of the Hemolymph

To analyze the compounds present in *H. axyridis'* hemolymph GC-MS (EI) was employed. The GC-MS technique was chosen because it is not only fast and reproducible but also a very sensitive method to separate and detect even minor compounds. Furthermore, various data bases containing plenty of (EI)-MS spectra of authentic reference standards are available that facilitate the identification of substance classes or even specific compounds.
Since the major defense compound harmonine ((*R*)-**5**)[28] is a diamine and therefore not volatile enough for GC-MS analysis a suitable derivatization reagent had to be selected. The obvious requirements for the derivatization reagent were reproducibility, complete derivatization to yield only one specific product and a broad functional group acceptance. Underlying the proposed biosynthesis of (*R*)-**5**[57] amines and alcohols should be the main functional groups present in the hemolymph. Therefore, *N*-methyl-bis(trifluoroacetamide) (MBTFA) was chosen as standard derivatization reagent. This acylation reagent had already proven to be convenient for GC-MS detection of (*R*)-**5**. Sloggett *et al*.[102] and Kijita *et al*.[103] used MBTFA-derivatized full body (or egg) extracts of various lady beetle species to study intraguild predation through the presence of foreign alkaloids. Furthermore, MBTFA forms only a neutral, volatile acylamide as by-product, which does not interfere with the analytes.

Prior to the collection of the hemolymph all beetles had unlimited access to water to facilitate the sample collection. For each hemolymph analysis at least five beetles were used (biological replicates) to confirm the results. Additionally the hemolymph of each beetle was split in two halves directly after the collection (technical replicate) to confirm the reproducibility of the procedure as such. To allow comparability between different analyses DCM with *n*-bromodecane (50 µg ml^{-1}) as internal standard was used as the solvent.
Since all larvae were kept on *Sitotroga* eggs, only beetles from group-A, which preyed on aphids for at least three months were used for analysis.

The GC-MS chromatograms of a hemolymph sample of group-S (**Fig. 3.1 A**) and of group-A (**Fig. 3.1 B**) after derivatization with MBTFA are shown in **Figure 3.1**. Besides the standard (11.8 min) only one major peak was prominent in both samples. The concentration of this peak did not differ significantly between both feed groups.

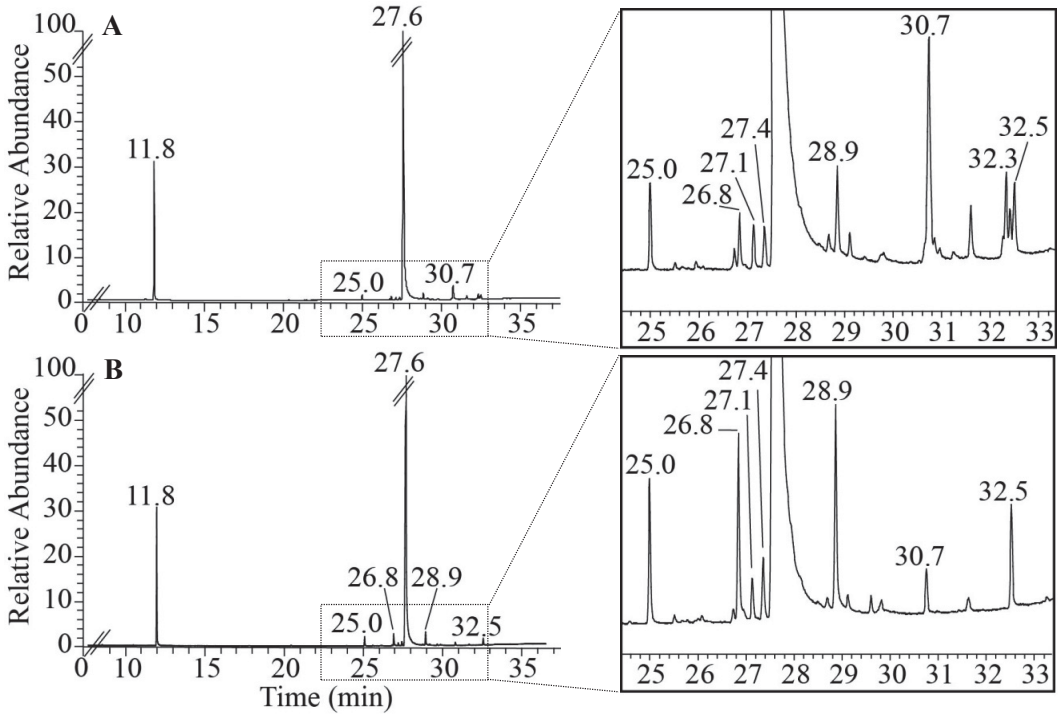

Figure 3.1: Comparison of the hemoplymph composition via GC-MS after derivatization with MBTFA. *n*-Bromodecane served as internal standard (RT = 11.8). **A**) TIC chromatogram of the hemolymph of a group-S beetle fed exclusively on *Sitotroga* eggs with detail magnification (20fold) of minor compounds (upper black box). **B**) TIC chromatogram of the hemolymph of a group-A beetle fed exclusively on *A. pisum* with detail magnification (20fold) of minor compounds (lower black box).

A detail magnification from minute 25 to 33 revealed, however, the presence of various minor components in both hemolymph samples. The profile of these minor compounds was comparable but not completely identical (**Fig. 3.1 black boxes**).

To identify the substances present in the hemolymph samples the MS spectra were analyzed. Four MS spectra typical for the substance classes found are displayed in **Figure 3.2**.

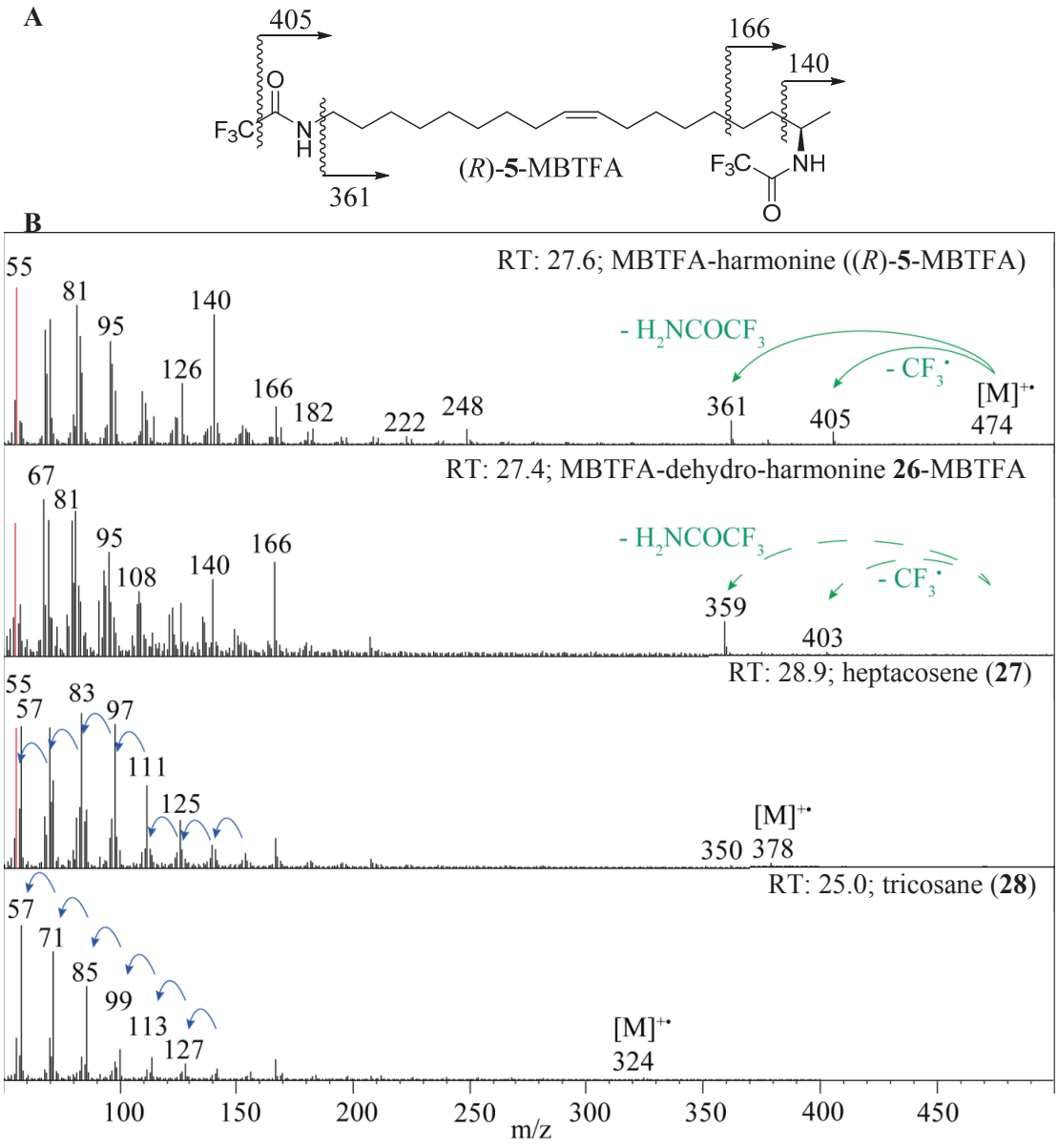

Figure 3.2: **A**) Structure of derivatized harmonine ((*R*)-**5**-MBTFA) with characteristic fragmentation points. **B**) Comparison of the fragmentation pattern of hemolymph compounds after derivatization with MBTFA (GC-MS, EI). The blue arrows display a mass loss of 14 amu and the green arrows show a mass loss of typical MBTFA derived fragments. The characteristic fragment indicating double bonds (55 amu) is drawn in red.

The major compound (RT = 27.6, upper spectrum) was identified to be double-derivatized harmonine ((*R*)-**5**-MBTFA). The spectrum did not only show a characteristic fragmentation pattern for MBTFA-derivatives but corresponded also exactly to the spectrum published by Sloggett *et al.*[102] The substance eluting at RT = 27.4 displayed a similar spectrum to

(*R*)-**5**-MBTFA. The MS fragment of 55 amu indicated at least one double bond and iterative mass losses of 14 amu the presence of a long alkyl chain. Strikingly was the 2 amu difference of the higher mass fragments compared to the fragments of (*R*)-**5**-MBTFA. This mass difference together with all other similarities suggested a harmonine-like structure with an additional double bond. The further structural elucidation of this dehydro-harmonine **26** is detailed in chapter 3.1.3.

For the other two compound types found in the hemolymph two representative spectra are shown (**Fig. 3.2**). The second last MS spectrum (peak eluting at RT = 28.9) exhibited the typical fragment of 55 amu indicating a certain degree of unsaturation as well as repeated mass losses of 14 amu. Furthermore, the relative abundance of the fragments was decreasing with increasing mass of the fragment. Together these facts indicated the presence of (mono)-unsaturated hydrocarbons in the hemolymph samples.[104] The lower spectrum (peak eluting at RT = 25.0) showed a typical MS spectrum for a saturated long-chain hydrocarbon. The saturated hydrocarbons were easily identified by comparison of their retention times with those of a C_7 - C_{30} hydrocarbon-standard. Additionally, the NIST MS spectral data base and massbank.jp were used. All identified compounds of the hemolymph samples are summarized in **Table 3.1**.

Table 3.1: Summary of compounds found in the hemolymph of *H. axyridis*.

RT	$[M]^{+\cdot}$	double bond	molecular formula	compound
25.0	324	-	*n*-$C_{23}H_{48}$	tricosane (**28**)
26.8	350	+	$C_{25}H_{50}$	pentacosene (**29**)
27.1	352	-	*n*-$C_{25}H_{52}$	pentacosane (**30**)
27.4	"472"	+	$C_{22}H_{34}F_6N_2O_2$	**26**-MBTFA
27.6	474	+	$C_{22}H_{36}F_6N_2O_2$	(*R*)-**5**-MBTFA
28.9	378	+	$C_{27}H_{54}$	heptacosene (**27**)
30.7	406	+	$C_{29}H_{58}$	nonacosene (**31**)
32.3	432	+	$C_{31}H_{60}$	untriacontadiene (**32**)
32.5	434	+	$C_{31}H_{62}$	untriacontene (**33**)

Since radical sites can migrate along the chain in unsaturated compounds, the fragmentation patterns of alkenes are similar, and normal MS spectra are not sufficient to determine the

position of the double bond. The first attempt to completely identify the unsaturated hydrocarbons was a literature research about known long-chain hydrocarbons in *H. axyridis*. This research revealed the use of long-chain saturated and unsaturated hydrocarbons for substrate marking and navigation of aggregation behavior in winter. The beetles mark the surface with different blends of hydrocarbons. These blends underlie seasonal changes and evoke different behavior of the beetles. The quantification, as well as the characterization of the hydrocarbons, was published by Durieux *et al*.[105] The analysis of beetle markings in June and July revealed that **28**, **29**, **27** and **31** are the more abundant hydrocarbons in the substrate marking. This finding correlated with the obtained spectra (beetles were reared at 22 °C) and strongly suggested that the hydrocarbons found in the hemolymph sample had the same structure as published previously, and that they were not originally part of the hemolymph but rather represent contaminants from the insect cuticle (hemolymph collection by cutting a leg). The structures of compounds found in the hemolymph sample are shown in **Figure 3.3**.

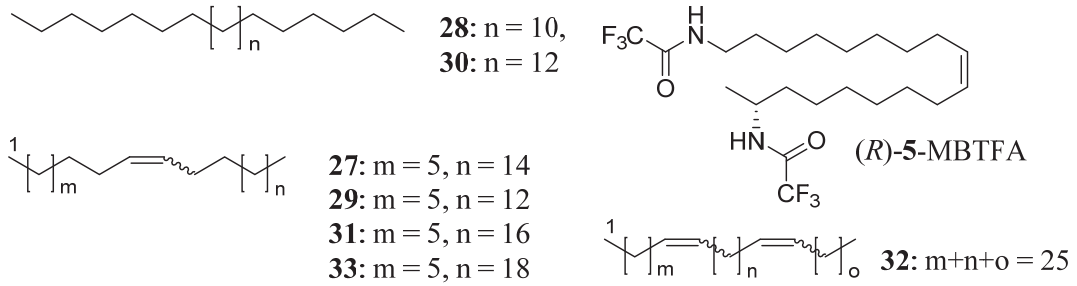

Figure 3.3: Likeliest structures of compounds found in *H. axyridis'* hemolymph sample after derivatization with MBTFA (except for **26**-MBTFA which is discussed in detail in chapter 3.1.3).

With the hydrocarbons most likely being cuticular contaminants and not part of the hemolymph they were excluded from further analyses. The remaining hemolymph composition did not show any difference between the two feed groups. In general, the hemolymph was rather clean. Besides of (*R*)-**5**-MBTFA only the dehydro-harmonine **26**-MBTFA was found.

3.1.3 AcN-CI-MS/MS Analysis of hemolymph compound 26

To determine the position of the second double bound in dehydro-harmonine **26** acetonitrile chemical ionization tandem mass spectrometry (AcN-CI-MS/MS) was used. This chemical ionization MS technique exploits acetonitrile as reagent gas and has been reported to facilitate the determination of double bond positions in monoene fatty acid methyl esters (FAME)[106] and in polyunsaturated FAME.[107-109]

Under AcN-CI-MS conditions, acetonitrile reacts with an ion of itself followed by decomposition. The resulting, diagnostically useful ion ($[CH_2=C=N=CH_2]^+$) was identified as 1-(methyleneimino)-1-ethenylium (MIE) and reacts rapidly with double bonds to form $[M+54]^+$ ions. Upon collision-induced dissociation of the $[M+54]^+$ adducts, two reproducible fragments are observed: the methyl ester end containing ion (α-ion) and the hydrocarbon end containing ion (ω-ion). Typically, monoenes experience bond cleavage at the allylic carbon of the double bond while dienes undergo cleavage at the vinylic carbon atom.[107]

Prior to AcN-CI-MS/MS analysis, the hemolymph was derivatized with MBTFA as described in chapter 6.4.2. Furthermore, the hemolymph sample was used as a whole since the molecule of interest was the minor hemolymph component (averaged: **26**-MBTFA/ (*R*)-**5**-MBTFA = 0.004).

The section of the AcN-CI-MS/MS spectrum of MBTFA-dehydro-harmonine **26**-MBTFA containing the characteristic MS^2 ions is shown in **Figure 3.4**. Two characteristic fragments of 303 amu and 345 amu were present. They allowed narrowing the positions of the double bonds down to being either at carbon 6 and 9 (**26b**-MBTFA) or at carbon 9 and 12 (**26a**-MBTFA). Furthermore, a fragment of 317 amu was dominant in the spectrum. This fragment arose from bond cleavage at the allylic carbon of the double bond. In FAME dienes mostly cleavage at the vinylic carbon is observed, however, minor peaks typical of monoene-type cleavages are also visible.[108] **26**-MBTFA features bulky functional groups at both sides of the molecule. These might have governed the normal hydrocarbon fragmentation pattern towards enhanced bond cleavage at the allylic carbon atom.

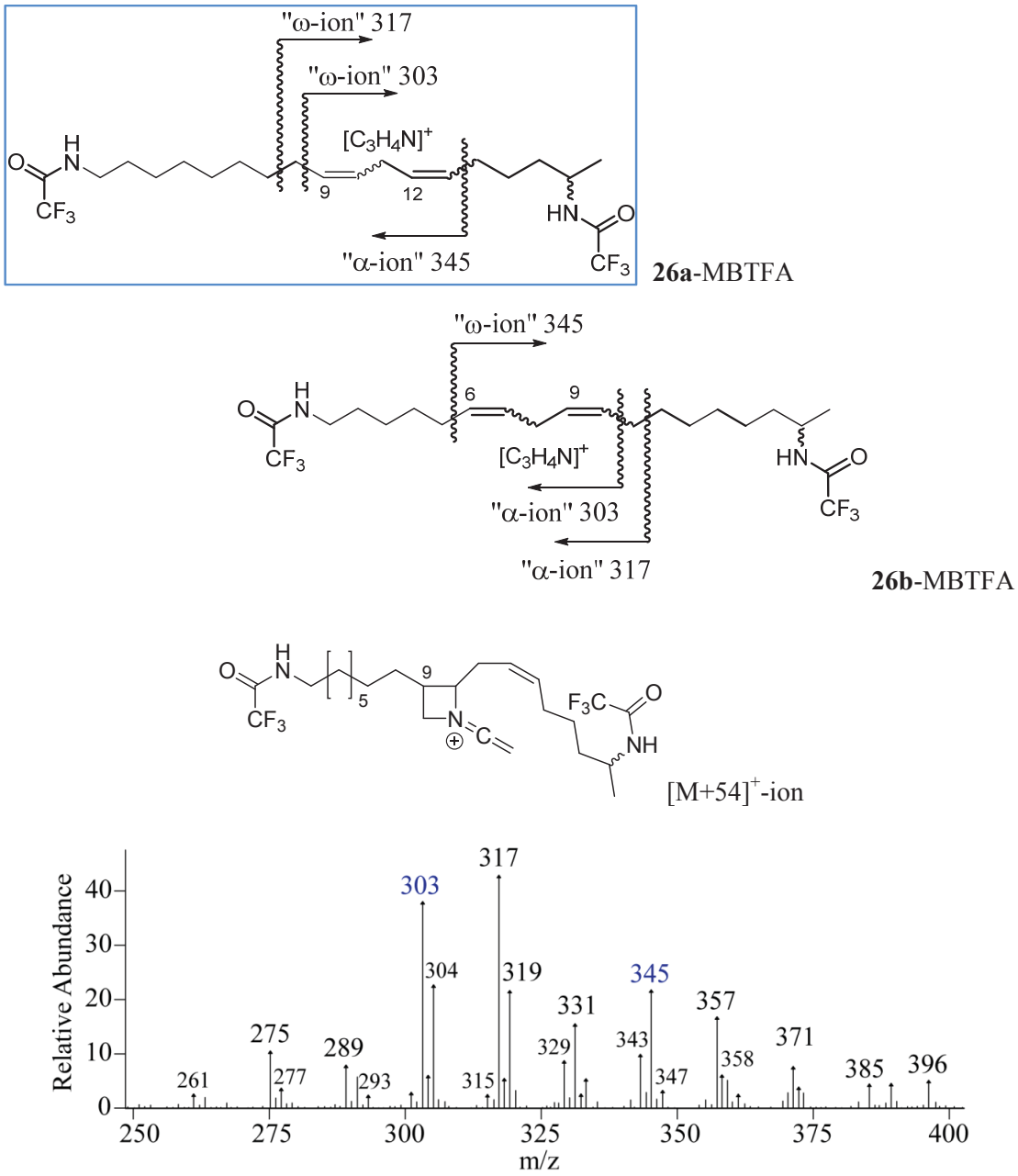

Figure 3.4: The 2 possible structures of **26**-MBTFA with typical bond cleavage positions and characteristic ions are shown. The more likely structure is highlighted in blue. Furthermore, one of the proposed $[M+54]^+$-ions (resulting from **26a**-MBTFA; modified from Van Pelt *et al.*[108] and Michaud *et al.*[110]) and the relevant section of the AcN-CI-MS/MS spectrum of MBTFA-dehydro-harmonine **26**-MBTFA are displayed.

Unfortunately, the exact position of the second double bond of dehydro-harmonine **26** could not be assigned, since the molecule is too symmetric for AcN-CI-MS/MS analysis. The emerging α-ion of structure **26a**-MBTFA showed the same mass as the ω-ion of **26b**-MBTFA

and *vice versa*. The fragment 317 could also emerge from both structures (**Fig. 3.4**). Since only a few per mille of **26** are present in the hemolymph, structural elucidation through NMR was not possible. Based on the circumstances that $\Delta^{9,12}$-unsaturation is a very common motive in nature and also existing in the omnipresent linoleic acid, a linoleic acid like structure with $\Delta^{9,12}$-unsaturation could be assumed for **26**. With this, **26a**-MBTFA is more likely to be the correct structure of the dehydro-harmonine **26** found in the hemolymph. For an impeccable structural elucidation the total synthesis of dehydro-harmonine **26** is the next step that should be accomplished.

3.2 Syntheses

Although harmonine ((*R*)-**5**) has been isolated[26] and synthesized[52-54] previously, there is still a need for an efficient and rapid synthesis of harmonine ((*R*)-**5**) as well as for derivatives and possible biosynthetic precursors. Since the mode of action is still unknown, larger quantities of (*R*)-**5** and related molecules are needed, in particular for bioassays and structure-activity studies. Especially at the beginning of this thesis only one time-consuming and lengthy synthesis of (*R*)-**5** was known.[53] Therefore the major aim of the following synthesis was not only to provide a quick and reliable access to harmonine ((*R*)-**5**) but also to generate a flexible synthetic route delivering derivatives and both enantiomers of **5** without the need of expensive catalysts or auxiliaries. The general concept of the synthesis was planned with a customizable key step enabling enantiomeric modifications and allowing necessary flexibility.

The retrosynthetic analysis of **5** is shown in **Scheme 3.1**. **5** could be obtained through functional group interconversion from isopropyl (9*Z*)-17-hydroxyoctadec-9-enoate (**34**). **34** itself could be generated following a Wittig-type reaction protocol starting from (9-iso-propoxy-9-oxononyl)triphenylphosphonium bromide (**35**) and 9-methyloxonan-2-one (**36**). The Wittig salt **35** could be easily prepared through functional group interconversion from commercially available bromoacid **37**. The lactone **36** is available through a Baeyer-Villiger oxidation of methyl-cyclooctanone **38** which itself could be prepared using commercially available cyclooctanone **39**.

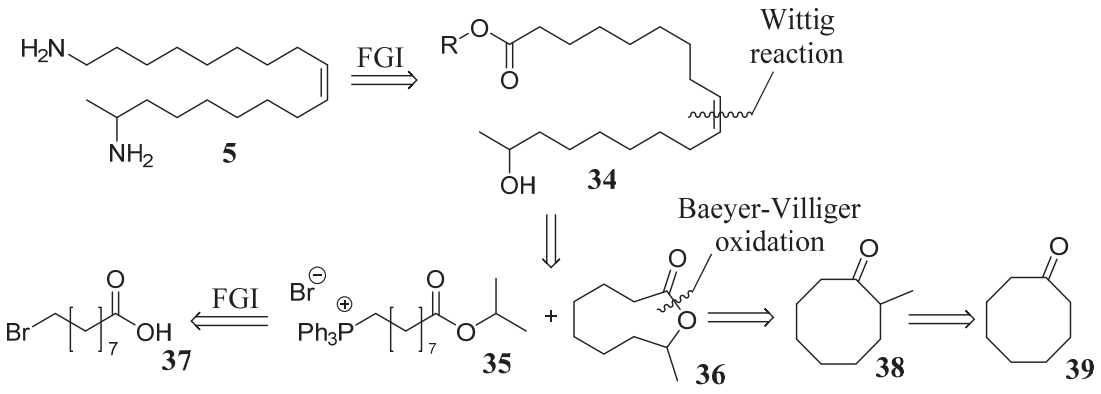

Scheme 3.1: Retrosynthetic analysis of harmonine (**5**); R = isopropyl.

The straightforward synthesis to *rac*- (*rac*-**5**), (*R*)- ((*R*)-**5**), and (*S*)-harmonine (*ent*-(*S*)-**5**)[1] as well as to harmonine-like compounds for structure-activity studies is described.

3.2.1 Synthesis of *rac*-Harmonine (*rac*-5) and OH-Analog *rac*-48

Initially the precursors for the assembly of the carbon backbone had to be synthesized. The ω-methylated lactone *rac*-**36** could be obtained in large quantities starting from commercially available cyclooctanone (**39**) following a protocol published by van Buijtenen *et al*.[111] (**Scheme 3.2**). First, **39** was methylated using methyl iodide (MeI). To avoid multiple alkylation reactions, low temperatures and only a minor excess of MeI were used. Under this reaction conditions the desired methyl-cyclooctanone **38** was obtained with high yield (up to 97%). The double alkylated product and **39** were only present in negligible quantities which allowed the usage of **38** without an additional purification step. Subsequently a Baeyer-Villiger oxidation employing *meta*-chloroperoxybenzoic acid (*m*-CPBA) as oxidant yielded *rac*-**36**. This reaction was improved with regard to the known protocol.[111] Although the duration is still long, the reaction time was reduced by 3 days and the yields were increased.

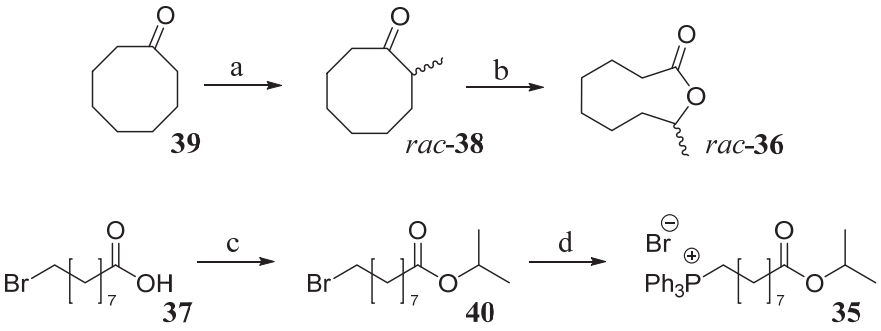

Scheme 3.2: Synthesis of the precursors for the Wittig-type reaction. Reagents and conditions: (a) (i) DIPA, BuLi, THF, 30 min, 0 °C; (ii) MeI, 15 min, -78 °C; (iii) rt, overnight, (97%); (b) *m*-CPBA, $CHCl_3$, 11 d at rt then 1 d reflux, (58%); (c) 2-propanol, H_2SO_4, 19 h, reflux, (86%); (d) PPh_3, toluene, 4 d, reflux, (77%).

The second precursor – the phosphonium salt **35** – could be prepared starting from ω-bromononanoic acid **37** (**Scheme 3.2**). **37** was converted into the isopropyl ester **40** exploiting a

[1] The stereochemistry of the synthesized substances is indicated using (*S*)- or (*R*)- or *rac*- in front of the assigned number.

classical esterification procedure (e.g. described in Yang *et al*.[112]). To shift the equilibrium towards the ester, a Dean-Stark apparatus was used to remove the released water. The isopropylester was chosen because it should allow minimization of side reactions during the following Wittig olefination. **40** was then reacted with PPh_3 to yield the desired phosphonium salt **35** in good quantities and high purity.[113]

With both precursors in hand, the actual synthesis of racemic harmonine (*rac*-**5**) could be conducted. The straightforward synthetic strategy is shown in **Scheme 3.3**.

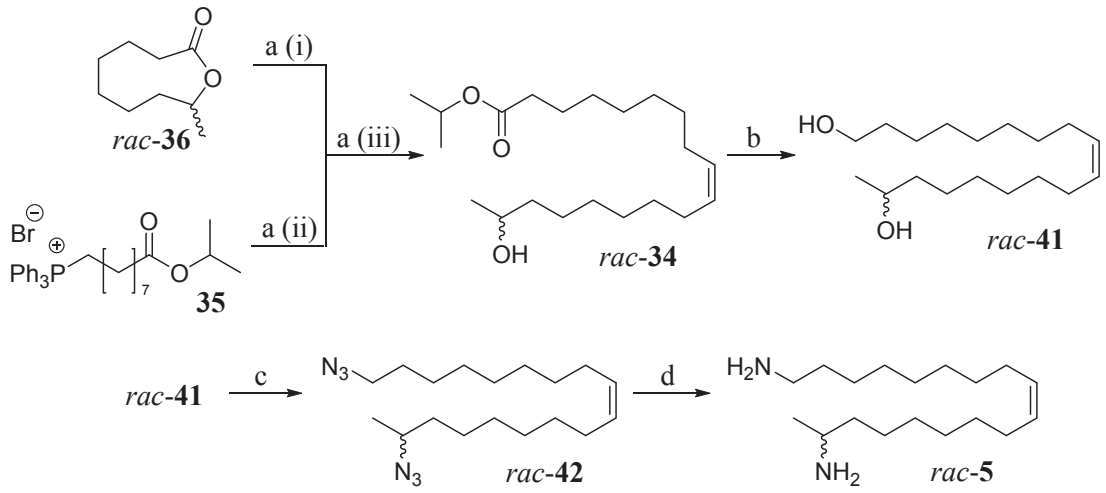

Scheme 3.3: Synthetic sequence to *rac*-harmonine (*rac*-**5**). Reagents and conditions: (a) (i) DiBAL-H, MeOH, toluene, −78 °C; (ii) KHMDS, THF, −78 °C; (iii) −78 °C to rt in 1 h, 1 h rt, (23-29%, *Z*/*E* > 98/2); (b) $LiAlH_4$, THF, 4.5 h, rt, (98%); (c) PPh_3, DPPA, DIAD, THF, 4 h, rt, (76%); (d) $LiAlH_4$, THF, 4 h, rt, (quant).

The carbon backbone of *rac*-**5** was established *via* reductive olefination of *rac*-**36** and phosphonium salt **35**. The used "one-pot Wittig-type" procedure was first reported in 1980 by Boland *et al*.[114] and exhibits various advantages over a normal two step reaction procedure (isolation and purification of hemiacetals with subsequent Wittig reaction): Obviously, it is one step shorter and has therefore also one purification procedure less minimizing possible losses of substance. Furthermore, there is no need to handle unstable hemiacetals or aldehydes.

The proposed reaction mechanism[114] of the "Wittig-type one-pot" reaction is detailed in **Scheme 3.4**. The use of DiBAL-H at temperatures below -65 °C allows the reduction of

lactone *rac*-**36** to the cyclic aluminum salt **43**, which undergoes ring opening at temperatures above -40 °C to form the free hydroxy aldehyde **44**. The hydroxyl group is protected as an aluminum alkoxide. In the presence of a suitable ylide, **44** readily reacts to form the desired olefin *rac*-**34**.

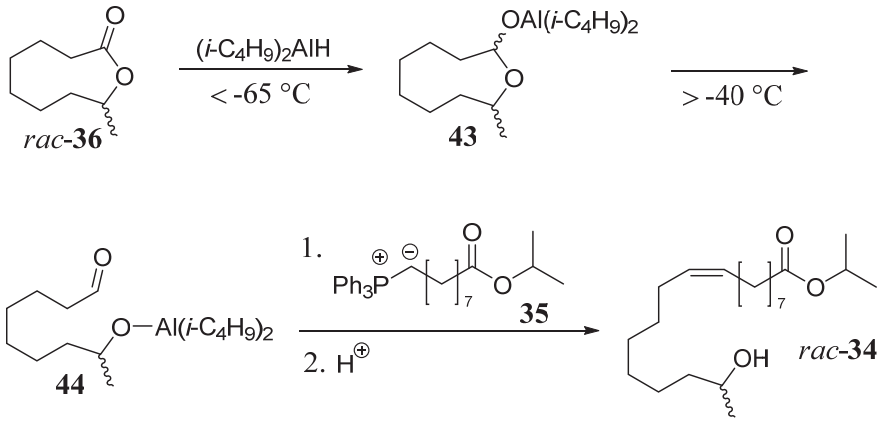

Scheme 3.4: Proposed mechanism for the "Wittig-type one-pot reaction" illustrated with 9-methyloxonan-2-one (*rac*-**36**) as reagent.[114]

The Wittig part of this one-pot reaction plays a pivotal role when it comes to formation of the *Z*- (or *E*-) alkene. Since high *Z*-selectivity was desirable, a non-stabilized ylide was used. Non-stabilized ylides react faster, favor the kinetically controlled formation of the *cis*-oxaphosphetane (OPA, **46**, **Fig. 3.5**) intermediate and thereby the formation of *Z*-alkenes.[115]

As it is widely known, the base used for the creation of the ylide, is essential to obtain high *Z*-selectivity. Although the Wittig-reaction was discovered more than 60 years ago, the exact mechanism has been controversial for a long time. While formerly the opinion was widespread that betaine-structures **45** are the first intermediate formed during the Wittig-reaction[116] the notions have changed these days. Various proposed mechanisms including evidences for these mechanisms were reviewed by Byrne and Gilheany.[115]

Figure 3.5: Schematic representation of a betaine **45** and a *cis*-OPA **46**.

They clearly state that there should be made a distinction between the well-established "Li^+ salt-free" and the up till now disputed "Li^+ present" Wittig mechanism. They claim that under Li^+ salt-free conditions all Wittig reactions occur under kinetic control. During the reaction an irreversible [2+2] cycloaddition of ylide and aldehyde is the first step that yields OPA. A following stereospecific cyclo-reversion yields the final product and phosphine oxide. The stereochemistry of the alkene is thereby defined by the stereochemistry of the OPA. Betaines or formerly proposed diradical species have been proven not to be present at any time of the reaction.[115]

In the mechanistically not yet completely clarified Wittig reactions in the presence of Li^+, reduced *Z*-selectivity is always observed. This arises probably from an effect of Li^+ on the formation of OPA. Furthermore, in some exceptional cases a non-correspondence between the *Z*/*E*-ratios of the alkene and the OPA was observed. This so-called "stereochemical drift" is mostly linked to the presence of Li^+ in the reaction mixture and favors the *E*- over the *Z*-isomer.[115]

The reduced *Z*-selectivity in presence of Li^+ ions could be also observed during the accomplishment of this thesis. The "Wittig-type one-pot" reaction was conducted with various reaction conditions to improve the yield and the *Z*/*E*-ratio of the formed isopropyl ester *rac*-**34**. The reductive part with DiBAL-H was kept constant, while the bases used for the Wittig part were varied. The results are summarized in **Table 3.2** and clearly demonstrate that KHMDS was the most suitable base for the Wittig reaction showing moderate yields and an excellent *Z*/*E*-ratio.

Table 3.2: Used reagents for ylide preparation during the "Wittig-type one-pot" reaction, obtained *Z*/*E*-ratios and yields.

reagent	***Z*/*E*-ratio**	**yield [%]**
***n*-BuLi**	$80/20 \leq Z/E \leq 86/14$	23 - 29
KHMDS	> 98/2	26
NaHMDS	98/2	13

Although the yields never exceed the 30%, this was not a serious drawback since the precursors could easily be obtained in abundance from commercially available substances. The

major aim of this reaction step was to create a distinguished excess of the *Z*-isomer for bioactivity studies, which was impeccably achieved.

The obtained isomer ratio was determined using GC-MS (exact method see chapter 6.1). The TIC chromatograms are shown in **Figure 3.6** and clearly demonstrate the advantages of KHMDS over *n*-BuLi in terms of *Z*-selectivity.

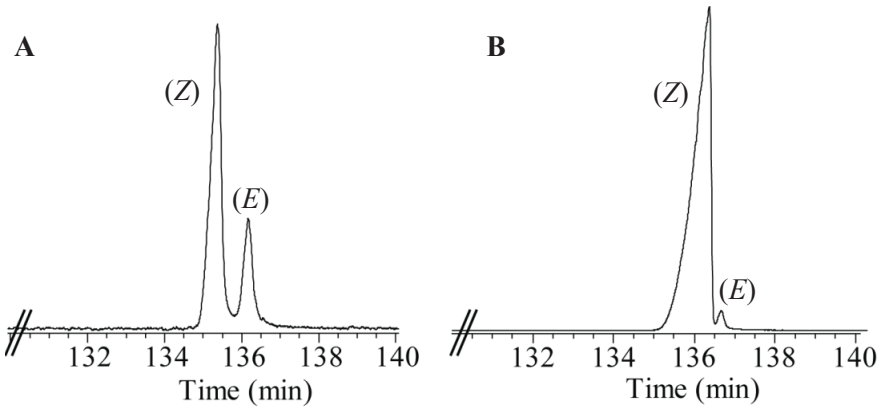

Figure 3.6: GC-MS chromatograms for *Z*/*E*-ratio determination of *rac*-**34**. **A**) *rac*-**34** prepared with *n*-BuLi; *Z*/*E* = 80/20. **B**) *rac*-**34** prepared with KHMDS; *Z*/*E* ≥ 98/2.

The next step in the sequence to harmonine (*rac*-**5**) was a reduction of *rac*-**34** using $LiAlH_4$ (LAH) (procedure modified from Ooi *et al*.[117]). This reducing agent allowed the quantitative generation of the racemic diol *rac*-**41** (**Scheme 3.3**). A subsequent Mitsunobu reaction utilizing triphenylphosphine (PPh_3), diphenyl phosphorazidate (DPPA) and diisopropyl azodicarboxylate (DIAD) converted *rac*-**41** into the diazide *rac*-**42** (modified from Jiao *et al*.[118]). Finally another reduction step with an excess of LAH afforded the desired product *rac*-**5**, which was extracted as a salt, in quantitative yield (modified from Jiao *et al*.[118]).
In total racemic harmonine (*rac*-**5**) could be prepared with an overall yield of 22% in only four reaction steps starting from the lactone *rac*-**36** and the phosphonium salt **35**.

The reaction sequence shown in **Scheme 3.3** could be easily altered to furnish a possible bio-synthetic precursor of harmonine (**5**), the (9*Z*)-18-aminooctadec-9-en-2-ol (*rac*-**48**)[2], in only two reaction steps. This OH-analog *rac*-**48** was of special interest for biological assays and structure-activity studies since it is structurally very similar to *rac*-**5** with only one different functional group.

[2] (9*Z*)-18-aminooctadec-9-en-2-ol (*rac*-**48**) is from now on called OH-analog

The synthetic sequence to the OH-analog *rac*-**48** starting from isopropyl ester *rac*-**34** is outlined in **Scheme 3.5**. Initially, the conversion of *rac*-**34** into the amide *rac*-**47** was conveniently achieved using magnesium nitride in MeOH at 80 °C.[119]

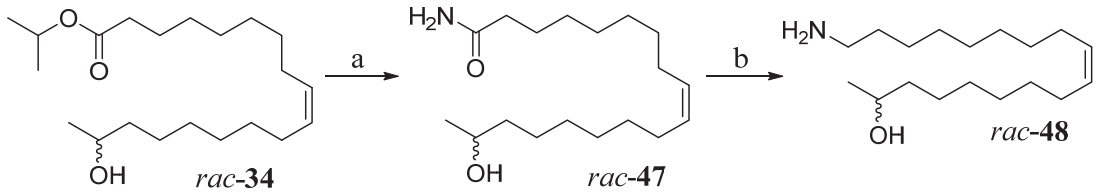

Scheme 3.5: Synthetic sequence to the OH-analog *rac*-**48**. Reagents and conditions: (a) Mg_3N_2, MeOH, 80 °C, 1 d, (87%); (b) $LiAlH_4$, THF, 45 °C, 20 h, (95%).

This so far relatively unknown procedure was chosen because it displays various decisive advantages over commonly used methods like the preparation of saturated ammonia solutions. Most importantly the use of toxic, gaseous ammonia was not necessary anymore, which also simplified the reaction set-up enormously. The required ammonia was prepared *in situ* from the reaction of magnesium nitride with a protic solvent such as MeOH. The release of ammonia could be simply observed by a distinctive color change. The initially brown reaction slurry turned white during the formation of magnesium salts. To ensure a complete reaction it was important to use thick-walled, tightly sealed glass vessels which could withstand the pressure built up from released ammonia and superheated MeOH.[119]

A subsequent reduction of the amide *rac*-**47** with LAH yielded the desired OH-analog *rac*-**48** in nearly quantitative yield (procedure modified from Csíki *et al*.[120]). Taken together *rac*-**48** could be obtained with an overall yield of 83% starting from the isopropyl ester *rac*-**34**.

3.2.2 Enantioselective Synthesis: (*R*)- ((*R*)-5) and (*S*)-Harmonine ((*S*)-5)

The synthesis of racemic harmonine (*rac*-**5**) could be readily modified to allow the generation of the natural occurring (*R*)-harmonine ((*R*)-**5**) as well as the synthesis of its non-natural enantiomeric (*S*)-harmonine (*ent*-(*S*)-**5**). Up until now the preparation of the (*S*)-enantiomer *ent*-(*S*)-**5** has never been described before and was achieved for the first time during the implementation of this thesis.

The racemic lactone *rac*-**36** served as starting material for the synthesis of both enantiomers. A kinetically controlled, enantioselective saponification of *rac*-**36** allowed the generation of the (*S*)-lactone (*S*)-**36** (*ee* > 99.5%) as well as the (*R*)-hydroxy acid (*R*)-**49** (*ee* > 99%) (**Scheme 3.6**).

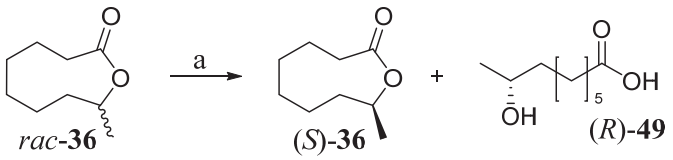

Scheme 3.6: Enzymatic, enantioselective saponification of *rac*-**36**. Reagents and conditions: (a) HLE, NaH_2PO_4, NaOH, 16 h, rt; (*S*)-**36**: 43%, *ee* ≥ 99.5%; (*R*)-**49**: 39%, *ee* ≥ 99%.

For this crucial key step, a procedure described by Fouque *et al*.[121] was modified. First, the lactone *rac*-**36** was suspended in a NaH_2PO_4-buffer (0.1 M) at pH = 7.2. Then horse liver esterase (HLE) was added as a lyophilized powder. With the addition of HLE, the hydrolysis started immediately. During the whole reaction the pH had to be kept constant by the dropwise addition of diluted NaOH (0.5 M) to avoid spontaneous hydrolysis and thereby racemization. The substrate/enzyme ratio could be lowered in regard to the previously published procedure. While Fouque *et al*.[121] used a ratio of 1/1 (w/w), the enzyme amount could be drastically reduced. An initial ratio of 10/1 (w/w) was found to be sufficient for complete reaction. To speed up the reaction procedure, an additional portion of HLE could be added (final ratio 8.3/1 (w/w)).

The progress of the hydrolysis was monitored using a GC-MS equipped with a chiral *β*-6TBDM-cyclodextrin column (**Fig. 3.7 A**). This column together with a newly developed method allowed a baseline separation of the lactone **36** enantiomers present in the reaction mixture and thereby a detailed evaluation of the reaction progress.

After complete hydrolysis of the (*R*)-lactone (*R*)-**36**, the reaction rate slowed down drastically. No hydrolysis of the (*S*)-lactone (*S*)-**36** was observed.

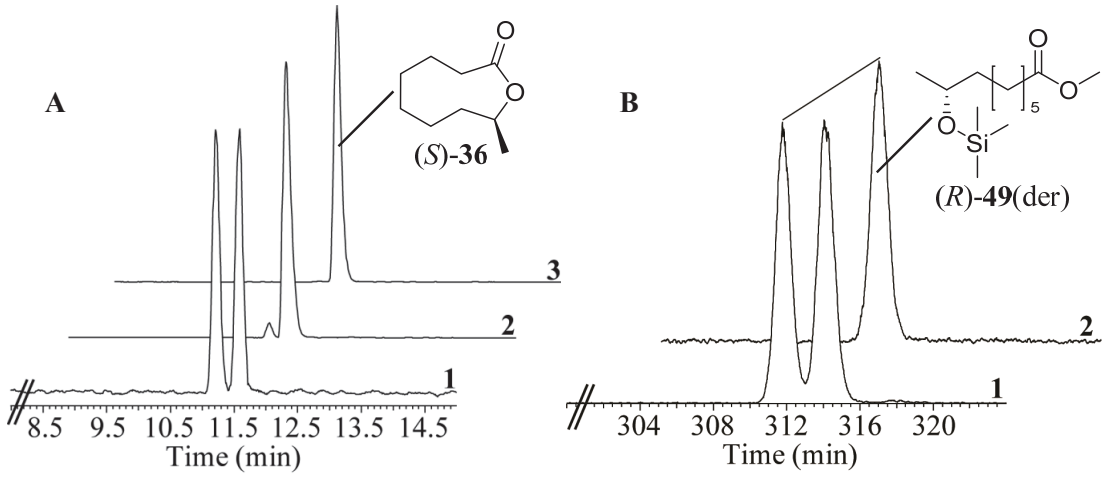

Figure 3.7: Enantiomeric GC analysis of (*S*)-**36** (**A**) and (*R*)-**49** (**B**) on a *β*-6TBDM-cyclodextrin column. **A**) **1**) Initial conditions: racemic lactone *rac*-**36**. **2**) 98% hydrolysis of (*R*)-lactone (*R*)-**36**. **3**) Isolated lactone (*S*)-**36** (*ee* ≥ 99.5%). **B**) **1**) Derivatized, racemic hydroxy acid *rac*-**49**(der) (derivatized with TMS-diazomethane/MSTFA). **2**) Derivatized, isolated (*R*)-**49**(der) (*ee* > 99%). (modified from Nagel *et al*.[55])

To develop an appropriate GC-MS method for the determination of the enantiomeric excess (*ee*) of the (*R*)-hydroxy acid (*R*)-**49**, the racemic hydroxy acid *rac*-**49** was needed. Therefore, the racemic lactone *rac*-**36** was dissolved in a mixture of THF and aqueous LiOH solution. The reaction mixture was stirred overnight, acidified with 3% HCl and extracted with DCM. The resulting, crude *rac*-**49** was initially derivatized with TMS-diazomethane, the solvent was evaporated and then the crude ester was derivatized with *N*-trimethylsilyl-*N*-methyl trifluoroacetamide (MSTFA). The obtained derivatized hydroxy acid *rac*-**49**(der) was used for the development of a GC-MS method (**Fig. 3.7 B**). Both methods developed for the determination of the *ee* of the (*S*)-lactone (*S*)-**36** and the (*R*)-hydroxy acid (*R*)-**49** can be found in detail in chapter 6.1.
In total, (*S*)-**36** and (*R*)-**49** could be obtained with good yields and excellent *ee* ((*S*)-**36**: 43%, *ee* > 99.5%, (*R*)-**49**: 39%, *ee* ≥ 99%).

The optically pure (*S*)-lactone (*S*)-**36** was now used to prepare the naturally occurring (*R*)-harmonine ((*R*)-**5**) (**Scheme 3.7**). For this, the same sequence of reactions was used as previously described in chapter 3.2.1 for the racemic harmonine (*rac*-**5**). The usage of the

Mitsunobu reaction protocol as the second last step involves the inversion of the stereocenter to finally result in the required (*R*)-configuration. In conclusion (*R*)-harmonine ((*R*)-**5**) could be obtained with an overall yield of 18% starting from the phosphonium salt **35** and the lactone (*S*)-**36**. All spectral data of (*R*)-**5** were identical to literature values.[28, 53, 56]

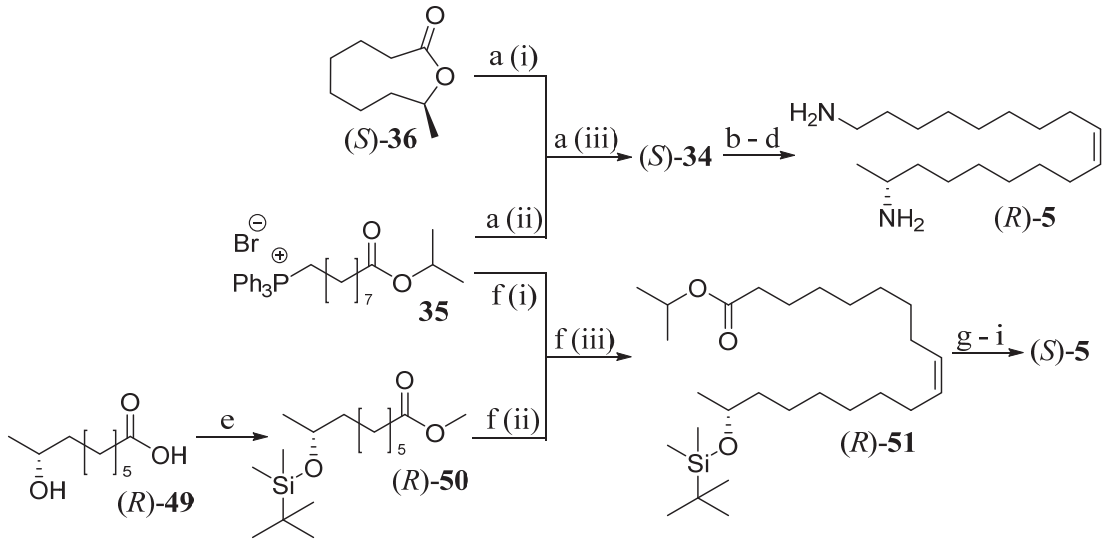

Scheme 3.7: Synthetic route to (*R*)- ((*R*)-**5**) and (*S*)-harmonine ((*S*)-**5**). Reagents and conditions: (a) (i) DiBAL-H, MeOH, toluene, −78 °C; (ii) *n*-BuLi, THF, −78 °C; (iii) −78 °C to rt in 1 h, 1 h rt, (23%, *Z*/*E* > 85/15); (b) $LiAlH_4$, THF, 4.5 h, rt, (98%); (c) PPh_3, DPPA, DIAD, THF, 4 h, rt, (81%); (d) $LiAlH_4$, THF, 4 h, rt, (quant); (e) (i) TMS-diazomethane, DCM/MeOH, 1.5 h, rt; (ii) AcOH; (iii) imidazole, TBDMSCl, DCM, 16.5 h, rt, (84%); (f) (i) DiBAL-H, MeOH, toluene, −78 °C; (ii) KHMDS, THF, −78 °C; (iii) −78 °C to rt in 1 h, 1 h rt, (29%, *Z*/*E* > 98/2); (g) (i) $LiAlH_4$, THF, 4 h, rt; (ii) 40% HF, AcN, 2 h, rt, (73%); (h) PPh_3, DPPA, DIAD, THF, 4 h, rt, (87%); (i) $LiAlH_4$, THF, 4 h, rt, (95%).

For the preparation of the non-natural (*S*)-harmonine (*ent*-(*S*)-**5**) the chiral (*R*)-hydroxy acid (*R*)-**49** was used as starting material.

At first, the overall reaction concept applied for the synthesis of (*R*)-**5** and *rac*-**5** should not be altered. Therefore, a re-lactonization of the hydroxy acid (*R*)-**49** to the (*R*)-lactone (*R*)-**36** was attempted. The used methods and results are summarized in **Table 3.3**.

For macrolactone formation from the corresponding hydroxy acid it is important to achieve a rapid lactonization to overcome polymerization.[122] The first entry (**Table 3.3**) displays a lactonization attempt with slightly modified Yamaguchi macrolactonization conditions employing the 2,4,6-trichlorobenzoyl chloride (TCBC) to form a mixed anhydride, which

could be attacked from the intramolecular alcohol function. Since these reaction conditions did not show any product formation (NMR, GC-MS) an approach following the protocol of Shiina *et al*.[123] was tested. In this case, the mixed anhydride was prepared with 2-methyl-6-nitrobenzoic anhydride (MNBA). The reaction resulted in the formation of traces of the desired product (*R*)-**36** but also in the formation of dimeric or trimeric large ring lactones. The reaction conditions were varied several times but the amount of (*R*)-**36** could not be increased.

Table 3.3: Macrolactonization methods used for the preparation of (*R*)-lactone (*R*)-**36**.

Reagents	no. of attempts	(*R*)-36 [a]	side products [a]
TCBC, Et_3N, DMAP[124]	1	/	reagents
MNBA, DMAP[123]	5	traces	"dimer"[b]
ethoxyacetylene, $[RuCl_2(p\text{-cymene})]_2$, *p*-TsOH[125]	2	~ 50%	"dimer"[b], (*R*)-**49**

[a] Substances and amounts were determined via GC-MS from the crude reaction mixture.
[b] Dimeric or trimeric lactones were observed showing a similar fragmentation pattern as the monomeric lactone. The molecular ion was not visible. The exact ring size was not determined.

Therefore a different method was applied (**Table 3.3** entry 3). First the ethoxyvinyl ester was prepared from the hydroxy acid (*R*)-**49** and ethoxyacetylene in the presence of a ruthenium catalyst. The catalyst had to be removed and afterwards the solution was added dropwise to a highly diluted solution of *p*-TsOH in 1,2-dichloroethane.[125] This procedure afforded the desired lactone (*R*)-**36** in around 50% yield. However, the hydroxy acid (*R*)-**49** and dimeric products were always observed.

Since all lactonization methods would lead to a substantial substance loss, the overall reaction concept to (*S*)-harmonine ((*S*)-**5**) was slightly altered (**Scheme 3.7**). At first, the hydroxy acid (*R*)-**49** was converted into the TBDMS-protected hydroxy methyl ester (*R*)-**50** in a one-pot reaction. The ester (*R*)-**50** could easily be used in the "Wittig-type one-pot" reaction to form the protected isopropyl ester (*R*)-**51**. (*R*)-**51** was then reduced with LAH and subsequently deprotected with HF to yield the (*R*)-diol (*R*)-**41**. At that point, the same sequence of reactions was used as described for the synthesis of the racemic harmonine (*rac*-**5**). In

summary, (*S*)-harmonine ((*S*)-**5**) could be obtained with an overall yield of 15% starting from the hydroxy acid (*R*)-**49** and the phosphonium salt **35**.

All spectral data of (*S*)-**5** (except for the optical rotation) were identical to literature values.[28, 53, 56] As expected, the optical rotation showed a similar numeric value with the opposite sign.

3.2.3 Synthesis of the short-chain Harmonine Derivative: C_{17}-Harmonine (*rac*-58)

Finally the complete reaction sequence should be used to obtain a short-chain derivative of (*R*)-**5**. This shorter harmonine derivative was mainly synthesized because it should give interesting insights into the chain length dependency of the biological activities of harmonine ((*R*)-**5**).

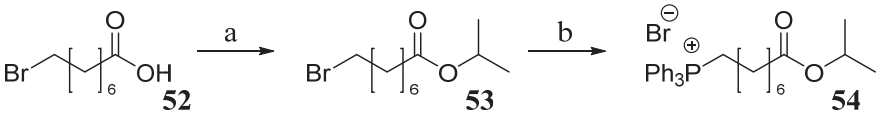

Scheme 3.8: Synthesis of the short-chain phosphonium salt **54**. Reagents and conditions: (a) 2-propanol, H_2SO_4, 19 h, reflux, (83%); (b) PPh_3, toluene, 4 d, reflux, (61%).

For the alteration of the carbon backbone the C_8-phosphonium salt **54** was prepared (**Scheme 3.8**). **54** was only one carbon atom shorter than the previously used phosphonium salt **35**. In general, the same procedure was conducted as detailed in chapter 3.2.1. The isopropyl group was again chosen to minimize side reactions during the following "Wittig-type one-pot" reaction.

Interestingly C_8-phosphonium salt **54** proved to be hygroscopic, which aggravated the process of drying as well as the handling of the syrup-like compound.

The following Wittig-type reaction was performed between the racemic lactone *rac*-**36** and the C_8-phosphonium salt **54** (**Scheme 3.9**). Due to the slightly elevated amount of moisture in **54**, the ylide preparation was not complete and the yield of the "Wittig-type one-pot" reaction decreased to some extent. The resulting C_{17}-isopropyl ester *rac*-**55** was then subjected to the

same sequence of reactions (see chapter 3.2.1, **Scheme 3.3**) as previously described yielding the C_{17}-harmonine derivative *rac*-**58**.

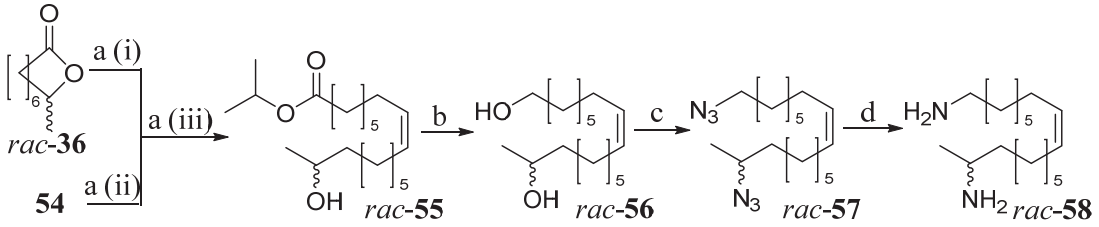

Scheme 3.9: Outline of the synthetic sequence to C_{17}-harmonine (*rac*-**58**). Reagents and conditions: (a) (i) DiBAL-H, MeOH, toluene, −78 °C; (ii) KHMDS, THF, −78 °C; (iii) −78 °C to rt in 1 h, 1 h rt, (15%, *Z*/*E* > 97/3); (b) $LiAlH_4$, THF, 4.5 h, rt, (98%); (c) PPh_3, DPPA, DIAD, THF, 4 h, rt, (90%); (d) $LiAlH_4$, THF, 4 h, rt, (quant).

C_{17}-harmonine *rac*-**58** could be prepared with an overall yield of 13% starting form lactone *rac*-**36** and C_8-phosphonium salt **54**. Because of the shorter carbon chain containing the primary amino group of *rac*-**58**, the position of the *cis*-configured double bond was shifted from Δ^9 to Δ^8. The back part of the molecule carrying the second amino group and the stereocenter was completely identical to racemic harmonine *rac*-**5**. Consequently, biological assays should allow to study the influence of the length of the carbon backbone without any other structural influences.

3.3 Determination of Biological Activities

The synthesized substances were tested in diverse bioassays to allow the elucidation of structure-activity relationships in harmonine ((*R*)-**5**) and to discover interesting new biological activities.

With the synthesized compounds the importance of the features summarized in **Figure 3.8** was tested and evaluated:

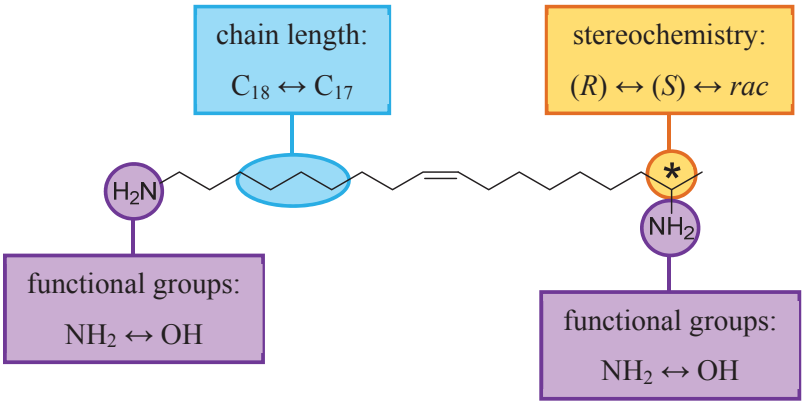

Figure 3.8: Modified structural features in the synthesized compounds.

At first, the role of the stereocenter of (*R*)-harmonine ((*R*)-**5**) should be clarified. Therefore, (*R*)-, (*S*)-, and *rac*-harmonine (**5**) were assayed. An importance of the stereocenter would suggest that the biological activity observed for harmonine (**5**) is due to a specific interaction with enzymes or receptors. Since most active sites of enzymes are structurally conserved and highly specific, changes in stereochemistry of an inhibitor or substrate should alter the observed activity. Next, the impact of the functional groups should be tested. A comparison of the biological activities of *rac*-harmonine (*rac*-**5**), OH-analog *rac*-**48** and diol *rac*-**41** could give important hints to functional group dependency of the observed activity. Finally, also the importance of the chain length of the carbon skeleton should be elucidated. Therefore, biological activities of *rac*-harmonine (*rac*-**5**) and C_{17}-harmonine *rac*-**58** were compared. A chain length dependency of the biological activities could also point towards effects of harmonine (**5**) on important enzymes of the assayed organisms.

3.3.1 Determination of Microbial Growth Inhibition

Initially, the antibacterial properties of various synthesized compounds were tested using a microbial growth inhibition assay. Therefore, bacteria were cultivated in LB medium, plated and the agar was pierced to allow the application of the substances. In this assay the compounds diffuse into the agar and the bacteria are exposed to a concentration gradient during their growth. Depending on the antibacterial activity (and the concentration) of the substance the occurring inhibition zones vary in size.
For the microbial growth inhibition assay *Escherichia coli* and *Bacillus subtilis* were chosen. *B. subtilis* is one of the well-known representatives of Gram-positive and *E. coli* of Gram-negative bacteria. The bacteria types can be differentiated through Gram staining.[126] A Gram-positive and a Gram-negative bacterium were used to cover both of the most important bacterial groups in this assay.

The efficiency of (*R*)-harmonine ((*R*)-**5**) against *E. coli* and *B. subtilis* was already proven by Röhrich *et al*.[27] who determined the minimal inhibitory concentration for *E. coli* to be 89 µM and 44 µM for *B. subtilis*.
Considering these data, solutions of the substances with concentrations of 0.1 mM and 10 mM in MeOH were prepared. MeOH was used because all of the substances are not water soluble under neutral conditions. To ensure that MeOH had no effect on the bacterial growth, each plate had one negative control in the form of pure MeOH. For the negative control a growth inhibition zone was never observed (**Figure 3.9**; hole (8)). The accuracy of each assay was assured by the use of a positive control. For this, ampicillin (1 mM) was applied.
All substances tested in the microbial growth inhibition assays are listed in **Table 3.4**. In preliminary tests, solutions with a concentration of 0.1 mM showed no growth inhibition. Therefore, only 10 mM solutions were used afterwards. Since the inhibition zones were not exactly circular, the diameter was measured from three different directions and averaged out.

Table 3.4: Tested substances in microbial growth inhibition assays with *E. coli* and *B. subtilis*. All compounds were dissolved in MeOH (c = 10 mM), except for ampicillin which was dissolved in water (c = 1 mM). The average diameters of the inhibition zones are given in cm (± SEM). "-" indicates no detected inhibition zone and "/" substance not tested.

	***E. coli* BW25113**	***B. subtilis* DSM10**
(*R*)-harmonine ((*R*)-5)	2.2 ± 0.09	2.6 ± 0.10
(*S*)-harmonine ((*S*)-5)	2.2 ± 0.10	2.6 ± 0.10
***rac*-harmonine (*rac*-5)**	2.2 ± 0.11	2.6 ± 0.10
***rac*-isopropyl ester *rac*-34**	-	/
(*S*)-diol (*S*)-41	-	/
***rac*-diol *rac*-41**	-	-
***rac*-diazide *rac*-42**	-	-
OH-analog *rac*-48	0.8 ± 0.05	1.4 ± 0.05
C_{17}-harmonine *rac*-58	2.1 ± 0.05	2.8 ± 0
ampicillin (positive control)	1.4 ± 0.05	1.3 ± 0.05

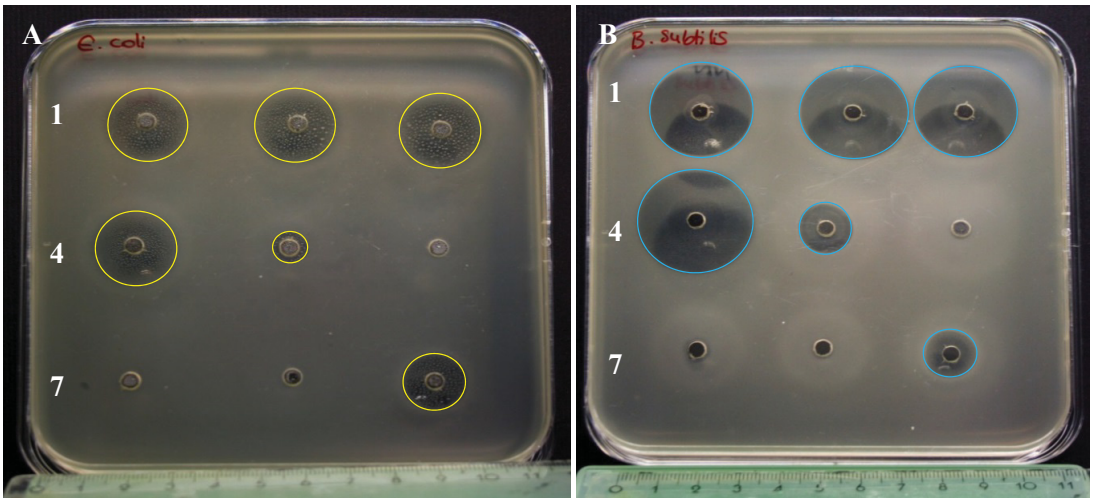

Figure 3.9: Microbial growth inhibition assays on LB-agar. Used substances and conditions: (1) *rac*-**5**; (2) (*R*)-**5**; (3) (*S*)-**5**; (4) *rac*-**58**; (5) *rac*-**48**; (6) *rac*-**42**; (7) *rac*-**41**; (8) MeOH (negative control); (9) ampicillin (positive control); Test substances: 10 mM in MeOH; ampicillin: 1 mM in H_2O; **A**) *E. coli*; **B**) *B. subtilis*.

After the application of the test substances the plates were incubated for 24 hours at 37 °C and then the diameter of the growth inhibition zones was determined (**Table 3.4**). The applied *rac*-isopropyl ester *rac*-**34** as well as (*S*)-diol (*S*)-**41**, *rac*-diol *rac*-**41**, and *rac*-diazide *rac*-**42** showed no growth inhibitory effect at all. Interestingly, the growth inhibition zones of both harmonine (**5**) enantiomers and of the racemic harmonine (*rac*-**5**) had the exact same size in the *E. coli* growth inhibition assay (**Figure 3.9 A**). In the assay using *B. subtilis* the diameters of the inhibition zones caused by the harmonine (**5**) enantiomers and the racemate were also identical (**Figure 3.9 B**). This fact reveals that the antibacterial activity of harmonine (**5**) is not dependent on the orientation of the amino group at C-17. The inhibition zone induced by the OH-analog *rac*-**48** was distinctly smaller in both bacterial assays, indicating that the antibacterial properties of *rac*-**48** are not as pronounced as the antibacterial properties of harmonine (**5**). An inhibiting effect by C_{17}-harmonine *rac*-**58** could also be observed. The inhibition zone measured for *E. coli* had nearly the same size as the ones for the harmonine (**5**) enantiomers. With *B. subtilis* only a slightly larger inhibition zone could be measured. Consequently, the observed antibacterial activity of *rac*-**58** is comparable to the activity of harmonine (**5**).

The diameters of the growth inhibition zones were measured again after another incubation at 37 °C for 24 hours and showed the same size as previously determined.

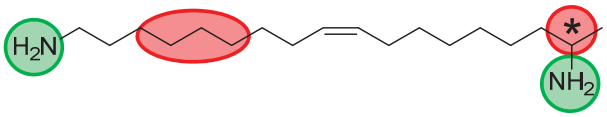

Figure 3.10: Graphical summary of the structural features moderating growth inhibition of *E. coli* and *B. subtilis*. “red”: changes show no effect on growth inhibition; “green”: changes effect growth inhibition.

All in all the structural dependency of the microbial growth inhibition can be summarized as shown in **Figure 3.10**. While chain length and stereochemistry do not matter when it comes to bacterial growth inhibition, the functional groups are of great importance. Substitution of one amino group through an alcohol function reduces the biological activity drastically. The replacement of both amino functions leads to a complete loss of inhibitory activity.
These observations suggest that the microbial growth inhibitory activity of harmonine (**5**) and its derivatives is a more general effect on the used bacteria.

A stronger response of *B. subtilis* to the harmonine enantiomers (**5**), the racemate *rac*-**5** as well as to *rac*-**48** and *rac*-**58** was noticed in this assay. This effect could generally arise from a greater susceptibility of Gram-positive bacteria – like *B. subtilis* – to the growth inhibitory and also killing effects of most antibacterial agents resulting at least partly from the absence of a protecttive outer membrane.[127]

3.3.2 Studies for the Determination of AChE-Inhibitory Activity

Alam *et al*.[28] reported 47% inhibition of the enzyme acetylcholinesterase (AChE) through a 40 μg ml^{-1} (*R*)-harmonine ((*R*)-**5**) solution. Although they did not provide further information about the used solvent, the origin of the enzyme or the general assay procedure, this observation represented a good starting point for the development of a new structure-activity relationship assay system.
Consequently, the biological activity of (*R*)-harmonine ((*R*)-**5**) as well as the properties of the synthesized enantiomer (*S*)-**5** and the derivatives were evaluated using AChE. This vital enzyme plays an important role in the transmission of action potentials across the synaptic cleft. It is responsible for the hydrolysis of the neurotransmitter ACh and thereby the termination of the current synaptic transmission.[68] A malfunction of ACh release or uptake can lead to severe diseases like dementia or the Alzheimer's disease. Through the development of AChE inhibiting drugs the course of the disease should be stopped or slowed down drastically.

With this assay the inhibitory properties of (*R*)-harmonine ((*R*)-**5**) were further qualified, the IC_{50} values of all synthesized compounds were established and new insights into the structure dependent activity of harmonine-like molecules were obtained.

For the determination of the IC_{50} values of the synthetic compounds a colorimetric AChE assay kit (AAT Bioquest Inc.) was used. This kit contains AChE isolated from the electric organ of *Electrophorus electricus* and was primarily developed to detect the presence of AChE in tissue or blood samples. However, through some modifications of the protocol this kit could be conveniently used to determine the inhibitory activity of the synthesized substances (detailed method described in chapter 6.5.2).

The quantification of AChE activity is based on Ellman's method (**Scheme 3.10**): In principal the AChE mediated hydrolysis of acetylthiocholine (**59**) is measured by the reaction of the product thiocholine (**60**) with the DTNB ion **61**. The resulting 5-thio-2-nitro-benzoate ion (**63**) displays a bright yellow color. This last reaction step is thereby sufficiently rapid to not be rate limiting. The absorption intensity of **63** can be measured with a photometer and is proportional to the formation of thiocholine (**60**), thus AChE activity.[128]

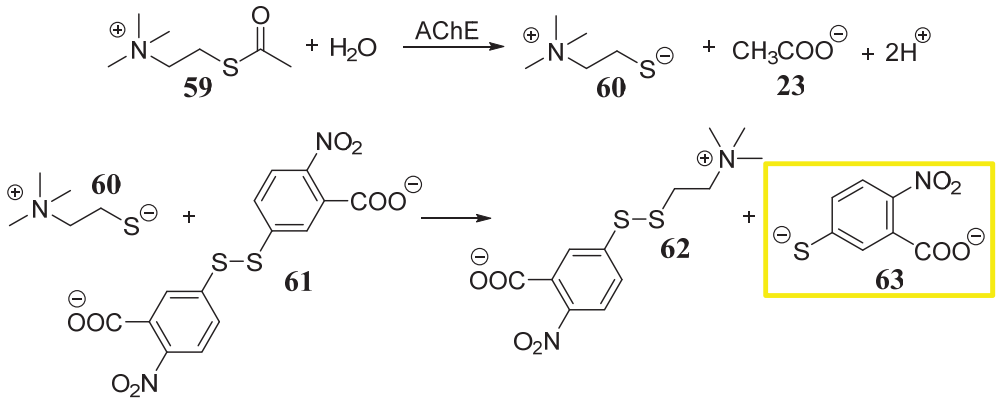

Scheme 3.10: Reaction mechanism proposed for Ellman's method.[128]

The AChE inhibition assays were conducted as descried in chapter 6.5.2. To introduce the synthesized substances into the assay system small amounts of MeOH had to be used. Since the aqueous assay buffer had a pH of 7.4 (manufacturer's information) some test substances could not be sufficiently dissolved. The introduction of MeOH had only minor effects on the enzyme. The longevity of AChE was shortened, which had no impact on the conducted assays since only the enzymatic reaction speed within the linear range (0 - 20 min) was needed for IC_{50} determination. The overall enzyme activity was only slightly reduced through the presence of MeOH and was effectively compensated by MeOH addition to positive control and blanks, too.

To determine the IC_{50} value of (*R*)-harmonine ((*R*)-**5**) preliminary tests were conducted, that involved the use of methanolic (*R*)-harmonine ((*R*)-**5**) solutions of a broad range of different concertations. This range was necessary to ensure complete inhibition as well as no inhibition of AChE. Based on these results a preliminary IC_{50} value could be calculated as described by Järvinen *et al*.[129]

The actual assay concentrations of (*R*)-harmonine ((*R*)-**5**) were then developed in accordance to the preliminary IC_{50} value to obtain accurate results. A graph containing the photometrically measured absorbance changes per minute plotted against the logarithmic concentrations of (*R*)-harmonine ((*R*)-**5**) allowed the determination of the IC_{50} value (**Fig. 3.11**).

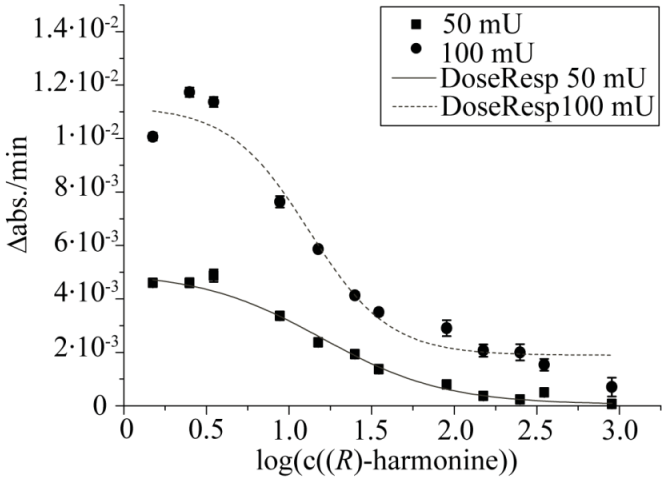

Figure 3.11: Concentration-dependency curve of (*R*)-harmonine (*R*)-**5** with sigmoidal dose-response fitting (variable slope, n = 3, ± SEM). Concentration of (*R*)-**5**: µM.

The obtained IC_{50} value of (*R*)-harmonine ((*R*)-**5**) as well as the IC_{50} values of the other test substances are listed in **Table 3.5**. The graphs can be found in **Appendix A.8**.

All IC_{50} values were determined for an enzyme concentration of 100 mU and of 50 mU to add a further control. Under ideal assay conditions the IC_{50} values obtained for both enzyme concentrations should be identical. This requirement was fairly fulfilled.

Table 3.5: Determined IC_{50}-values for two different AChE concentrations. "-." indicates no inhibition.

	IC_{50} [µM]	
	50 mU	**100 mU**
(*R*)-harmonine ((*R*)-5)	14.6 ± 1.10	12.8 ± 1.12
(*S*)-harmonine ((*S*)-5)	22.6 ± 1.11	27.7 ± 1.10
***rac*-harmonine (*rac*-5)**	30.6 ± 1.21	36.1 ± 1.21
OH-analog *rac*-48	"245.8 ± 3.77" [a]	56.5 ± 1.18 [a]
***rac*-diol *rac*-41**	-[a]	-[a]
C_{17}-harmonine *rac*-58	61.4 ± 1.23	73.3 ± 1.16

[a] These values could not be precisely determined because of solubility problems at higher concentrations.

The determined IC_{50} values of (*R*)-, (*S*)-, and *rac*-harmonine (**5**) were in a similar range and showed no considerable difference. This was an interesting result since most enzymes are highly specialized and changes in stereochemistry of substrates/inhibitors should alter the existing interactions and thereby the activity/IC_{50} values drastically. For AChE it was proven that a change of the stereochemistry of inhibiting phosphotriesters[130] or chemical warfare nerve agents[131] evokes different inhibition or inactivation rates.

Since the stereochemistry of harmonine (**5**) does apparently not matter for AChE inhibition, it is reasonable to suggest that the interactions between harmonine (**5**) and AChE do not involve binding to the active center or specific binding pockets but are more to the peripheral parts of the enzyme. At these parts, the interactions might be less conserved and stereochemical changes of the inhibitor do probably not evoke different reactions of the enzyme. In this case, the inhibitory activity of harmonine (**5**) could arise from a simple blockage of the active center. Since the active center is situated in a narrow and deep gorge (chapter 1.2.1, **Fig. 1.4 B**) an inhibitor blocking the entrance of this gorge or slightly changing the conformation of the enzyme could stop the catalytic reaction.

Furthermore, it is proposed that AChE can only function with such a high efficiency because there are alternative entrances (additional to the main door of the gorge) leading to the active site. These doors allow the passage of water and small ions and would therefore smoothen the overall reaction procedure and the entering of reactants. For these doors a gating mechanism is described which is explained as a temporary side chain movement of specific amino acid

residues.[132] A binding of harmonine (**5**) could therefore also block one of the amino acids responsible for gate opening/closing.

In general, harmonine (**5**) shows only moderate inhibition of AChE compared to other well-known inhibitors.[129]

The IC_{50} value of the racemic C_{17}-harmonine *rac*-**58** was determined to be slightly higher than the one for harmonine (**5**), however on a similar scale. This might suggest that the chain length of the carbon backbone is important but that the shortage of only one carbon atom is not enough to completely prevent interactions.

Unfortunately, the IC_{50} value of the OH-analog *rac*-**48** could only be approximated. The obtained concentration-dependency curve of *rac*-**48** is shown in **Figure 3.12** and the critical range is marked in gray.

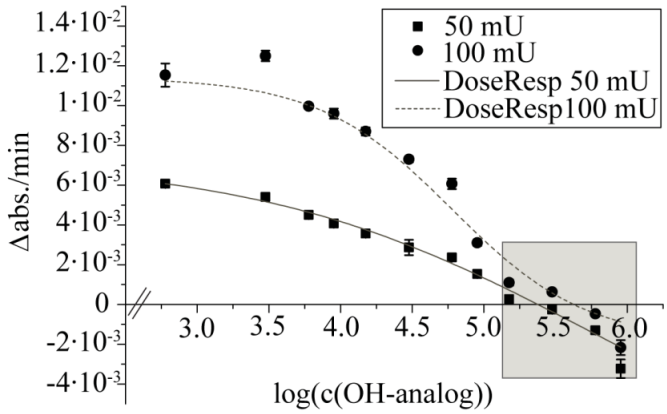

Figure 3.12: Complete concentration-dependency curve of OH-analog *rac*-**48** with sigmoidal dose-response fitting (variable slope, n = 3, ± SEM) (12 data points). Concentration of *rac*-**48**: nM.

The values in the grey rectangle were obtained for the highest used concentrations of *rac*-**48**. At these concentrations *rac*-**48** was not completely soluble under the assay conditions. Therefore, the initial absorbance was higher than usually. Over time *rac*-**48** started to dissolve and the absorbance decreased. This fact afforded a contrary effect to the assay during which the increase in absorbance was measured. Close to the point of complete inhibition of AChE, the obtained slopes of the absorbance increase were extremely small and were therefore covered by the decreasing absorbance due to solvation of *rac*-**48**. The measured absorbance appeared smaller than it actually was and "simulated" complete

inhibition. Especially with an enzyme concentration of 50 mU, which only gave small slopes, severe problems like the complete loss of the sigmoidal curve shape needed for calculation were encountered. The IC_{50} value obtained for this concentration is consequently not accurate. To get an approximate IC_{50} value of an enzyme concentration of 100 mU the highest concentration was left out of calculation (**Fig. A.8.4**; Appendix). The obtained value is, however, smaller than it would actually be and feigns thereby better inhibition.

The *rac*-diol *rac*-**41** showed already during the preliminary testing (high concentrations) absolutely no inhibition. The absorbance curve for this test is shown in **Figure 3.13**. For the diol *rac*-**41** even worse solubility was observed. In the obtained curves the solubility problems are mirrored in the high observed absorbance compared to the positive control.

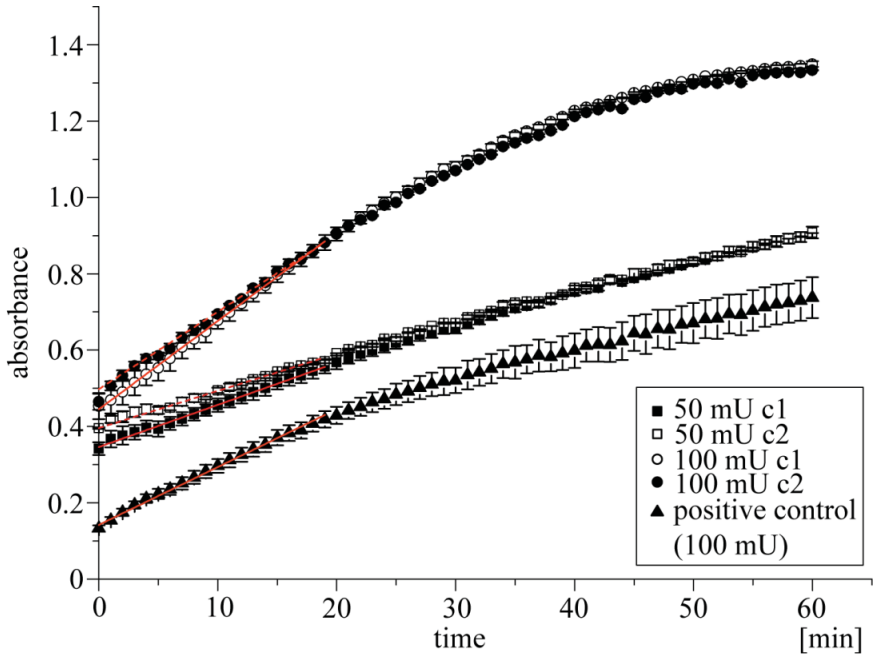

Figure 3.13: Absorbance curve of (9*Z*)-octadec-9-ene-1,17-diol (*rac*-**41**) with linear fitting (0 - 20 min; red line) and positive control (n = 3, ± SEM). In-well-concentrations of c1 = 6 10^{-3} µmol µl^{-1} and c2 = 2.8·10^{-3} µmol µl^{-1}. Positive control: 100 mU enzyme with 5 µl MeOH.

The structural dependency observed for AChE inhibition can be summarized as shown in **Figure 3.14**. The stereochemistry of harmonine (**5**) again does not seem to play an important role when it comes to AChE inhibition. However, replacement of the functional groups as well as a variation of the chain length affects the inhibitory activity.

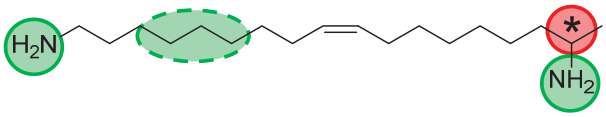

Figure 3.14: Graphical summary of the structural features influencing AChE inhibition. "red": changes do not alter activity; "green": changes effect activity.

Taken together these observations, the mechanism of AChE inhibition shows moderate selectivity (based on the lack of activity differences of the enantiomers of harmonine (**5**)).

3.3.3 Proof of Antileishmanial Activity

The synthesized compounds which proved to be the most active ones so far were also tested against the causative agent of cutaneous leishmaniasis – *L. major*. Annually around 800 000 – 1.3 million new infections of CL are estimated to occur.[133] The available chemotherapy is thereby not only limited but also accompanied by severe side effects. Resistances of the parasites against the available medication are also regularly reported.[134] With the ongoing search for new and safer drugs, naturally derived compounds are screened to identify and develop new antileishmaniasis treatments.
The activity of (*R*)-harmonine ((*R*)-**5**) against the malaria causing parasite *P. falciparum* was already reported[27] and prompted the evaluation of (*R*)-**5**'s activity against *L. major*.

Antileishmanial assays were kindly performed by Dr. Anita Masic and Martina Schultheis in the laboratories of the former research group of Dr. Uta Schurigt (Institute for Molecular Infection Biology, Würzburg).

At first the naturally occurring (*R*)-harmonine ((*R*)-**5**) was tested against the parasite. The AlamarBlue assay with *L. major* promastigotes and the Britelite assay with Luciferase-transgenic *L. major* amastigotes were performed (detailed in chapter 6.5.3). The IC_{50} value of (*R*)-**5** against *L. major* promastigotes was determined to be 14.2 µM and against *L. major* amastigotes 2.4 µM (**Table 3.6**). Miltefosine (**24**) – the current drug in use – exhibited IC_{50} values of 36.2 µM (promastigotes) and 33.0 µM (amastigotes).[135] In comparison to these values, (*R*)-harmonine ((*R*)-**5**) showed antileishmanial activity already at distinctly lower concentrations and thereby higher potency than **24**.

Table 3.6: Antileishmanial activity of (*R*)-harmonine ((*R*)-**5**) in comparison to the commonly used drug miltefosine (**24**). (Nagel *et al*.[55])

	IC_{50} [µM]			
	***L. major* promastigotes**	***L. major* amastigotes**	**BMDM**	**SI** [b]
(*R*)-harmonine ((*R*)-5) [a]	14.2	2.4	36.5	15.2
miltefosine (24)	36.2	33.0	65.5	2.0

[a] isolated from *H. axyridis*

[b] SI: IC_{50} for BMDM/IC_{50} for *L. major*

To examine the cytotoxic effect of (*R*)-**5** and **24** against host cells, bone marrow derived macrophages (BMDM) were used. The IC_{50} values against BMDM were determined to be 36.5 µM for (*R*)-**5** and 65.5 µM for **24**. The cytotoxicity of an antileishmanial drug against host cells divided through its antileishmanial efficacy is defined as selectivity index (SI). In general, SIs > 20 are considered to be magnificent.[136] In this assay, (*R*)-harmonine ((*R*)-**5**) demonstrates a very good SI = 15.2 towards *L. major* while miltefosine (**24**) shows only a SI of 2.0.

A further investigation of the antileishmanial effect of (*R*)-harmonine ((*R*)-**5**) was possible via transmission light microscopy. To determine the cell morphological changes of *L. major* promastigotes, they were treated with (*R*)-**5** for 6 h, 10 h, and 24 h (**Fig. 3.15**). Changes of the cell morphology were rapidly visible. After 6 h upon (*R*)-**5** treatment rounding of the cells was induced and after 10 h first dead cells were observed. After 24 h only dead cells were visible. In the DMSO treated control *L. major* promastigotes showed no significant changes. After 6 h and 10 h of cultivation, the characteristic flagellated parasite with its slender shape was observed (**Fig. 3.15**).

To study the type of cell death induced by (*R*)-harmonine ((*R*)-**5**) a flow cytometric approach was used. For this approach the different mechanisms of necrosis (unregulated cell death) and apoptosis (programmed cell death) were exploited. While during necrosis the membrane integrity is lost and DNA is exposed to the surrounding environment, apoptotic cells translocate phosphatidylserine (PS) to the outside of the cellular membrane. A double staining with Annexin V-fluorescein isothiocyanate (AV, binds PS) and propidium iodide (PI, binds DNA)[137] can therefore be used to differentiate all four possible *Leishmania* cell

death phenotypes: alive (AV−/PI−), early necrotic (AV−/PI+), early apoptotic cells (AV+/PI−), and late necrotic/late apoptotic (AV+/PI+).[137, 138]

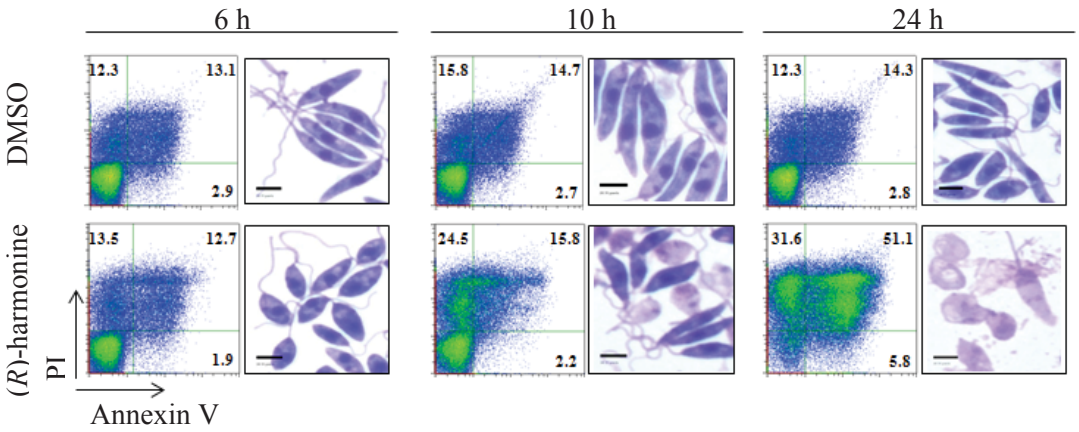

Figure 3.15: Observation of (*R*)-harmonine ((*R*)-**5**) induced cell death in *L. major* promastigotes. *L. major* promastigotes were treated with 1% DMSO (control) or 30 µM (*R*)-harmonine ((*R*)-**5**) solution for 6 h, 10 h, and 24 h. Double staining (Annexin V, PI) was performed to determine the cell death phenotype (dot-blots, left). Diff-Quick staining allowed investigation of cell morphological changes via transmission light microscopy (pictures, right). Scale bars: 10 µm. Number in quadrants: cells [%] showing early necrotic, late necrotic, or apoptotic cell death. (modified from Nagel *et al.*[55])

In general, cell death during treatment with (*R*)-**5** increased over time. In total, after 6 h 26.2% and after 10 h 40.3% of cells were dead (PI staining, **Fig. 3.15**). The successful PI-staining indicates binding to the DNA, loss of membrane integrity and thereby the early necrotic cell death type. After 10 h a population of 24.5% early necrotic cells was detected (**Fig. 3.15**). In the 24 h treatment, (*R*)-harmonine ((*R*)-**5**) induced early necrotic cell death in 31.6% and late necrotic/late apoptotic cell death in 51.1% of all treated cells. In total, 82.8% of cells were dead. Under normal growth conditions 73.4% of all cells were viable.

These results clearly indicate that (*R*)-harmonine ((*R*)-**5**) induces necrosis in *L.major* promastigotes. The increase of late necrotic/late apoptotic cells after 24 h results from the rupture of the cell membrane during necrosis. After loss of cell membrane integrity, AV can bind to PS of the dead parasites.

For structure-activity relationship studies more substances were tested against the promastigote form of the *Leishmania* parasite. The determined IC_{50} values are summarized in **Table 3.7**.

Table 3.7: Antileishmanial activity of (*R*)-, (*S*)-, *rac*-harmonine (**5**), and OH-analog *rac*-**48**.

	***L. major* promastigotes; IC_{50} [µM]**
(*R*)-harmonine ((*R*)-5)	8.6
(*S*)-harmonine ((*S*)-5)	9.1
***rac*-harmonine (*rac*-5)**	13.2
OH-analog *rac*-48	32.1

To evaluate the importance of the amino group orientation at the stereocenter, the two harmonine (**5**) enantiomers as well as the racemate *rac*-**5** were tested against *L. major* promastigotes using the AlamarBlue assay. The obtained IC_{50} values showed no considerable difference. All three IC_{50} values were below the determined IC_{50} value for miltefosine (**24**) (36.2 µM), which shows that even the racemic harmonine (*rac*-**5**) is more active *in vitro* than the current drug in use.
The IC_{50} value of the OH-analog *rac*-**48** was determined to be 32.1 µM. This means that *rac*-**48** is again less active than the harmonine enantiomers (**5**) but its activity against the promastigote form is still comparable to **24**.

In general, the pronounced activity of all enantiomers of harmonine (**5**) and the OH-analog *rac*-**48** against *L. major* was shown for the first time during the implementation of this thesis and is an encouraging result for antileishmanial drug development. The indifference of the stereochemistry is thereby especially interesting since complex or costly stereocontrol of chemical synthesis does not seem to be necessary to achieve antileishmanial activity.

When it comes to structure-activity relationship the general picture observed so far is again confirmed (**Fig. 3.16**). Interestingly, the stereochemistry does not play an important role when it comes to antileishmanial activity. An exchange of an amino group through a hydroxy group at the carbon backbone nevertheless reduces the activity slightly.

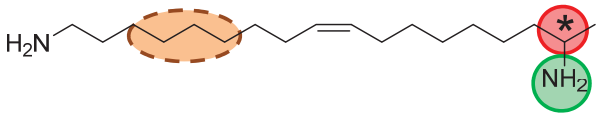

Figure 3.16: Graphical summary of the structural features moderating antiparasitic activity against *L. major*. "red": changes do not alter activity; "green": changes effect activity, "brown": effect not tested.

Unfortunately, the impact of the chain length of the carbon backbone could not be examined so far. The research group of the collaborators was closed before an assay with C_{17}-harmonine *rac*-**58** could be conducted. As perspective, this assay can hopefully be completed with the help of another research group working with the *L. major* parasites.

3.3.4 Modeling and Docking Studies

The search for a connection between the biological activities of the harmonine enantiomers (**5**) against AChE (chapter 3.3.2) and against the *Leishmania* parasite (chapter 3.3.3) was initiated following two key observations:

At first, the IC_{50} values of the harmonine enantiomers (**5**) as well as of the OH-analog *rac*-**48** were comparable in scale in both tested assay systems. Besides, a similar behavior to structural changes of the introduced inhibitors was visible.

The hypothesis that both activities are connected with each other was promoted by the proof of the presence of an AChE in *Trypanosoma evansi* by subcellular localization and confocal microscopy.[139] This protozoan parasite causes surra in animals but is not pathogenic to humans. The non-neuronal role of AChE in *T. evansi* respectively the Trypanosomatidae family is not yet completely understood. However, Mijares *et al*.[139] proposed that AChE is mostly located in the glycosome and that it is responsible for the regulation of the flow of Ca^{2+} between this organelle and the cytosol. Since the *Leishmania* parasites belong to the same family the presence of an AChE or a carboxylesterase with similar structure and function was assumed. Hereafter, the search for the "leishmanial AChE" as well as modeling and docking studies proving the inhibitory activity of the harmonine enantiomers (**5**) are presented.

3.3.4.1 Identification of "AChE-like proteins" in *L. major*

At first the "AChE-like proteins" in *L. major* had to be identified. Therefore, the protein sequence of a known AChE from the model organism *Caenorhabditis elegans* (NP_510660.1) was blasted against the protein sequence of *L. major*. The BLAST identified two possible candidates: a conserved hypothetical protein (XP_001681951.1) and a putative ecotin (XP_001681950.1). Both sequences showed relatively low identities and query covers. Interestingly, the identical parts of the sequences were at important and conserved sites of the AChE sequence. Most matches could be found from amino acid 129 - 228 (conserved hypothetical protein) or from amino acid 124 - 238 (putative ecotin). In this sequence region, amino acids which are part of the substrate binding pocket as well as the serine from the catalytic triad are located.

This fact suggested that even with substandard identities and query covers two good candidates were found. Since both candidates showed matches with the important, catalytic or substrate binding part of the AChE, they were both considered for docking studies.

3.3.4.2 Modeling of possible Candidates and Docking Studies

Modeling and docking studies of the two possible "leishmanial AChE" candidates were kindly performed by PD Dr. Wolfgang Brandt (Leibniz Institute of Plant Biochemistry, Halle). The exact approach is described in chapter 6.5.4.

For the putative ecotin (XP_001681950.1) no reasonable models could be created. For the conserved hypothetical protein (XP_001681951.1), however, an interesting model could be obtained (**Fig. 3.17**). This model was based on homology modeling. After search for templates in the protein database[140] and various refinement steps, a model resembling the template 1qz3 (**Fig. 6.3**, chapter 6.5.4) appeared as most fitting. Interestingly, this template can be complexed with hexadecanesulfonate which is structurally comparable to harmonine (**5**).

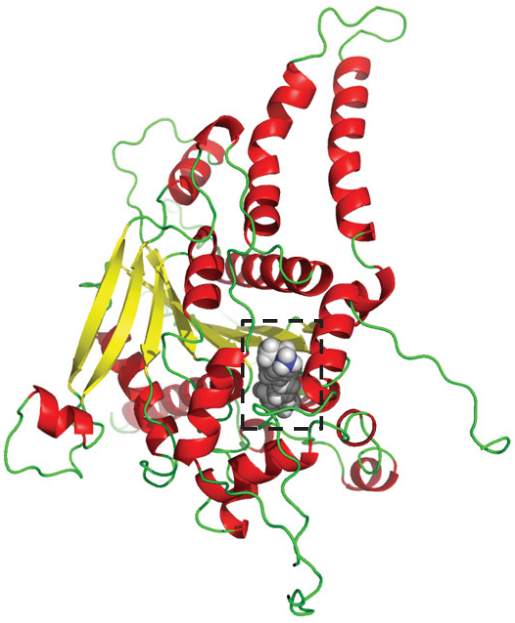

Figure 3.17: Model of the sequence XP_001681951.1 with bond harmonine. The amino groups interact with E406 (surface; no specificity of the chiral carbon) and with D739 (bottom, probably near the active site).

The model of the full sequence of the conserved hypothetical protein bound with harmonine (**5**) is shown in **Figure 3.17**. This model already suggests that harmonine (**5**) is bound to aspartate 739 at the bottom of the visible gorge of the protein and with this probably near the active site.

A more detailed view (**Fig. 3.18**) clearly shows that harmonine (**5**) is able to form two salt bridges (dashed lines) with aspartate 739 and glutamate 406. The glutamate residue is located near the surface of the protein and the amino group at the chiral center of **5** is probably interacting with it. Near the surface of the protein no space limitations can be found. Therefore, the stereochemistry of harmonine (**5**) is not important and the (*S*)- as well as the (*R*)-enantiomer of **5** are able to form a salt bridge with glutamate.

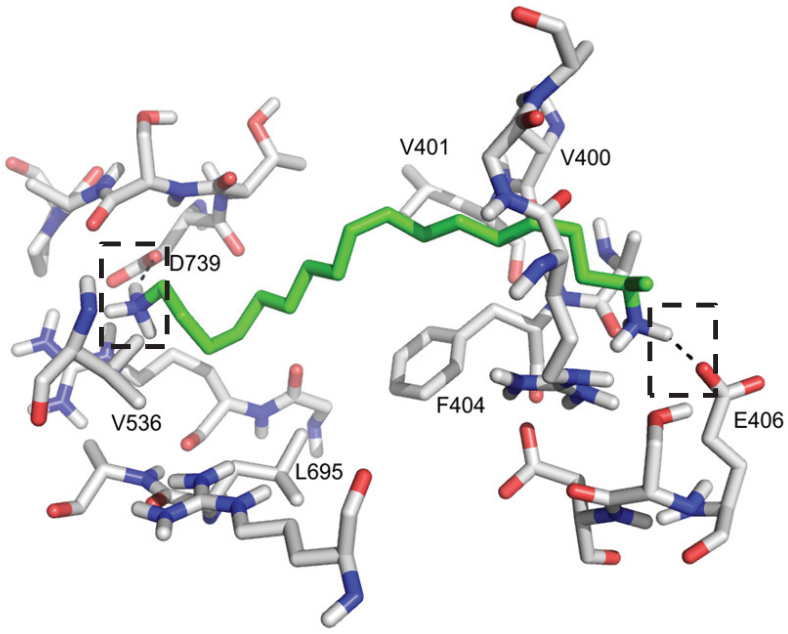

Figure 3.18: The most favored docking arrangement of harmonine (**5**) (interaction energy: -47.5 kcal mol^{-1}). Interactions based on the hydrophobic effect (F404, V400, V401, L695, V536) are identifiable. Furthermore, the ligand's length is ideal to form two salt bridges with E406 and D739.

The non-polar middle part of **5** is probably interacting with various non-polar amino acids such as leucine, valine, and phenylalanine. Obviously the length of the carbon backbone plays an important role for the observed interactions. Even though harmonine (**5**) is not

bound to the active center it fits perfectly into the gorge forming two salt bridges at either side.

This assumption was confirmed by the model of the conserved hypothetical protein bound to the short-chain C_{17}-harmonine *rac*-**58** (**Fig. 3.19** and **Fig. A.9.2, Appendix**). It is clearly visible that *rac*-**58** is too short to fit perfectly. With the C_{17}-backbone only one salt bridge can be formed - either with aspartate or with glutamate. The hydrophobic interactions were nevertheless present. In total, the shortage of one carbon atom reduced the calculated interaction energy from -47.5 kcal mol^{-1} with harmonine (**5**) to -40.1 kcal mol^{-1} (with D739) or -39.2 kcal mol^{-1} (with E406) with C_{17}-harmonine *rac*-**58**.

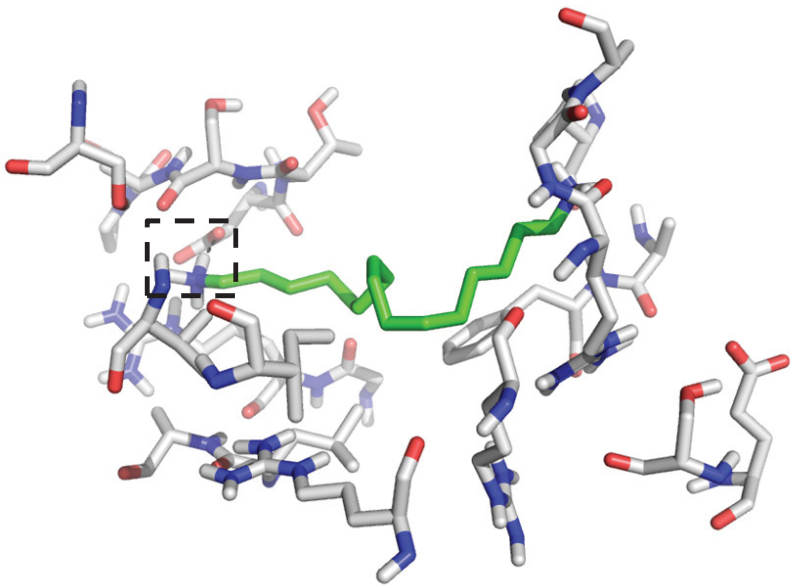

Figure 3.19: Favored docking arrangement of C_{17}-harmonine (*rac*-**58**) (interaction energy: -40.1 kcal mol^{-1}). Interactions based on the hydrophobic effect (F404, V400, V401, L695, V536) are present. However, the length of the ligand is too short to form two salt bridges but only one with D739.

Even though these modeling studies confirmed that harmonine (**5**) is not bound to the active center it was nicely shown that the interactions between **5** and this putative "leishmanial AChE" are strong, defined and near the active center. Therefore a possible blockage of the substrate on its way to the active center of the AChE and/or the enforced retention of the enzyme conformation are possible inhibition mechanisms (see also chapter 3.3.2).

The desired linkage between the observed AChE-inhibitory activity as well as the determined antileishmanial activity of harmonine (**5**) and its derivatives could be nicely established. With this model of the possible "leishmanial AChE" and the docking studies explaining perfectly the observed structure-activity relationship in both biological assay systems, the presence of an AChE or at least a carboxylesterase with structural similarity can be suggested in *L.major*. In the future, the C_{17}-harmonine *rac*-**58** can hopefully be tested against *L. major* to confirm these above discussed results.

4 Summary

The Asian lady beetle *Harmonia axyridis* gained enormous attention over the past years. This vivid, carnivorous beetle is natively distributed in the Asian range[31, 37] and shows a voracious feeding behavior of coccids, aphids and mites[39] which qualified *H. axyridis* as a suitable biological control agent. However, over time populations began to establish and already more than two decades ago *H. axyridis* became an invasive species threatening and decimating the native lady beetle populations wherever it occurred.[44, 50] The enormous invasive success derives from various factors: First of all, the cannibalistic Asian lady beetles act as aggressive inraguild predators dominating other lady beetle species.[10] Second, *H. axyridis* is less likely to be eaten by coccinellid predators[13] and is more resistant to pathogens[17]. This resistance most likely derives from harmonine ((*R*)-**5**), the defense compound of *H. axyridis*.
This long-chain, aliphatic alkaloid (*R*)-**5** is present in the hemolymph and displays a variety of interesting biological properties. For example, harmonine ((*R*)-**5**) is active against 12 different bacterial strains, against the yeast *Candida albicans* and against four fast-growing mycobacteria strains including *Mycobacterium tuberculosis*.[27] (*R*)-**5** demonstrates multi-stage antimalarial activity by inhibiting the growth of the protozoan parasite *P. falciparum*[27] and is also cytotoxic to five human tumor cell lines[28].
Although *H. axyridis* and harmonine ((*R*)-**5**) have been studied over the past years, many details and connections are not clarified yet. The main objective of this thesis was to contribute to the body of knowledge about this beetle and harmonine ((*R*)-**5**) in particular by analytical, chemical and biological means.

Analysis of *H. axyridis*' hemolymph (chapter 3.1)
To study the hemolymph composition of *H. axyridis* a beetle rearing was established starting from field collected specimens. The beetles were kept on two different food sources (moth eggs (*Sitotroga*) or pea aphids (*A. pisum*)) to examine their effect on the hemolymph composition. After hemolymph collection, the samples were derivatized using MBTFA and analyzed via GC-MS. The GC-MS technique was chosen because it is a fast, reproducible, and very sensitive method to separate and detect even minor compounds. In the hemolymph samples were, however, only very few compounds detected. In general, the hemolymph composition of both feed groups was comparable and showed no considerable differences. Harmonine ((*R*)-**5**) was the major component in both feed groups. Besides (*R*)-**5**, contaminants from the cuticula were identified as well as one minor component present in only

4 ‰ compared to (*R*)-**5**. This minor component showed a similar fragmentation pattern as (*R*)-**5** along with a 2 amu difference in molecular mass and was consequently identified as dehydro-harmonine **26** with one additional double bond. To elucidate the structure of the previously unknown hemolymph compound **26** the AcN-CI-MS/MS technique was applied. This technique exploits acetonitrile as reagent gas and allows the localization of double bonds especially in fatty acid methyl esters. Since **26** is too symmetric for this technique, the position of the double bond could not be unambiguously assigned, however, a $\Delta^{9,12}$-dehydro-harmonine structure is assumed. To confirm the structure, a synthesis of **26** and a comparison of the natural and the synthetic compound would be the next step.

Synthesis of *rac*-, (*R*)-, and (*S*)-harmonine (5), OH-analog *rac*-48 and the short chain derivative C_{17}-harmonine *rac*-58 (chapter 3.2)

Since harmonine ((*R*)-**5**) displays a lot of interesting biological activities, a constant demand for synthetic material can be observed. However, at the beginning of this thesis only one lengthy synthesis[53] was known to provide synthetic (*R*)-**5**. Within this work, a short and efficient synthetic method was developed to obtain the natural (*R*)-harmonine ((*R*)-**5**) as well as the racemic form *rac*-**5** and the previously undescribed non-natural enantiomer (*S*)-harmonine (*ent*-(*S*)-**5**). Based on a "Wittig-type one-pot" reaction as key step a flexible approach was designed to allow the synthesis of a whole spectrum of compounds starting from commercially available cyclooctanone (**39**) and ω-bromononanoic acid (**37**).

Cyclooctanone (**39**) was easily converted into the racemic lactone *rac*-**36** and the bromo acid **37** into the corresponding Wittig salt **35**. The "Wittig-type one-pot" reaction of both compounds yielded the carbon skeleton of harmonine (**5**) with high *Z*-selectivity ($Z/E \geq 98/2$). Through subsequent functional group modifications, harmonine (*rac*-**5**) was readily available. To obtain both harmonine enantiomers (**5**), horse liver esterase was used for enantioselective, enzymatic saponification of the lactone *rac*-**36**. This yielded the (*S*)-lactone (*S*)-**36** and the (*R*)-hydroxy acid (*R*)-**49** with excellent *ee* ((*S*)-**36**: $ee \geq 99.5\%$, (*R*)-**49**: $ee \geq 99\%$) and good yields. The optically pure precursors were then used to synthesize the natural harmonine ((*R*)-**5**) and the (*S*)-harmonine (*ent*-(*S*)-**5**).

This flexible synthetic protocol was subsequently altered to gain access to the possible biosynthetic intermediate, the OH-analog *rac*-**48**, as well as to the short chain derivative C_{17}-harmonine *rac*-**58**. Both substances were designed to provide insights into structure-activity relationships. The synthetic strategy is shown in **Scheme 4.1**.

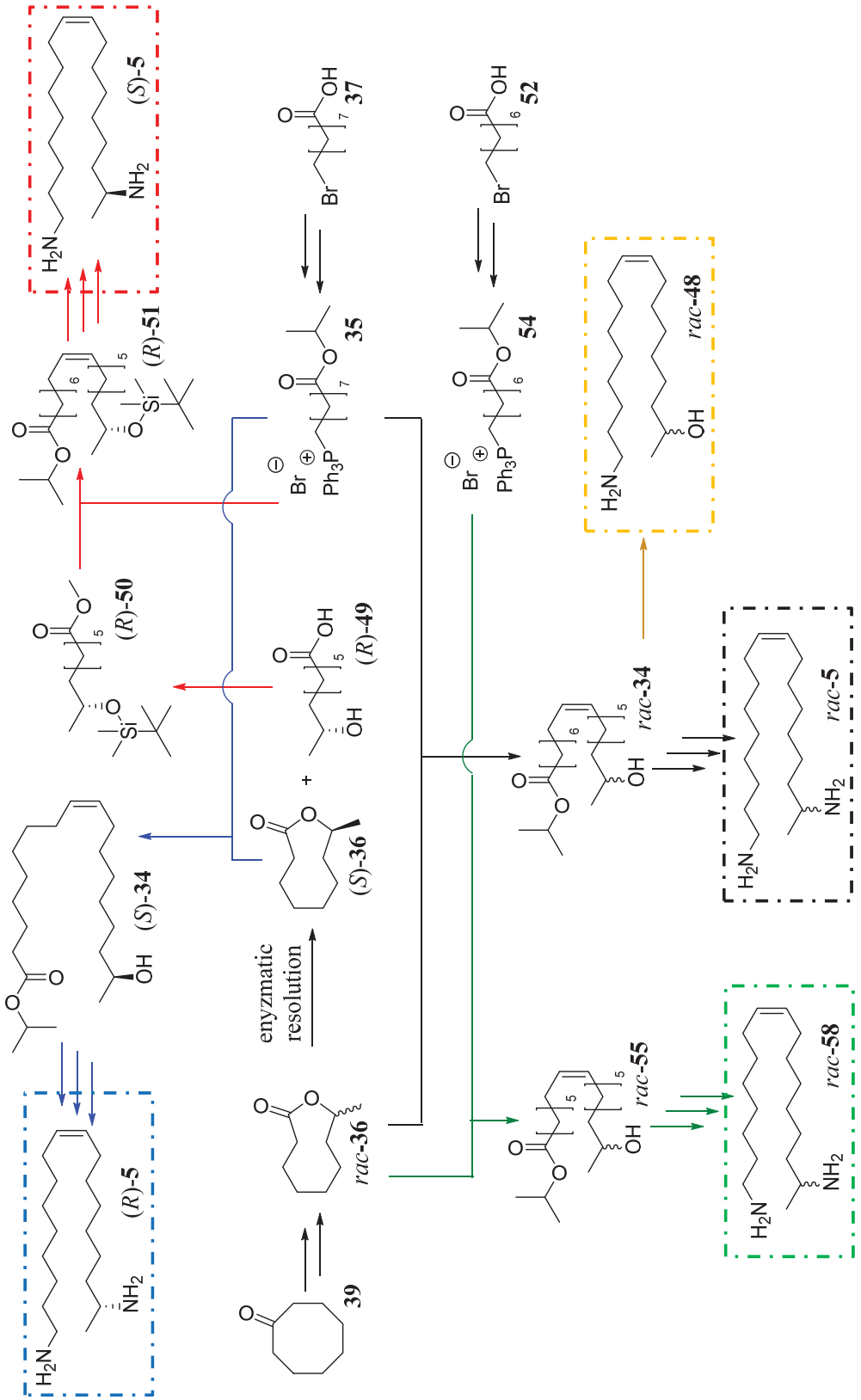

Scheme 4.1: Schematic representation of the synthetic protocol used to generate the harmonine enantiomers (**5**) as well as the OH-analog *rac*-**48** and C_{17}-harmonine *rac*-**58**.

Bioactivity and structure-activity relationship studies of the synthesized compounds (chapter 3.3)

The previously synthesized compounds were used to determine the biological activities of harmonine (**5**) as well as to study structure-activity relationships. At first, microbial growth inhibition assays with the Gram-negative bacterium *E. coli* and the Gram-positive bacterium *B. subtilis* were conducted. These assays confirmed an antibacterial activity of both harmonine enantiomers (**5**) and showed that C_{17}-harmonine *rac*-**58** is equally active. The OH-analog *rac*-**48** showed a lower antibacterial activity. In terms of structure-activity relationships, this assay led to the conclusion that neither the stereochemistry of the amino group at C-17 of harmonine (**5**) nor the chain length of the carbon backbone is important for the antibacterial activity. The replacement of the amino groups through one or two alcohol functions reduces the activity drastically.

Next, the acetylcholinesterase (AChE) inhibitory activity of the synthesized compounds was evaluated. In general, both harmonine enantiomers (**5**) showed the same, moderate AChE inhibitory activity. The C_{17}-harmonine *rac*-**58** showed a slightly reduced activity, but on the same scale. The inhibitory activity of *rac*-**48** could only be approximated due to solubility problems under the assay conditions but is, however, lower than the activities of **5** and *rac*-**58**. The inhibitory effect on AChE seems to be more specific than the antibacterial effect. Since the stereochemistry of the amino group is again not important, an interaction of the compounds with the periphery of the enzyme is assumed.

The most active compounds could also be tested against the *Leishmania* parasite *L. major* with the help of the research group of Dr. Uta Schurigt. During the accomplishment of this thesis the antileishmanial activity of (*R*)-harmonine ((*R*)-**5**) was demonstrated for the first time. The determined IC_{50} value was considerably lower than the one obtained for miltefosine (**24**), the current drug in use. Again, both harmonine enantiomers (**5**) showed the same activity and *rac*-**48** was slightly less active.

Due to the discovery of non-neuronal AChEs in the Trypanosomatidae family[139] the possibility of a “leishmanial AChE” was examined. Candidates were selected using BLAST and subsequently modeled with the help of PD Dr. Wolfgang Brandt. Docking studies with the obtained model confirmed that harmonine (**5**) binds close to the active center of the possible “leishmanial AChE” with the amino group at C-17 in the periphery of the enzyme nicely explaining the observed structure-activity relationships.

In conclusion, an efficient synthesis of the harmonine enantiomers (**5**) was developed and, inter alia, their antileishmanial activity was proven for the first time.

5 Zusammenfassung

Der asiatische Marienkäfer *Harmonia axyridis* hat im Laufe der letzten Jahre enorme Aufmerksamkeit auf sich gezogen. Dieser karnivore Käfer ist im asiatischen Raum beheimatet[31, 37] und vertilgt große Mengen an Blattläusen, Schildläusen und Milben.[39] Dies führte zu seinem großflächigen Einsatz in der biologischen Schädlingsbekämpfung. Mit der Zeit siedelten sich allerdings erste *H. axyridis* Populationen an, welche bereits vor 20 Jahren begannen invasiv zu werden und sich weltweit zu verbreiten.[44, 50] Für die einheimischen Marienkäferarten stellt *H.axyridis* dabei eine große Bedrohung dar, da er deren Bestände beträchtlich dezimiert.[44, 50] Der außergewöhnliche, invasive Erfolg von *H. axyridis* ist auf mehrere Faktoren zurückzuführen: Zunächst dominiert der kannibalische asiatische Marienkäfer trophische Wechselwirkungen mit natürlichen Gegenspielern (*intraguild predator*).[10] Weiterhin wird *H. axyridis* seltener von Fressfeinden attakiert[13] und ist resistenter gegenüber Krankheitserregern[17]. Diese Resistenzen lassen sich auf Harmonin ((*R*)-**5**), die sich in der Hämolymphe befindliche Abwehrsubstanz von *H. axyridis* zurückführen.

Das langkettige, aliphatische Alkaloid (*R*)-**5** weist eine Vielzahl interessanter biologischer Eigenschaften auf. So ist Harmonin ((*R*)-**5**) unter anderem wirksam gegen 12 verschiedene Bakterienstämme, zeigt Aktivität gegen *Candida albicans* und vier Mykobakterien Stämme; *Mycobacterium tuberculosis* eingeschlossen.[27] Des Weiteren inhibiert (*R*)-**5** auch das Wachstum des Parasiten *P. falciparum* und demonstriert damit anti-Malaria Aktivität.[27] Gegen fünf humane Krebszelllinien erweist sich Harmonine ((*R*)-**5**) als zytotoxisch.[28]

Obwohl *H. axyridis* und Harmonin ((*R*)-**5**) in den letzten Jahren mehrfach untersucht wurden, sind immer noch viele Zusammenhänge ungeklärt. Das Hauptaugenmerk dieser Dissertation lag deshalb darauf, den gegenwärtigen Wissensfundus über Harmonin ((*R*)-**5**) mittels analytischer, chemischer und biologischer Methoden zu erweitern.

Analyse der Hämolymphe von *H. axyridis* (Kapitel 3.1)

Zunächst wurde die Zusammensetzung der Hämolymphe von *H. axyridis* untersucht. Dazu wurde eine verlässliche Käferzucht etabliert. Um einen möglichen Effekt der Futtermittel auf die Hämolymph-Zusammensetzung zu studieren, wurden die Käfer entweder auf Motteneiern (*Sitotroga*) oder auf Erbsenblattläusen (*A. pisum*) gehalten. Nach der Entnahme der Hämolymphe wurden die Proben mit MBTFA derivatisiert und mittels GC-MS analysiert um

schnelle und reproduzierbare Ergebnisse zu erhalten und selbst die Identifikation von Minderkomponenten zu ermöglichen. Im Allgemeinen konnten in der Hämolymphe nur wenige Verbindungen detektiert werden und die Zusammensetzungen beider Fütterungsgruppen war annähernd identisch. Harmonin ((*R*)-**5**) war in beiden Proben die Hauptkomponente. Neben (*R*)-**5** wurden noch Verunreinigungen von der Cuticula sowie eine der wenigen Minderkomponenten (4 ‰ verglichen mit (*R*)-**5**) identifiziert. Diese zeigte im MS Spektrum ein dem Harmonin ((*R*)-**5**) ähnliches Fragmentierungsmuster sowie eine geringe Massendifferenz der größeren Fragmentionen von 2 *amu*. Um die Struktur dieser als Dehydro-Harmonin **26** bestimmten Hämolymph-Verbindung aufzuklären wurde die AcN-CI-MS/MS Technik angewendet, welche Acetonitril als Reaktandgas verwendet und die Lokalisierung von Doppelbindungen – vor allem in Fettsäuremethylestern – ermöglicht. Die symmetrische Struktur von **26** erlaubte allerdings keine exakte Bestimmung der Lage der Doppelbindung. Man kann jedoch davon ausgehen dass es sich um eine $\Delta^{9,12}$-Dehydro-Harmonin-Struktur handelt. Zur Bestätigung der Struktur von **26** ist eine Synthese unabdingbar.

Synthese von *rac*-, (*R*)-, und (*S*)-Harmonin (5), OH-Analogon *rac*-48 und dem kurzkettigen Derivat C_{17}-Harmonin *rac*-58 (Kapitel 3.2)

Da Harmonin ((*R*)-**5**) viele interessante biologische Aktivitäten aufweist, besteht eine konstante Nachfrage nach synthetischem Material. Zu Beginn dieser Dissertation gab es allerdings nur eine aufwändige und teure Synthese,[53] die diesem Bedürfnis nicht vollständig nachkommen konnte.

Im Rahmen dieser Arbeit wurde eine kurze und effektive Synthese entwickelt um das natürlich vorkommende (*R*)-Harmonin ((*R*)-**5**) sowie die racemische Form *rac*-**5** und das bislang noch nicht dargestellte unnatürliche Enantiomer (*S*)-Harmonin (*ent*-(*S*)-**5**) zu erhalten. Basierend auf einer „Wittig-ähnlichen One-Pot“ Reaktion wurde eine flexible Synthese ausgearbeitet, die die Herstellung eines ganzen Substanzspektrums ausgehend von kommerziell erhältlichem Cyclooctanon (**39**) und ω-Bromnonansäure (**37**) ermöglichte.

Zunächst wurde aus Cyclooctanon (**39**) das racemische Lacton *rac*-**36** und aus der Bromnonansäure **37** das korrespondierende Wittig-Salz **35** hergestellt. Die „Wittig-ähnliche One-Pot“ Reaktion beider Verbindungen ergab das Kohlenstoffgerüst des Harmonins (**5**). Die Doppelbindung wurde dabei mit hoher *Z*-Selektivität dargestellt ($Z/E \geq 98/2$). Durch nachfolgende Modifikationen der funktionellen Gruppen konnte Harmonin *rac*-**5** einfach erhalten werden.

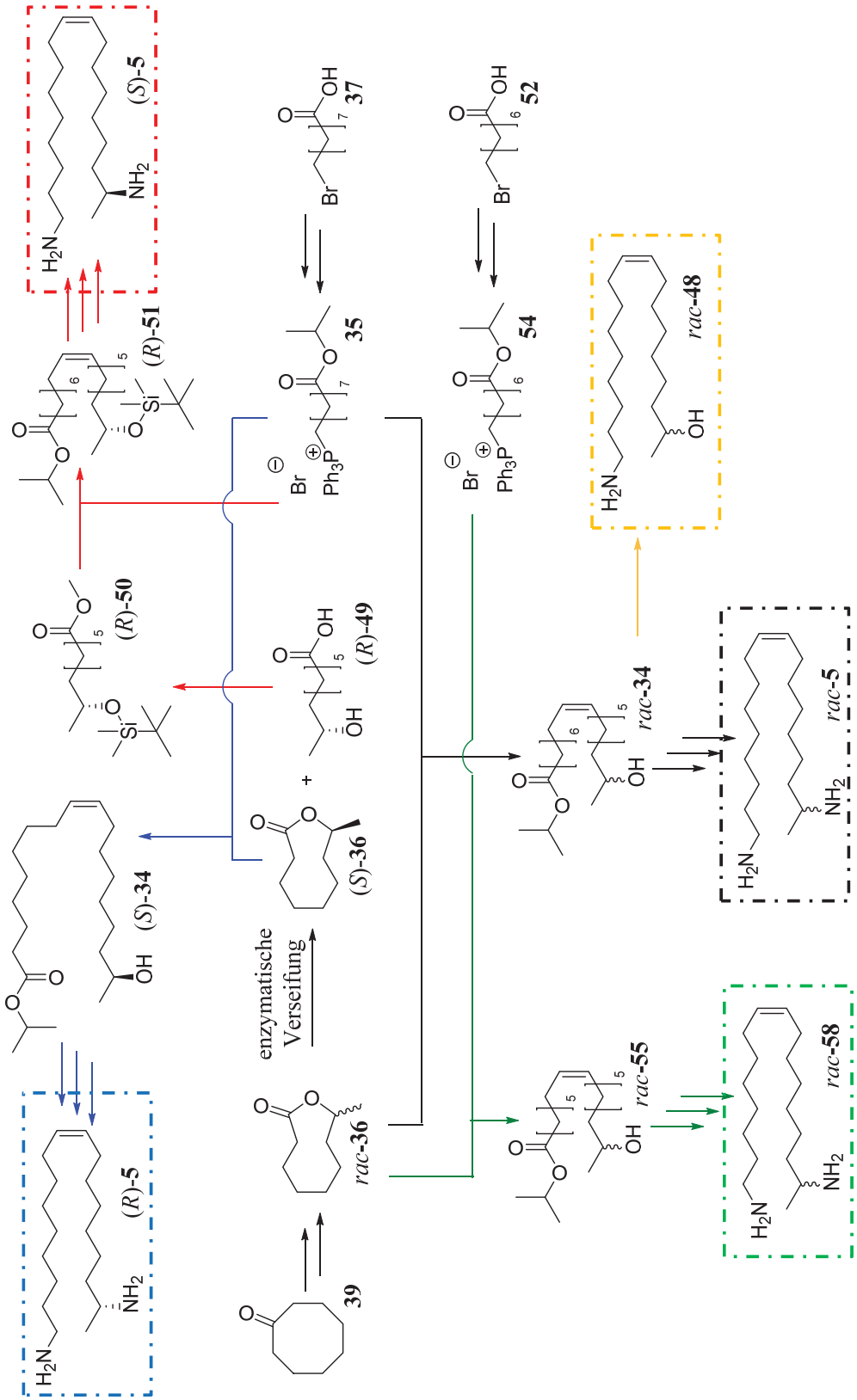

Schema 5.1: Schematische Darstellung des Syntheseprotokolls zur Gewinnung der Harmonin Enantiomere (**5**), sowie des OH-Analogons *rac*-**48** und des C_{17}-Harmonins *rac*-**58**.

Um beide Harmonin Enantiomere (**5**) zu erhalten wurde Pferdeleberesterase zur enantioselektiven Verseifung des Lactons *rac*-**36** eingesetzt. Diese ergab das (*S*)-Lacton (*S*)-**36** und die (*R*)-Hydroxysäure (*R*)-**49** in guten Ausbeuten und mit exzellentem Enantiomerenüberschuß ((*S*)-**36**: *ee* ≥ 99.5%, (*R*)-**49**: *ee* ≥ 99%). Die optisch reinen Ausgangsstoffe wurden anschließend zur Synthese des natürlichen Harmonins ((*R*)-**5**) und des (*S*)-Harmonins (*ent*-(*S*)-**5**) eingesetzt.

Das flexible Syntheseprotokoll konnte einfach modifiziert werden um eine mögliche, biosynthetische Zwischenstufe (OH-Analogon *rac*-**48**) sowie ein kurzkettiges Harmonin-Derivat (C_{17}-Harmonin *rac*-**58**) zu erhalten. Beide Substanzen wurden synthetisiert um Erkenntnisse über die Struktur-Wirkbeziehungen von Harmonin ((*R*)-**5**) zu erlangen. Eine Zusammenfassung der Synthesestrategie ist in **Schema 5.1** gezeigt.

Bioaktivitätsstudien und Struktur-Wirkbeziehungs-Studien der synthetisierten Verbindungen (Kapitel 3.3)

Die synthetisierten Verbindungen wurden nun zur Bestimmung der biologischen Aktivitäten des Harmonins (**5**) sowie zur Analyse von Struktur-Wirkbeziehungen eingesetzt. Zunächst wurden Hemmhoftests mit *E. coli* und *B. subtilis*, als Modelle für Gram-positive beziehungsweise Gram-negative Bakterienstämme, durchgeführt. Diese bestätigten die antibakterielle Wirkung der Harmonin Enantiomere (**5**) und zeigten, dass C_{17}-Harmonin *rac*-**58** ähnlich aktiv ist. Lediglich das OH-Analogon *rac*-**48** zeigte eine geringere Aktivtät. In Bezug auf die durchgeführten Hemmhoftests ist ersichtlich, dass weder die Stereochemie der Aminogruppe an C-17 des Harmonins (**5**) noch die Kettenlänge des Kohlenstoffgrundgerüsts Einfluss auf die antibakterielle Aktivität haben. Der Austausch einer oder beider Aminogruppen durch Alkoholfunktionen reduziert die Aktivität allerdings deutlich.

Weiterhin wurde die Acetylcholinesterase-hemmende (AChE) Wirkung der Verbindungen evaluiert. Im Allgemeinen zeigten die Harmonin Enantiomere (**5**) erneut die gleiche, moderate Aktivität. C_{17}-Harmonin *rac*-**58** wies eine ähnliche, allerdings leicht geringere Aktivität auf. Die inhibitorische Aktivität von *rac*-**48** konnte nur abgeschätzt werden, da sich dieses unter Assay-Bedingungen nicht vollständig löste. Sie war allerdings geringer als die ermittelten Aktivitäten für **5** und *rac*-**58**. Die AChE-inhibierende Wirkung des Harmonins (**5**) scheint spezifischer zu sein als sein antibakterieller Effekt. Da die Stereochemie der Aminogruppe an C-17 des Harmonins (**5**) allerdings nicht von Bedeutung ist, wird eine Interaktion der Verbindungen mit der Peripherie des Enzyms angenommen.

Die aktivsten Verbindungen konnten mit Hilfe der Forschungsgruppe von Frau Dr. Uta Schurigt ebenfalls auf ihre Wirkung gegen den Humanparasiten *L. major* getestet werden. Im Rahmen dieser Dissertation wurde zum ersten Mal die anti-Leishmaniose Wirkung von (*R*)-Harmonin ((*R*)-**5**) gezeigt. Der bestimmte IC_{50} Wert war dabei deutlich geringer als der ermittelte Wert des momentan verwendeten Medikaments Miltefosin (**24**). Beide Harmonin Enantiomere (**5**) waren gleich effektiv gegen *L. major*; *rac*-**48** wies eine geringere Aktivität auf.

Da in der Trypanosomatidae Familie nicht-neuronale AChEs nachgewiesen werden konnten,[139] wurde das Vorhandensein einer „*Leishmania*-AChE“ überprüft. Mögliche Kandidaten wurden mittels BLAST ermittelt und mit Hilfe von PD Dr. Wolfgang Brandt modelliert. *Docking* Studien mit dem erhaltenen Modell bestätigten, dass Harmonin (**5**) nahe des aktiven Zentrums der möglichen „*Leishmania*-AChE“ bindet, aber auch dass sich die Aminogruppe an C-17 in der Peripherie des Enzyms befindet. Dieses Ergebnis erklärt ausgezeichnet die beobachteten Struktur-Wirkbeziehungen sowohl in den AChE-Assays als auch in den Leishmanien-Assays.

Im Rahmen dieser Dissertation wurde somit eine effektive Synthese beider Harmonin Enantiomere (**5**) entwickelt und, unter anderem, deren anti-Leishmaniose Wirkung erstmals gezeigt.

6 Materials and Methods

6.1 General Information

The NMR spectra were recorded with a Bruker AV 400 spectrometer (Bruker, Rheinstetten/ Karlsruhe, Germany) operating at 400 MHz (^{1}H) or 100 MHz (^{13}C). All chemical shifts (δ) are reported in ppm and referenced to the residual solvent peak ($CDCl_3$: 7.27 (^{1}H), 77.0 (^{13}C)). For structural elucidation COSY, HSQC and HMBC spectra were used.
Infrared spectra (700 – 4000 cm^{-1}, resolution: 2 cm^{-1}) were recorded using a Bruker Equinox 55 FTIR spectrophotometer in transmission mode.
GC-MS analysis of synthesized compounds or of hemolymph samples were conducted with a Trace MS connected to a Trace GC 2000 Series (ThermoQuest, Austin, TX, USA) and an Alltech DB5 column (30 m × 0.25 m, 0.25 µm) with helium as carrier gas (1.5 ml min^{-1}) and EI (70 eV) for ionization. 1 µl of the sample was automatically injected with an A200SE (CTCAnalytics, Zwingen, Switzerland). The data were acquired using the software package Finnigan Xcalibur 2.07. The following methods were used:

Hemolymph Analysis:	50 °C (3 min) - 7.5 °C min^{-1} - 280 °C (4 min) - 10 °C min^{-1} - 300 °C (1 min), inlet T: 250 °C, split flow: 15 ml min^{-1}, split ratio: 10:1
Z/*E* Determination:	50 °C (2 min) - 1 °C min^{-1} - 280 °C - 30 °C min^{-1} - 300 °C (5 min), inlet T: 250 °C, split flow: 15 ml min^{-1}, split ratio: 10:1
Synthesis I:	60 °C (1 min) - 7 °C min^{-1} - 250 °C - 30 °C min^{-1} - 300 °C (2 min), inlet T: 250 °C, split flow: 20 ml min^{-1}, split ratio: 13:1
Synthesis II:	50 °C (2 min) - 10 °C min^{-1} - 280 °C - 30 °C min^{-1} - 300 °C (5 min), inlet T: 250 °C, split flow: 15 ml min^{-1}, split ratio: 10:1
Volatile Compounds:	45 °C (2 min) - 5 °C min^{-1} - 180 °C - 30 °C min^{-1} - 300 °C (2 min), inlet T: 250 °C, split flow: 15 ml min^{-1}, split ratio: 10:1

For the determination of the enantiomeric excess of chiral compounds an ITQ 900 (Thermo Fisher Scientific, Waltham, MA, USA) connected to a Trace GC Ultra (Thermo Fisher Scientific, Waltham, MA, USA) equipped with a Hydrodex-β-6TBDM column (25 m × 0.25 m) was used. Helium was used as carrier gas (1.0 ml min^{-1}) and EI (70 eV) for ionization. An

A200SE (CTCAnalytics, Zwingen, Switzerland) automatic sampler injected 1 µl of the sample. For data acquisition the software package Finnigan Xcalibur 2.07 was used.

ee Lactone: 100 °C (20 min) - 15 °C min^{-1} - 200 °C (2 min), inlet T: 200 °C, split flow: 10 ml min^{-1}, split ratio: 10:1

ee Hydroxy acid: 60 °C (5 min) - 0.1 °C min^{-1} - 120 °C (5 min) - 40 °C min^{-1} - 200 °C (3 min), inlet T: 200 °C, split flow: 10 ml min^{-1}, split ratio: 10:1

To detect molecular ions of synthetic compounds the same device was used in CI mode (CI gas: methane) equipped with a Restek RTX-200MS (30 m x 0.25 mm, 0.25 µm; Restek, Bad Homburg, Germany) column. Helium was used as carrier gas (1.0 ml min^{-1}).

CI positive: 50 °C (2 min) - 10 °C min^{-1} - 230 °C (2 min), inlet T: 240 °C, split flow: 14 ml min^{-1}, split ratio: 9:1

The HPLC-MS spectra were obtained using a Finnigan LTQ (Thermo Electron Company, Waltham, MA, USA) MS in APCI mode connected to a Purospher STAR RP 18 column (250 mm × 4 mm, 5 µm). Flow rate: 1 ml min^{-1}. Solvents: A: H_2O + 0.1% formic acid, B: AcN + 0.1% formic acid.

LC Method: 20% B (0 min - 5 min, isocratic) - 100% B (5 min - 36 min, gradient) - 100% B (36 min - 41 min, isocratic) - 20% B (41 min - 42 min, gradient) - 20% B (42 min - 50 min, isocratic)

HR-MS spectra were either recorded with a QExactive Plus MS (Thermo Fisher Scientific, Waltham, MA, USA)) running with a RP-18 column (150 mm × 2.1 mm, 120 Å) or through direct injection into the ESI source (capillary T = 275 °C) or with a Hewlett Packgard 6890 GC equipped with a Phenomenex ZB5HT column (30 m × 0.25 m, 0.25 µm) and linked to a Masspec MS02 (Mircomass, UK) (ionization: EI, 70 eV).

The optical rotation of enantiopure compounds was determined with a JASCO P1030 polarimeter at a specific wavelength of 589 nm (T = 22 - 24 °C).

For thin layer chromatography silica gel 60 F_{254} on aluminum sheets (Merck, Darmstadt, Germany) was used. The separated compounds were detected using Hanessian's stain, potassium permanganate stain or vanillin.

Preparative column chromatography was conducted with silica gel (40 - 63 µm, Macherey-Nagel, Düren, Germany) or Lichroprep RP-18 silica gel (40 - 63 µm, Merck, Darmstadt, Germany).

Solvents were purchased in HPLC grade and used without further purification. Except for diethyl ether, which was distilled prior to use. Anhydrous solvents were purchased as such. Horse liver esterase was obtained as lyophilized powder (0.5-1.0 U/mg, Sigma Aldrich, Schnelldorf, Germany).

H. axyridis larvae (third and fourth instar) were collected in spring in Jena, Germany or in Mitwitz, Germany. The larvae – and later beetles – were kept in *Gerda* boxes (20 cm × 20 cm × 9,5 cm, Westmark, Lennestadt-Elspe, Germany) equipped with a fine-meshed net for air circulation in a climate chamber (Vötsch Industrietechnik, Type VB 1014/S, Balingen, Germany). *Sitotroga* eggs (Katz Biotech AG, Baruth, Germany) or pea aphids (*A. pisum*) reared on bean plants (Broad Bean "The Sutton", Hazera Seeds UK Ltd., Rothwell, UK) in *rotho* boxes (23 cm × 22,5 cm × 27,5 cm, Rotho Kunststoff AG, Würenlingen, Switzerland) were used as feed.

Dissections were conducted with a StemiDV4 microscope (Carl Zeiss Lichtmikroskopie, Göttingen, Germany), spring steel tweezers and micro scissors. Hemolymph samples were dried using an eppendorf Concentrator*plus* (Eppendorf AG, Hamburg, Germany). The default derivatization reagent was *N*-methyl-bis(triflouroacetamide) (Sigma-Aldrich, St. Louis, MO, USA).

For microbial growth inhibition assays LB-agar (Lennox) and LB-medium (Lennox) (both Carl Roth GmbH + Co. KG, Karlsruhe, Germany) were used.

AChE inhibition assays were conducted in crystal-clear 96 well microplates (Greiner Bio-one GmbH, Kremsmünster, Austria). Amplite Colorimetric Acetylcholinesterase Assay Kit (AAT Bioquest Inc., Sunnydale, CA, USA) and a Spectra MAX 190 (Molecular Devices LLC., Sunnyvale, CA, USA) were used to determine the enzymatic activity. IC_{50} values were calculated using GraphPad Prism 5.04 software (nonlinear regression, log(inhibitor) vs. response – variable slope; Fitting method: least squares (ordinary) fit) and graphs were illustrated using Origin8.

6.2 Syntheses

Most of the following syntheses in chapter 6.2.1, 6.2.2 and 6.2.4 were already published in "Efficient synthesis of (*R*)-harmonine – the toxic principle of the multicolored Asian lady beetle (*Harmonia axyridis*)" (authors: Nagel, N. C. *et al*.)[55] and are subsequently cited thereof.

6.2.1 Synthesis of *rac*-Harmonine (*rac*-5)

6.2.1.1 Synthesis of 2-Methylcyclooctan-1-one (*rac*-38)

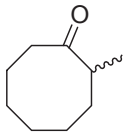
rac-**38**

Diisopropylamine (18.0 ml, 127.3 mmol) was dissolved in dry THF (230 ml) under argon atmosphere and cooled to 0 °C. *n*-BuLi (1.6 M in hexane, 86.6 ml, 138.6 mmol) was added dropwise and the reaction mixture was stirred at 0 °C for another 30 minutes before cyclooctanone (**39**) (15.9 g, 125.9 mmol) dissolved in dry THF (75 ml) was added. The solution was again stirred for 30 minutes, cooled to -78 °C and MeI (11.0 ml, 176.4 mmol) was added. After 15 minutes, the cooling bath was removed, the reaction mixture was allowed to warm to room temperature and stirred for 17 hours. Then it was poured into saturated NH_4Cl solution (150 ml) and extracted with Et_2O (150 ml). The phases were separated and the organic phase was first washed with saturated Na_2CO_3 solution (150 ml), HCl (1 M, 100 ml) and saturated $MgCl_2$ solution (150 ml) and then dried over $MgSO_4$. The solvent was removed under reduced pressure yielding the crude 2-methyl-cyclooctan-1-one (*rac*-**38**) which was used without further purification (17.1 g, 121.9 mmol, 97%).[111]

HRMS *m*/*z* calcd for $C_9H_{16}O$ 140.1199 $[M]^{+\cdot}$, found 140.1201
IR (thin film, cm^{-1}) *v* 2930 (s), 2858 (m), 1704 (s), 1448 (m), 1373 (m), 1242 (w), 1160 (w), 1122 (w), 1082 (w)
^{1}H NMR (400 MHZ, $CDCl_3$) δ 2.65 – 2.53 (m, 1 H, H-2), 2.43 – 2.33 (m, 2 H, H-8), 1.96 – 1.88 (m, 2 H, H-3a/H-7a), 1.80 – 1.71 (m, 1 H, H-7b), 1.70 – 1.56 (m, 2 H, H-3b/H-5a), 1.56 – 1.29 (m, 4 H, H-4a/H-5b/H-6), 1.26 – 1.13 (m, 1 H, H-4b), 1.02 (d, $^3J_{9,8}$ = 7.0 Hz, 3 H, H-1')

^{13}C NMR (100 MHz, $CDCl_3$) δ 220.3 (C-1), 45.2 (C-2), 40.3 (C-8), 33.1 (C-3), 26.9 (C-6), 26.5, 25.6, 24.5 (C-4/C-5/C-7), 16.8 (C-1')

MS (GC-MS, EI) *m*/*z* (%) 140 ($[M]^{+\cdot}$, 20), 112 (40), 98 (76), 83 (100), 67 (38), 55 (62)

6.2.1.2 Synthesis of 9-Methyloxonan-2-one (*rac*-36)

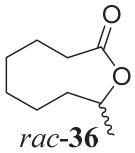

rac-**36**

2-Methylcyclooctan-1-one (*rac*-**38**) (2.2 g, 15.88 mmol) was dissolved in chloroform (20 ml) and *m*-CPBA (5.2 g, 30.17 mmol) was added at room temperature. The solution was stirred for 11 days. Then, additional *m*-CPBA (548 mg, 3.18 mmol) was added and the reaction mixture was heated to reflux for 24 hours. The solution was cooled to room temperature, filtered over Celite and the solvent was removed under reduced pressure. The residue was dissolved in Et_2O (20 ml) and washed with saturated $Na_2S_2O_3$ solution (2 × 20 ml), saturated Na_2CO_3 solution (2 × 20 ml) and saturated $MgCl_2$ solution (20 ml). The ethereal phase was dried over $MgSO_4$ and the solvent was removed under reduced pressure. After purification by column chromatography on silica gel using DCM as eluent, (*rac*-**36**) was obtained as colorless liquid (1.4 g, 9.20 mmol, 58%). R_f = 0.62 (DCM).[111]

HRMS *m*/*z* calcd for $C_9H_{16}O_2$ 156.1150 $[M]^{+\cdot}$, found 156.1156

IR (thin film, cm^{-1}) ν 2929 (s), 2857 (m), 1710 (s), 1461 (w), 1410 (w), 1375 (w), 1258 (s), 1100 (w), 940 (w)

^{1}H NMR (400 MHZ, $CDCl_3$) δ 5.07 (m_c, 1 H, H-9), 2.25 (m_c, 2 H, H-3), 1.93 (m_c, 1 H, H-5a), 1.82 – 1.74 (m, 1 H, H-8a), 1.72 – 1.64 (m, 1 H, H-4a), 1.67 – 1.55 (m, 2 H, H-7a/ H-4b), 1.55 – 1.43 (m, 3 H, H-8b/H-6a/H-5b), 1.37 – 1.27 (m, 2 H, H-7b/H-6b), 1.25 (d, $^3J_{9,8}$ = 6.5 Hz, 3 H, H-1')

^{13}C NMR (100 MHz, $CDCl_3$) δ 175.6 (C-2), 71.6 (C-9), 35.7 (C-3), 35.1 (C-8), 29.4 (C-6), 25.0 (C-5), 23.9 (C-4), 21.9 (C-7), 20.7 (C-1')

MS (GC-MS, EI) *m*/*z* (%) 156 ($[M]^{+\cdot}$, 0.8), 138 (18), 113 (48), 97 (77), 95 (43), 83 (77), 67 (100)

6.2.1.3 Synthesis of Isopropyl 9-Bromononanoate (40)

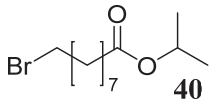

40

9-Bromononanoic acid (**37**) (5.2 g, 21.92 mmol) was dissolved in dry 2-propanol (50 ml) and sulfuric acid (1 ml) was added. The flask was equipped with a Dean-Stark apparatus and the solution was heated to reflux for 19 hours. After the solution cooled down to room temperature, 2-propanol was removed under reduced pressure, the residue was dissolved in Et_2O (20 ml) and the organic solution was washed with saturated Na_2CO_3 solution (20 ml), distilled water (20 ml) and saturated NaCl solution (20 ml). The ethereal solution was dried over $MgSO_4$, the solvent was removed and the crude product was purified by column chromatography on silica gel (DCM). After removal of the solvent **40** was obtained as a colorless oil (5.23g, 18.73 mmol, 86%). R_f = 0.70 (DCM).[55]

HRMS m/z calcd for $C_{12}H_{23}O_2BrNa$, $C_{12}H_{23}O_2{}^{81}BrNa$ 301.0774, 303.0753 $[M + Na]^{+\cdot}$, found 301.0776, 303.0753

IR (thin film, cm^{-1}) *v* 2979 (m), 2932 (s), 2857 (m), 1731 (s), 1466 (m), 1374 (m), 1256 (m), 1181 (m), 1145 (w), 1110 (s), 964 (w)

^{1}H NMR (400 MHz, $CDCl_3$) δ 5.00 (sp, $^3J_{1',2'} = {}^3J_{1',2''}$ = 6.2 Hz, 1 H, H-1'), 3.40 (t, $^3J_{9,8}$ = 6.9 Hz, 2 H, H-9), 2.26 (t, $^3J_{2,3}$ = 7.6 Hz, 2 H, H-2), 1.85 (m_c, 2 H, H-8), 1.61 (m_c, 2 H, H-3), 1.42 (m_c, 2 H, H-7), 1.34 – 1.28 (m, 6 H, H-6 – H-4), 1.22 (d, $^3J_{2',1'} = {}^3J_{2'',1'}$ =6.2 Hz, 6 H, H-2'/H-2'')

^{13}C NMR (100 MHz, $CDCl_3$) δ 173.3 (C-1), 67.3 (C-1'), 34.6 (C-2), 33.9 (C-9), 32.7 (C-8), 29.0, 29.0 (C-5/C-4), 28.5 (C-6), 28.1 (C-7), 24.9 (C-3), 21.8 (C-2', C-2'')

MS (GC-MS, EI) *m/z* (%) 280, 278 ($[M]^{+\cdot}$, 0.04), 265 (0.08), 263 (0.08), 239 (14), 237 (14), 221 (48), 219 (48), 157 (58), 139 (100), 121 (34), 97 (38), 73 (16), 61 (38), 55 (40)

6.2.1.4 Synthesis of (9-Isopropoxy-9-oxononyl)triphenylphosphonium Bromide (35)

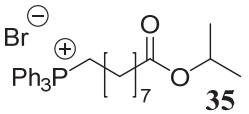

35

Isopropyl 9-bromononanoate (**40**) (2.89 g, 10.35 mmol) was dissolved in dry toluene (65 ml) and PPh_3 (2.71 g, 10.35 mmol) was added. The solution was refluxed for 24 hours under argon, cooled to room temperature and the supernatant was transferred to a new flask. There again PPh_3 (1.36 g, 5.18 mmol) was added and the solution was stirred under reflux for 3 days. After

cooling to room temperature, the supernatant was discarded and both bottom layers were combined and purified by column chromatography on silica gel (DCM/MeOH 14:1). The solvents were removed under reduced pressure and **35** was obtained as a sticky syrup (4.33 g, 8.00 mmol, 77%). R_f = 0.51 (DCM/MeOH 14:1).[55]

HRMS *m*/*z* calcd for $C_{30}H_{38}O_2P$ 461.2604 $[M]^+$, found 461.2601

IR (thin film, cm^{-1}) *v* 3057 (w), 2977 (w), 2855 (s), 2802 (w), 1720 (s), 1587 (w), 1522 (w), 1485 (m), 1104 (m), 856 (s), 842 (s)

^{1}H NMR (400 MHZ, $CDCl_3$) δ 7.88 – 7.76 (m, 9 H, H_{ar}-6/H_{ar}-2/H_{ar}-4), 7.74 – 7.67 (m, 6 H, H_{ar}-5/H_{ar}-3), 4.96 (sp, $^3J_{1',2'} = {}^3J_{1',2''}$ = 6.2 Hz, 1 H, H-1'), 3.82 – 3.71 (m, 2 H, H-1), 2.19 (t, $^3J_{2,3}$ = 7.5 Hz, 2 H, H-8), 1.68 – 1.56 (m, 4 H, H-3/H-2), 1.52 (m_c, 2 H, H-7), 1.30 – 1.21 (m, 6 H, H-6 - H-4), 1.20 (d, $^3J_{2',1'} = {}^3J_{2'',1'}$ = 6.2 Hz, 6 H, H-2''/H-2')

^{13}C NMR (100 MHz, $CDCl_3$) δ 173.3 (C-9), 134.9, 134.9 (C_{ar}-4), 133.7, 133.6 (C_{ar}-6/C_{ar}-2), 130.5, 130.4 (C_{ar}-5/C_{ar}-3), 118.7, 118.1 (C_{ar}-1), 67.3 (C-1'), 34.6 (C-8), 30.3, 30.2 (C-3), 28.9, 28.9, 28.7 (C-6 – C-4), 24.8 (C-7), 22.9, 22.6 (C-1), 22.6, 22.6 (C-2), 21.8 (C-2'/C-2'')

6.2.1.5 Synthesis of Isopropyl (9*Z*)-17-Hydroxyoctadec-9-enoate (*rac*-34)

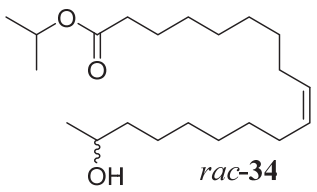

rac-**34**

A cold solution (-78 °C) of 9-methyloxonan-2-one (*rac*-**36**) (78 mg, 0.5 mmol) in dry toluene (2.7 ml) was treated within 10 min with DiBAL-H (0.6 ml, 0.6 mmol, 1 M in hexane). Stirring was continued for another 40 minutes and excess of DiBAL-H was quenched by addition of dry MeOH (5 µl). Next, the cold solution was transferred into a cold solution (-78 °C) of the phosphorous ylid, prepared from (9-isopropoxy-9-oxononyl)triphenylphosphonium bromide (**35**) (325 mg, 0.6 mmol) in dry THF (3.5 ml) and KHMDS (120 mg, 0.6 mmol). The reaction mixture was warmed to room temperature during 1 hour. Stirring was carried on for 1 hour and the mixture was hydrolyzed by the addition of 5% HCl (2.6 ml). The layers were separated and the aqueous phase was extracted with Et_2O (2 × 5 ml). The combined organic extracts were washed with 5% HCl (20 ml), saturated $NaHCO_3$ solution (20 ml) and water (20 ml). After removal of the solvents under reduced pressure, the crude product was purified by column chromatography on silica gel using hexane/ethyl acetate (5:1) for elution. Removal of the solvents yielded (*rac*-**34**) as a colorless oil (49 mg, 0.13 mmol, 26%,

Z/*E* > 98/2; Ylid preparation with *n*-BuLi: 29%, *Z*/*E* 80/20). R_f = 0.18 (hexane/ethyl acetate 5:1).[55]

HRMS *m*/*z* calcd for $C_{21}H_{40}O_3$ 340.2978 $[M]^{+\cdot}$, found 340.2985

IR (thin film, cm^{-1}) *v* 3401 (br, m), 2977 (m), 2964 (m), 2925 (s), 2854 (s), 1732 (s), 1655 (w), 1465 (m), 1374 (m), 1247 (m), 1181 (m), 1145 (m), 1109 (s)

^{1}H NMR (400 MHZ, $CDCl_3$) δ 5.40 – 5.31 (m, 2 H, H-10/H-9), 5.01 (sp, $^3J_{1',2'} = {}^3J_{1',2''}$ = 6.2 Hz, 1 H, H-1'), 3.79 (tq, $^3J_{17,18} = {}^3J_{17,16}$ = 6.1 Hz, 1 H, H-17), 2.26 (t, $^3J_{2,3}$ = 7.7 Hz, 2 H, H-2), 2.04 – 1.96 (m, 4 H, H-11/H-8), 1.61 (m_c, 2 H, H-3), 1.48 – 1.38 (m, 2 H, H-16), 1.36 – 1.27 (m, 16 H, H-15 – H-12/H-7 – H-4), 1.23 (d, $^3J_{2',1'} = {}^3J_{2'',1'}$ = 6.3 Hz, 6 H, H-2'/H-2''), 1.19 (d, $^3J_{18,17}$ = 6.2 Hz, 3 H, H-18)

^{13}C NMR (100 MHz, $CDCl_3$) δ 173.4 (C-1), 129.8 (C-10/C-9), 68.1 (C-17), 67.3 (C-1'), 39.4 (C-16), 34.7 (C-2), 29.7, 29.5, 29.2, 29.1, 29.1, 25.7 (C-15 – C-12/C-7 – C-4), 27.2, 27.2 (C-11/C-8), 25.0 (C-3), 23.5 (C-18), 21.9 (C-2'/C-2'')

MS (GC-MS, EI) *m*/*z* (%) 340 ($[M]^{+\cdot}$, 0.3), 322 (1.5), 279 (26), 123 (37), 109 (56), 95 (87), 81 (98), 67 (92), 55 (100), 43 (80), 41 (71)

6.2.1.6 Synthesis of (9*Z*)-Octadec-9-ene-1,17-diol (*rac*-41)

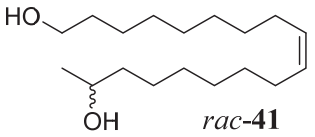

rac-**41**

$LiAlH_4$ (99 mg, 2.62 mmol) was suspended at 0 °C in dry THF (7.5 ml) and the ester *rac*-**34** (297 mg, 0.87 mmol) was added slowly. The reaction mixture was allowed to come to room temperature and stirred for 4.5 hours. Et_2O (9 ml) and water (10 ml) were added, the phases were separated and the aqueous layer was extracted with Et_2O (3 × 10 ml). The combined organic extracts were washed with water (30 ml) and dried over Na_2SO_4. The solvent was removed under reduced pressure and the residue was purified by column chromatography on silica gel using hexane/ethyl acetate (1:1) for elution. After removal of the solvents, *rac*-**41** was obtained as slightly yellow oil (243 mg, 0.85 mmol, 98%). R_f = 0.35 (hexane/ethyl acetate 1:1).[55]

HRMS *m*/*z* calcd for $C_{18}H_{36}O_2$ 284.2715 $[M]^{+\cdot}$, found 284.2705

IR (thin film, cm^{-1}) *v* 3332 (br, m), 3004 (w), 2926 (s), 2854 (s), 1654 (w), 1462 (m), 1373 (m)

^{1}H NMR (400 MHZ, $CDCl_3$) δ 5.40 – 5.30 (m, 2 H, H-10/H-9), 3.79 (tq, $^3J_{17,18} = {}^3J_{17,16}$ = 5.9 Hz, 1 H, H-17), 3.63 (t, $^3J_{1,2}$ = 6.6 Hz, 2 H, H-1), 2.06 – 1.95 (m, 4 H, H-11/H-8), 1.95 – 1.80 (br, 2 H, O-H), 1.56 (tt, $^3J_{2,3} = {}^3J_{2,1}$ = 6.7 Hz, 2 H, H-2), 1.49 – 1.38 (m, 2 H, H-16), 1.38 – 1.25 (m, 18 H, H-15 – H-12/H-7 – H-3), 1.18 (d, $^3J_{18,17}$ = 6.0 Hz, 3 H, H-18)

^{13}C NMR (100 MHz, $CDCl_3$) δ 129.9, 129.8 (C-10/C-9), 68.2 (C-17), 63.0 (C-1), 39.3 (C-16), 32.7 (C-2), 29.7, 29.7, 29.5, 29.4, 29.4, 29.2, 29.1 (C-14 – C-12/C-7 – C-4), 27.1 (C-11/C-8), 25.7 (C-15/C-3), 23.4 (C-18)

MS (GC-MS, EI) *m*/*z* (%) 284 ([M]$^{+\cdot}$, 0.6), 266 (10), 149 (6), 135 (14), 124 (24), 110 (56), 96 (84), 95 (82), 82 (85), 81 (98), 67 (98), 55 (100)

6.2.1.7 Synthesis of (9*Z*)-1,17-Diazidooctadec-9-ene (*rac*-42)

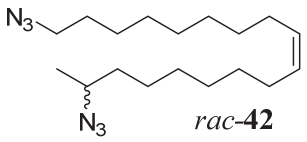

rac-**42**

(9*Z*)-Octadec-9-ene-1,17-diol (*rac*-**41**) (218 mg, 0.77 mmol) was dissolved in dry THF (13 ml) and cooled to 0 ºC. PPh_3 (836 mg, 3.19 mmol), DPPA (0.97 ml, 4.51 mmol) and DIAD (0.85 ml, 4.29 mmol) were successively added with stirring and the reaction mixture was allowed to warm to room temperature. After 4 hours the solvent was removed and the reaction product was purified by column chromatography on silica gel using hexane/DCM (3:1) for elution. Removal of solvents afforded *rac*-**42** as a colorless oil (195 mg, 0.58 mmol, 76%). R_f = 0.30 (hexane/DCM 3:1).[55]

HRMS *m*/*z* calcd for $C_{18}H_{34}N_6Na$ 357.2737 $[M + Na]^+$, found 357.2737

IR (thin film, cm^{-1}) *v* 3004 (w), 2928 (s), 2855 (s), 2094 (s), 1653 (w), 1459 (m), 1378 (w), 1249 (s)

^{1}H NMR (400 MHZ, $CDCl_3$) δ 5.42 – 5.30 (m, 2 H, H-10/H-9), 3.42 (tq, $^3J_{17,18} = {}^3J_{17,16}$ = 6.5 Hz, 1 H, H-17), 3.26 (t, $^3J_{1,2}$ = 7.0 Hz, 2 H, H-1), 2.07 – 1.94 (m, 4 H, H-11/H-8), 1.61 (tt, $^3J_{2,3} = {}^3J_{2,1}$ = 7.0 Hz, 2 H, H-2), 1.57 – 1.28 (m, 20 H, H-16 – H-12/H-7 – H-3), 1.25 (d, $^3J_{18,17}$ = 6.6 Hz, 3 H, H-18)

^{13}C NMR (100 MHz, $CDCl_3$) δ 129.9, 129.8 (C-10/C-9), 58.0 (C-17), 51.5 (C-1), 36.2 (C-16), 29.7, 29.6, 29.4, 29.3, 29.2, 29.1, 29.1 (C-14 – C-12/C-7 – C-4), 28.8 (C-2), 27.2, 27.1 (C-11/C-8), 26.7 (C-3), 26.1 (C-15), 19.5 (C-18)

6.2.1.8 Synthesis of (9*Z*)-Octadec-9-ene-1,17-diamine (*rac*-5)

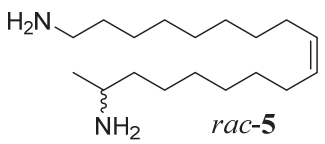

rac-**5**

$LiAlH_4$ (177 mg, 3.95 mmol) was suspended with stirring in dry THF (11 ml) and cooled to 0 ºC. A solution of (9*Z*)-1,17-diazidooctadec-9-ene (*rac*-**42**) (165 mg, 0.49 mmol) in dry THF (5 ml) was added dropwise and the suspension was warmed to room temperature. After stirring for 4 hours water (30 ml) and $CHCl_3$ (30 ml) were added, the layers were separated and the aqueous phase was extracted with $CHCl_3$ (6 × 30 ml). The organic extracts were combined and solvents were removed under reduced pressure. The product was taken up in MTBE (80 ml) and 2% HCl (80 ml). The layers were separated, the aqueous phase was carefully extracted with MTBE (3 × 20 ml) and the combined organic extracts were washed with 2% HCl (30 ml). The aqueous solutions were combined and MTBE (40 ml) and NH_3 (25% aqueous solution, 80 ml) were added. After separation of the two layers, the aqueous phase was extracted with MTBE (3 × 60 ml). The combined organic extracts were dried over Na_2SO_4 and the solvent was evaporated under reduced pressure to yield (*rac*-**5**) as colorless oil (139 mg, 0.49 mmol, quant.).[55]

HRMS *m*/*z* calcd for $C_{18}H_{39}N_2$ 283.3108 $[M + H]^+$, found 283.3106

IR (thin film, cm^{-1}) *v* 3320 (m), 3004 (w), 2921 (s), 2851 (s), 1639 (w), 1564 (m), 1468 (m), 1430 (w), 1390 (m), 1331 (m)

^{1}H NMR (400 MHZ, $CDCl_3$) δ 5.38 – 5.27 (m, 2 H, H-10/H-9), 2.85 (tq, $^3J_{17,18} = {}^3J_{17,16}$ = 6.0 Hz, 1 H, H-17), 2.66 (t, $^3J_{1,2}$ = 7.0 Hz, 2 H, H-1), 2.04 – 1.91 (m, 4 H, H-11/H-8), 1.50 – 1.38 (m, 6 H, H-2, N-H_2), 1.36 – 1.21 (m, 20 H, H-16 – H-12/H-7 – H-3), 1.03 (d, $^3J_{18,17}$ = 6.2 Hz, 3 H, H-18)

^{13}C NMR (100 MHz, $CDCl_3$) δ 129.8, 129.8 (C-10/C-9), 46.9 (C-17), 42.1 (C-1), 40.1 (C-16), 33.7 (C-2), 29.7, 29.6, 29.6, 29.4, 29.4, 29.2, 29.2 (C-14 – C-12/C-7 – C-4), 27.1 (C-11/C-8), 26.8 (C-3), 26.3 (C-15), 23.8 (C-18)

MS (HPLC, APCI) *m*/*z* (%) 283 ($[M + H]^+$, 100), 264 (8)

6.2.2 Synthesis of (*R*)-Harmonine ((*R*)-5)

6.2.2.1 Enzymatic hydrolysis of 9-Methyloxonan-2-one (*rac*-36)

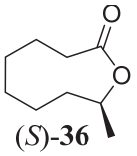
(*S*)-**36**

Racemic 9-methyloxonan-2-one (*rac*-**36**) (3.50 g, 22.4 mmol) was suspended in NaH_2PO_4 buffer (0.1 M, pH = 7.2, 100 ml) and stirred for 15 minutes. Then horse liver esterase (350 mg, lyophilized powder) was added and the pH was kept constant by dropwise addition of 0.5 M NaOH during the whole reaction time. After 12 hours, another portion of horse liver esterase (70 mg) was added and stirring was continued for 4 hours. Then Celite (3.50 g) and ice (7.00 g) were added, the suspension was stirred for 5 minutes and the solids were filtered off. The filter cake was washed with Et_2O (2 × 50 ml). The layers of the filtrate were separated and the aqueous phase was extracted with Et_2O (3 × 50 ml). The combined organic extracts were washed with saturated $NaHCO_3$ solution (100 ml) and dried over Na_2SO_4. Evaporation of the solvent yielded (9*S*)-9-methyloxonan-2-one ((*S*)-**36**) as a colorless liquid.[55]

(9*S*)-9-Methyl-oxonan-2-one ((*S*)-36): Yield: 1.51 g (9.67 mmol, 86% of (*S*)-enantiomer, *ee* ≥ 99.5%).

$[\alpha]_D^{23}$ + 31.8 (c 1.00, THF). All other spectral data were identical to *rac*-**36**.

(8*R*)-8-Hydroxynonanoic acid ((*R*)-49)

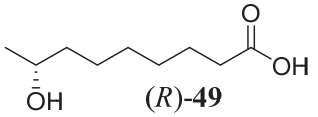
(*R*)-**49**

The water phase was covered with Et_2O (100 ml) and 2 M HCl (60 ml) was added. The layers were separated and the aqueous phase was extracted with Et_2O (3 × 100 ml). The combined organic extracts were washed with saturated NaCl solution (150 ml) and dried over Na_2SO_4. The solvent was removed under reduced pressure to yield (8*R*)-8-hydroxynonanoic acid ((*R*)-**49**) as a colorless wax.[55]

(8*R*)-8-Hydroxynonanoic acid ((*R*)-49): Yield: 1.52 g (8.72 mmol, 78% of (*R*)-enantiomer, *ee* ≥ 99%).

$[\alpha]_D^{23}$ – 8.5 (c 1.00, THF).

HRMS *m*/*z* calcd for $C_9H_{18}O_3Na$ 197.1148 $[M + Na]^+$, found 197.1146

IR (thin film, cm^{-1}) *v* 3391 (br, s), 2933 (s), 2858 (s), 1711 (s), 1462 (m), 1410 (m), 1376 (m), 1261 (m), 1127 (m), 1103 (m)

^{1}H NMR (400 MHZ, $CDCl_3$) δ 5.25 (br, 2 H, O-H, COO-H), 3.81 (tq, $^{3}J_{8,9} = {}^{3}J_{8,7}$ = 6.1 Hz, 1 H, H-8), 2.36 (t, $^{3}J_{2,3}$ = 7.5 Hz, 2 H, H-2), 1.65 (tt, $^{3}J_{3,4} = {}^{3}J_{3,2}$ = 7.5 Hz, 2 H, H-3), 1.50 – 1.40 (m, 3 H, H-7/H-6a), 1.40 – 1.30 (m, 5 H, H-6b/H-5/H-4), 1.20 (d, $^{3}J_{9,8}$ = 6.1 Hz, 3 H, H-9)

^{13}C-NMR (100 MHz, $CDCl_3$) δ 179.0 (C-1), 68.2 (C-8), 39.2 (C-7), 33.9 (C-2), 29.2, 29.0 (C-5/C-4), 25.5 (C-6), 24.6 (C-3), 23.5 (C-9)

MS (GC-MS, EI) *m*/*z* (%) 174 ($[M]^{+\cdot}$, 0.1), 141 (18), 130 (30), 95 (26), 87 (60), 73 (100), 69 (20), 55 (30), 45 (72)

6.2.2.2 Subsequent synthesis steps to (*R*)-Harmonine ((*R*)-5)

Isopropyl (17*S*,9*Z*)-17-hydroxyoctadec-9-enoate ((*S*)-34):

Prepared from (9*S*)-9-methyloxonan-2-one ((*S*)-**36**) (750 mg, 4.80 mmol) as described in chapter 6.2.1.5 (ylide preparation with *n*-BuLi). After purification, (*S*)-**34** was obtained as colorless oil (366 mg, 1.08 mmol, 23%, *Z*/*E* > 85/15).[55]

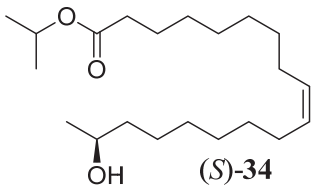

(*S*)-**34**

$[\alpha]_D^{22}$ + 2.9 (c 1.00, $CHCl_3$). All other spectral data were identical to *rac*-**34**.

(17*S*,9*Z*)-Octadec-9-ene-1,17-diol ((*S*)-41):

Prepared from isopropyl (17*S*,9*Z*)-17-hydroxyoctadec-9-enoate ((*S*)-**34**) (295 mg, 0.87 mmol) as described in chapter 6.2.1.6. After column chromatography, (*S*)-**41** was obtained as a colorless oil (245 mg, 0.86 mmol, 98%).[55]

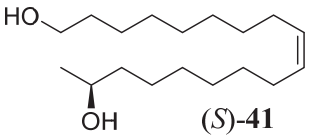

(*S*)-**41**

$[\alpha]_D^{22}$ + 3.8 (c 1.00, $CHCl_3$). All other spectral data were identical to *rac*-**41**.

(17*R*,9*Z*)-1,17-Diazidooctadec-9-ene ((*R*)-42):

Prepared from (17*S*,9*Z*)-octadec-9-ene-1,17-diol ((*S*)-**41**) (200 mg, 0.70 mmol) as depicted in chapter 6.2.1.7. Purification by column chromatography afforded (*R*)-**42** as a colorless oil (189 mg, 0.57 mmol, 81%).[55]

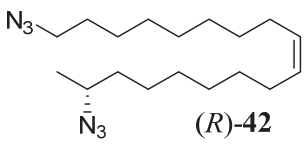

(*R*)-**42**

$[\alpha]_D^{22}$ – 19.7 (c 1.06, $CHCl_3$). All other spectral data were identical to *rac*-**42**.

(17*R*,9*Z*)-Octadec-9-ene-1,17-diamine ((*R*)-5)/(*R*)-Harmonine:

Prepared from (17*R*,9*Z*)-1,17-diazidooctadec-9-ene ((*R*)-**42**) (161 mg, 0.48 mmol) as described in chapter 6.2.1.8. Harmonine ((*R*)-**5**) was obtained as a slightly yellow oil (135 mg, 0.48 mmol, 99%).[55]

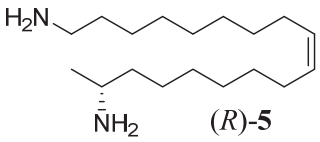

(*R*)-**5**

$[\alpha]_D^{24}$ – 3.4 (c 1.04, C_6H_6). Spectroscopic data were identical with *rac*-**5**.

6.2.3 Synthesis of (*S*)-Harmonine ((*S*)-5)

6.2.3.1 Synthesis of Methyl (8*R*)-8-((*tert*-Butyldimethylsilyl)oxy)nonanoate ((*R*)-50)

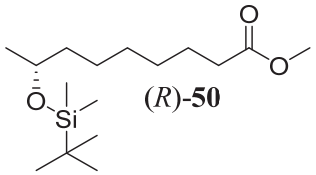

(*R*)-**50**

(8*R*)-8-Hydroxynonanoic acid ((*R*)-**49**) (558 mg, 3.20 mmol) was dissolved in a DCM/MeOH (95 ml/ 9.5 ml) mixture and the solution was stirred for 2 minutes. Then, (TMS)-diazomethane solution (2.0 M in Et_2O) was added dropwise until a slightly yellow color remained (~ 2.3 ml). The reaction mixture was stirred for 1.5 hours at room temperature. Acetic acid was added until the yellow color fainted and the solvents were removed under reduced pressure. The residue was dissolved in dry DCM (43 ml) and the solution was henceforward treated under an argon atmosphere. Imidazole (1.36 g, 20.00 mmol) was added, the reaction mixture was cooled to 0 °C and TBDMSCl (1.21 g, 8.00 mmol) was added in small portions. After additional stirring for 10 minutes, the solution was allowed to warm to room temperature and was stirred for another 17 hours before water (25 ml) and DCM (25 ml) were added. The aqueous phase was extracted with DCM (3 × 25 ml) and the combined organic extracts were washed with saturated NaCl solution (35 ml) and dried over $MgSO_4$. The solvent was removed under reduced pressure and the residue was purified by column chromatography on silica gel (hexane/ethyl acetate 12:1) yielding methyl (8*R*)-8-((*tert*-butyl-dimethylsilyl)oxy)-nonanoate ((*R*)-**50**) as a colorless oil (812 mg, 2.68 mmol, 84%). R_f = 0.44 (hexane/ethyl acetate 12:1).

$[\boldsymbol{\alpha}]_{\mathbf{D}}^{\mathbf{23}}$ – 12.0 (c 1.00, THF)

HRMS *m*/*z* calcd for $C_{15}H_{31}O_3Si$ 287.2042 $[M\text{-}Me^{\cdot}]^+$, found 287.2054

IR (thin film, cm^{-1}) *v* 2957 (s), 2931 (s), 2857 (s), 1743 (s), 1463 (m), 1436 (m), 1374 (m), 1361 (m), 1254 (s), 1198 (s), 1168 (s), 1134 (s), 1104 (s), 1068 (s), 1005 (s), 939 (s), 892 (m)

^{1}H NMR (400 MHZ, $CDCl_3$) δ 3.77 (m_c, 1 H, H-8), 3.67 (s, 3 H, H-1‘), 2.31 (t, 2 H, H-2, $^3J_{2,3}$ = 7.5 Hz), 1.63 (m_c, 2 H, H-3), 1.46 – 1.23 (m, 8 H, H-4 – H-7), 1.11 (d, 3 H, H-9, $^3J_{9,8}$ = 6.1 Hz), 0.89 (s, 9 H, H-3* - H-3***), 0.05, 0.05 (2 × s, 2 × 3 H, H-1*/H-1**)

^{13}C NMR (100 MHz, $CDCl_3$) δ 174.3 (C-1), 68.6 (C-8), 51.4 (C-1‘), 39.6 (C-7), 34.1 (C-2), 29.3, 29.2, 25.6 (C-4/C-5/C-6), 25.9 (C-3* - C-3***), 24.9 (C-3), 23.8 (C-9), 18.2 (C-2*), -4.4, -4.7 (C-1*/C-1**)

MS (GC-MS, EI) *m*/*z* (%) 287 ($[M\text{-}Me^{\cdot}]^{+\cdot}$, 0.4), 245 (10), 213 (50), 159 (20), 107 (35), 89 (32), 75 (100), 73 (65), 69 (69), 55 (57)

6.2.3.2 Synthesis of Isopropyl (17*R*,9*Z*)-17-((*tert*-Butyldimethylsilyl)oxy)octadec-9-enoate ((*R*)-51)

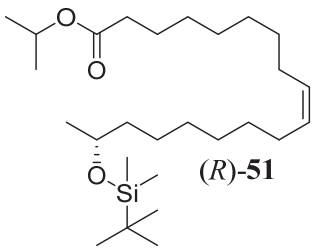

(*R*)-**51**

(8*R*)-8-((*tert*-Butyldimethylsilyl)oxy)nonanoate ((*R*)-**50**) (576 mg, 1.90 mmol) was reacted with (9-isopropoxy-9-oxo-nonyl)triphenylphosphonium bromide (**35**) (1.24 g, 2.28 mmol) following the "Wittig-type one-pot" reaction protocol described in chapter 6.2.1.5. The crude product was purified by column chromatography on silica gel using pure DCM as eluent. Removal of the solvent in reduced pressure yielded ((*R*)-**51**) as a colorless oil (248 mg, 0.55 mmol, 29%, *Z*/*E* > 98/2). R_f = 0.49 (DCM).

$[\boldsymbol{\alpha}]_{\mathbf{D}}^{\mathbf{21}}$ – 4.0 (c 1.00, $CHCl_3$)

HRMS *m*/*z* calcd for $C_{27}H_{54}O_3Si$ 454.3842 $[M]^{+\cdot}$, found 454.3854

IR (thin film, cm^{-1}) *v* 3007 (m), 2928 (s), 2856 (s), 1735 (s), 1699 (w), 1464 (m), 1374 (m), 1253 (m), 1180 (w), 1134 (w), 1110 (m), 1066 (w), 1005 (w), 939 (w)

^{1}H NMR (400 MHZ, $CDCl_3$) δ 5.40 – 5.30 (m, 2 H, H-10/H-9), 5.01 (sp, 1 H, H-1‘, $^3J_{1‘,2‘/2‘‘}$ = 6.2 Hz), 3,77 (m_c, 1 H, H-17), 2.26 (t, 2 H, H-2, $^3J_{2,3}$ = 7.5 Hz), 2.02 (m_c, 4 H, H-11/H-8), 1.66 – 1.56 (m, 2 H, H-3), 1.46 – 1.26 (m, 18 H, H-4 – H-7/H-12 – H-16), 1.23 (d, 6 H, H-2‘/H-2“, $^3J_{2‘/2‘‘,1‘}$ = 6.2 Hz), 1.12 (d, 3 H, H-18, $^3J_{18,17}$ = 6.1 Hz), 0.89 (s, 9 H, H-3* - H-3***), 0.05, 0.05 (2 × s, 2 × 3 H, H-1*/H-1**)

^{13}C NMR (100 MHz, $CDCl_3$) δ 173.4 (C-1), 129.9, 129.8 (C-10/C-9), 68.7 (C-17), 67.3 (C-1‘), 39.7 (C-16), 34.7 (C-2), 29.7, 29.7, 29.6, 29.3, 29.2, 29.1, 29.1, 25.8 (C-4 – C-7/C-12 – C-15), 27.2, 27.2 (C-11/C-8), 25.9 (C-3* - C-3***), 25.0 (C-3), 23.8 (C-18), 21.9 (C-2‘/C-2‘‘), 18.2 (C-2*), - 4.4, -4.7 (C-1*/C-1**)

MS (GC-MS, EI) *m*/*z* (%) 454 ($[M]^{+\cdot}$, 0.02), 337 (48), 159 (16), 109 (10), 95 (19), 81 (21), 75 (100), 73 (42), 69 (19), 67 (20), 55 (30)

6.2.3.3 Synthesis of (17*R*,9*Z*)-Octadec-9-ene-1,17-diol ((*R*)-41)

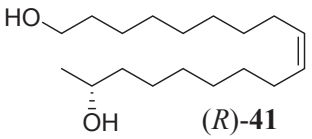

(*R*)-**41**

LAH (55 mg, 1.44 mmol) was suspended in dry THF (2.4 ml) under an argon atmosphere and the slurry was cooled to 0 °C. Then, isopropyl (17*R*,9*Z*)-17-((*tert*-butyldimethylsilyl)oxy)-octadec-9-enoate ((*R*)-**51**) (218 mg, 0.48 mmol) dissolved in 2.2 ml THF was added dropwise and the reaction mixture was warmed to room temperature. After 4 hours, water (7.3 ml) and Et_2O (7.3 ml) were added, the layers were separated and the aqueous phase was extracted with Et_2O (3 × 10 ml). The combined organic extracts were washed with water (20 ml), dried over $MgSO_2$ and the solvent was evaporated under reduced pressure. The residue was dissolved in AcN (4.4 ml) and HF (40% aq, 85 µl) was added dropwise. The reaction mixture was stirred for 2.5 hours and then K_2CO_3 (847 mg, 6.13 mmol) was added. Water was poured into the reaction vessel until all solids were dissolved. The mixture was extracted with MTBE (4 × 20 ml), the organic extracts were combined and dried over $MgSO_2$. Evaporation of the solvent yielded the crude product which was purified by column chromatography using hexane/ethyl acetate (1:1). The Diol ((*R*)-**41**) was obtained as a colorless oil (100 mg, 0.35 mmol, 73%).

$[\boldsymbol{\alpha}]_{\mathbf{D}}^{\mathbf{22}}$ – 4.7 (c 1.00, $CHCl_3$). All other spectral data were identical to *rac*-**41** and (*S*)-**41**.

6.2.3.4 Subsequent synthesis steps to (*S*)-Harmonine ((*S*)-5)

(17*S*,9*Z*)-1,17-Diazidooctadec-9-ene ((*S*)-42):

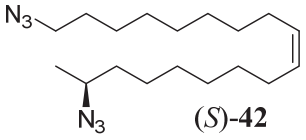

(*S*)-**42**

Prepared from (17*R*,9*Z*)-octadec-9-ene-1,17-diol ((*R*)-**41**) (28 mg, 0.10 mmol) according to the procedure described in chapter 6.2.1.7. After purification, ((*S*)-**42**) was obtained as a colorless oil (29 mg, 0.09 mmol, 87%).

$[\boldsymbol{\alpha}]_{\mathbf{D}}^{\mathbf{22}}$ + 18.8 (c 1.00, $CHCl_3$). All other spectral data were identical to *rac*-**42** and (*R*)-**42**.

(17*S*,9*Z*)-Octadec-9-ene-1,17-diamine ((*S*)-5):

The reduction of (17*S*,9*Z*)-1,17-diazidooctadec-9-ene ((*S*)-**42**) (25 mg, 0.08 mmol) using LAH (26 mg, 0.70 mmol) was executed as described in chapter 6.2.1.8. The desired (*S*)-harmonine ((*S*)-**5**) was obtained as a slightly yellow oil (20 mg, 0.07 mmol, 95%).

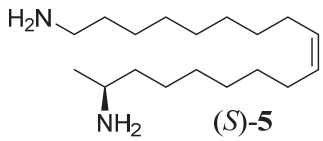

(*S*)-**5**

$[\alpha]_D^{24}$ + 2.9 (c 0.87, C_6H_6). All other spectral data were identical to *rac*-**5** and (*R*)-**5**.

6.2.4 Synthesis of (*Z*)-18-Aminooctadec-9-en-2-ol (*rac*-48)

6.2.4.1 Synthesis of (9*Z*)-17-Hydroxyoctadec-9-enamide (*rac*-47)

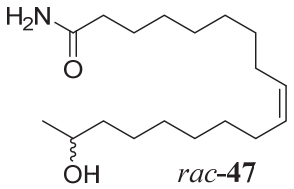

rac-**47**

Isopropyl (9*Z*)-17-hydroxyoctadec-9-enoate (*rac*-**34**) (237 mg, 0.70 mmol) was dissolved at 0 °C in MeOH (2.25 ml). Mg_3N_2 (353 mg, 3.48 mmol) was quickly added in one portion, the reaction vessel was carefully closed and the suspension was allowed to warm to room temperature. Stirring was continued for 1 hour. The reaction was heated to 80 ºC and stirring was continued for 24.5 hours. After cooling to room temperature, $CHCl_3$ (25 ml) and water (25 ml) were added. The aqueous phase was neutralized with 3 M HCl, the layers were separated and the aqueous phase was extracted with $CHCl_3$ (2 × 25 ml). The organic layers were combined and the solvent was removed under reduced pressure. The residue was purified by column chromatography on RP-18 silica gel using H_2O/MeOH (1:9) for elution. $CHCl_3$ was added and the solvents were removed under reduced pressure. This procedure was repeated three times with $CHCl_3$ and three times with benzene to remove last traces of water. The residue was concentrated under high vacuum to yield *rac*-**47** as a colorless, sticky oil. (182 mg, 0.61 mmol, 87%). R_f = 0.43 (H_2O/MeOH 1:9, RP-18).[55]

HRMS *m*/*z* calcd for $C_{18}H_{36}NO_2$ 298.2741 $[M + H]^+$, found 298.2734

IR (thin film, cm^{-1}) *v* 3358 (s), 3191 (br, m), 3003 (w), 2967 (w), 2924 (s), 2852 (s), 1703 (w), 1659 (s), 1633 (s), 1468 (m), 1423 (m), 1412 (m)

^{1}H NMR (400 MHZ, $CDCl_3$) δ 5.68 (d, $^2J_{NH,NH'}$ = 81.9 Hz, 2 H, N-H_2), 5.40 – 5.27 (m, 2 H, H-10/H-9), 3.78 (tq, $^3J_{17,18} = {}^3J_{17,16}$ = 5.7 Hz, 1 H, H-17), 2.20 (t, $^3J_{2,3}$ = 7.5 Hz, 2 H, H-2), 2.05 – 1.92 (m, 4 H, H-11/H-8), 1.84 (brs, 1 H, O-H), 1.62 (tt, $^3J_{3,4} = {}^3J_{3,2}$ = 7.1 Hz, 2 H, H-3), 1.51 – 1.37 (m, 2 H, H-16), 1.37 – 1.23 (m, 16 H, H-15 – H-12/H-7 – H-4), 1.17 (d, $^3J_{18,17}$ = 6.1 Hz, 3 H, H-18)

^{13}C NMR (100 MHz, $CDCl_3$) δ 175.8 (C-1), 129.9, 129.8 (C-10/C-9), 68.0 (C-17), 39.3 (C-16), 35.9 (C-2), 29.6, 29.6, 29.5, 29.5, 29.2, 29.2, 29.0 (C-14 – C-12/C-7 – C-4), 27.1, 27.1 (C-11/C-8), 25.7 (C-15), 25.5 (C-3), 23.4 (C-18)

MS (GC-MS, EI) *m*/*z* (%) 297 ($[M]^{+\cdot}$, 1), 279 (2), 262 (5), 207 (6), 109 (28), 95 (43), 81 (33), 72 (64), 69 (34), 67 (54), 59 (98), 55 (100), 41 (68)

6.2.4.2 Synthesis of (9*Z*)-18-Aminooctadec-9-en-2-ol (*rac*-48)

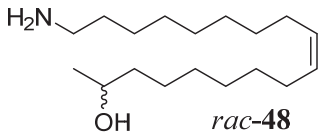

rac-**48**

$LiAlH_4$ (106 mg, 3.00 mmol) was suspended with stirring in dry THF (3 ml) and cooled to 0 ºC. (9*Z*)-17-Hydroxyoctadec-9-enamide (*rac*-**47**) (168 mg, 0.56 mmol), dissolved in dry THF (2 ml), was added dropwise. The reaction was allowed to warm to room temperature, stirred for 4 hours at room temperature and for 19.5 hours at 45 ºC. After cooling to room temperature, water (10 ml) and $CHCl_3$ (10 ml) were added. The layers were separated and the aqueous phase was extracted with $CHCl_3$ (5 × 10 ml). The organic extracts were combined and the solvents were removed under reduced pressure. The residue was separated between MTBE (80 ml) and 2% HCl (80 ml). The aqueous phase was extracted with MTBE (3 × 20 ml) and the combined organic extracts were washed with 2% HCl (35 ml). Both aqueous solutions were combined and MTBE (50 ml) and NH_3 (25% aqueous solution, 80 ml) were added. The layers were separated and the aqueous phase was extracted with MTBE (3 × 80 ml). The combined organic extracts were dried over Na_2SO_4 and the solvent was evaporated under reduced pressure yielding *rac*-**48** as an oily, colorless wax (151 mg, 0.53 mmol, 95%).[55]

HRMS *m*/*z* calcd for $C_{18}H_{38}NO$ 284.2948 $[M + H]^+$, found 284.2935

IR (thin film, cm^{-1}) *v* 3332 (br, m), 3004 (m), 2925 (s), 2853 (s), 1632 (m), 1572 (m), 1464 (m), 1372 (m), 1315 (m)

^{1}H NMR (400 MHZ, $CDCl_3$) δ 5.38 – 5.28 (m, 2 H, H-10/H-9), 3.75 (tq, $^3J_{17,18} = {}^3J_{17,16}$ = 6.1 Hz, 1 H, H-2), 2.66 (t, $^3J_{1,2}$ = 7.0 Hz, 2 H, H-18), 2.04 – 1.91 (m, 4 H, H-11/H-8), 1.82 – 1.76 (m, 3 H, N-H_2, O-H), 1.48 – 1.35 (m, 5 H, H-17/H-4a/H-3), 1.35 – 1.23 (m, 17 H, H-4b/ H-16 – H-12/H-7 – H-5), 1.15 (d, $^3J_{18,17}$ = 6.1 Hz, 3 H, H-1)

^{13}C-NMR (100 MHz, $CDCl_3$) δ 129.8, 129.8 (C-10/C-9), 67.7 (C-2), 42.1 (C-18), 39.4 (C-3), 33.6 (C-17), 29.6, 29.6, 29.5, 29.4, 29.4, 29.2, 29.1, (C-15 – C-12/C-7 – C-5), 27.1 (C-11/ C-8), 26.8 (C-16), 25.8 (C-4), 23.5 (C-1)

MS (GC-MS, EI) *m*/*z* (%) 283 ($[M]^{+\cdot}$, 30), 268 (40), 250 (10), 238 (26), 222 (12), 210 (12), 196 (20), 182 (35), 168 (38), 154 (92), 140 (40), 123 (18), 109 (32), 95 (86), 81 (87), 79 (53), 67 (100), 55 (42)

6.2.5 Synthesis of C_{17}-Harmonine (*rac*-58)

Isopropyl 8-Bromooctanoate (53):

Prepared from 8-bromooctanoic acid (**52**) (9.0 g, 40.34 mmol) as described in chapter 6.2.1.3. Isopropyl 8-bromooctanoate (**53**) was obtained as sweet smelling, colorless oil (8.9 g, 33.56 mmol, 83%).

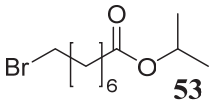

53

HRMS *m/z* calcd for $C_{11}H_{21}O_2Br$ 264.0734 $[M]^{+\cdot}$, found 264.0725
IR (thin film, cm^{-1}) *v* 2979 (s), 2933 (s), 2858 (s), 1728 (s), 1466 (m), 1374 (m), 1238 (s), 1181 (s), 1145 (m), 1109 (s), 964 (w)
^{1}H NMR (400 MHz, $CDCl_3$) δ 4.99 (sp, $^3J_{1',2'} = {}^3J_{1',2''}$ = 6.2 Hz, 1 H, H-1'), 3.39 (t, $^3J_{8,7}$ = 7.0 Hz, 2 H, H-8), 2.25 (t, $^3J_{2,3}$ = 7.5 Hz, 2 H, H-2), 1.84 (m_c, 2 H, H-7), 1.61 (m_c, 2 H, H-3), 1.43 (m_c, 2 H, H-6), 1.37 – 1.29 (m, 4 H, H-5/H-4), 1.22 (d, $^3J_{2',1'} = {}^3J_{2'',1'}$ =6.2 Hz, 6 H, H-2'/ H-2")
^{13}C NMR (100 MHz, $CDCl_3$) δ 173.2 (C-1), 67.3 (C-1'), 34.6 (C-2), 33.8 (C-8), 32.7 (C-7), 28.8, 28.4 (C-5/C-4), 27.9 (C-6), 24.8 (C-3), 21.8 (C-2', C-2")
MS (GC-MS, CI) *m/z* (%) 267, 265 ($[M+H]^+$, 70), 252, 250 (14), 224, 222 (84), 206, 204 (29), 143 (32), 125 (100), 97 (58), 55 (39)

(8-Isopropoxy-8-oxooctyl)triphenylphosphonium Bromide (54):

Compound **54** was prepared from isopropyl 8-bromooctanoate (**53**) (8.7 g, 32.92 mmol) and PPh_3 (12.9 g, 49.38 mmol) as described in chapter 6.2.1.4. After purification, **54** was obtained as a slightly yellow, sticky syrup (10.6 g, 20.07 mmol, 61%).

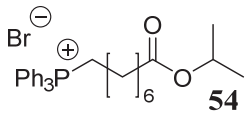

54

HRMS *m/z* calcd for $C_{29}H_{36}O_2P$ 447.2447 $[M]^+$, found 447.2437
IR (thin film, cm^{-1}) *v* 3054 (m), 2980 (s), 2934 (s), 2860 (s), 2795 (w), 1722 (s), 1622 (w), 1587 (m), 1486 (w), 1466 (s), 1374 (m), 1185 (m), 1110 (s), 996 (m)
^{1}H NMR (400 MHZ, $CDCl_3$) δ 7.85 – 7.75 (m, 9 H, H_{ar}-6/H_{ar}-2/H_{ar}-4), 7.73 – 7.65 (m, 6 H, H_{ar}-5/H_{ar}-3), 4.93 (sp, $^3J_{1',2'} = {}^3J_{1',2''}$ = 6.2 Hz, 1 H, H-1'), 3.79 – 3.68 (m, 2 H, H-1), 2.17 (t,

$^{3}J_{2,3}$ = 7.5 Hz, 2 H, H-7), 1.66 – 1.56 (m, 4 H, H-3/H-2), 1.51 (m_c, 2 H, H-6), 1.31 – 1.20 (m, 4 H, H-5/H-4), 1.17 (d, $^{3}J_{2',1'} = {}^{3}J_{2'',1'}$ = 6.2 Hz, 6 H, H-2''/H-2')

^{13}C NMR (100 MHz, $CDCl_3$) δ 173.2 (C-8), 135.0, 134.9 (C_{ar}-4), 133.6, 133.5 (C_{ar}-6/C_{ar}-2), 130.5, 130.4 (C_{ar}-5/C_{ar}-3), 118.7, 117.9 (C_{ar}-1), 67.3 (C-1'), 34.4 (C-7), 30.2, 30.0 (C-3), 28.7, 28.5 (C-5/C-4), 24.7 (C-6), 22.9, 22.5 (C-1), 22.5, 22.5 (C-2), 21.8 (C-2'/C-2'')

Isopropyl (8*Z*)-16-Hydroxyheptadec-8-enoate (*rac*-55):

This "Wittig-type one-pot reaction" between (8-isopropoxy-8-oxooctyl)triphenylphosphonium bromide (**54**) (3.0 g, 5.76 mmol) and 9-methyloxonan-2-one (*rac*-**36**) (750 mg, 4.80 mmol) was carried out as described in chapter 6.2.1.5 and yielded *rac*-**55** as a colorless oil (219 mg, 0.67 mmol, 15%, (*Z*)/(*E*) > 97/3).

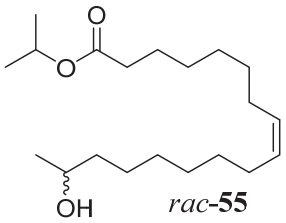

rac-**55**

HRMS *m*/*z* calcd for $C_{20}H_{38}O_3$ 326.2821 $[M]^{+\cdot}$, found 326.2808

IR (thin film, cm^{-1}) *v* 3418 (br, m), 3003 (m), 2974 (s), 2926 (s), 2855 (s), 1732 (s), 1657 (w), 1465 (m), 1374 (m), 1254 (m), 1180 (m), 1145 (m), 1109 (s)

^{1}H NMR (400 MHZ, $CDCl_3$) δ 5.40 – 5.29 (m, 2 H, H-9/H-8), 5.01 (sp, $^{3}J_{1',2'} = {}^{3}J_{1',2''}$ = 6.2 Hz, 1 H, H-1'), 3.79 (tq, $^{3}J_{16,17} = {}^{3}J_{16,15}$ = 6.1 Hz, 1 H, H-16), 2.26 (t, $^{3}J_{2,3}$ = 7.7 Hz, 2 H, H-2), 2.07 – 1.95 (m, 4 H, H-10/H-7), 1.61 (m_c, 2 H, H-3), 1.50 (brs, 1 H, OH), 1.48 – 1.39 (m, 2 H, H-15), 1.39 – 1.28 (m, 14 H, H-14 – H-11/H-6 – H-4), 1.23 (d, $^{3}J_{2',1'} = {}^{3}J_{2'',1'}$ = 6.3 Hz, 6 H, H-2'/H-2''), 1.19 (d, $^{3}J_{17,16}$ = 6.2 Hz, 3 H, H-17)

^{13}C NMR (100 MHz, $CDCl_3$) δ 173.4 (C-1), 129.9, 129.8 (C-9/C-8), 68.1 (C-16), 67.3 (C-1'), 39.4 (C-15), 34.7 (C-2), 29.7, 29.5, 29.5, 29.2, 29.0, 28.9, 25.7 (C-14 – C-11/C-6 – C-4), 27.2, 27.1 (C-10/C-7), 25.0 (C-3), 23.5 (C-17), 21.8 (C-2'/C-2'')

MS (GC-MS, EI) *m*/*z* (%) 326 ($[M]^{+\cdot}$, 0.3), 308 (2.2), 265 (28), 137 (20), 123 (34), 109 (48), 95 (80), 81 (100), 67 (92), 55 (92), 45 (44)

(8*Z*)-Heptadec-8-ene-1,16-diol (*rac*-56):

The reduction of isopropyl (8*Z*)-16-hydroxyheptadec-8-enoate (*rac*-**55**) (150 mg, 0.46 mmol) was conducted as described in chapter 6.2.1.6. Diol *rac*-**56** was obtained as a colorless oil (121 mg, 0.45 mmol, 98%).

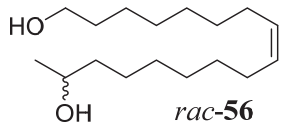

rac-**56**

HRMS *m*/*z* calcd for $C_{17}H_{34}O_2$ 270.2559 $[M]^{+\cdot}$, found 270.2566

IR (thin film, cm^{-1}) *v* 3333 (br, m), 3004 (w), 2926 (s), 2854 (s), 1656 (w), 1463 (m), 1373 (m), 1128 (w), 1057 (m)

^{1}H NMR (400 MHZ, $CDCl_3$) δ 5.42 – 5.29 (m, 2 H, H-9/H-8), 3.80 (m_c, 1 H, H-16), 3.64 (t, $^3J_{1,2}$ = 6.6 Hz, 2 H, H-1), 2.06 – 1.97 (m, 4 H, H-10/H-7), 1.57 (m_c, 2 H, H-2), 1.53 (brs, 2 H, O-H), 1.50 – 1.41 (m, 2 H, H-15), 1.41 – 1.27 (m, 16 H, H-14 – H-11/H-6 – H-3), 1.19 (d, $^3J_{17,16}$ = 6.1 Hz, 3 H, H-17)

^{13}C NMR (100 MHz, $CDCl_3$) δ 129.9 (C-9/C-8), 68.2 (C-16), 63.0 (C-1), 39.4 (C-15), 32.8 (C-2), 29.7, 29.6, 29.5, 29.3, 29.2, 29.2 (C-13 – C-11/C-6 – C-4), 27.2 (C-10/C-7), 25.7, 25.7 (C-14/C-3), 23.5 (C-17)

MS (GC-MS, EI) *m*/*z* (%) 270 ($[M]^{+\cdot}$, 0.6), 252 (4.7), 135 (12), 121 (20), 110 (38), 95 (62), 81 (100), 67 (98), 55 (98), 45 (31)

(8*Z*)-1,16-Diazidoheptadec-8-ene (*rac*-57):

Prepared from (8*Z*)-heptadec-8-ene-1,16-diol (*rac*-**56**) (71 mg, 0.26 mmol) as described in chapter 6.2.1.7. After column chromatography, *rac*-**57** was obtained as a colorless oil (75 mg, 0.24 mmol, 90%).

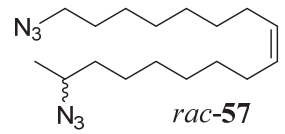

rac-**57**

HRMS *m*/*z* calcd for $C_{17}H_{32}N_6Na$ 343.2581 $[M + Na]^+$, found 343.2578

IR (thin film, cm^{-1}) *v* 3004 (w), 2929 (s), 2856 (s), 2095 (s), 1459 (m), 1379 (w), 1260 (s), 1095 (m), 1018 (m)

^{1}H NMR (400 MHZ, $CDCl_3$) δ 5.42 – 5.31 (m, 2 H, H-9/H-8), 3.43 (m_c, 1 H, H-16), 3.27 (t, $^3J_{1,2}$ = 6.8 Hz, 2 H, H-1), 2.08 – 1.97 (m, 4 H, H-10/H-7), 1.61 (tt, $^3J_{2,3} = {}^3J_{2,1}$ = 6.8 Hz, 2 H, H-2), 1.55 – 1.29 (m, 18 H, H-15 – H-11/H-6 – H-3), 1.25 (d, $^3J_{17,16}$ = 7.0 Hz, 3 H, H-17)

^{13}C NMR (100 MHz, $CDCl_3$) δ 129.9, 129.8 (C-9/C-8), 58.0 (C-16), 51.5 (C-1), 36.2 (C-15), 29.6, 29.6, 29.3, 29.1, 29.1, 29.0 (C-13 – C-11/C-6 – C-4), 28.8 (C-2), 27.1 (C-10/C-7), 26.7 (C-3), 26.0 (C-14), 19.5 (C-17)

(8*Z*)-Heptadec-8-ene-1,16-diamine (*rac*-58):

The C_{17}-harmonine (*rac*-**58**) was synthesized from (8*Z*)-1,16-diazidoheptadec-8-ene (*rac*-**57**) (24 mg, 0.08 mmol) and LAH (22.7 mg, 0.60 mmol) as depicted in chapter 6.2.1.8. *Rac*-**58** was obtained as a slightly yellow oil (22 mg, quant.).

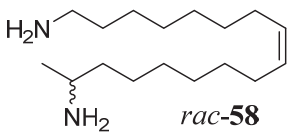

rac-**58**

HRMS *m*/*z* calcd for $C_{17}H_{37}N_2$ 269.2951 $[M + H]^+$, found 269.2951

IR (thin film, cm^{-1}) ν 3338 (m), 3005 (w), 2918 (s), 2850 (s), 1605 (s), 1461 (s), 1392 (m), 1345 (m), 1320 (w)

^{1}H NMR (400 MHZ, $CDCl_3$) δ 5.41 – 5.30 (m, 2 H, H-9/H-8), 2.89 (m_c, 1 H, H-16), 2.70 (t, $^3J_{1,2}$ = 7.0 Hz, 2 H, H-1), 2.06 – 1.96 (m, 4 H, H-10/H-7), 1.72 (brs, 4 H, N-H_2), 1.46 (m_c, 2 H, H-2), 1.39 – 1.27 (m, 18 H, H-15 – H-11/H-6 – H-3), 1.07 (d, $^3J_{17,16}$ = 6.2 Hz, 3 H, H-17)

^{13}C NMR (100 MHz, $CDCl_3$) δ 129.9 (C-9/C-8), 47.0 (C-16), 42.1 (C-1), 40.0 (C-15), 33.6 (C-2), 29.7, 29.7, 29.6, 29.4, 29.3, 29.2 (C-13 – C-11/C-6 – C-4), 27.2 (C-10/C-7), 26.8 (C-3), 26.4 (C-14), 23.8 (C-17)

6.3 Rearing of the Beetles

H. axyridis were collected as fourth (or third) instar larvae and kept in groups of ~ 10 individuals before pupation. Larvae were fed with *Sitotroga* eggs. Eppendorf tubes plugged with cotton were used as water supply. Feed and water were renewed twice a week (Monday and Friday). Each Friday, the larvae were provided with a slice of fresh apple.
H. axyridis beetles were kept in groups of 20 - 30 sorted by their hatching dates. Sufficient water supply was also provided in Eppendorf tubes plugged with cotton. 80% of the beetles were fed with *Sitotroga* eggs twice a week (Monday and Friday) and 20 % were fed with pea aphids three times a week (Monday, Wednesday, Friday). On Fridays, all beetles were offered a slice of fresh apple. A piece of kitchen tissue was placed in each box to encourage oviposition.
Eggs were collected three times a week and placed into separate boxes. Larvae were reared with separation of instars and in small groups.
The boxes of the beetles were cleaned and disinfected every Monday. Therefore, the beetles were moved to new boxes. Larvae boxes were cleaned after pupation when the newly hatched beetles were moved to different boxes.

Larvae and beetle boxes were kept together in a climate chamber to ensure a controlled environment (60% humidity, 22 °C (light), 19 °C (darkness), 16:8 (light:darkness)).

6.4 Hemolymph Analysis

6.4.1 Collection of the Hemolymph

Prior to the collection of the hemolymph it was assured that the beetles had unlimited access to fresh water.

The beetle was stuck with its elytra on adhesive tape placed under the microscope and held in place with a gloved hand. One of its hind legs was cut directly at the metathorax using a pair of micro scissors and the resulting droplet of hemolymph was collected with a pipette tip filled with 10 µl of MeOH. The content of the pipette tip was thoroughly washed into a GC vial filled with 50 µl of MeOH. These 60 µl were split into halves and the solvent and the water content of the hemolymph were removed using a Concentrator*plus* (program: V_{aq},

30 min, 30 °C). The residue was dissolved in 100 µl DCM with *n*-bromodecane (50 µg ml^{-1}) as standard.

6.4.2 Derivatization and GC-MS Analysis

The previously prepared hemolymph samples in 100 µl DCM with *n*-bromodecane were entirely transferred into smaller inserts and 4 µl of MBTFA were added. Then, the vials were placed into a preheated thermo-shaker and derivatized at 60 °C for 1 hour.

GC-MS analyses were executed on a Trace MS using the method "hemolymph analysis" described in chapter 6.1. To avoid contamination from preceding samples, DCM blanks were measured between each hemolymph sample.

6.4.3 Acetonitrile Chemical Ionization Tandem Mass Spectrometry

The collection of the hemolymph was similarly conducted to the procedure described in chapter 6.4.1. However, for AcN-CI-MS/MS experiments, the hemolymph of one beetle was not split into halves but used as one sample. Furthermore, no standard was added. The procedure detailed in chapter 6.4.2 was used for the derivatization with MBTFA.

All AcN-CI-MS/MS experiments were performed with the help of Dr. Tobias Engl in the former laboratory of Dr. Martin Kaltenpoth (Max Planck Research Group Insect Symbioses, Jena). The following equipment and method were used:
CI-GC-MS analyses were conducted on a Varian 240MS ion-trap mass detector with internal ionization configuration coupled to a Varian 450GC (Varian, Inc., Palo Alto, CA, USA). For separation of the compounds a DB-5 ms column (30 m×0.25 mm ID; 0.25 µm df, Agilent, Santa Clara, CA, USA) was used.

CI-GC-MS Method: 45 °C (3 min) - 7.5 °C min^{-1} - 280 °C (4 min) - 10 °C min^{-1} - 300 °C (1 min), inlet T: 250 °C, splitless

Helium (1 ml min^{-1}) served as carrier gas and AcN as reagent gas. The CI spectra were recorded with a mass range of m/z = 90-1000. MS/MS experiments of the $[M+54]^+$ adducts were accomplished with the resonant waveform type for precursor ion excitation (m/z = 526),

an isolation window of m/z = 3, and 20 ms excitation time. The automatic "q" calculator was used for the product ion mass range and the determination of precursor ion excitation energy. An ion-trap temperature of 160 °C and a manifold temperature of 50 °C were used for all CI measurements. Data analyses were performed with a MS Workstation software (version 6.9.3, Varian Inc., Palo Alto, CA, USA).[141]

6.5 Bioactivity Studies

6.5.1 Microbial Growth Inhibition Assays

The microbial growth inhibition assays were conducted with *E. coli* BW25113- and *B. subtilis* DSM 10. The substances which should be tested were dissolved in MeOH and the concentration was adjusted to 10 mM. MeOH was used as a negative control and Ampicillin (1 mM) as a positive control.

First, precultures of *E. coli* and *B. subtilis* were prepared. 5 ml LB-medium were inoculated with bacteria from a cryostock and the cultures were grown for 17 hours at 37 °C (220 rpm). The optical density of the cultures was measured and was adjusted to OD_{600} = 1 with LB-medium.
2 ml of a preculture from the respective bacterial strain were mixed with 48 ml of LB-agar. Next, 2 plates (12 cm × 12 cm) were poured with 25 ml of agar in each plate and left to dry upside down for 2 hours. The agar was pierced with a metal stick to result in 3 × 3 holes with a diameter of 0.5 cm. Each hole was filled with 8 µl of one of the test compound solutions. The standard assay design is shown in the following scheme:

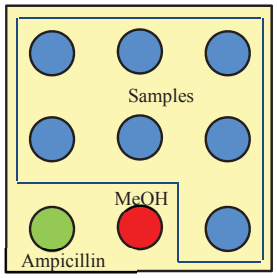

Figure 6.1: Pipetting scheme of the Microbial Growth Inhibiton Assay (mirror-inverted to photographs). Ampicillin as positive control (green), MeOH as negative control (red), test compounds (blue).

The plates were cultivated for 24 hours at 37 °C. Afterwards, the clear inhibition zones were measured in three different directions and the average was calculated.

6.5.2 AChE Inhibition Assays

All required stock solutions and the acetylthiocholine reaction mixture were prepared according to the technical information sheet obtained with the kit (chapter 6.1). However, the overall assay procedure was altered and is described hereafter:

1. To determine the correct concentration range for the inhibition assay, preliminary tests were performed for each substance. Solutions of the possible inhibitor in MeOH were prepared using 6 different concentrations. The concentrations were calculated referring to the final concentration in the wells and were chosen to be within a broad range from $9 \cdot 10^{-4}$ mol l-^{1} to $6 \cdot 10^{-7}$ mol l^{-1} (in-well-concentration). The enzyme solution was diluted to concentrations of 50 mU and 100 mU. Each plate contained 3 blank wells and 3 standard wells to facilitate comparability between plates. There were 3 replicates with 100 mU and 3 replicates with 50 mU enzyme for each inhibitor concentration on each plate.

Table 6.1: Filling of the wells in preliminary tests and AChE inhibition assays.

Blank	5 µl MeOH, 50 µl buffer, 50 µl enzyme (100 mU)
Standard	5 µl MeOH, 50 µl acetylthiocholine reaction mixture, 50 µl enzyme (100 mU)
Assay 100	5 µl inhibitor solution, 50 µl acetylthiocholine reaction mixture, 50 µl enzyme (100 mU)
Assay 50	5 µl inhibitor solution, 50 µl acetylthiocholine reaction mixture, 50 µl enzyme (50 mU)

The preliminary test was conducted as follows: The plate was put on ice and the whole assay was pipetted on ice with exclusion of light. First, MeOH or the inhibitor solution was pipetted in the wells directly followed by the enzyme solution or buffer. This mixture was incubated for 10 minutes on ice before the acetylthiocholine reaction mixture was added. The plate was again incubated for 5 minutes at room temperature and then the absorbance increase was monitored every minute for 1 hour using a microplate reader at 410 nm.

2. For preliminary tests an approximate value of the IC_{50} was calculated using Microsoft Excel and the GraphPad Prism software: First, the mean of the blank values was calculated and subtracted from all other values. Then, the mean of the standard wells was divided by the mean of the standard wells of the first plate measured to obtain comparability between plates. All values were multiplied by this factor. The absorbance of each assay well was then plotted

against the time and a linear regression curve fit of the data points from minute 0 to minute 20 (linear range) resulted in the change of absorbance per minute (Δabs./min). This change of absorbance was plotted against the logarithmic concentration of the possible inhibitor. A sigmoidal dose-response fit revealed finally the IC_{50} value.[129]

3. The AChE inhibition assay was conducted according to the results from the preliminary testing. 12 methanolic solutions of the possible inhibitor were prepared with in-well-concentrations around the preliminarily calculated IC_{50} value. The filling of the wells, the replicate number per inhibitor concentration and the blank and standard well quantity was kept the same as in the preliminary test. The pipetting scheme for all AChE inhibiton assays is shown here:

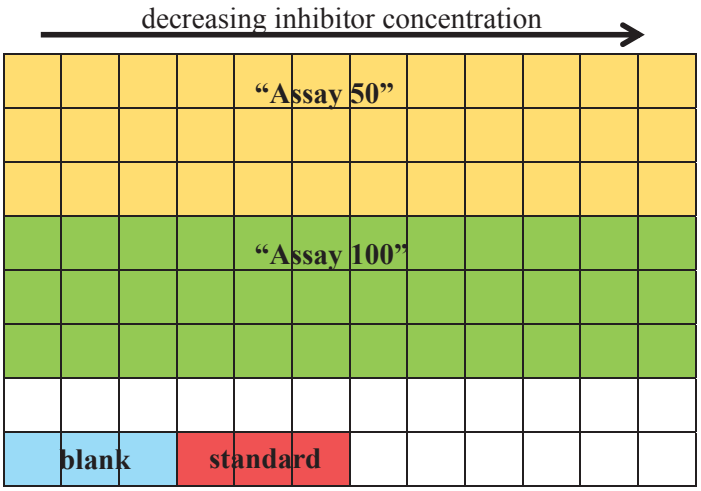

Figure 6.2: Pipetting scheme for AChE inhibiton assays. Preliminary tests had the same pipetting structure but less inhibitor concentrations.

The inhibition assay was likewise performed as the preliminary test described above. After measurement of the absorbance increase per minute the IC_{50} value was calculated as detailed in 2. using Microsoft Excel and the GraphPad Prism software.

6.5.3 Antileishmanial Activity

All assays with the *L. major* parasite were performed by Dr. Anita Masic and Martina Schultheis in the laboratories of the former research group of Dr. Uta Schurigt (Institute for Molecular Infection Biology, Würzburg) and were already partly published in "Efficient synthesis of (*R*)-harmonine – the toxic principle of the multicolored Asian lady beetle (*Harmonia axyridis*)" (authors: Nagel, N. C. *et al*.).[55] The following methods are cited thereof.

Antileishmanial activity. The virulent *L. major* isolate (MHOM/IL/81/FE/BNI) and Luciferase-transgenic (Luc-tg.) *L. major* were maintained by continuous passage in female BALB/c mice. *L. major* amastigotes were isolated from lesions as described previously[142, 143] and promastigotes were grown *in vitro* in blood-agar cultures at 27 °C, 5% CO2, and 95% humidity. AlamarBlue assays for the determination of antileishmanial activities against *L. major* promastigotes and BMDM cytotoxicity and Britelite plus (PerkinElmer, Waltham, MA, USA) assays against intracellular Luc-tg. *L. major* amastigotes were performed as previously reported[143] [55].

Diff-Quick staining for transmitted light microscopy. After incubation for 6 h, 10 h, and 24 h in the presence of 30 μM harmonine or 1% DMSO as solvent control, *L. major* promastigotes were harvested and centrifuged in a Cytospin 3 centrifuge (Shandon, Frankfurt, Germany) on microscopic slides. Cytospin preparations were stained using the Differential Quick Stain (Diff-Quick) dye (Medion Diagnostics AG, Düdingen, Switzerland), according to the manufacturers' protocol. Diff-Quick stains the leishmanial nuclei and the kinetoplasts dark purple and the cytoplasm light purple allowing the observation of phenotypic changes within the parasite. Stained cells were analyzed by transmitted light microscopy under a 50 × objective on a Nikon ECLIPSE 50i microscope equipped with a digital camera (Nikon, Tokyo, Japan). The images were proceeded using NIS Elements D software (Nikon).[55]

Determination of cell death phenotype by flow cytometric analysis. *L. major* promastigotes were either treated for 6 h, 10 h, and 24 h with 30 µM harmonine or 1% DMSO as solvent control. Cell staining was performed using an Annexin V-FITC Apoptosis detection kit (Sigma-Aldrich, Saint Louis, MO, USA) according to the manufacturers´ protocol. Stained samples were immediately analyzed by flow cytometry using MACS Quant Analyzer (Miltenyi Biotech, Bergisch Gladbach, Germany).[55]

6.5.4 Identification of "AChE-like Proteins" in *L. major* and Docking Studies

The identification of putative "AChE-like proteins" in *L. major* was performed with the help of Ding Wang (MPI CE, Jena).

First the protein sequence of the AChE from *Caenorhabditis elegans* (ace-1, sequence ID: NP_510660.1, length: 620) was blasted against the protein sequence of *L. major* strain Friedlin (taxid: 347515). The BLAST revealed 2 possible candidates:

1. Conserved hypothetical protein (sequence ID: XP_001681951.1, length: 1022, identities: 29%, query cover: 16%)
2. Putative ecotin (sequence ID: XP_001681950.1, length: 761, identities: 27%, query cover: 18%)

Modeling and docking studies were performed by PD Dr. Wolfgang Brandt (Leibniz Institute of Plant Biochemistry, Halle).

YASARA version 14.7.17[144] was used for homology modeling of the proteins. After search for templates in the protein database[140] 23 models were created based on alternative sequence alignments including secondary structure predictions and comparisons with found appropriate X-ray templates.

Based on these most favored templates, a final hybrid model was created by replacing some small better folded fragments (loops) from other models. The model (after quality analysis, blow) based on 1qz3 appeared as best one (**Fig. 6.3**).

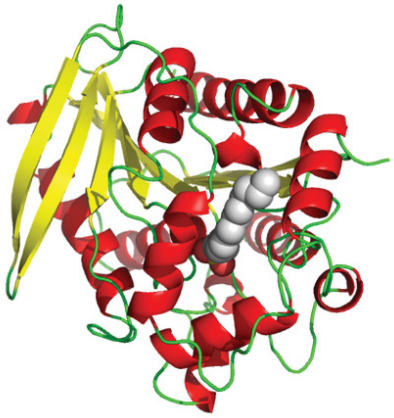

Figure 6.3: Template of the X-ray structure of 1qz3 (crystal structure of M211S/R215L mutant of carboxylesterase EST2; complexed with hexadecanesulfonate).[145]

The quality of the resulting homology models was evaluated using PROCHECK[146] and ProSA.[147, 148] Only models of excellent quality (more than 87% of the residues being in the most favored region of the Ramachandran plot and two outliers; ProSA energy graphs all in negative range and calculated z-scores in the range of natively folded proteins) were used further on.

The substrates were docked using the molecular modeling environment program MOE 2014.09 (https://www.chemcomp.com/). All models with docked substrates were refined by energy minimization using the MMFF94[149] force field implemented in MOE.

7 References

1. Lewie, C.R., *Ladybug, Ladybug: What's in a Name?* The Coleopterists Bulletin, 1960. **14**(1): p. 21-25.

2. Seago, A.E., *et al*., *Phylogeny, classification and evolution of ladybird beetles (Coleoptera: Coccinellidae) based on simultaneous analysis of molecular and morphological data.* Molecular Phylogenetics and Evolution, 2011. **60**(1): p. 137-151.

3. Kovář, I., *Morphology and Anatomy*, in *Ecology of Coccinellidae*, I. Hodek and A. Honěk, Editors. 1996, Kluwer Academic Publishers. p. 1-18.

4. Britton, G., *et al*., *Pigmentation of the ladybird beetle Coccinella septempunctata by carotenoids not of plant origin.* Nature, 1977. **266**(5597): p. 49-50.

5. Hodek, I. and A. Honěk, *Distribution in Habitats*, in *Ecology of Coccinellidae*, I. Hodek and A. Honěk, Editors. 1996, Kluwer Academic Publishers. p. 95-142.

6. Hodek, I., *Food Relationships*, in *Ecology of Coccinellidae*, I. Hodek and A. Honěk, Editors. 1996, Kluwer Academic Publishers. p. 143-238.

7. Waldbauer, G.P. and S. Friedman, *Self-Selection of Optimal Diets by Insects.* Annual Review of Entomology, 1991. **36**(1): p. 43-63.

8. Martini, X., *et al*., *Evolution of cannibalism and female's response to oviposition-deterring pheromone in aphidophagous predators.* Journal of Animal Ecology, 2009. **78**(5): p. 964-972.

9. Meisner, M.H., J.P. Harmon, and A.R. Ives, *Response of Coccinellid Larvae to Conspecific and Heterospecific Larval Tracks: A Mechanism That Reduces Cannibalism and Intraguild Predation.* Environmental Entomology, 2011. **40**(1): p. 103-110.

10. Yasuda, H., *et al*., *Relationships Between Attack and Escape Rates, Cannibalism, and Intraguild Predation in Larvae of Two Predatory Ladybirds.* Journal of Insect Behavior, 2001. **14**(3): p. 373-384.

11. Kenis, M., *et al*., *Current and potential management strategies against Harmonia axyridis.* BioControl, 2008. **53**(1): p. 235-252.

12. de Clercq, P., *et al*., *Interaction between Podisus maculiventris and Harmonia axyridis, two predators used in augmentative biological control in greenhouse crops.* BioControl, 2003. **48**: p. 39-55.

13. Yasuda, H. and T. Kimura, *Interspecific interactions in a tri-trophic arthropod system: effects of a spider on the survival of larvae of three predatory ladybirds in relation to aphids.* Entomologia Experimentalis et Applicata, 2001. **98**(1): p. 17-25.

14. Obrycki, J.J., M.J. Tauber, and C.A. Tauber, *Perilitus coccinellae (Hymenoptera: Braconidae): Parasitization and Development in Relation to Host-stage Attacked.* Annals of the Entomological Society of America, 1985. **78**(6): p. 852-854.

15. Shapiro-Ilan, D.I. and T.E. Cottrell, *Susceptibility of lady beetles (Coleoptera: Coccinellidae) to entomopathogenic nematodes.* Journal of Invertebrate Pathology, 2005. **89**(2): p. 150-156.

16. Roy, H.E., *et al*., *BIZARRE INTERACTIONS AND ENDGAMES: Entomopathogenic Fungi and Their Arthropod Hosts.* Annual Review of Entomology, 2006. **51**(1): p. 331-357.

17. Roy, H., *et al*., *Interactions between the fungal pathogen Beauveria bassiana and three species of coccinellid: Harmonia axyridis, Coccinella septempunctata and Adalia bipunctata.* BioControl, 2008. **53**(1): p. 265-276.

18. Rogers, S.M. and S.J. Simpson, *Thanatosis.* Current Biology, 2014. **24**(21): p. R1031-R1033.

19. Ceryngier, P., *Enemies of Coccinellidae*, in *Ecology of Coccinellidae*, I. Hodek and A. Honěk, Editors. 1996, Kluwer Academic Publishers. p. 319-350.

20. Al Abassi, S., *et al*., *Ladybird beetle odour identified and found to be responsible for attraction between adults.* CMLS, Cellular and Molecular Life Sciences, 1998. **54**(8): p. 876-879.

21. Galvan, T.L., S. Kells, and W.D. Hutchison, *Determination of 3-Alkyl-2-methoxypyrazines in Lady Beetle-Infested Wine by Solid-Phase Microextraction Headspace Sampling.* Journal of Agricultural and Food Chemistry, 2008. **56**(3): p. 1065-1071.

22. Daloze, D., J.-C. Braekman, and J. Pasteels, *Ladybird defence alkaloids: Structural, chemotaxonomic and biosynthetic aspects (Col.: Coccinellidae).* Chemoecology, 1994. **5/6**(3/4): p. 173-183.

23. Tursch, B., *et al*., *A defense alkaloid in a carnivorous beetle.* Experientia, 1971. **27**(12): p. 1380-1381.

24. Tursch, B., *et al*., *Chemical ecology of arthropods, VI. Adaline, a novel alkaloid from Adalia bipunctata L, (Coleoptera, Coccinellidae).* Tetrahedron Letters, 1973. **14**(3): p. 201-202.

25. Ayer, W.A., *et al*., *Defensive substances of Coccinella transversoguttata and Hippodamia caseyi, ladybugs indigenous to western Canada.* Canadian Journal of Chemistry, 1976. **54**(11): p. 1807-1813.

26. Braconnier, M.F., *et al*., *(Z)-1,17-diaminooctadec-9-ene, a novel aliphatic diamine from coccinellidae.* Experientia, 1985. **41**(4): p. 519-520.

27. Röhrich, C.R., *et al*., *Harmonine, a defence compound from the harlequin ladybird, inhibits mycobacterial growth and demonstrates multi-stage antimalarial activity.* Biology Letters, 2012. **8**(2): p. 308-311.

28. Alam, N., *et al*., *A New Alkaloid from Two Coccinellid Beetles Harmonia axyridis and Aiolocaria hexaspilota.* Bulletin of the Korean Chemical Society, 2002. **23**(3): p. 497-499.

29. Schroeder, F.C., *et al*., *Polyazamacrolides from ladybird beetles: Ring-size selective oligomerization.* Proceedings of the National Academy of Sciences, 1998. **95**(23): p. 13387-13391.

30. Vilcinskas, A., *et al*., *Invasive Harlequin Ladybird Carries Biological Weapons Against Native Competitors.* Science, 2013. **340**(6134): p. 862-863.

31. Koch, R.L., *The multicolored Asian lady beetle, Harmonia axyridis: A review of its biology, uses in biological control, and non-target impacts.* Journal of Insect Science, 2003. **3**(32): p. 1-16.

32. Kovář, I., *Phylogeny*, in *Ecology of Coccinellidae*, I. Hodek and A. Honěk, Editors. 1996, Kluwer Academic Publishers. p. 19-31.

33. Lee, D.H., *et al*., *Molecular identification of AFLP fragments associated with elytra color variation of the Asian ladybird beetle, Harmonia axyridis (Coleoptera: Coccinellidae).* Journal of Asia-Pacific Entomology, 2011. **14**(1): p. 99-105.

34. Komai, T., *Genetics of ladybeetles.* Advances in Genetics, 1956. **8**: p. 155–189.

35. Stewart, L.A. and A.F.G. Dixon, *Why Big Species of Ladybird Beetles are Not Melanic.* Functional Ecology, 1989. **3**(2): p. 165-171.

36. Hodek, I., *Life History and Biological Properties*, in *Biology of Coccinellidae*, J. Mařan and K. Hůrka, Editors. 1973, Dr. W. JUNK N. V. p. 70-76.

37. Chapin, J.B. and V.A. Brou, *Harmonia axyridis (PALLAS), the third species of the genus to be found in the United States (COLEOPTERA: COCCINELLIDAE).* Proceedings of the Entomological Society of Washington, 1991. **93**(3): p. 630-635.

38. Tedders, W.L. and P.W. Schaefer, *Release And Establishment Of Harmonia axyridis (Coleoptera, Coccinellidae) In The Southeastern United states.* Entomological News, 1994. **105**(4): p. 228-243.

39. Lucas, É., D. Coderre, and C. Vincent, *Voracity and feeding preferences of two aphidophagous coccinellids on Aphis citricola and Tetranychus urticae.* Entomologia Experimentalis et Applicata, 1997. **85**(2): p. 151-159.

40. Brown, P.M.J., *et al*., *Harmonia axyridis in Europe: spread and distribution of a non-native coccinellid.* BioControl, 2008. **53**(1): p. 5-21.

41. de Almeida, L.M. and V.B. da Silva, *First record of Harmonia axyridis (Pallas) (Coleoptera, Coccinellidae): a lady beetle native to the Palaearctic region.* Revista Brasileira de Zoologia, 2002. **19**: p. 941-944 (abstract in English).

42. Ferran, A., *et al*., *Introduction and release of the coccinellid Harmonia axyridis Pallas for controlling Aphis craccivora Koch on faba beans in Egypt.* Egyptian Journal of Biological Pest Control, 2000. **10**: p. 129-136 (abstract only).

43. Stals, R. and G. Prinsloo, *Discovery of an alien invasive, predatory insect in South Africa: the multicoloured Asian ladybird beetle,Harmonia axyridis (Pallas) (Coleoptera: Coccinellidae): research in action.* South African Journal of Science, 2007. **103**(3/4): p. 123-126.

44. Roy, H., P. Brown, and M. Majerus, *HARMONIA AXYRIDIS: A SUCCESSFUL BIOCONTROL AGENT OR AN INVASIVE THREAT?*, in *An Ecological and Societal Approach to Biological Control*, J. Eilenberg and H.M.T. Hokkanen, Editors. 2006, Springer Netherlands. p. 295-309.

45. Brown, P.J., *et al*., *The global spread of Harmonia axyridis (Coleoptera: Coccinellidae): distribution, dispersal and routes of invasion.* BioControl, 2011. **56**(4): p. 623-641.

46. Lombaert, E., *et al*., *Bridgehead Effect in the Worldwide Invasion of the Biocontrol Harlequin Ladybird.* PLoS ONE, 2010. **5**(3): p. e9743.

47. Koch, R. and T. Galvan, *Bad side of a good beetle: the North American experience with Harmonia axyridis*, in *From Biological Control to Invasion: the Ladybird Harmonia axyridis as a Model Species*, H. Roy and E. Wajnberg, Editors. 2008, Springer Netherlands. p. 23-35.

48. Nalepa, C.A., G.G. Kennedy, and C. Brownie, *Role of Visual Contrast in the Alighting Behavior of Harmonia axyridis (Coleoptera: Coccinellidae) at Overwintering Sites.* Environmental Entomology, 2005. **34**(2): p. 425-431.

49. van Lenteren, J.C., *et al*., *Environmental risk assessment of exotic natural enemies used in inundative biological control.* BioControl, 2003. **48**(1): p. 3-38.

50. Roy, H. and E. Wajnberg, *From biological control to invasion: the ladybird Harmonia axyridis as a model species.* BioControl, 2008. **53**(1): p. 1-4.

51. Pasteels, J.M., *et al*., *Distribution et activités des alcaloïdes défensifs des Coccinellidae.* Journal of Insect Physiology, 1973. **19**(9): p. 1771-1784.

52. Braconnier, M.F., J.C. Braekman, and D. Daloze, *Synthesis of the Racemic Form of (Z)-1, 17-Diaminooctadec-9-Ene, An Aliphatic Diamine From Coccinellidae, Determination of the Absolute Configuration of the (+)-Naturally-Occurring Antipode.* Bulletin des Sociétés Chimiques Belges, 1985. **94**(8): p. 605-613.

53. Enders, D. and D. Bartzen, *Enantioselective total synthesis of harmonine, a defence alkaloid of ladybugs (Coleoptera: Coccinellidae).* Liebigs Annalen der Chemie, 1991. **1991**(6): p. 569-574.

54. Philkhana, S.C., *et al*., *Access to harmonine, a chemical weapon of ladybird beetles.* RSC Advances, 2014. **4**(58): p. 30923-30926.

55. Nagel, N.C., *et al*., *Efficient synthesis of (R)-harmonine - the toxic principle of the multicolored Asian lady beetle (Harmonia axyridis).* Organic & Biomolecular Chemistry, 2015. **13**(18): p. 5139-5146.

56. Abel, S.-A.G., *et al*., *Complete Stereocontrol in the Synthesis of Harmonine and Novel Analogues Facilitated by a Grubbs Z-Selective Cross-Metathesis Catalyst.* Australian Journal of Chemistry, 2015. **68**(12): p. 1815-1820.

57. Haulotte, E., P. Laurent, and J.-C. Braekman, *Biosynthesis of Defensive Coccinellidae Alkaloids: Incorporation of Fatty Acids in Adaline, Coccinelline, and Harmonine.* European Journal of Organic Chemistry, 2012. **2012**(10): p. 1907-1912.

58. Laurent, P., *et al*., *Biosynthesis of Defensive Compounds from Beetles and Ants.* European Journal of Organic Chemistry, 2003. **2003**(15): p. 2733-2743.

59. Tursch, B., *et al*., *Chemical ecology of arthropods—X.* Tetrahedron, 1975. **31**(13): p. 1541-1543.

60. Laurent, P., *et al*., *Biosynthetic studies on adaline and adalinine, two alkaloids from ladybird beetles (Coleoptera: Coccinellidae).* Tetrahedron, 2001. **57**(16): p. 3403-3412.

61. Ivarsson, P., G.J. Blomquist, and S.J. Seybold, *In Vitro Production of the Pheromone Intermediates Ipsdienone and Ipsenone by the Bark Beetles Ips pini (Say) and I. paraconfusus Lanier (Coleoptera: Scolytidae).* Naturwissenschaften, 1997. **84**(10): p. 454-457.

62. Laurent, P., *et al*., *In vitro production of adaline and coccinelline, two defensive alkaloids from ladybird beetles (Coleoptera: Coccinellidae).* Insect Biochemistry and Molecular Biology, 2002. **32**(9): p. 1017-1023.

63. Vilcinskas, A., *et al*., *Evolutionary ecology of microsporidia associated with the invasive ladybird Harmonia axyridis.* Insect Science, 2015. **22**(3): p. 313-324.

64. Vilcinskas, A. and H. Schmidtberg, *Der Asiatische Marienkäfer als Modell.* Biologie in unserer Zeit, 2014. **44**(6): p. 386-391.

65. Abrams, P., *et al*., *Muscarinic receptors: their distribution and function in body systems, and the implications for treating overactive bladder.* British Journal of Pharmacology, 2006. **148**(5): p. 565-578.

66. Jones, C.K., N. Byun, and M. Bubser, *Muscarinic and Nicotinic Acetylcholine Receptor Agonists and Allosteric Modulators for the Treatment of Schizophrenia.* Neuropsychopharmacology, 2012. **37**(1): p. 16-42.

67. Quinn, D.M., *Acetylcholinesterase: enzyme structure, reaction dynamics, and virtual transition states.* Chemical Reviews, 1987. **87**(5): p. 955-979.

68. Soreq, H. and S. Seidman, *Acetylcholinesterase - new roles for an old actor.* Nature Reviews Neuroscience, 2001. **2**(4): p. 294-302.

69. Silman, I. and J.L. Sussman, *Acetylcholinesterase: How is structure related to function?* Chemico-Biological Interactions, 2008. **175**(1–3): p. 3-10.

70. Bon, S., M. Vigny, and J. Massoulié, *Asymmetric and globular forms of acetylcholinesterase in mammals and birds.* Proceedings of the National Academy of Sciences of the United States of America, 1979. **76**(6): p. 2546-2550.

71. Dvir, H., *et al*., *Acetylcholinesterase: From 3D structure to function.* Chemico-Biological Interactions, 2010. **187**(1–3): p. 10-22.

72. Sussman, J., *et al*., *Atomic structure of acetylcholinesterase from Torpedo californica: a prototypic acetylcholine-binding protein.* Science, 1991. **253**(5022): p. 872-879.

73. Sussman, J.L., M. Harel, and I. Silman, *Three-dimensional structure of acetylcholinesterase and of its complexes with anticholinesterase drugs.* Chemico-Biological Interactions, 1993. **87**(1–3): p. 187-197.

74. Rosenberry, T.L., *Acetylcholinesterase*, in *Advances in Enzymology and Related Areas of Molecular Biology*. 1975, John Wiley & Sons, Inc. p. 103-218.

75. Francis, P.T., *et al*., *The cholinergic hypothesis of Alzheimer's disease: a review of progress.* Journal of Neurology, Neurosurgery & Psychiatry, 1999. **66**(2): p. 137-147.

76. Van Marum, R.J., *Current and future therapy in Alzheimer's disease.* Fundamental & Clinical Pharmacology, 2008. **22**(3): p. 265-274.

77. Nikolaev, A., *et al*., *APP binds DR6 to trigger axon pruning and neuron death via distinct caspases.* Nature, 2009. **457**(7232): p. 981-990.

78. Kitisripanya, N., *et al*., *Binding of huperzine A and galanthamine to acetylcholinesterase, based on ONIOM method.* Nanomedicine: Nanotechnology, Biology, and Medicine, 2011. **7**(1): p. 60-68.

79. Bern, C., J.H. Maguire, and J. Alvar, *Complexities of Assessing the Disease Burden Attributable to Leishmaniasis.* PLoS Neglected Tropical Diseases, 2008. **2**(10): p. e313.

80. WHO, *Control of the leishmaniases. Report of a WHO Expert Committee.* World Health Organization Technical Report Series, 1990. **793**: p. 1-158.

81. Van Assche, T., *et al*., *Leishmania–macrophage interactions: Insights into the redox biology.* Free Radical Biology and Medicine, 2011. **51**(2): p. 337-351.

82. de Vries, H.J., S.H. Reedijk, and H.D. Schallig, *Cutaneous Leishmaniasis: Recent Developments in Diagnosis and Management.* American Journal of Clinical Dermatology, 2015. **16**(2): p. 99-109.

83. WHO, *Control of the leishmaniases. Report of a WHO Expert Committee.* World Health Organization Technical Report Series, 2010. **949**: p. 1-186.

84. McGwire, B.S. and A.R. Satoskar, *Leishmaniasis: clinical syndromes and treatment.* QJM: An International Journal of Medicine, 2014. **107**(1): p. 7-14.

85. Kedzierski, L., *Leishmaniasis Vaccine: Where are We Today?* Journal of Global Infectious Diseases, 2010. **2**(2): p. 177-185.

86. Bailey, M.S. and D.N.J. Lockwood, *Cutaneous leishmaniasis.* Clinics in Dermatology, 2007. **25**(2): p. 203-211.

87. Marsden, P.D., *Mucosal leishmaniasis ("espundia" Escomel, 1911).* Transactions of The Royal Society of Tropical Medicine and Hygiene, 1986. **80**(6): p. 859-876.

88. Kaye, P. and P. Scott, *Leishmaniasis: complexity at the host–pathogen interface.* Nature Reviews Microbiology, 2011. **9**(8): p. 604-615.

89. Mathers, C.D., M. Ezzati, and A.D. Lopez, *Measuring the Burden of Neglected Tropical Diseases: The Global Burden of Disease Framework.* PLoS Neglected Tropical Diseases, 2007. **1**(2): p. e114.

90. Alvar, J., S. Yactayo, and C. Bern, *Leishmaniasis and poverty.* Trends in Parasitology, 2006. **22**(12): p. 552-557.

91. Ranjan, A., *et al*., *Risk factors for Indian kala-azar.* The American Journal of Tropical Medicine and Hygiene, 2005. **73**(1): p. 74-78.

92. Cerf, B.J., *et al*., *Malnutrition as a risk factor for severe visceral leishmaniasis.* The Journal of Infectious Diseases, 1987. **156**(6): p. 1030-1033.

93. Hussain, H., *et al*., *Fruitful Decade for Antileishmanial Compounds from 2002 to Late 2011.* Chemical Reviews, 2014. **114**(20): p. 10369-10428.

94. Sangshetti, J.N., *et al*., *Antileishmanial drug discovery: comprehensive review of the last 10 years.* Royal Society of Chemistry Advances, 2015. **5**(41): p. 32376-32415.

95. Dorlo, T.P.C., *et al*., *Miltefosine: a review of its pharmacology and therapeutic efficacy in the treatment of leishmaniasis.* Journal of Antimicrobial Chemotherapy, 2012. **67**(11): p. 2576-2597.

96. Seifert, K., *Structures, Targets and Recent Approaches in Anti-Leishmanial Drug Discovery and Development.* The Open Medicinal Chemistry Journal, 2011. **5**: p. 31-39.

97. Sindermann, H. and J. Engel, *Development of miltefosine as an oral treatment for leishmaniasis.* Transactions of The Royal Society of Tropical Medicine and Hygiene, 2006. **100**(Supplement 1): p. S17-S20.

98. Olliaro, P., *et al*., *Cost-effectiveness projections of single and combination therapies for visceral leishmaniasis in Bihar, India.* Tropical Medicine & International Health: TM & IH, 2009. **14**(8): p. 918-925.

99. Sundar, S., *et al*., *Injectable paromomycin for Visceral leishmaniasis in India.* The New England Journal of Medicine, 2007. **356**(25): p. 2571-2581.

100. Sundar, S., *et al*., *Failure of pentavalent antimony in visceral leishmaniasis in India: report from the center of the Indian epidemic.* Clinical Infectious Diseases, 2000. **31**(4): p. 1104-1107.

101. Krengel, S., *et al*., *A Comparative Study on Effects of Normal Versus Elevated Temperatures During Preimaginal and Young Adult Period on Body Weight and Fat Body Content of Mature Coccinella septempunctata and Harmonia axyridis (Coleoptera: Coccinellidae).* Environmental Entomology, 2012. **41**(3): p. 676-687.

102. Sloggett, J.J., J.J. Obrycki, and K.F. Haynes, *Identification and quantification of predation: novel use of gas chromatography–mass spectrometric analysis of prey alkaloid markers.* Functional Ecology, 2009. **23**(2): p. 416-426.

103. Kajita, Y., *et al*., *Intraspecific alkaloid variation in ladybird eggs and its effects on con- and hetero-specific intraguild predators.* Oecologia, 2010. **163**(2): p. 313-322.

104. Budzikiewicz, H., C. Djerassi, and D.H. Williams, *Mass Spectrometry of Organic Compounds*. 1967: Holden-Day, Inc.

105. Durieux, D., *et al*., *Substrate Marking by an Invasive Ladybeetle: Seasonal Changes in Hydrocarbon Composition and Behavioral Responses.* PLoS ONE, 2013. **8**(4): p. e61124.

106. Oldham, N.J. and A. Svatoš, *Determination of the double bond position in functionalized monoenes by chemical ionization ion-trap mass spectrometry using acetonitrile as a reagent gas.* Rapid Communications in Mass Spectrometry, 1999. **13**(5): p. 331-336.

107. Van Pelt, C.K. and J.T. Brenna, *Acetonitrile Chemical Ionization Tandem Mass Spectrometry To Locate Double Bonds in Polyunsaturated Fatty Acid Methyl Esters.* Analytical Chemistry, 1999. **71**(10): p. 1981-1989.

108. Van Pelt, C.K., B.K. Carpenter, and J.T. Brenna, *Studies of structure and mechanism in acetonitrile chemical ionization tandem mass spectrometry of polyunsaturated fatty acid methyl esters.* Journal of the American Society for Mass Spectrometry, 1999. **10**(12): p. 1253-1262.

109. Michaud, A.L., *et al*., *Double bond localization in minor homoallylic fatty acid methyl esters using acetonitrile chemical ionization tandem mass spectrometry.* Analytical Biochemistry, 2002. **307**(2): p. 348-360.

110. Michaud, A.L., *et al*., *On the formation of conjugated linoleic acid diagnostic ions with acetonitrile chemical ionization tandem mass spectrometry.* Rapid Communications in Mass Spectrometry, 2005. **19**(3): p. 363-368.

111. van Buijtenen, J., *et al*., *Switching from S- to R-Selectivity in the Candida antarctica Lipase B-Catalyzed Ring-Opening of ω-Methylated Lactones: Tuning Polymerizations by Ring Size.* Journal of the American Chemical Society, 2007. **129**(23): p. 7393-7398.

112. Yang, Y., *et al*., *Synthesis, Crystal Structure, and Resolution of [10](1,6)Pyrenophane: An Inherently Chiral [n]Cyclophane.* The Journal of Organic Chemistry, 2011. **77**(1): p. 57-67.

113. Woo, S.H., *et al*., *Structurally Simple Trichostatin A-Like Straight Chain Hydroxamates as Potent Histone Deacetylase Inhibitors.* Journal of Medicinal Chemistry, 2002. **45**(13): p. 2877-2885.

114. Boland, W., P. Ney, and L. Jaenicke, *"One-Pot" Conversion of Carboxylic Acid Esters and Lactones to Olefinic Compounds.* Synthesis, 1980. **1980**(12): p. 1015-1017.

115. Byrne, P.A. and D.G. Gilheany, *The modern interpretation of the Wittig reaction mechanism.* Chemical Society Reviews, 2013. **42**(16): p. 6670-6696.

116. Schlosser, M. and K.F. Christmann, *Olefinierungen mit Phosphor-Yliden, I. Mechanismus und Stereochemie der Wittig-Reaktion.* Justus Liebigs Annalen der Chemie, 1967. **708**(1): p. 1-35.

117. Ooi, T., Y. Uematsu, and K. Maruoka, *New, Improved Procedure for the Synthesis of Structurally Diverse N-Spiro C2-Symmetric Chiral Quaternary Ammonium Bromides.* The Journal of Organic Chemistry, 2003. **68**(11): p. 4576-4578.

118. Jiao, L., E. Herdtweck, and T. Bach, *Pd(II)-Catalyzed Regioselective 2-Alkylation of Indoles via a Norbornene-Mediated C–H Activation: Mechanism and Applications.* Journal of the American Chemical Society, 2012. **134**(35): p. 14563-14572.

119. Veitch, G.E., K.L. Bridgwood, and S.V. Ley, *Magnesium Nitride as a Convenient Source of Ammonia: Preparation of Primary Amides.* Organic Letters, 2008. **10**(16): p. 3623-3625.

120. Csíki, Z. and P. Fügedi, *Synthesis of glycosaminoglycan oligosaccharides. Part 4: Synthesis of aza-l-iduronic acid-containing analogs of heparan sulfate oligosaccharides as heparanase inhibitors.* Tetrahedron, 2010. **66**(39): p. 7821-7837.

121. Fouque, E. and G. Rousseau, *Enzymatic Resolution of Medium-Ring Lactones. Synthesis of (S)-(+)-Phoracantholide I.* Synthesis, 1989. **1989**(09): p. 661-666.

122. Inanaga, J., *et al*., *A Rapid Esterification by Means of Mixed Anhydride and Its Application to Large-ring Lactonization.* Bulletin of the Chemical Society of Japan, 1979. **52**(7): p. 1989-1993.

123. Shiina, I., *et al*., *Stereoselective Total Synthesis of the Proposed Structure of 2-Epibotcinolide.* Organic Letters, 2006. **8**(23): p. 5279-5282.

124. Dalby, S.M., J. Goodwin-Tindall, and I. Paterson, *Total Synthesis of (−)-Rhizopodin.* Angewandte Chemie International Edition, 2013. **52**(25): p. 6517-6521.

125. Ohba, Y., *et al*., *A Highly Efficient Macrolactonization Method via Ethoxyvinyl Ester.* Chemistry – A European Journal, 2009. **15**(14): p. 3526-3537.

126. Mayer, F., *The Prokaryotic Cell*, in *Biology of the Prokaryotes*, J.W. Lengeler, G. Drews, and H.G. Schlegel, Editors. 1999, Georg Thieme Verlag. p. 20-47.

127. Salton, M.R.J., *The Bacterial Cell Envelope - a Historic Perspective*, in *Bacterial Cell Wall*, J.M. Ghuysen and R. Hakenbeck, Editors. 1994, Elsevier Science B.V. p. 1-22.

128. Ellman, G.L., *et al*., *A new and rapid colorimetric determination of acetylcholinesterase activity.* Biochemical Pharmacology, 1961. **7**(2): p. 88-95.

129. Järvinen, P., *et al*., *Potency determinations of acetylcholinesterase inhibitors using Ellman's reaction-based assay in screening: Effect of assay variants.* Analytical Biochemistry, 2011. **408**(1): p. 166-168.

130. Hong, S.-B. and F.M. Raushel, *Stereochemical Constraints on the Substrate Specificity of Phosphotriesterase.* Biochemistry, 1999. **38**(4): p. 1159-1165.

131. Benschop, H.P. and L.P.A. De Jong, *Nerve agent stereoisomers: analysis, isolation and toxicology.* Accounts of Chemical Research, 1988. **21**(10): p. 368-374.

132. Fang, L., *et al*., *Active site gating and substrate specificity of butyrylcholinesterase and acetylcholinesterase: insights from molecular dynamics simulations.* The Journal of Physical Chemistry B, 2011. **115**(27): p. 8797-8805.

133. Alvar, J., *et al*., *Leishmaniasis worldwide and global estimates of its incidence.* PLoS One, 2012. **7**(5): p. e35671.

134. Croft, S.L., S. Sundar, and A.H. Fairlamb, *Drug resistance in leishmaniasis.* Clinical microbiology reviews, 2006. **19**(1): p. 111-126.

135. Glaser, J., *et al*., *Antileishmanial Lead Structures from Nature: Analysis of Structure-Activity Relationships of a Compound Library Derived from Caffeic Acid Bornyl Ester.* Molecules, 2014. **19**(2): p. 1394-1410.

136. Nwaka, S. and A. Hudson, *Innovative lead discovery strategies for tropical diseases.* Nature reviews. Drug discovery, 2006. **5**(11): p. 941-955.

137. Vermes, I., *et al*., *A novel assay for apoptosis. Flow cytometric detection of phosphatidylserine expression on early apoptotic cells using fluorescein labelled Annexin V.* Journal of immunological methods, 1995. **184**(1): p. 39-51.

138. Zhang, G., *et al*., *Early detection of apoptosis using a fluorescent conjugate of annexin V.* Biotechniques, 1997. **23**(3): p. 525-531.

139. Mijares, A., *et al*., *Immune detection of acetylcholinesterase in subcellular compartments of Trypanosoma evansi.* Parasitology Research, 2011. **108**(1): p. 1-5.

140. Berman, H.M., *et al*., *The Protein Data Bank.* Nucleic Acids Research, 2000. **28**(1): p. 235-242.

141. Kroiss, J., A. Svatos, and M. Kaltenpoth, *Rapid identification of insect cuticular hydrocarbons using gas chromatography-ion-trap mass spectrometry.* Journal of Chemical Ecology, 2011. **37**(4): p. 420-427.

142. Bogdan, C., *et al*., *Tumor necrosis factor-alpha in combination with interferon-gamma, but not with interleukin 4 activates murine macrophages for elimination of Leishmania major amastigotes.* European Journal of Immunology, 1990. **20**(5): p. 1131-1135.

143. Bringmann, G., *et al*., *A novel Leishmania major amastigote assay in 96-well format for rapid drug screening and its use for discovery and evaluation of a new class of leishmanicidal quinolinium salts.* Antimicrobial Agents and Chemotherapy, 2013. **57**(7): p. 3003-3011.

144. Krieger, E., G. Koraimann, and G. Vriend, *Increasing the precision of comparative models with YASARA NOVA--a self-parameterizing force field.* Proteins, 2002. **47**(3): p. 393-402.

145. De Simone, G., *et al*., *A Substrate-induced Switch in the Reaction Mechanism of a Thermophilic Esterase: KINETIC EVIDENCES AND STRUCTURAL BASIS.* Journal of Biological Chemistry, 2004. **279**(8): p. 6815-6823.

146. Laskowski, R.A., *et al*., *PROCHECK: a program to check the stereochemical quality of protein structures.* Journal of Applied Crystallography, 1993. **26**(2): p. 283-291.

147. Sippl, M.J., *Recognition of errors in three-dimensional structures of proteins.* Proteins, 1993. **17**(4): p. 355-362.

148. Sippl, M.J., *Calculation of Conformational Ensembles from Potentials of Mean Force. An Approach to the Knowledge-based Prediction of Local Structures in Globular Proteins.* Journal of Molecular Biology, 1990. **213**(4): p. 859-883.

149. Halgren, T.A., *Merck molecular force field. I. Basis, form, scope, parameterization, and performance of MMFF94.* Journal of Computational Chemistry, 1996. **17**(5-6): p. 490-519.

A Appendix

A.1 NMR Spectra of Compounds from Chapter 6.2.1 (*rac*-Harmonine)

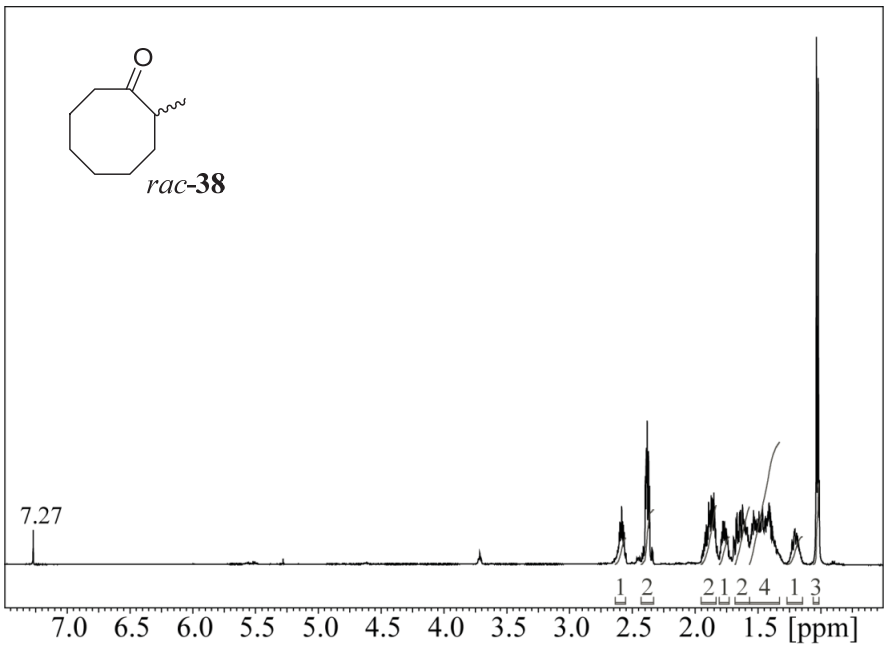

Figure A.1.1: ^{1}H NMR spectrum of 2-methylcyclooctan-1-one (*rac*-**38**).

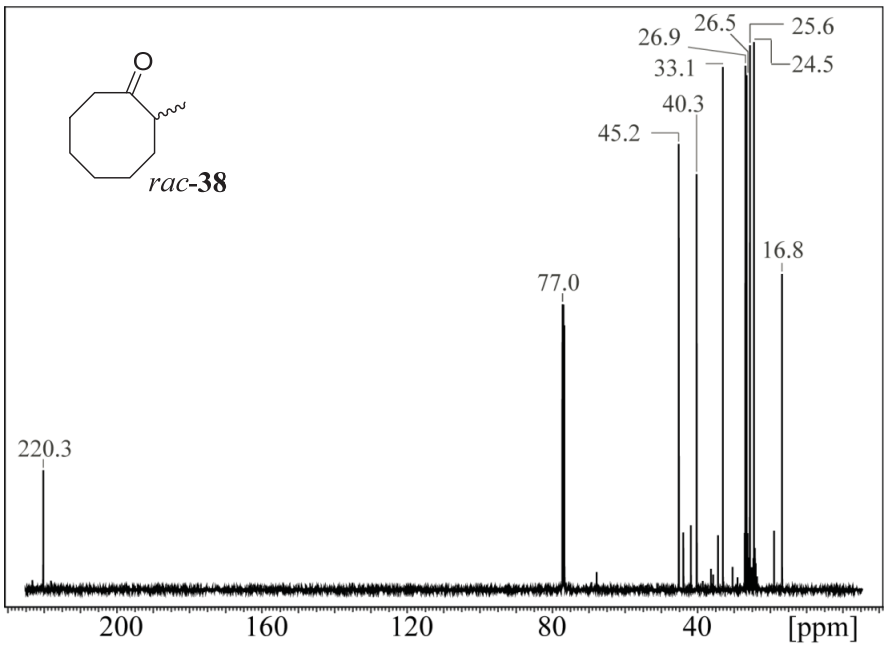

Figure A.1.2: ^{13}C NMR spectrum of 2-methylcyclooctan-1-one (*rac*-**38**).

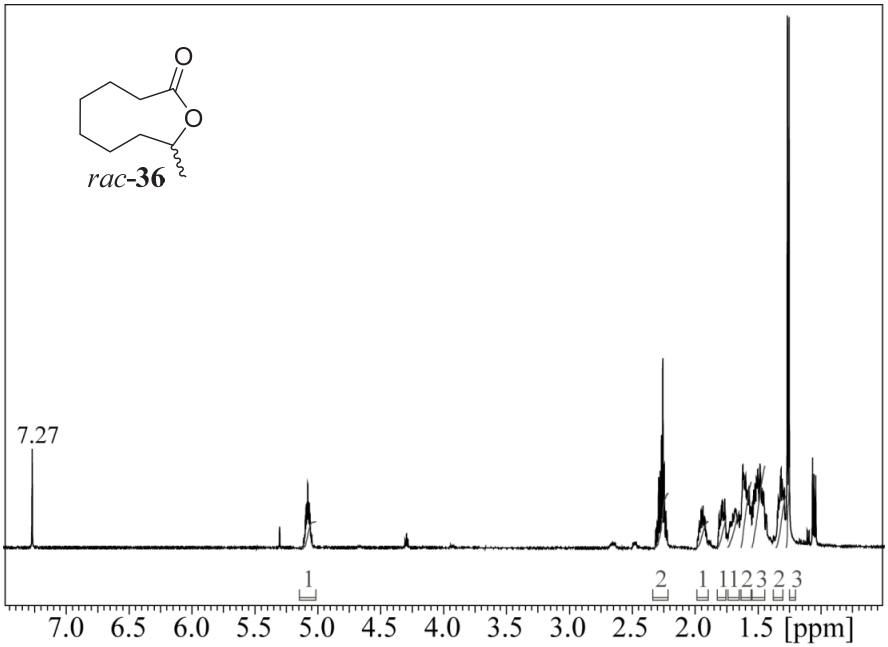

Figure A.1.3: ^{1}H NMR spectrum of 9-methyloxonan-2-one (*rac*-**36**).

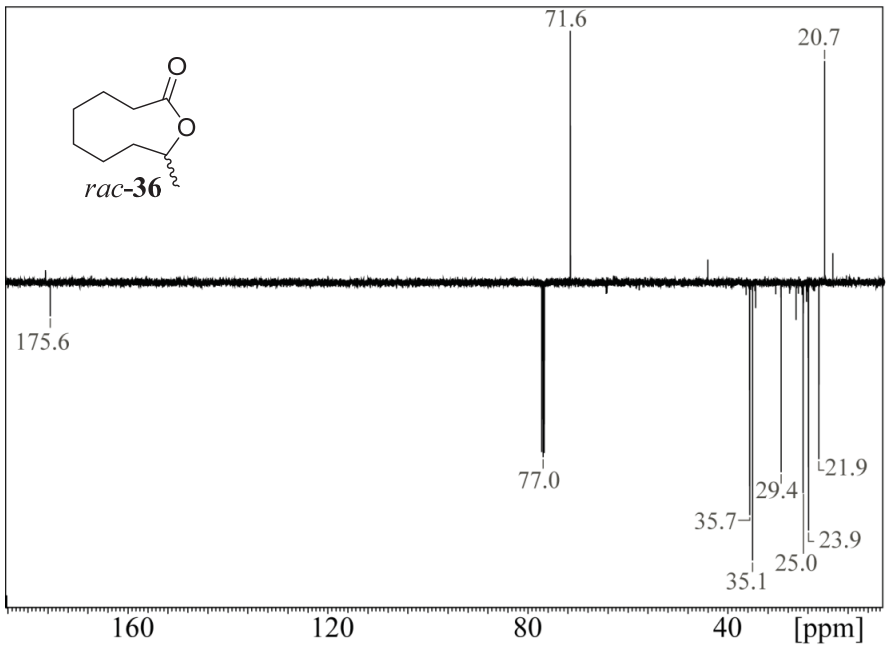

Figure A.1.4: APT spectrum of 9-methyloxonan-2-one (*rac*-**36**).

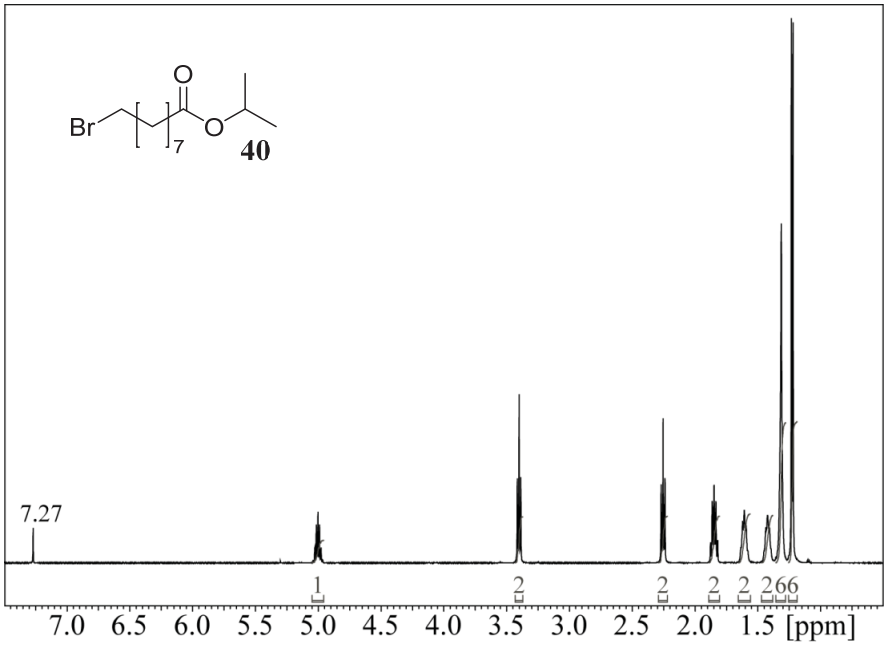

Figure A.1.5: ^{1}H NMR spectrum of isopropyl 9-bromononanoate (**40**).

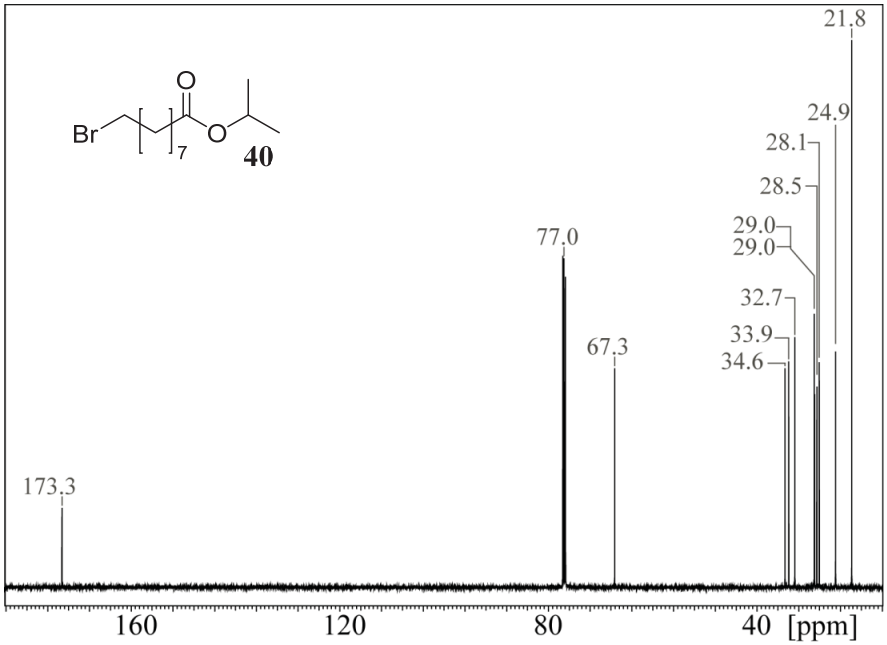

Figure A.1.6: ^{13}C NMR spectrum of isopropyl 9-bromononanoate (**40**).

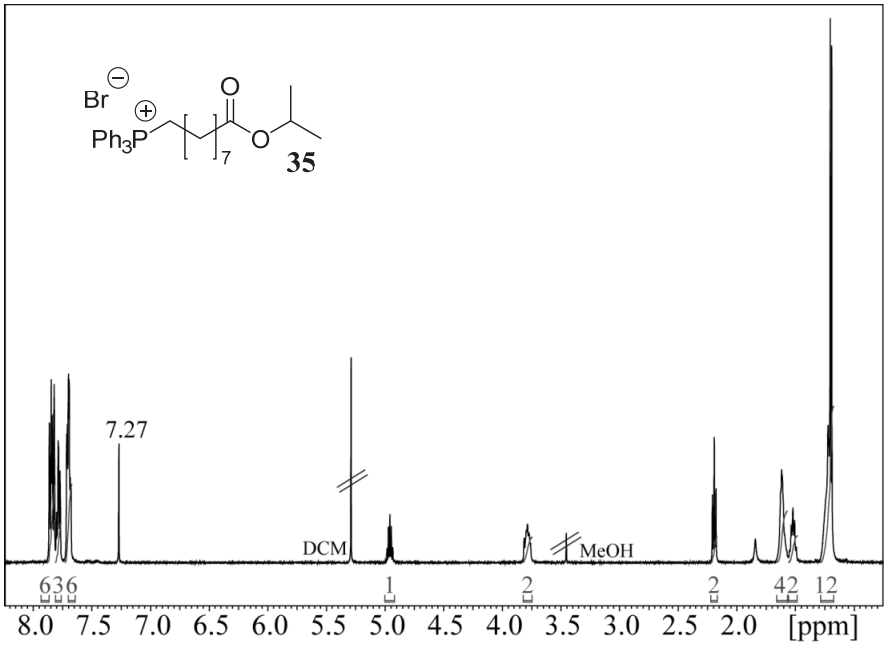

Figure A.1.7: ^{1}H NMR spectrum of (9-isopropoxy-9-oxononyl)triphenylphosphonium bromide (**35**).

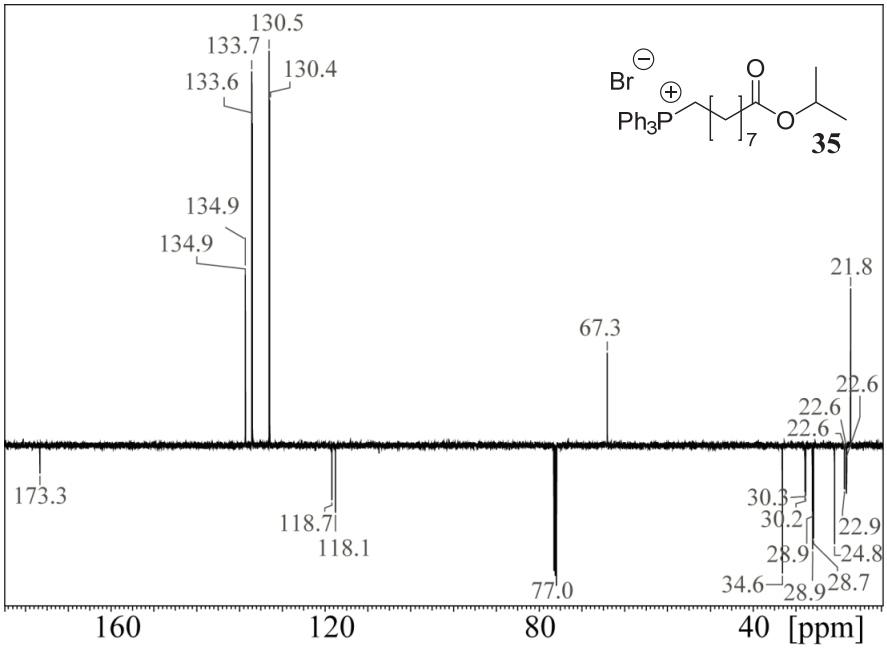

Figure A.1.8: APT NMR spectrum of (9-isopropoxy-9-oxononyl)triphenylphosphonium bromide (**35**).

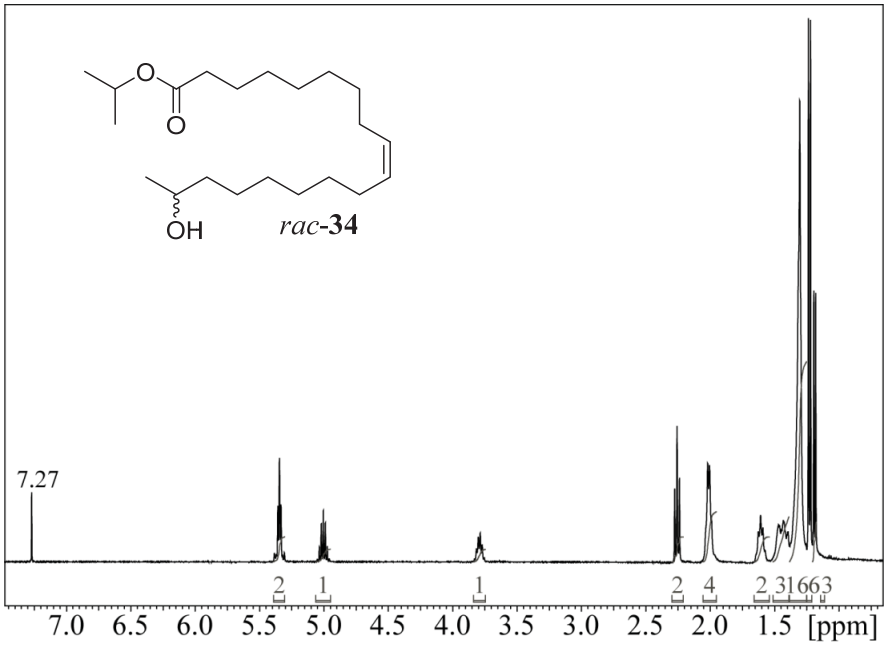

Figure A.1.9: ^{1}H NMR spectrum of isopropyl (9*Z*)-17-hydroxyoctadec-9-enoate (*rac*-**34**).

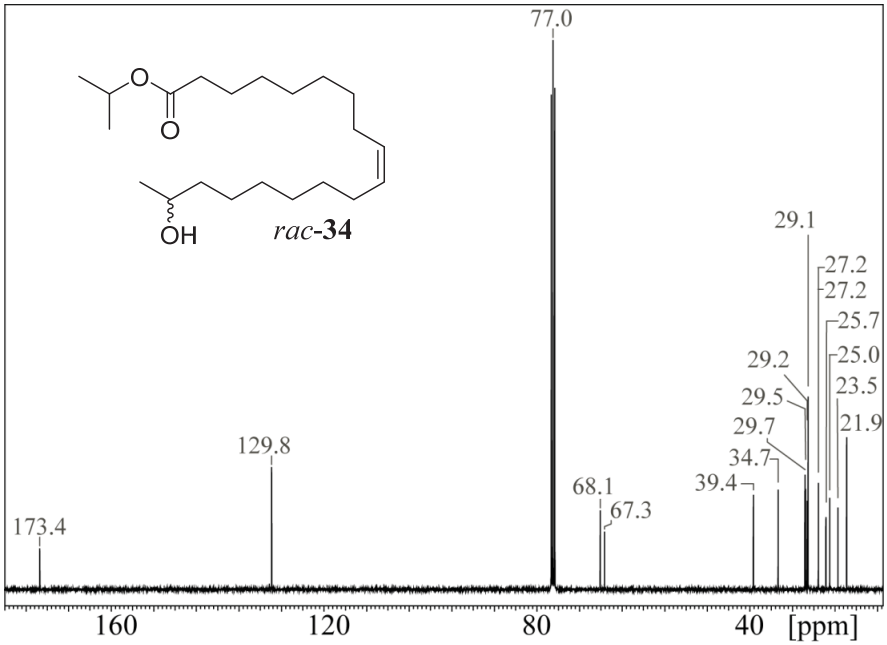

Figure A.1.10: ^{13}C NMR spectrum of isopropyl (9*Z*)-17-hydroxyoctadec-9-enoate (*rac*-**34**).

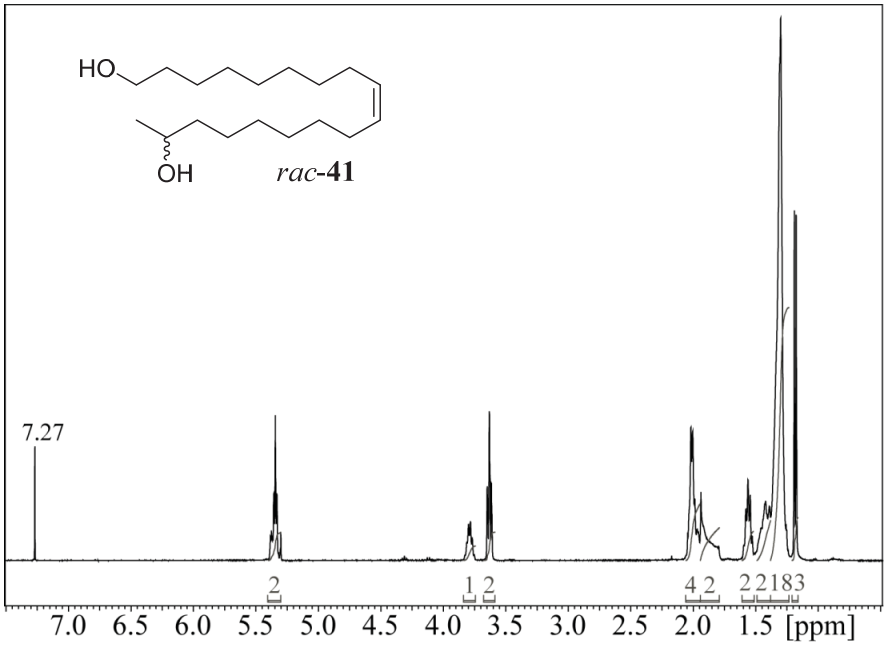

Figure A.1.11: ^{1}H NMR spectrum of (9*Z*)-octadec-9-ene-1,17-diol (*rac*-**41**).

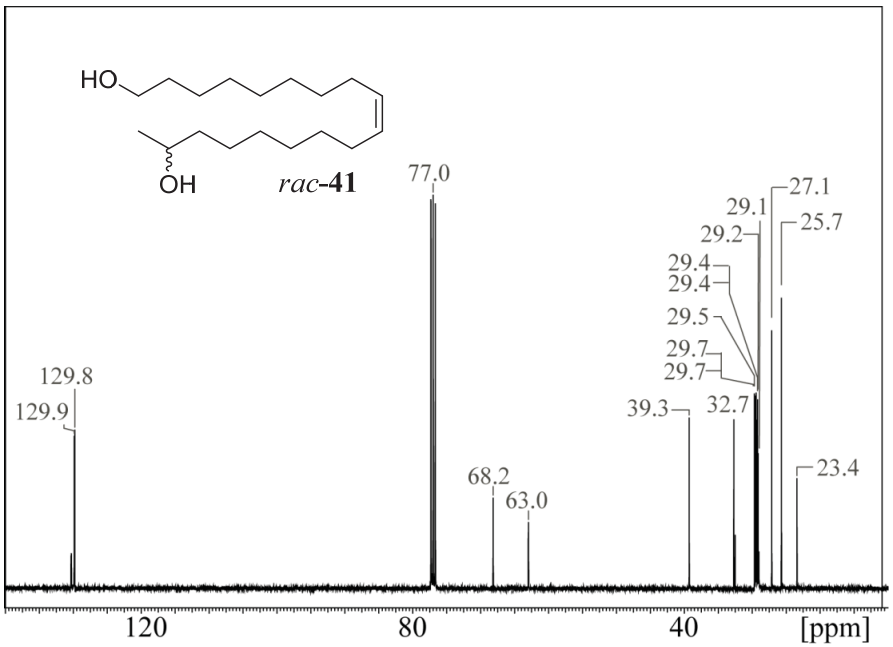

Figure A.1.12: ^{13}C NMR spectrum of (9*Z*)-octadec-9-ene-1,17-diol (*rac*-**41**).

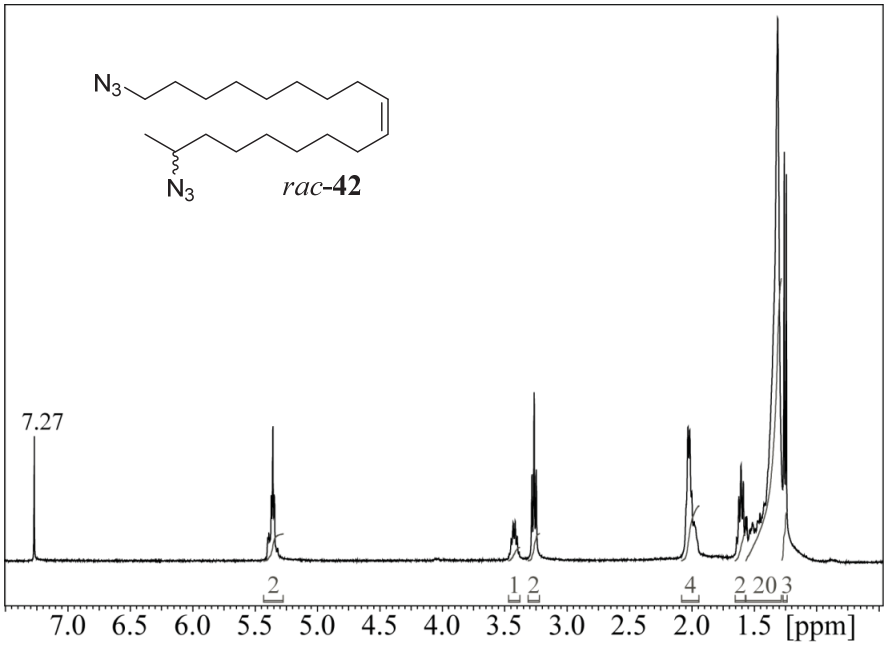

Figure A.1.13: ^{1}H NMR spectrum of (9*Z*)-1,17-diazidooctadec-9-ene (*rac*-**42**).

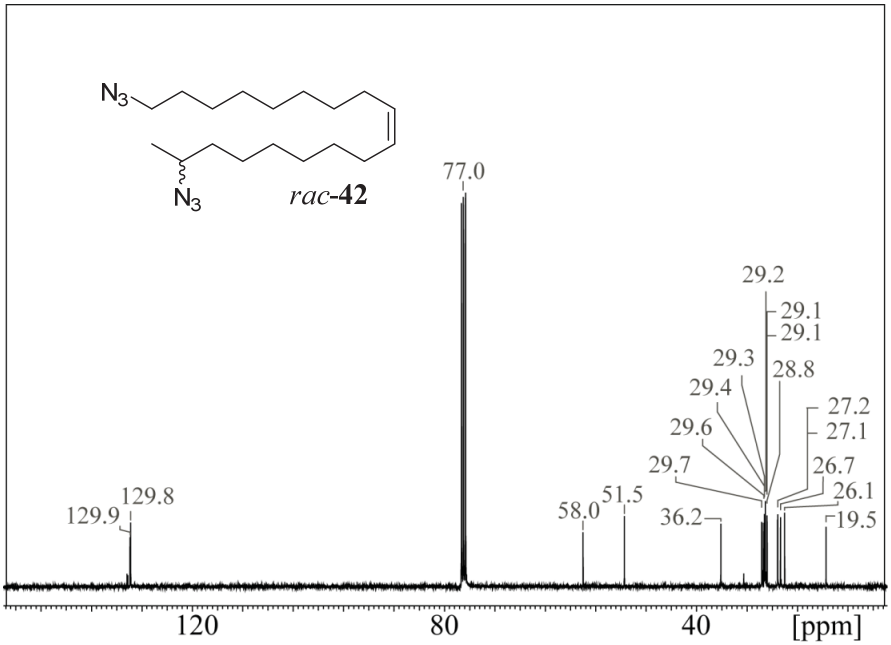

Figure A.1.14: ^{13}C NMR spectrum of (9*Z*)-1,17-diazidooctadec-9-ene (*rac*-**42**).

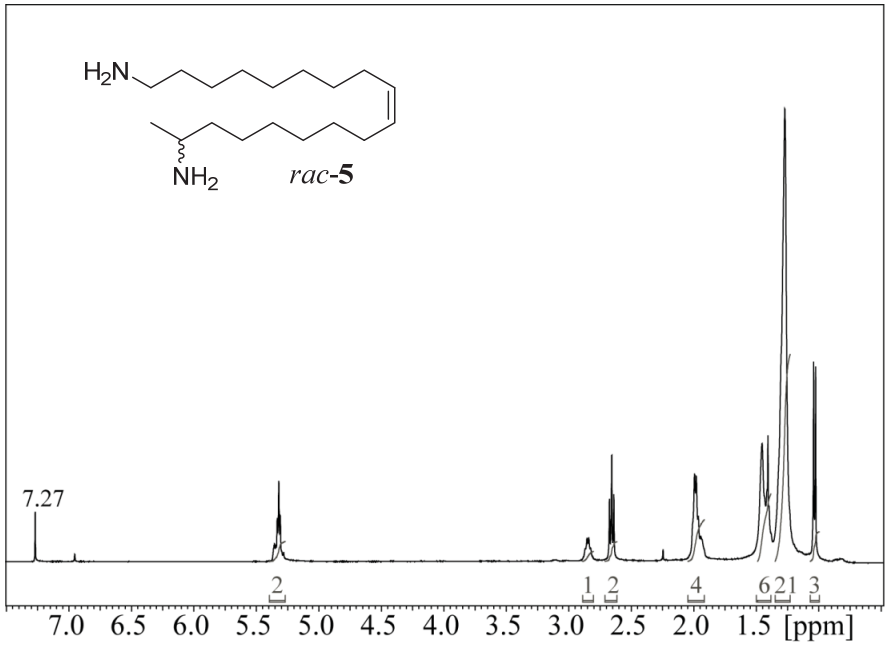

Figure A.1.15: ^{1}H NMR spectrum of (9*Z*)-octadec-9-ene-1,17-diamine (*rac*-**5**).

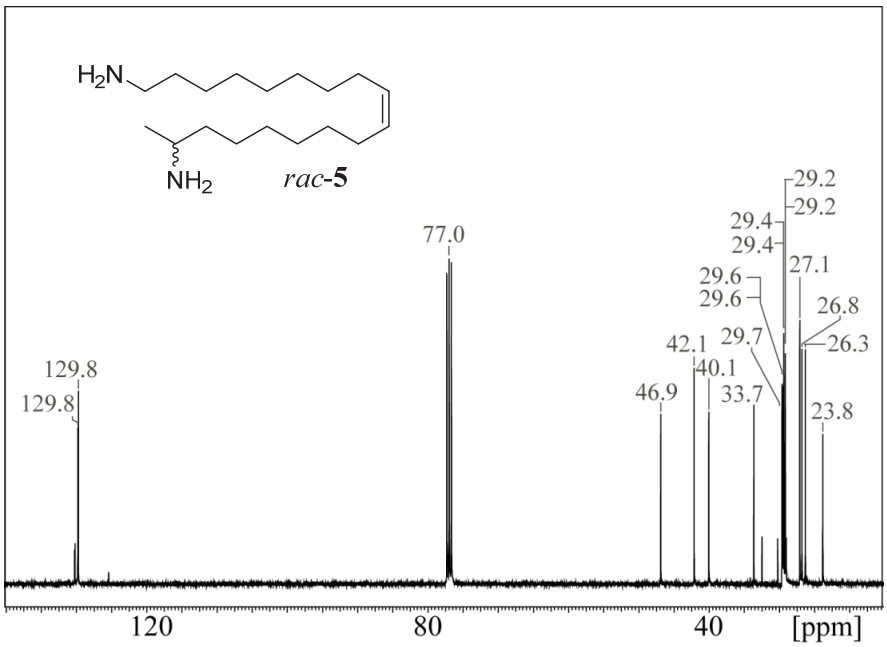

Figure A.1.16: ^{13}C NMR spectrum of (9*Z*)-octadec-9-ene-1,17-diamine (*rac*-**5**).

A.2 ^{1}H and ^{13}C NMR Spectra of Compounds from Chapter 6.2.2 ((*R*)-Harmonine)

"*" indicates compounds that exclusively differ in stereochemistry from previously shown substances. Therefore, only the proton spectrum is shown.

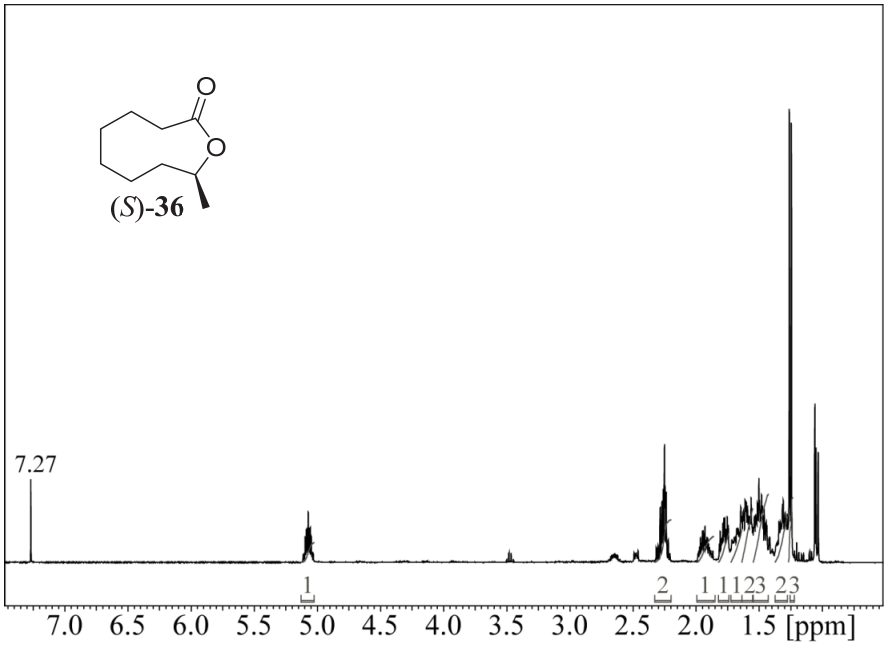

Figure A.2.1: ^{1}H NMR spectrum of 9-methyloxonan-2-one ((*S*)-**36**)*.

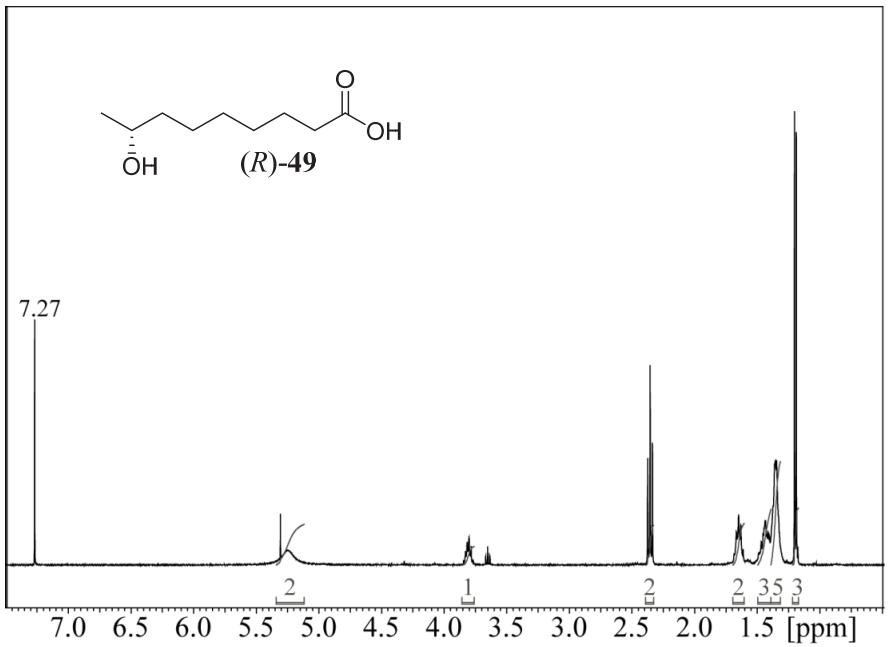

Figure A.2.2: ^{1}H NMR spectrum of (8*R*)-8-hydroxynonanoic acid ((*R*)-**49**).

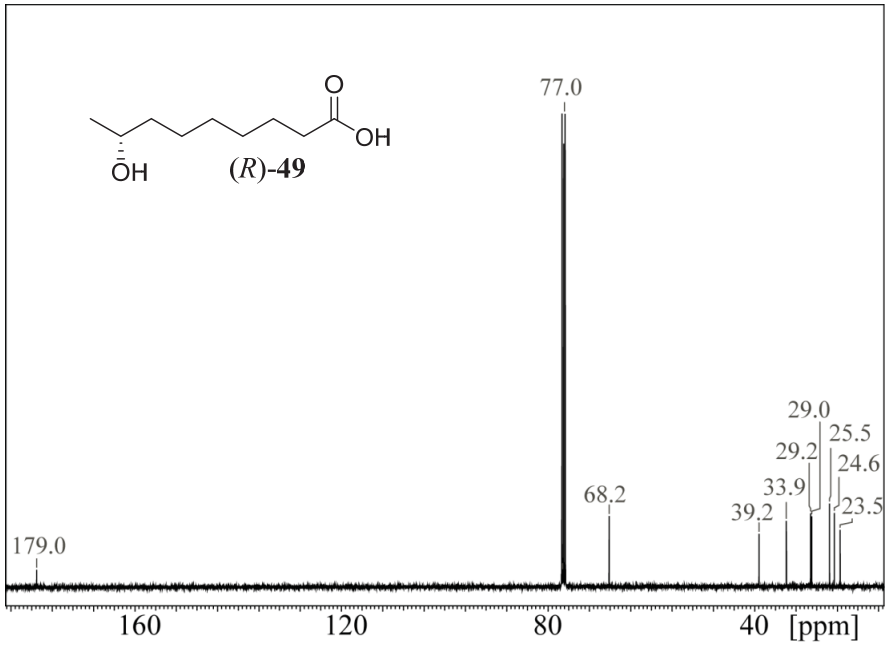

Figure A.2.3: ^{13}C NMR spectrum of (8*R*)-8-hydroxynonanoic acid ((*R*)-**49**).

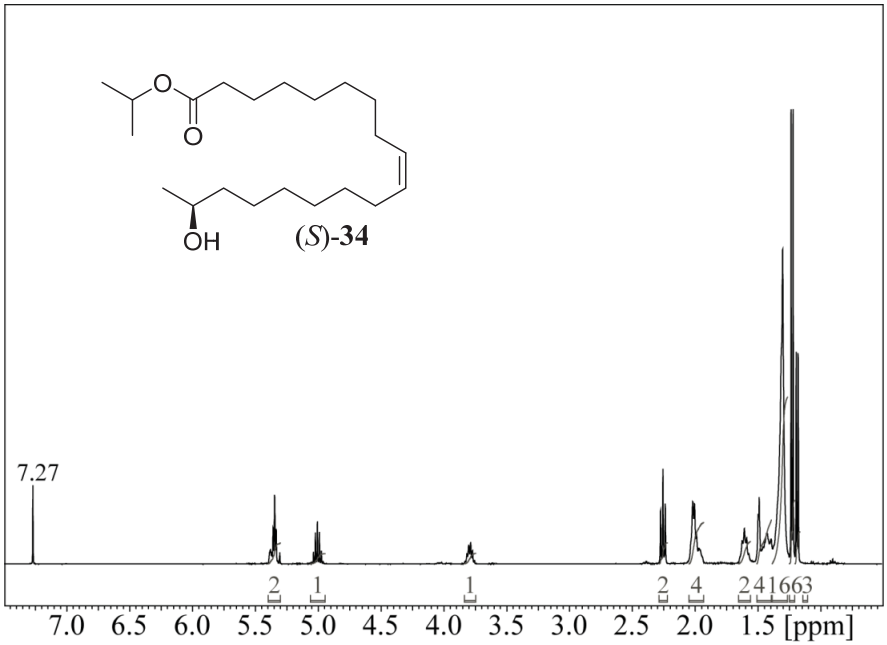

Figure A.2.4: ^{1}H NMR spectrum of isopropyl (17*S*,9*Z*)-17-hydroxyoctadec-9-enoate (**(*S*)-34**)*.

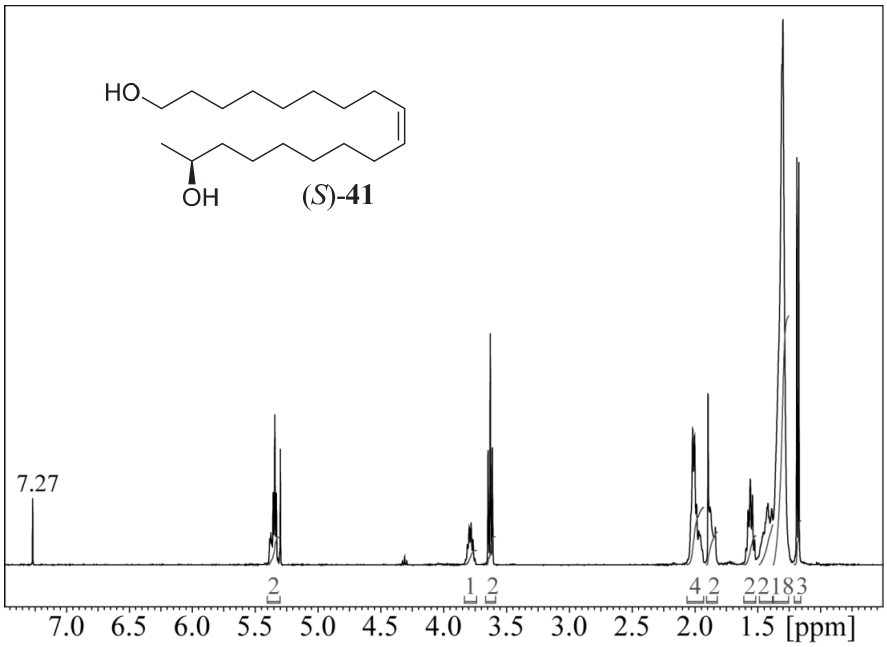

Figure A.2.5: ^{1}H NMR spectrum of (17*S*,9*Z*)-octadec-9-ene-1,17-diol (**(*S*)-41**)*.

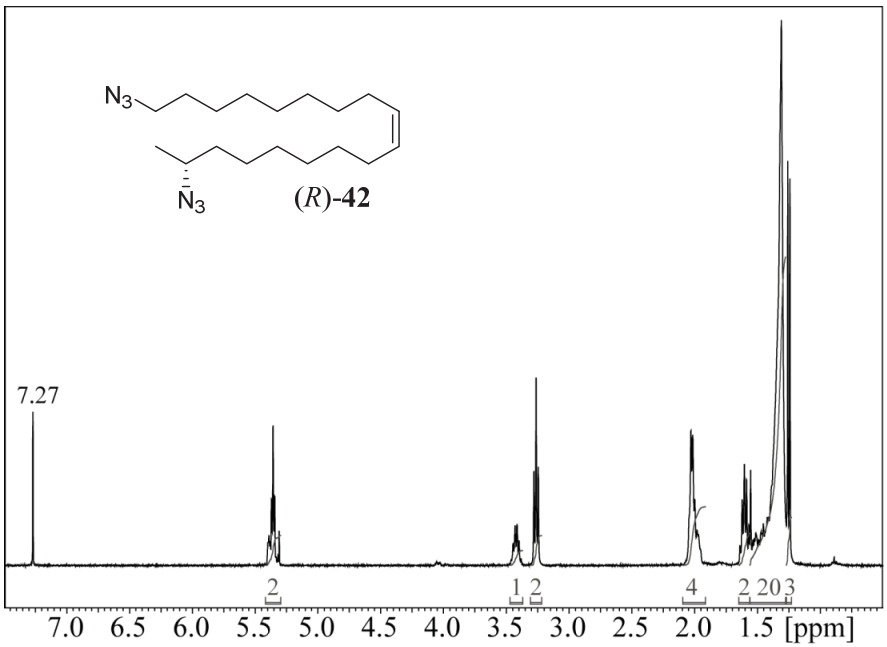

Figure A.2.6: ^{1}H NMR spectrum of (17*R*,9*Z*)-1,17-diazidooctadec-9-ene (**(*R*)-42**)*.

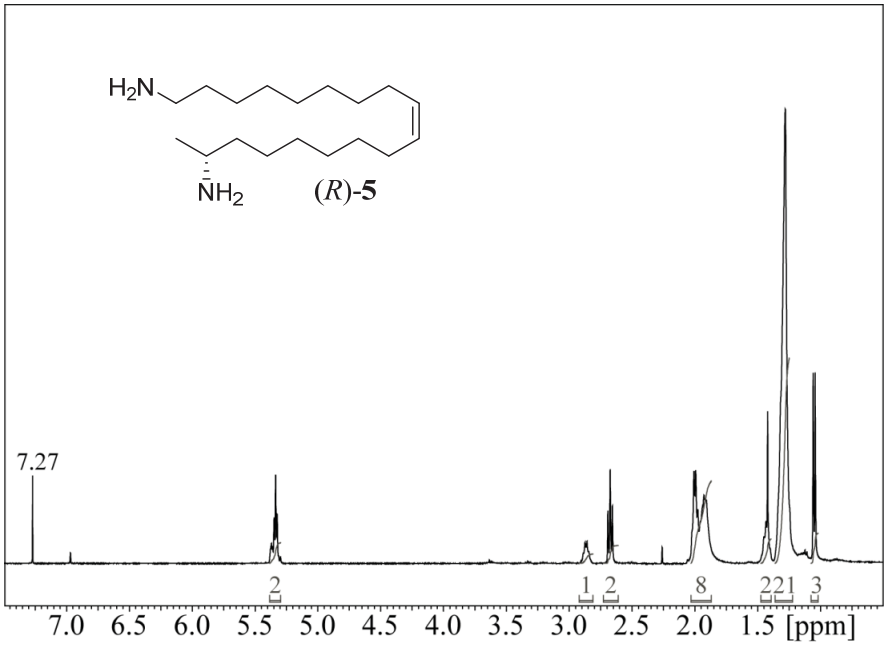

Figure A.2.7: ^{1}H NMR spectrum of (17*R*,9*Z*)-octadec-9-ene-1,17-diamine (**(*R*)-5**)*.

A.3 ^{1}H and ^{13}C NMR Spectra of Compounds from Chapter 6.2.3 ((*S*)-Harmonine)

"*" indicates compounds that exclusively differ in stereochemistry from previously shown substances. Therefore, only the proton spectrum is shown.

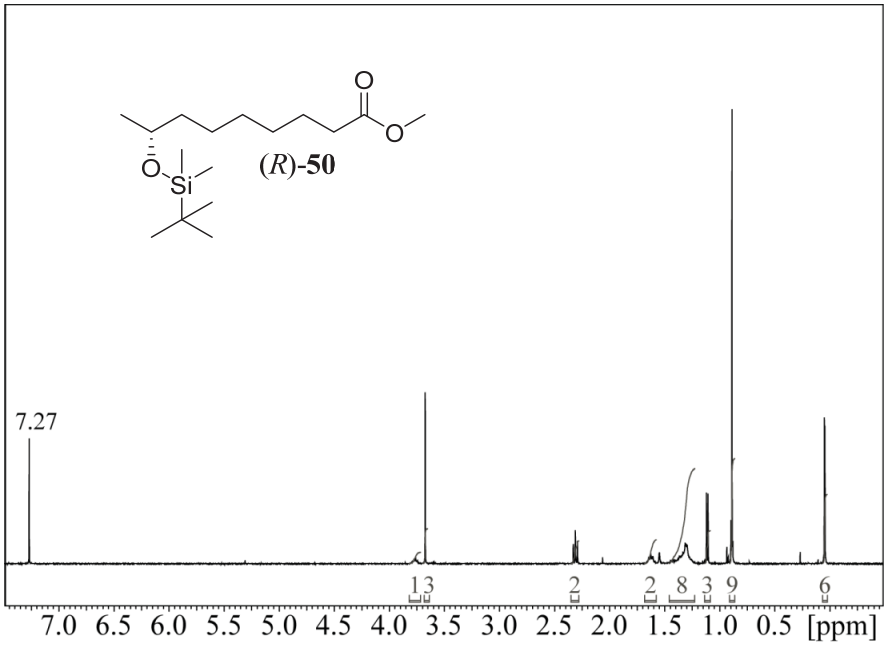

Figure A.3.1: ^{1}H NMR spectrum of methyl (8*R*)-8-((*tert*-butyldimethylsilyl)oxy)nonanoate ((*R*)-**50**).

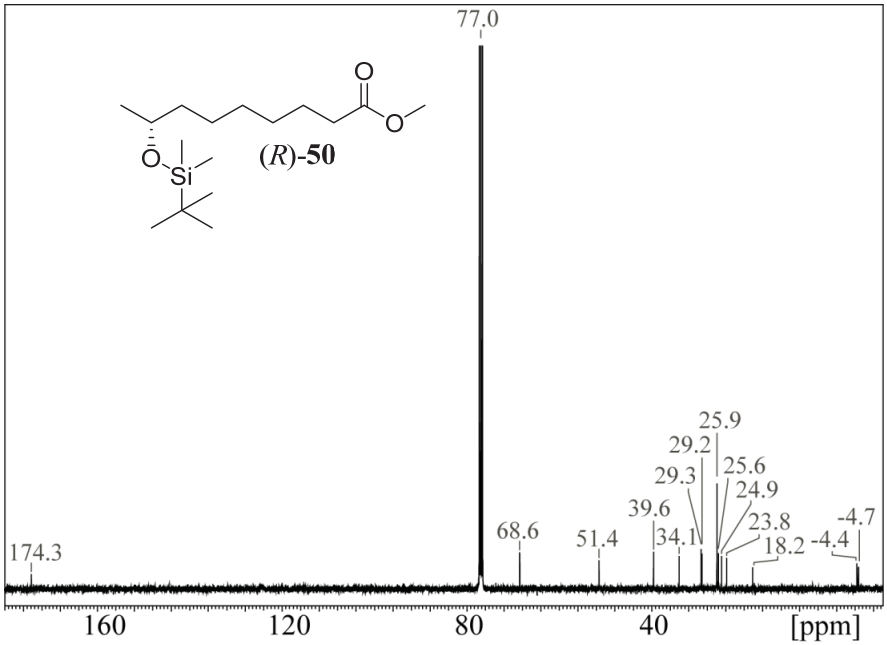

Figure A.3.2: ^{13}C NMR spectrum of methyl (8*R*)-8-((*tert*-butyldimethylsilyl)oxy)nonanoate ((*R*)-**50**).

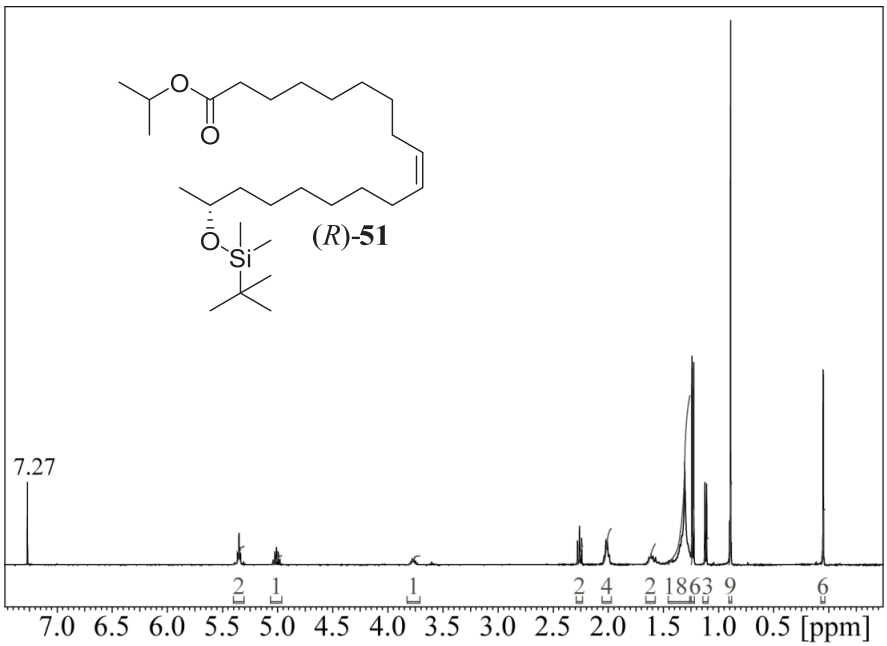

Figure A.3.3: ^{1}H NMR spectrum of isopropyl (17*R*,9*Z*)-17-((*tert*-butyldimethylsilyl)oxy)-octadec-9-enoate ((*R*)-**51**).

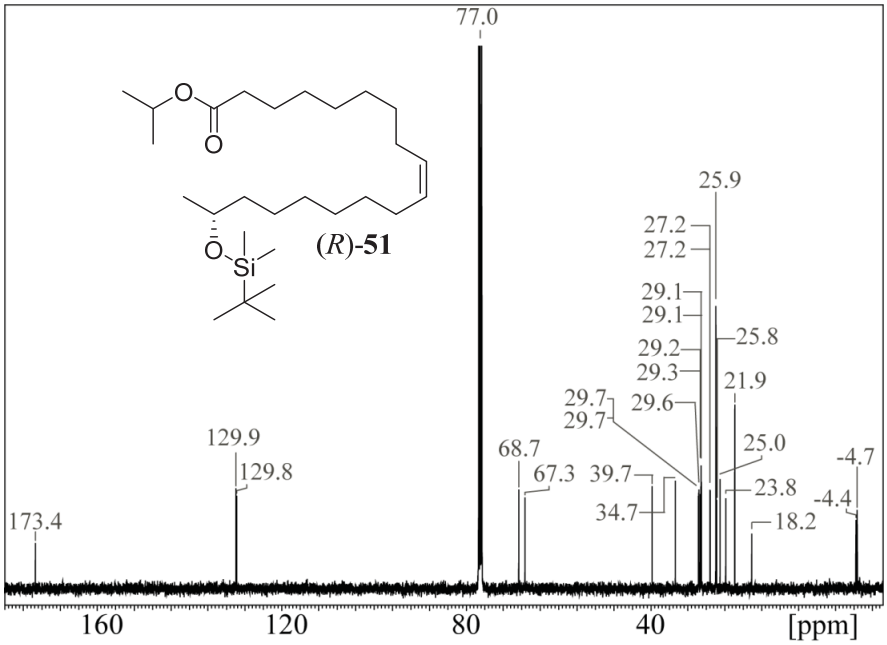

Figure A.3.4: ^{13}C NMR spectrum of isopropyl (17*R*,9*Z*)-17-((*tert*-butyldimethylsilyl)oxy)-octadec-9-enoate ((*R*)-**51**).

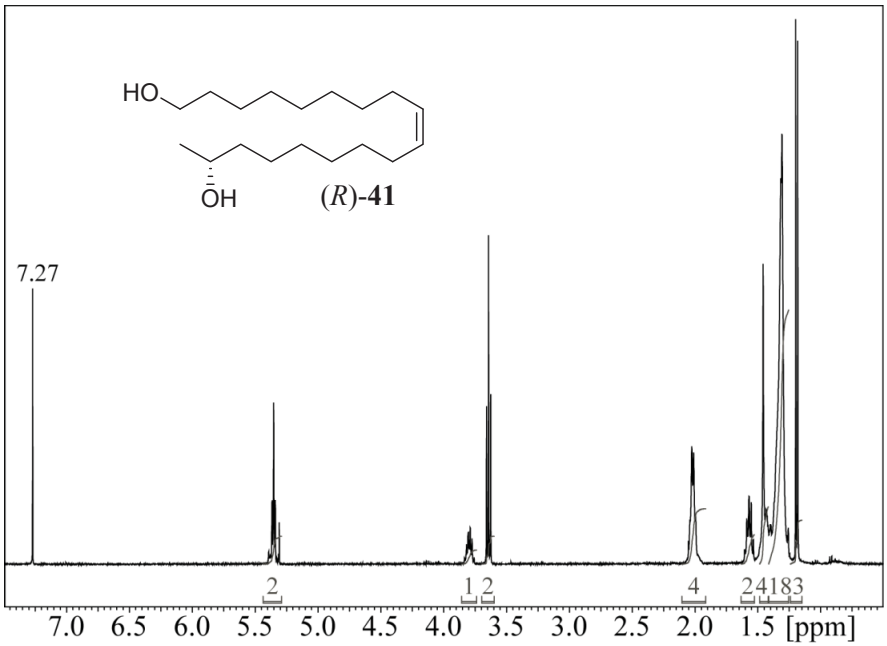

Figure A.3.5: ^{1}H NMR spectrum of (17*R*,9*Z*)-octadec-9-ene-1,17-diol ((*R*)-**41**)*.

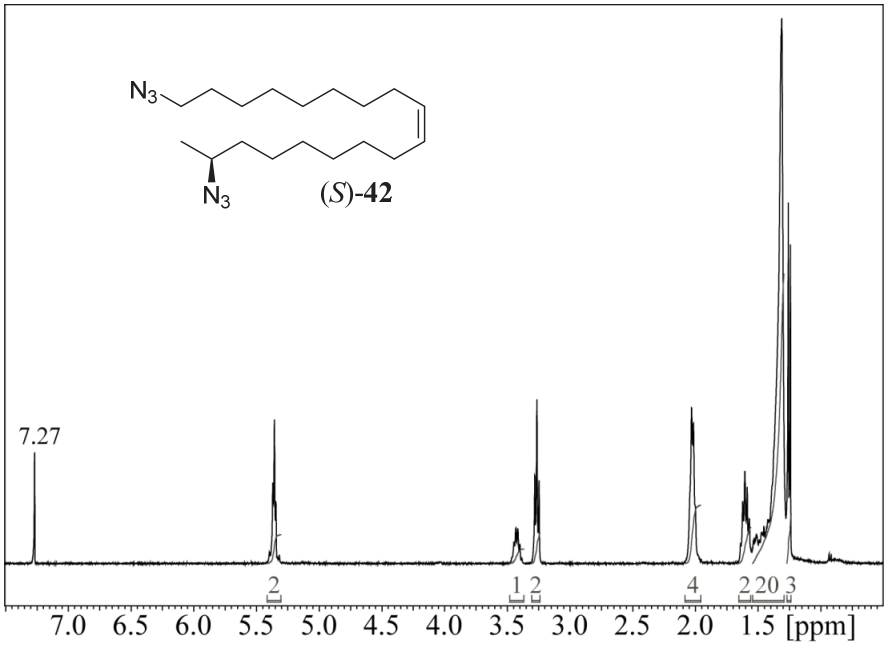

Figure A.3.6: ^{1}H NMR spectrum of (17*S*,9*Z*)-1,17-diazidooctadec-9-ene ((*S*)-**42**)*.

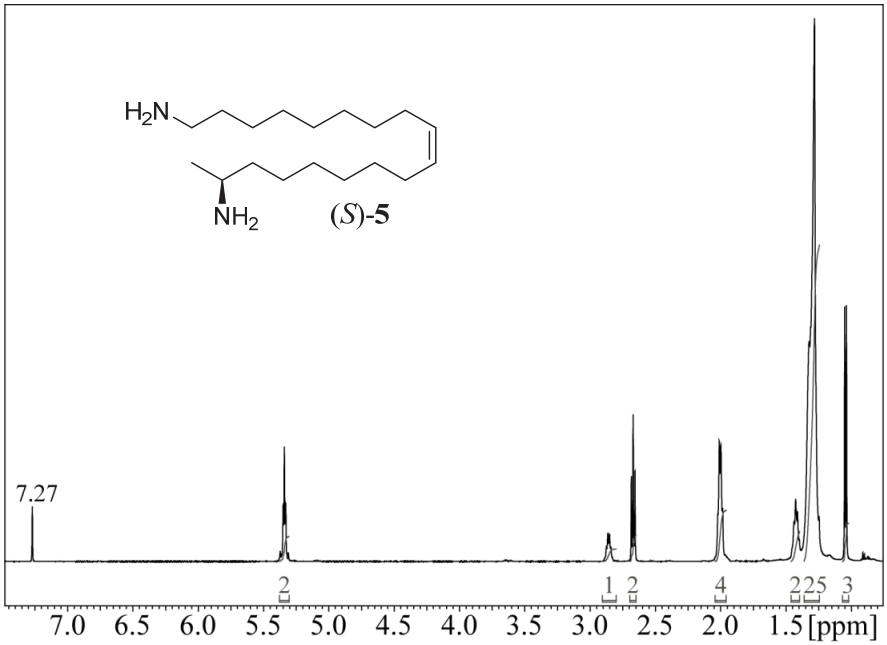

Figure A.3.7: ^{1}H NMR spectrum of (17*S*,9*Z*)-octadec-9-ene-1,17-diamine ((*S*)-**5**)*.

A.4 NMR Spectra of Compounds from Chapter 6.2.4 ((*Z*)-18-Aminooctadec-9-en-2-ol)

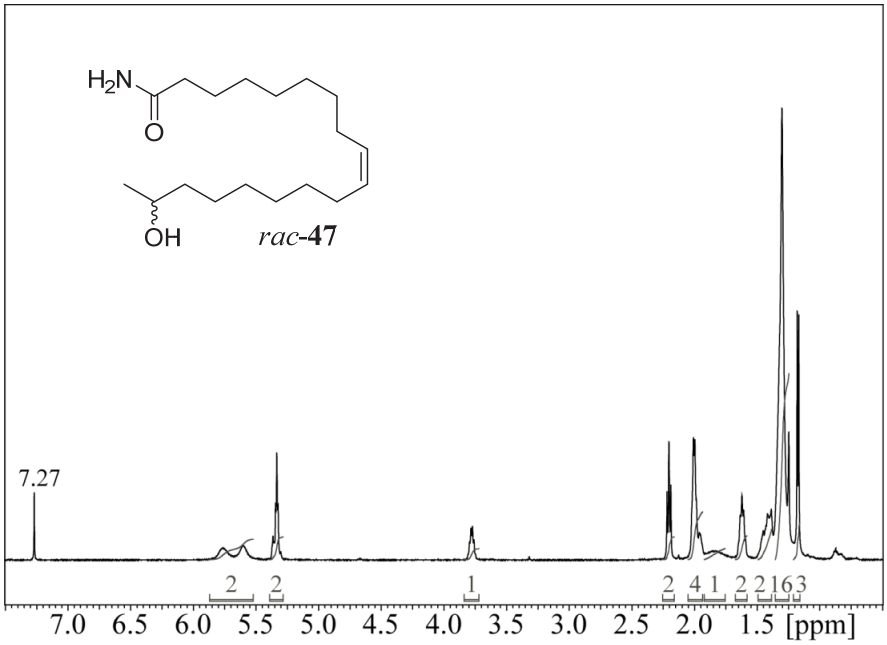

Figure A.4.1: ^{1}H NMR spectrum of (9*Z*)-17-hydroxyoctadec-9-enamide (*rac*-**47**).

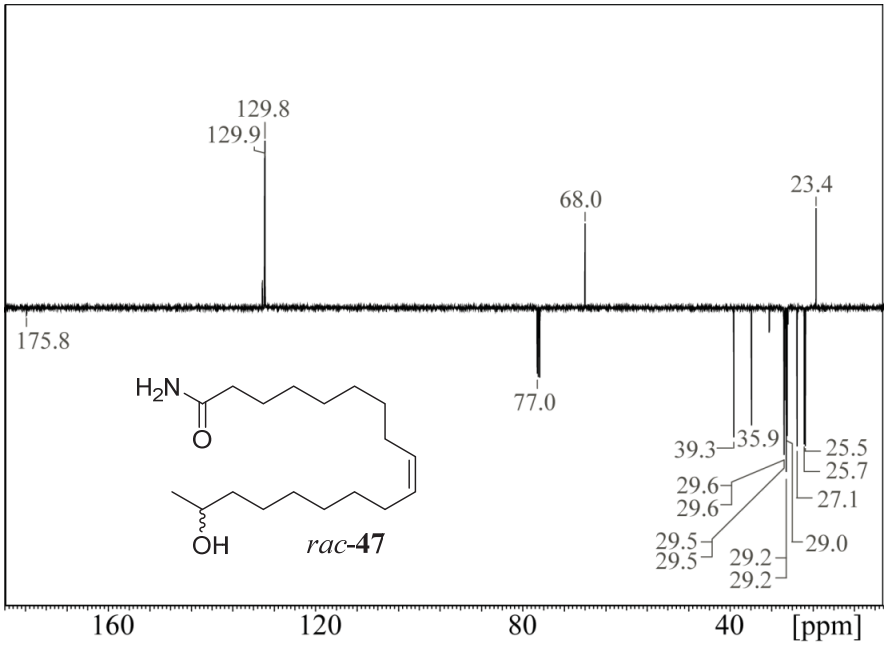

Figure A.4.2: APT spectrum of (9*Z*)-17-hydroxyoctadec-9-enamide (*rac*-**47**).

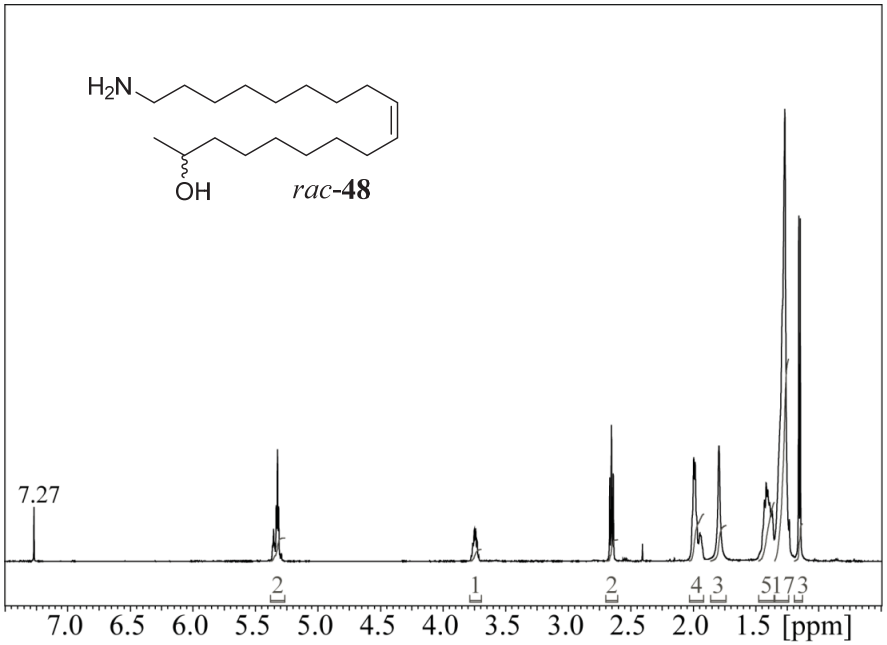

Figure A.4.3: ^{1}H NMR spectrum of (9*Z*)-18-aminooctadec-9-en-2-ol (*rac*-**48**).

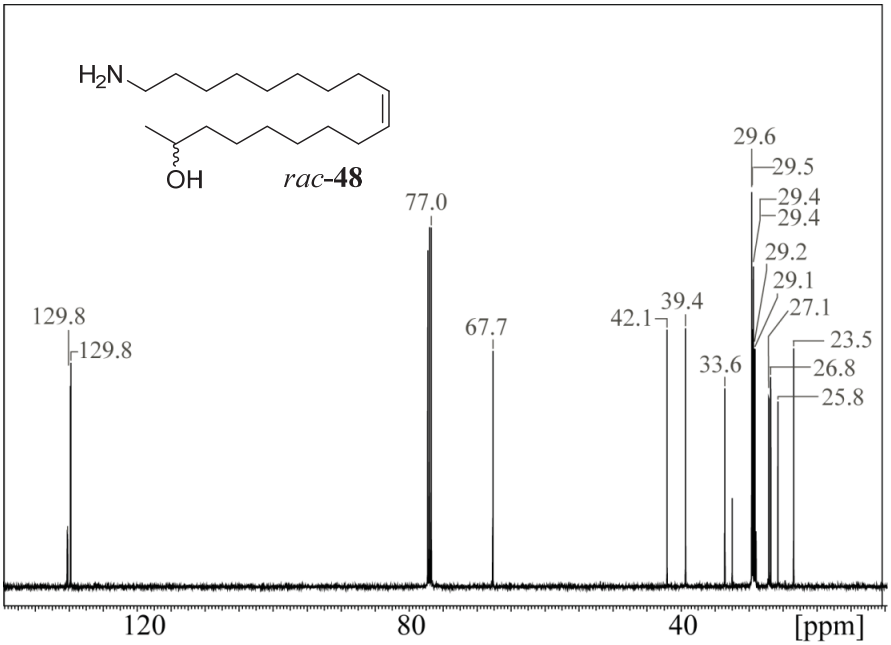

Figure A.4.4: ^{13}C NMR spectrum of (9*Z*)-18-aminooctadec-9-en-2-ol (*rac*-**48**).

A.5 ^{1}H and ^{13}C NMR Spectra of Compounds from Chapter 6.2.5 (C_{17}-Harmonine)

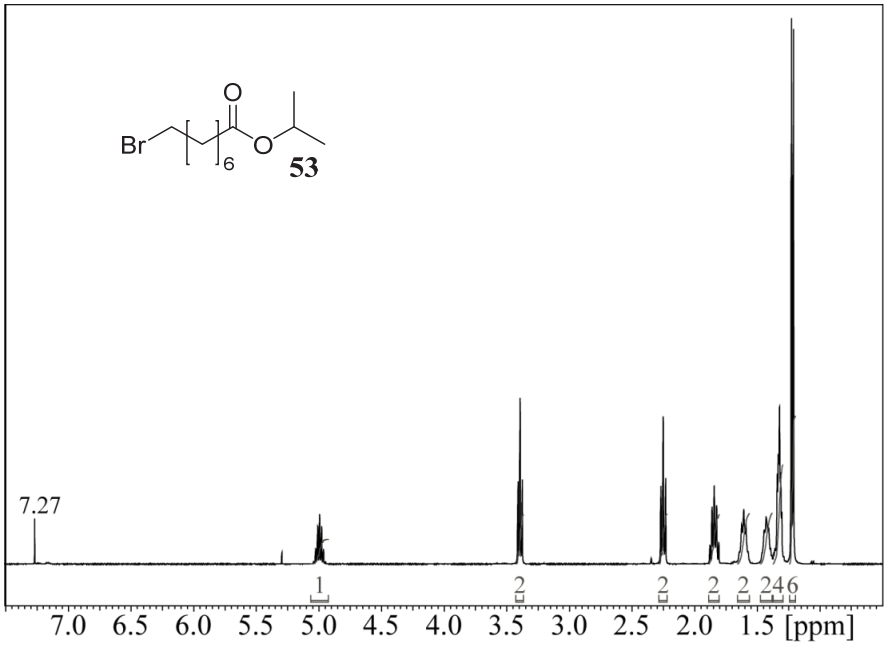

Figure A.5.1: ^{1}H NMR spectrum of isopropyl 8-bromooctanoate (**53**).

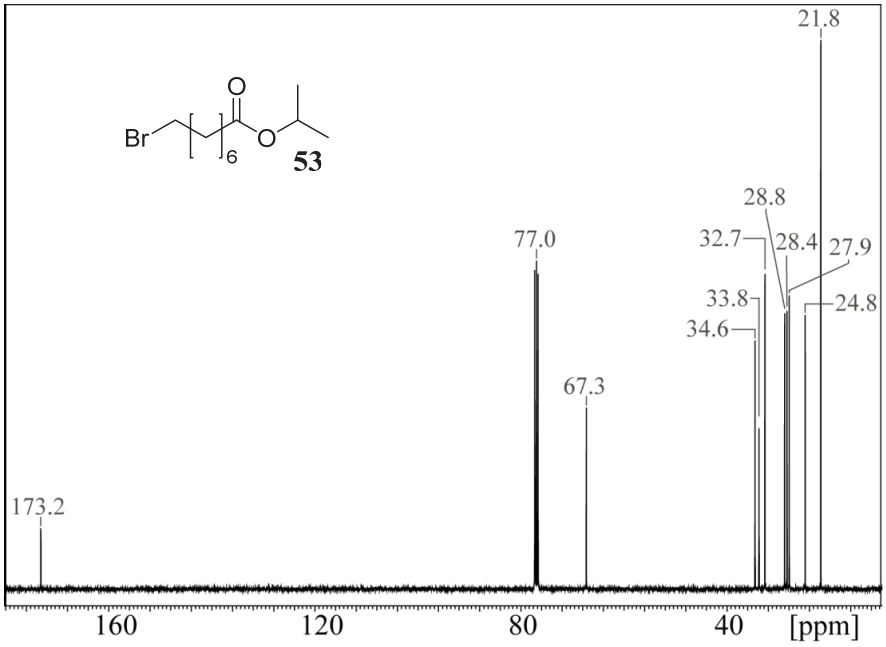

Figure A.5.2: ^{13}C NMR spectrum of isopropyl 8-bromooctanoate (**53**).

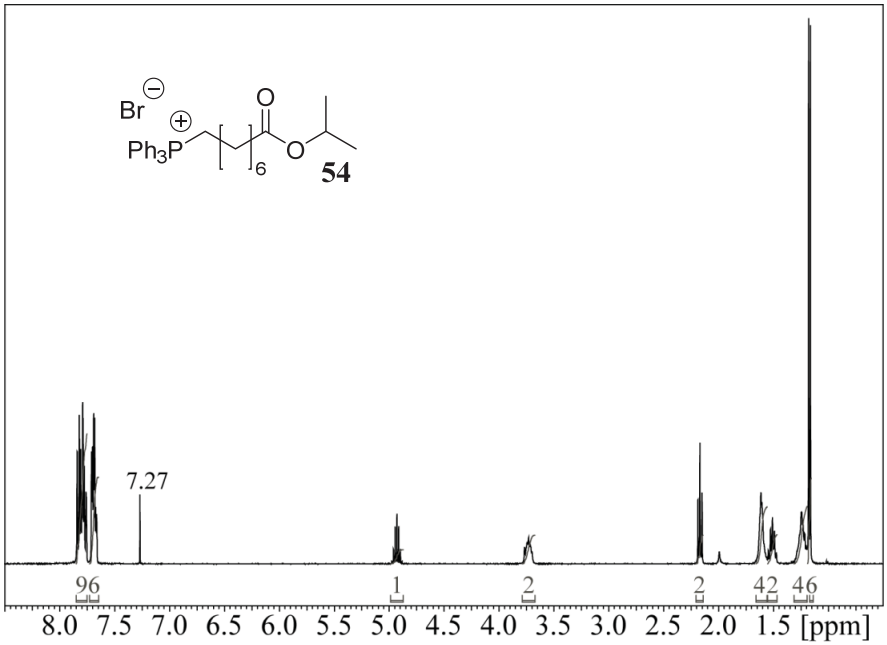

Figure A.5.3: ^{1}H NMR spectrum of (8-isopropoxy-8-oxooctyl)triphenylphosphonium bromide (**54**).

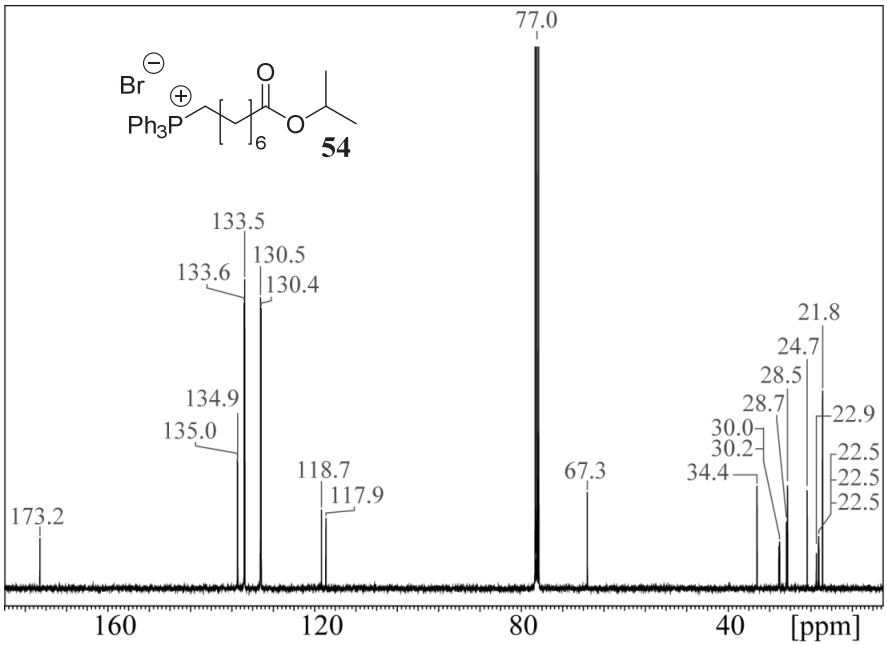

Figure A.5.4: ^{13}C NMR spectrum of (8-isopropoxy-8-oxooctyl)triphenylphosphonium bromide (**54**).

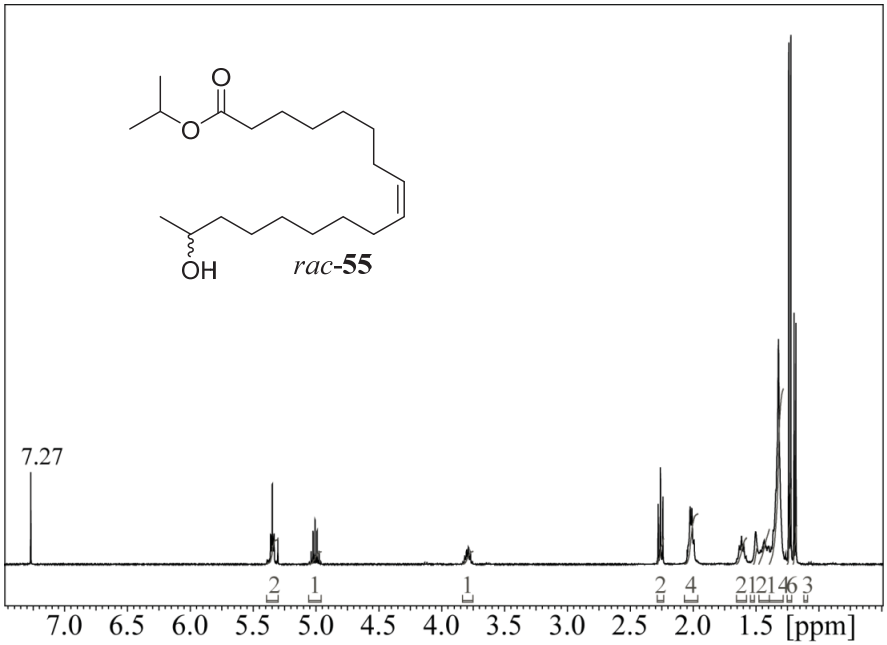

Figure A.5.5: ^{1}H NMR spectrum of isopropyl (8*Z*)-16-hydroxyheptadec-8-enoate (*rac*-**55**).

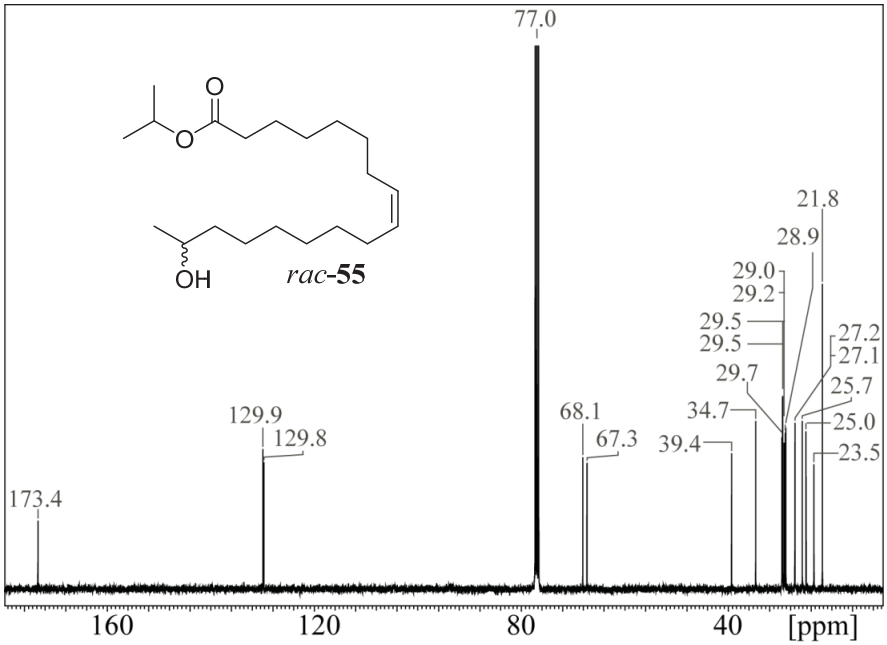

Figure A.5.6: ^{13}C NMR spectrum of isopropyl (8*Z*)-16-hydroxyheptadec-8-enoate (*rac*-**55**).

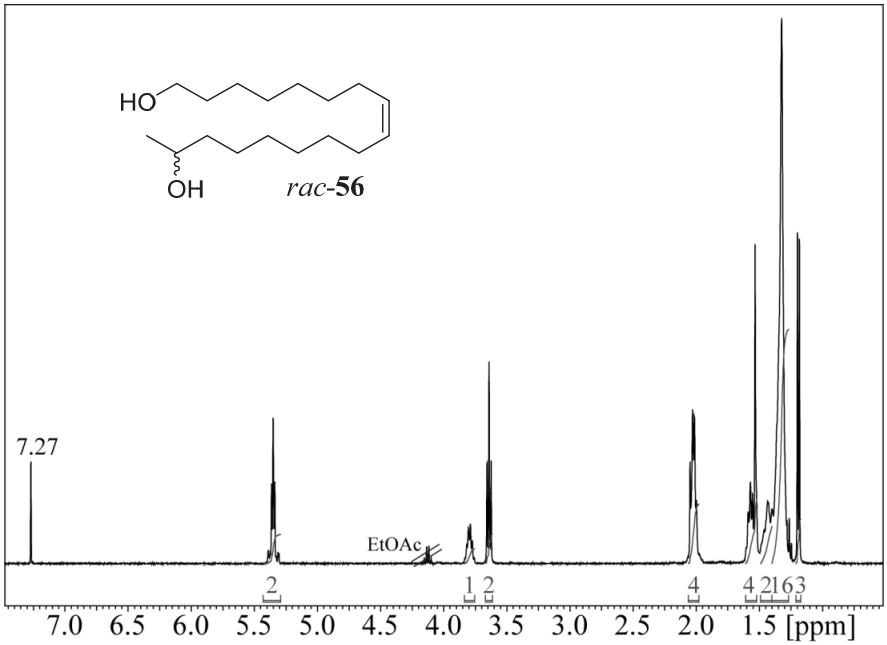

Figure A.5.7: ^{1}H NMR spectrum of (8*Z*)-heptadec-8-ene-1,16-diol (*rac*-**56**).

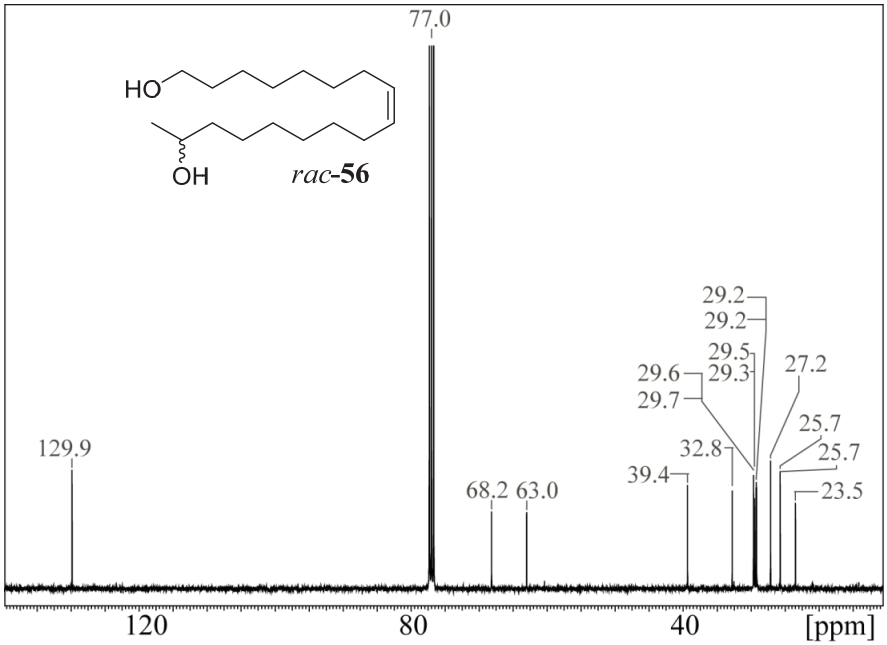

Figure A.5.8: ^{13}C NMR spectrum of (8*Z*)-heptadec-8-ene-1,16-diol (*rac*-**56**).

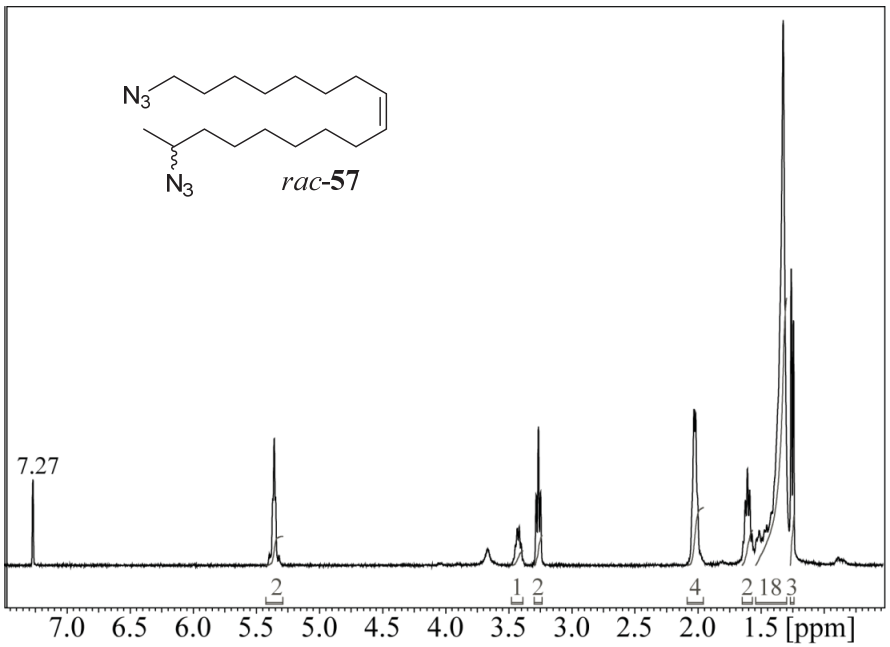

Figure A.5.9: ^{1}H NMR spectrum of (8*Z*)-1,16-diazidoheptadec-8-ene (*rac*-**57**).

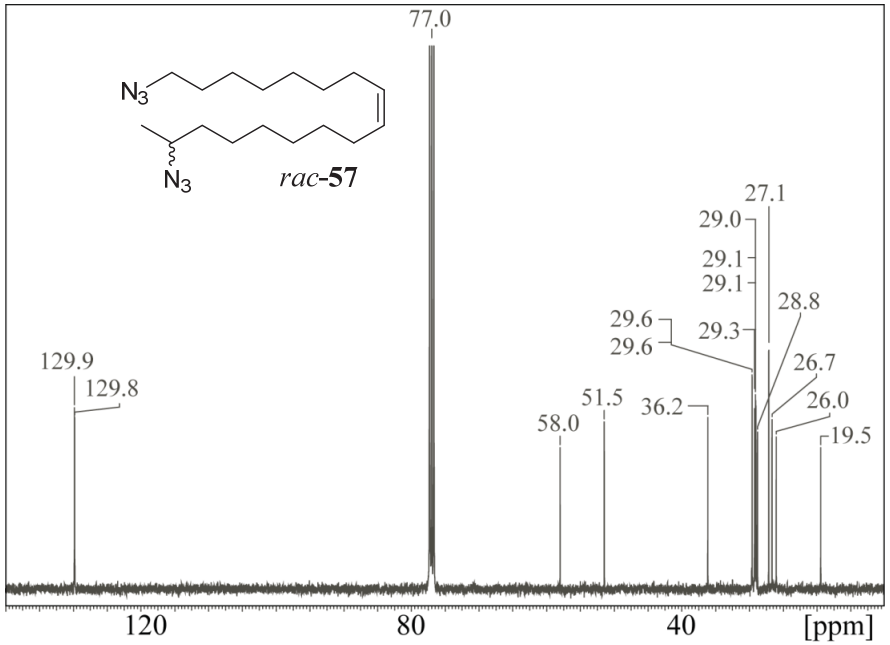

Figure A.5.10: ^{13}C NMR spectrum of (8*Z*)-1,16-diazidoheptadec-8-ene (*rac*-**57**).

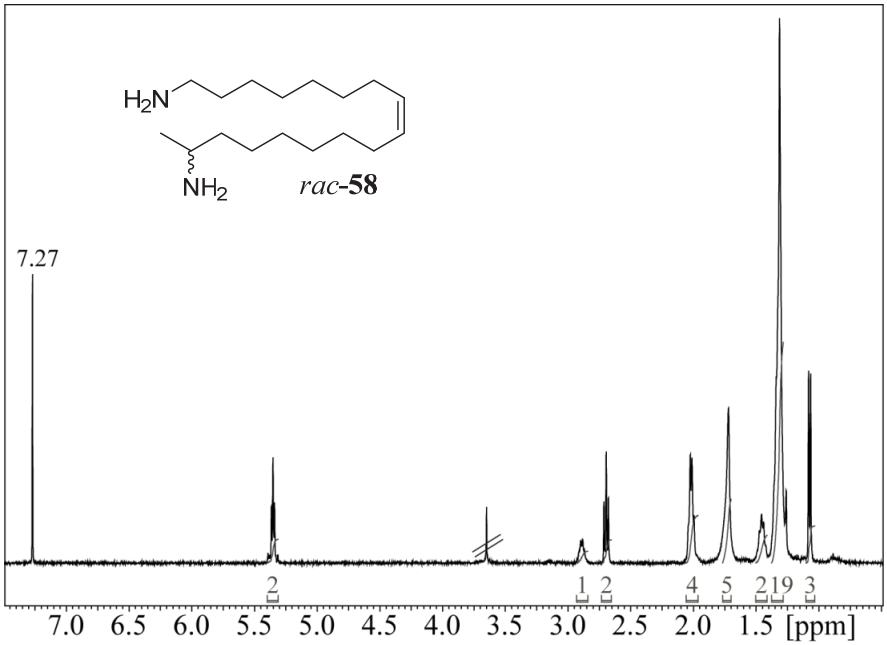

Figure A.5.11: ^{1}H NMR spectrum of (8*Z*)-heptadec-8-ene-1,16-diamine (*rac*-**58**).

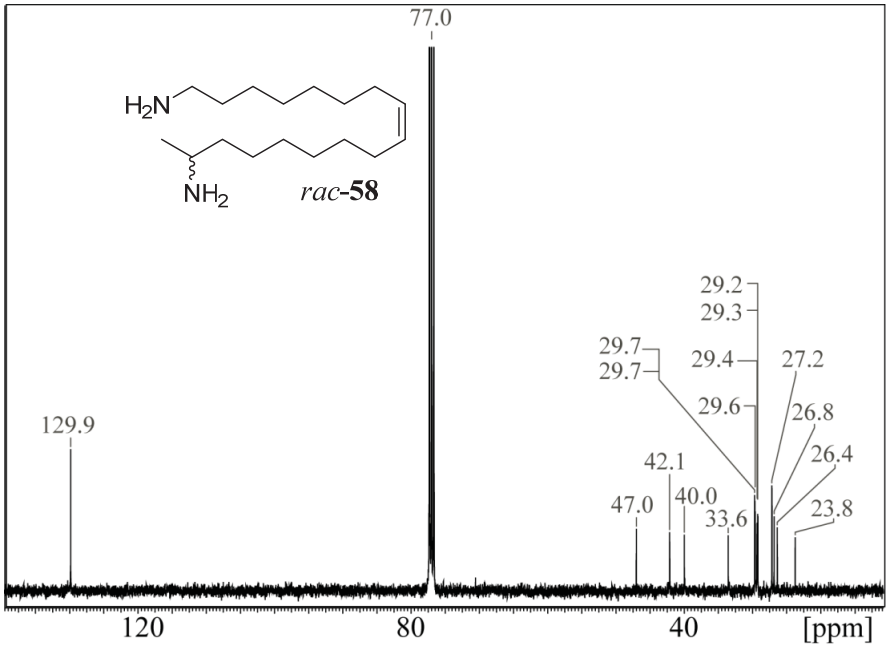

Figure A.5.12: ^{13}C NMR spectrum of (8*Z*)-heptadec-8-ene-1,16-diamine (*rac*-**58**).

A.6 FTIR Spectra

Only one of the spectra of compounds exclusively differing in stereochemistry at position C-17 is shown.

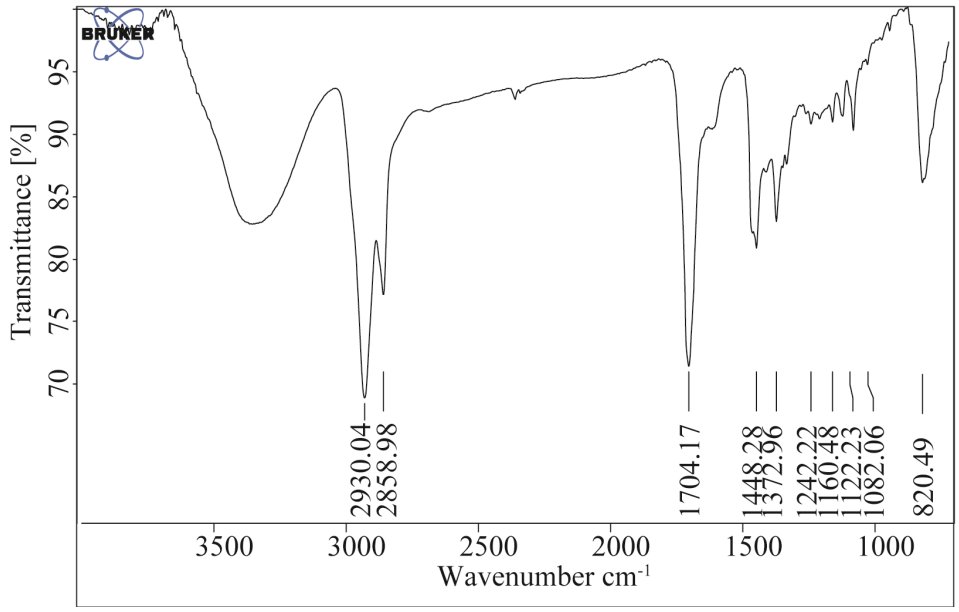

Figure A.6.1: FTIR spectrum of 2-methylcyclooctan-1-one (*rac*-**38**).

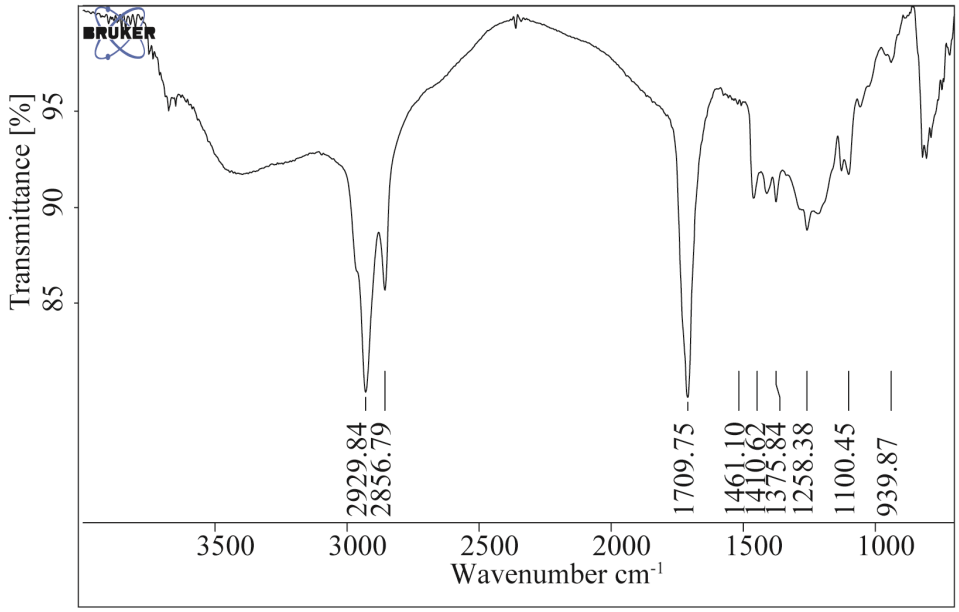

Figure A.6.2: FTIR spectrum of 9-methyloxonan-2-one (*rac*-**36**).

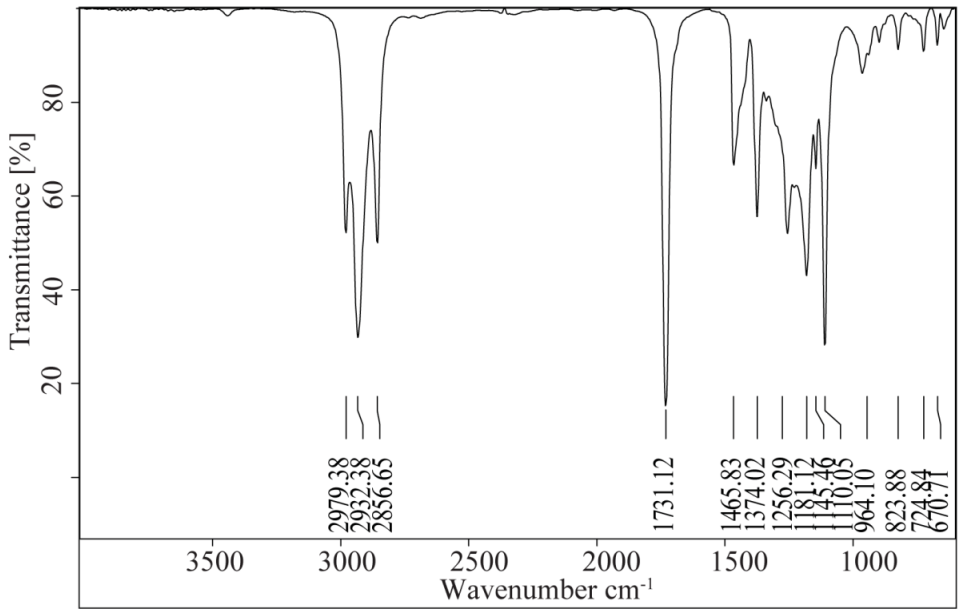

Figure A.6.3: FTIR spectrum of isopropyl 9-bromononanoate (**40**).

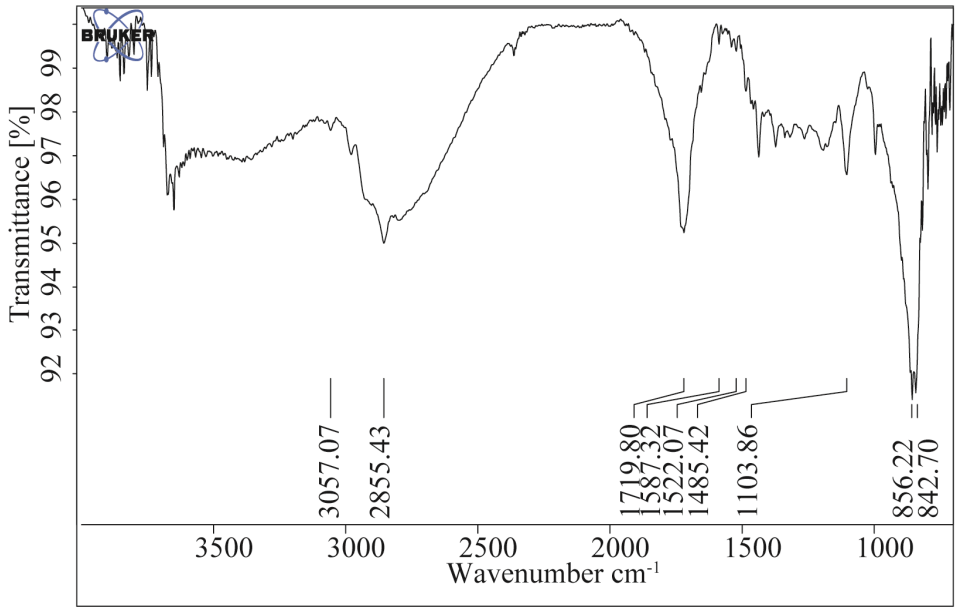

Figure A.6.4: FTIR spectrum of (9-isopropoxy-9-oxononyl)triphenylphosphonium bromide (**35**).

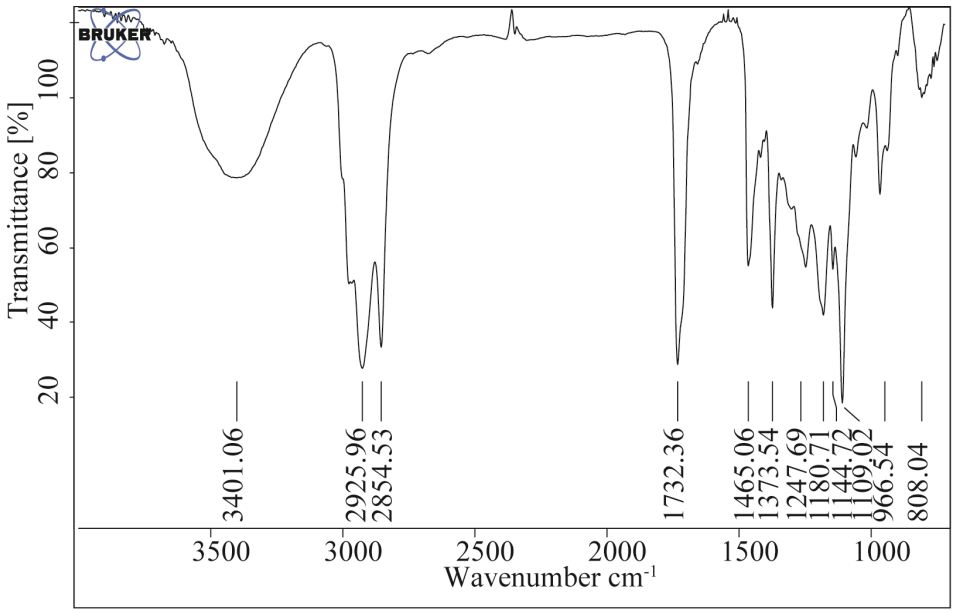

Figure A.6.5: FTIR spectrum of isopropyl (17*S*,9*Z*)-17-hydroxyoctadec-9-enoate ((*S*)-**34**).

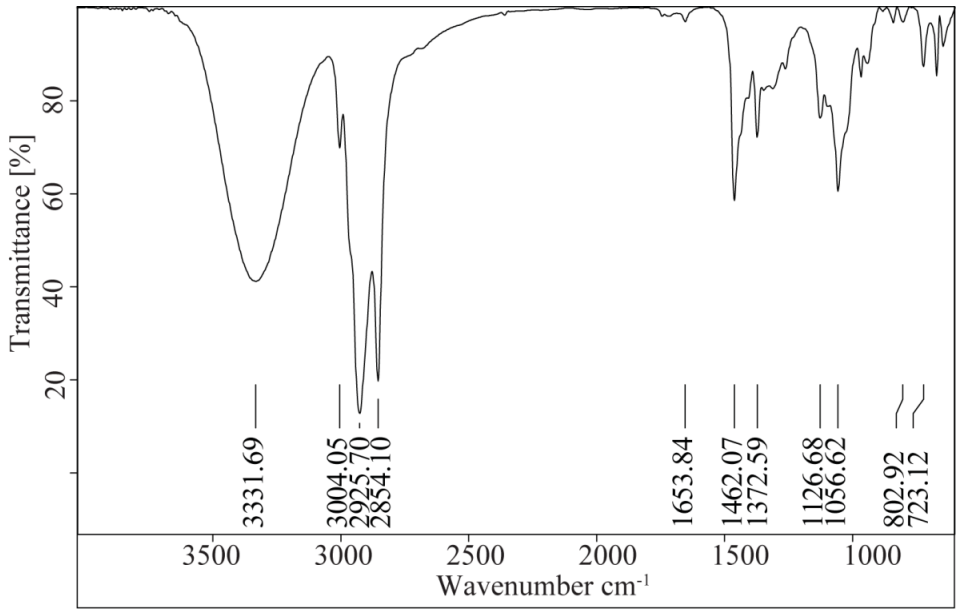

Figure A.6.6: FTIR spectrum of (9*Z*)-octadec-9-ene-1,17-diol (*rac*-**41**).

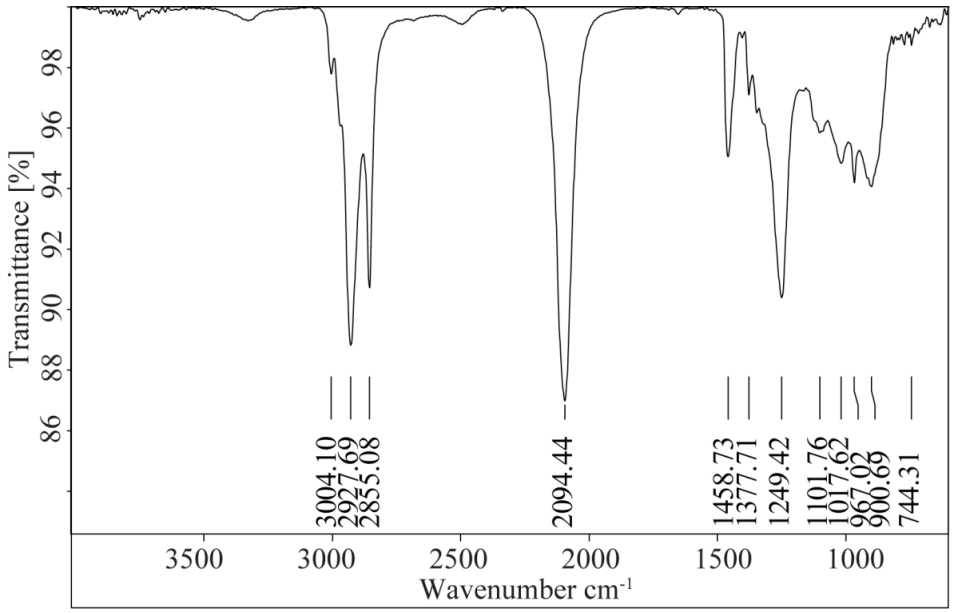

Figure A.6.7: FTIR spectrum of (9*Z*)-1,17-diazidooctadec-9-ene (*rac*-**42**).

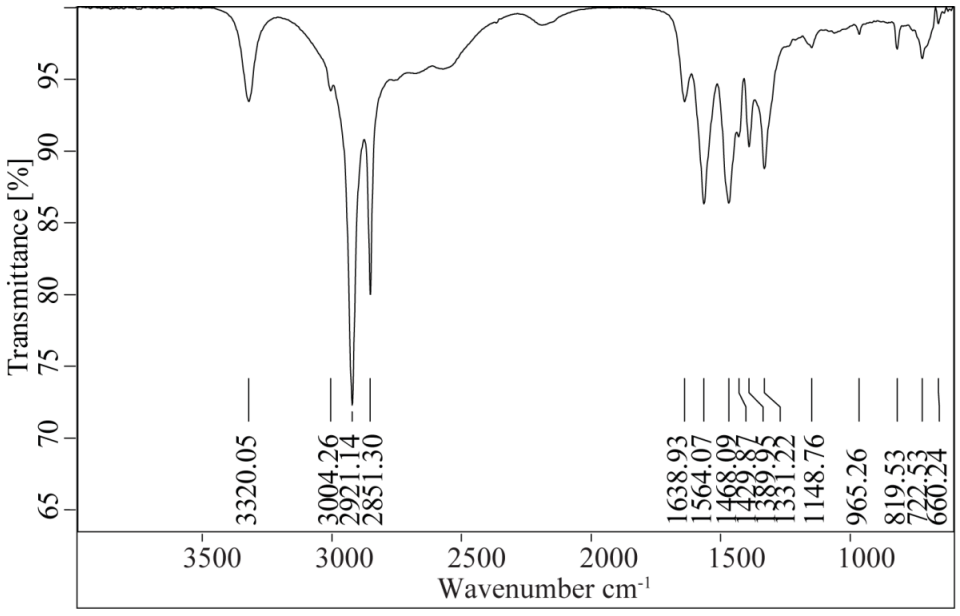

Figure A.6.8: FTIR spectrum of (9*Z*)-octadec-9-ene-1,17-diamine (*rac*-**5**).

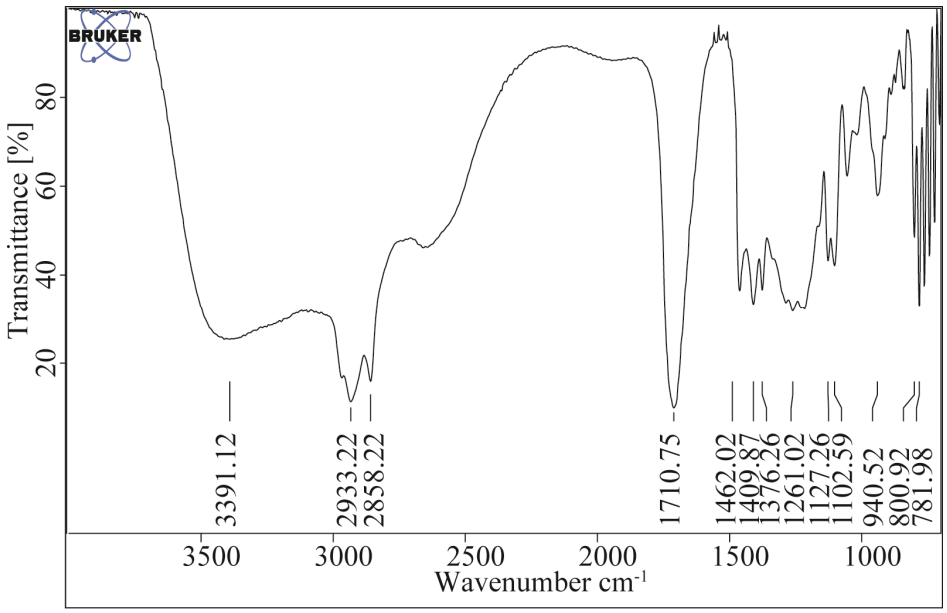

Figure A.6.9: FTIR spectrum of (8*R*)-8-hydroxynonanoic acid ((*R*)-**49**).

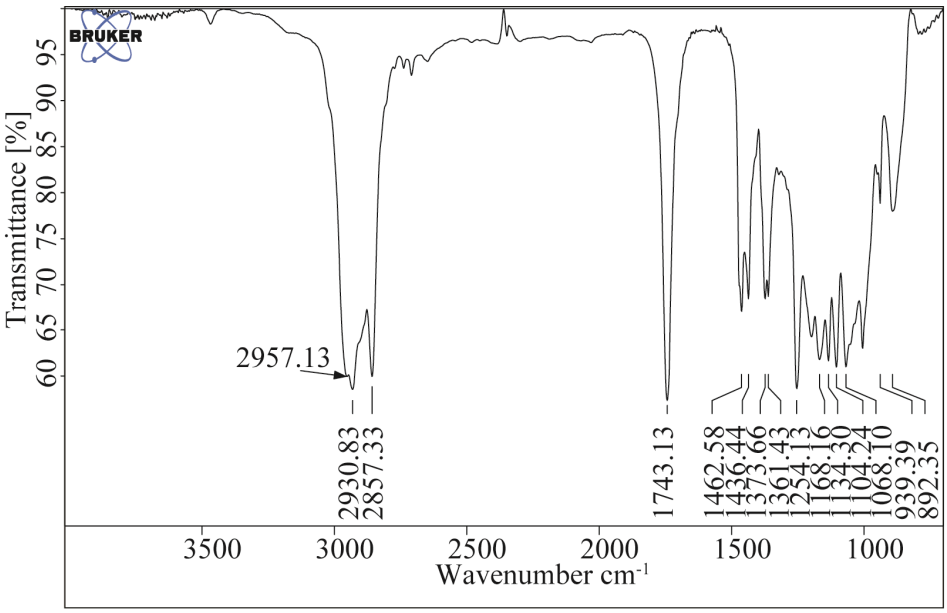

Figure A.6.10: FTIR spectrum of methyl (8*R*)-8-((*tert*-butyldimethylsilyl)oxy)nonanoate ((*R*)-**50**).

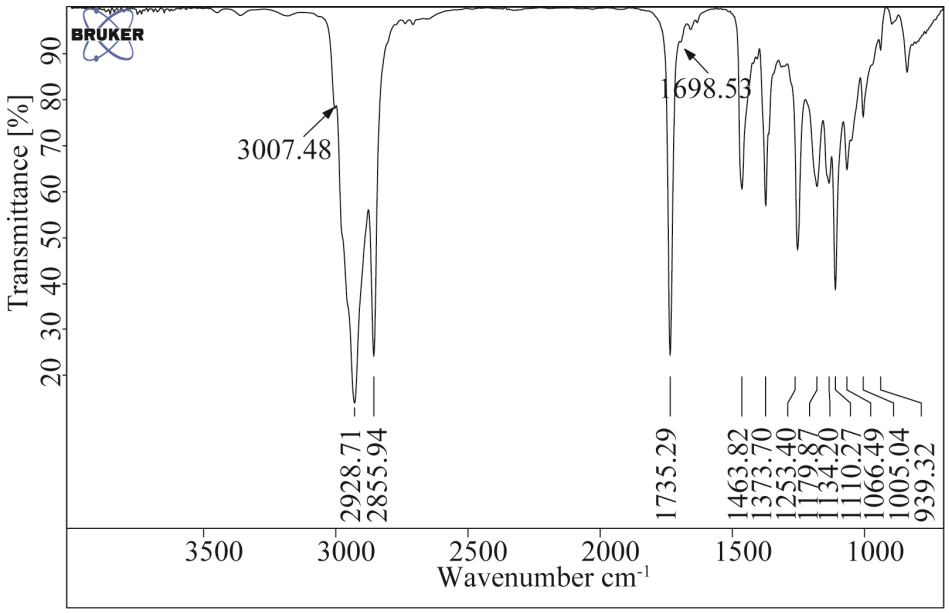

Figure A.6.11: FTIR spectrum of isopropyl (17*R*,9*Z*)-17-((*tert*-butyldimethylsilyl)oxy)-octadec-9-enoate ((*R*)-**51**).

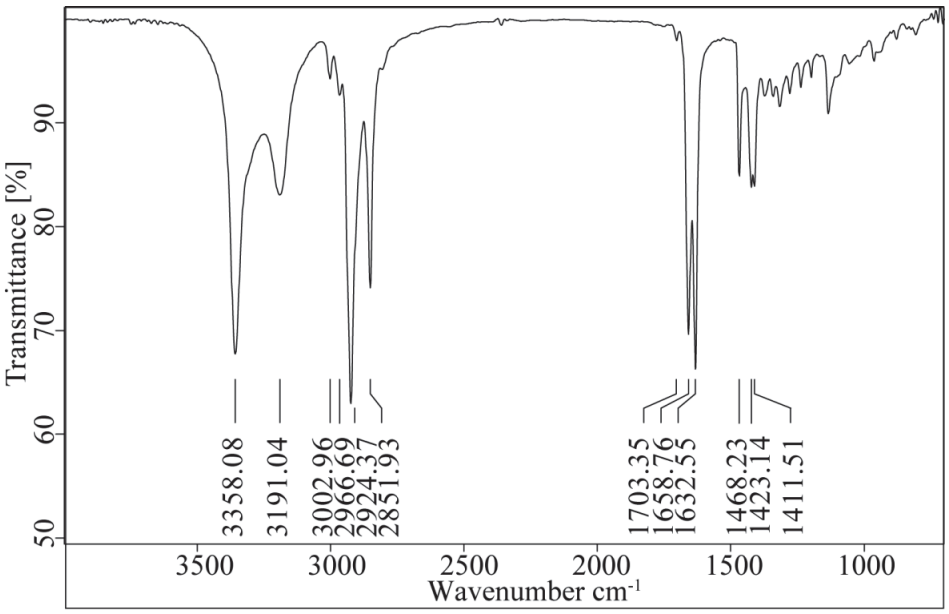

Figure A.6.12: FTIR spectrum of (9*Z*)-17-hydroxyoctadec-9-enamide (*rac*-**47**).

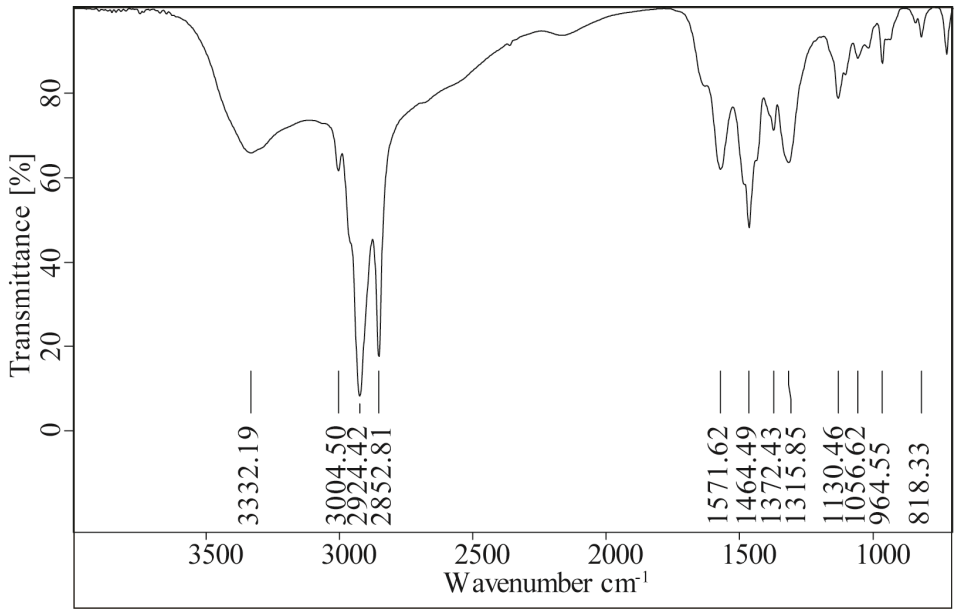

Figure A.6.13: FTIR spectrum of (9*Z*)-18-aminooctadec-9-en-2-ol (*rac*-**48**).

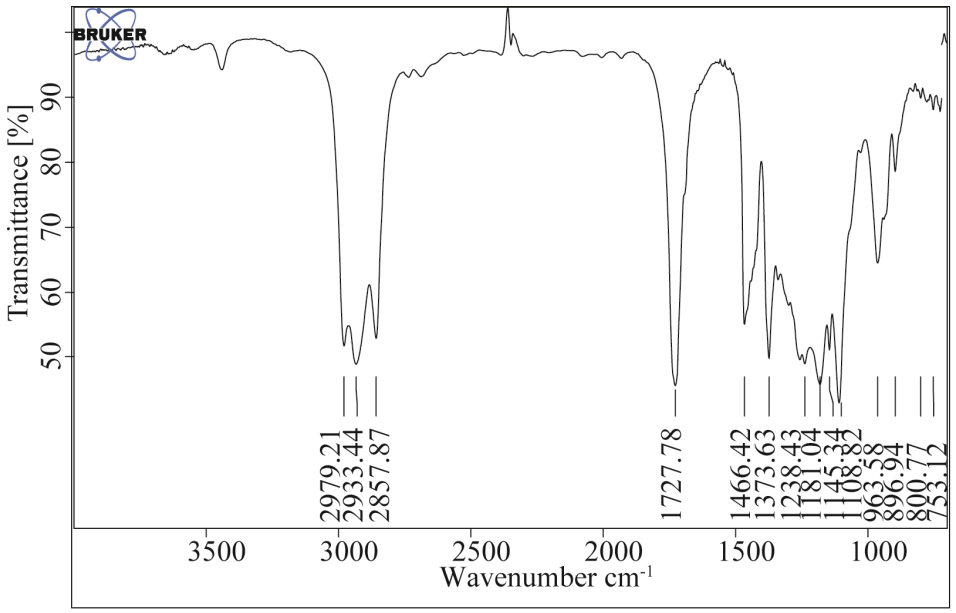

Figure A.6.14: FTIR spectrum of isopropyl 8-bromooctanoate (**53**).

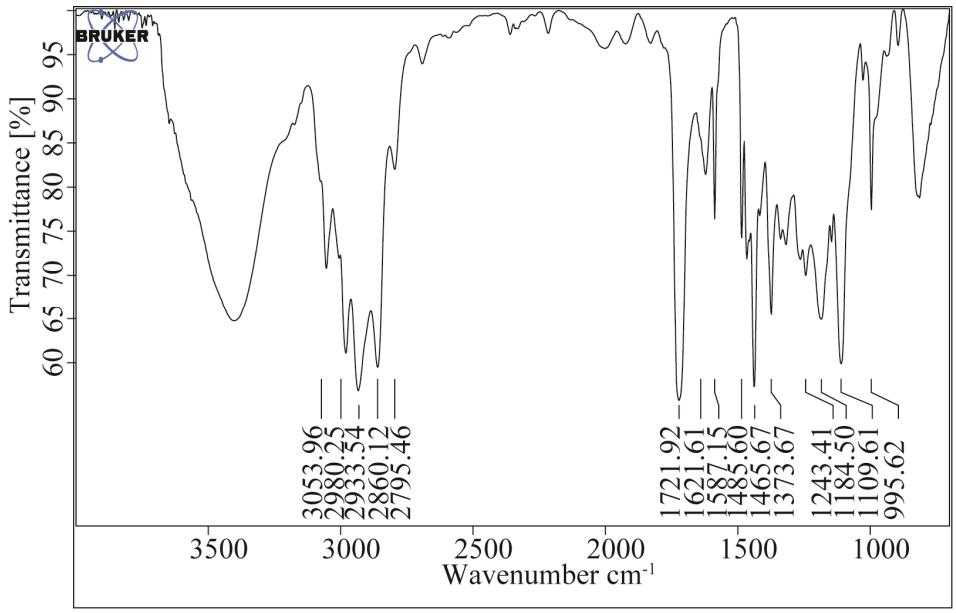

Figure A.6.15: FTIR spectrum of (8-isopropoxy-8-oxooctyl)triphenylphosphonium bromide (**54**).

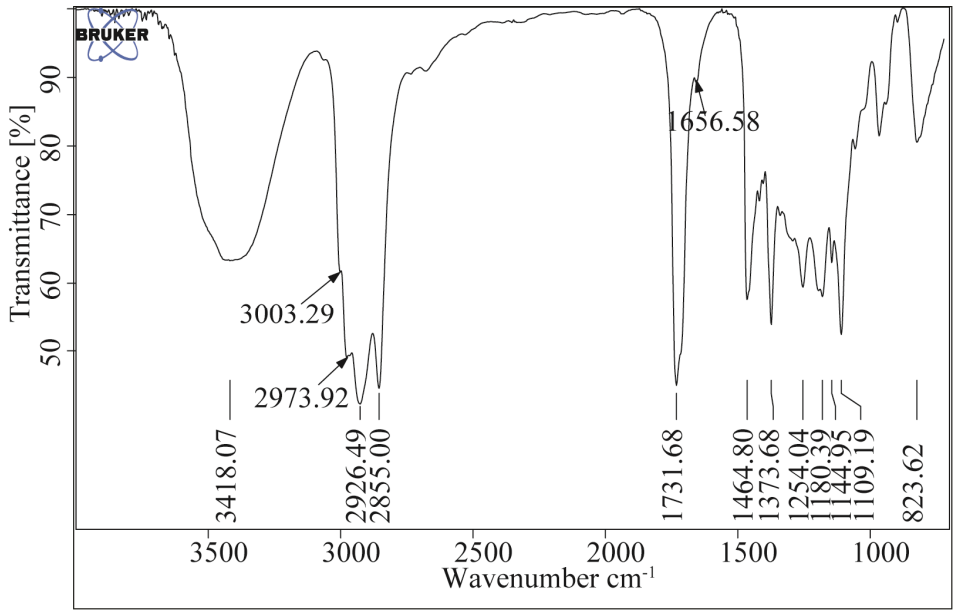

Figure A.6.16: FTIR spectrum of isopropyl (8*Z*)-16-hydroxyheptadec-8-enoate (*rac*-**55**).

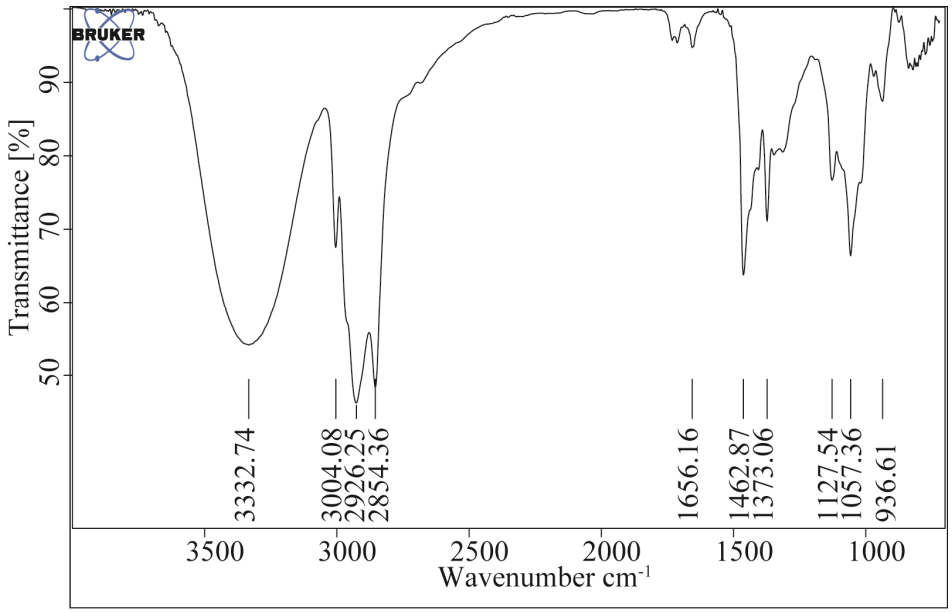

Figure A.6.17: FTIR spectrum of (8*Z*)-heptadec-8-ene-1,16-diol (*rac*-**56**).

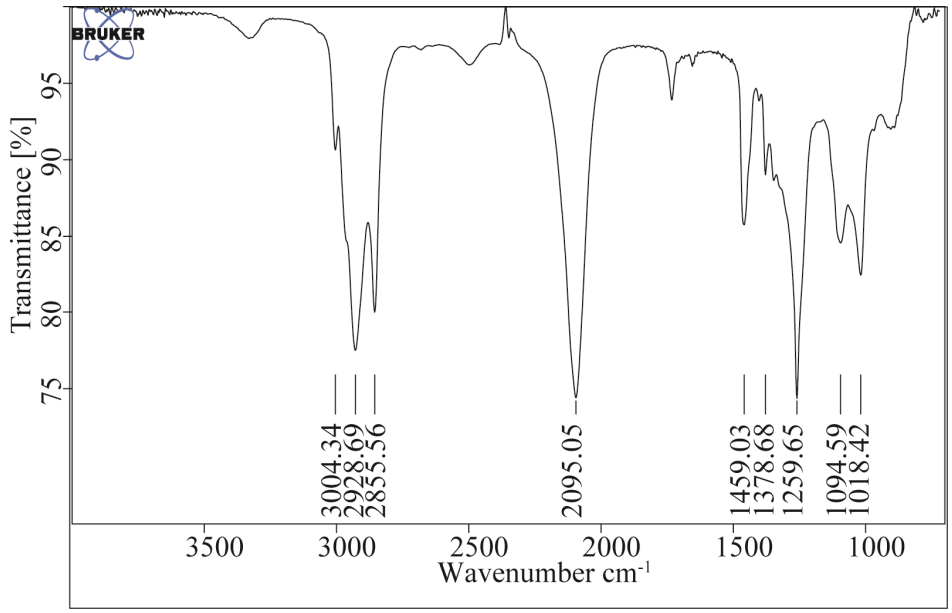

Figure A.6.18: FTIR spectrum of (8*Z*)-1,16-diazidoheptadec-8-ene (*rac*-**57**).

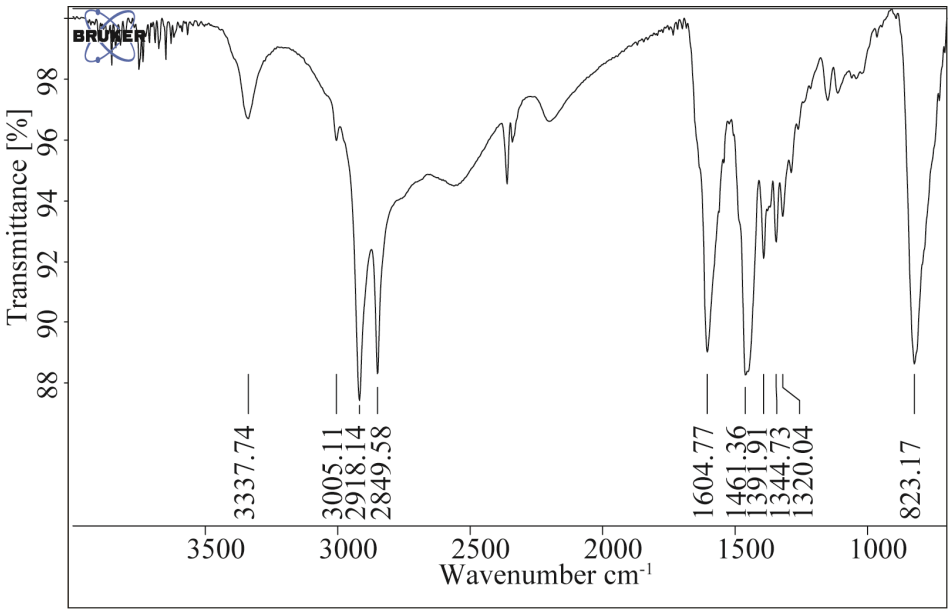

Figure A.6.19: FTIR spectrum of (8*Z*)-heptadec-8-ene-1,16-diamine (*rac*-**58**).

A.7 GC-MS Spectra

Only one of the spectra of compounds exclusively differing in stereochemistry at position C-17 is shown.

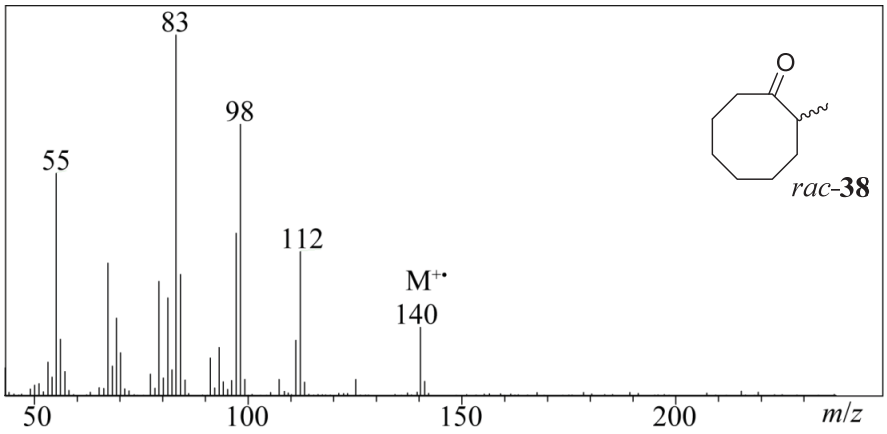

Figure A.7.1: MS (EI) spectrum of 2-methylcyclooctan-1-one (*rac*-**38**).

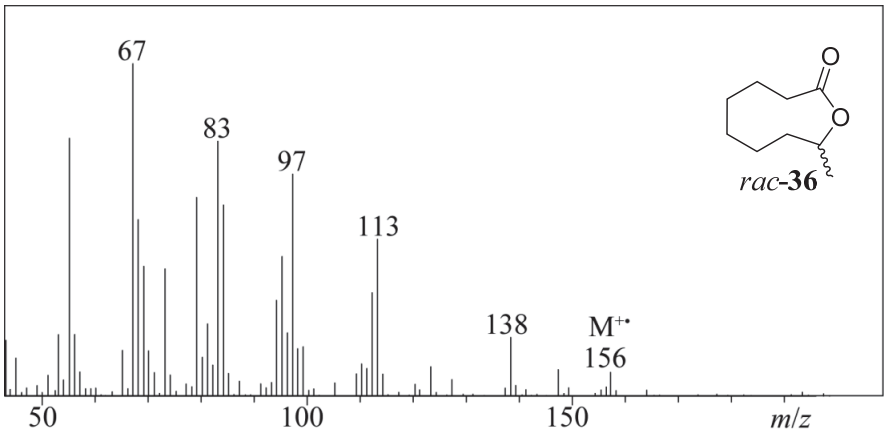

Figure A.7.2: MS (EI) spectrum of 9-methyloxonan-2-one (*rac*-**36**).

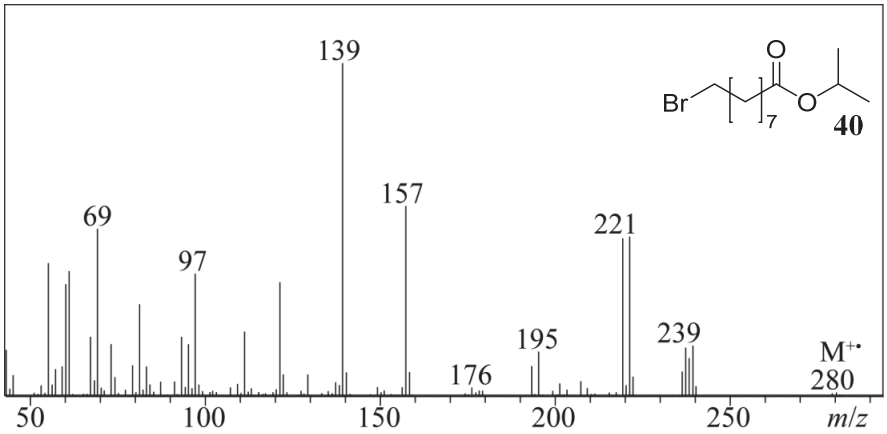

Figure A.7.3: MS (EI) spectrum of isopropyl 9-bromononanoate (**40**).

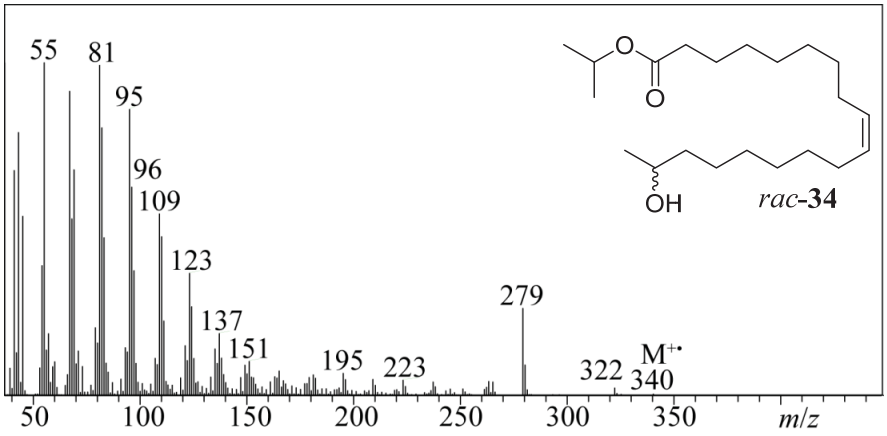

Figure A.7.4: MS (EI) spectrum of isopropyl (9*Z*)-17-hydroxyoctadec-9-enoate (*rac*-**34**).

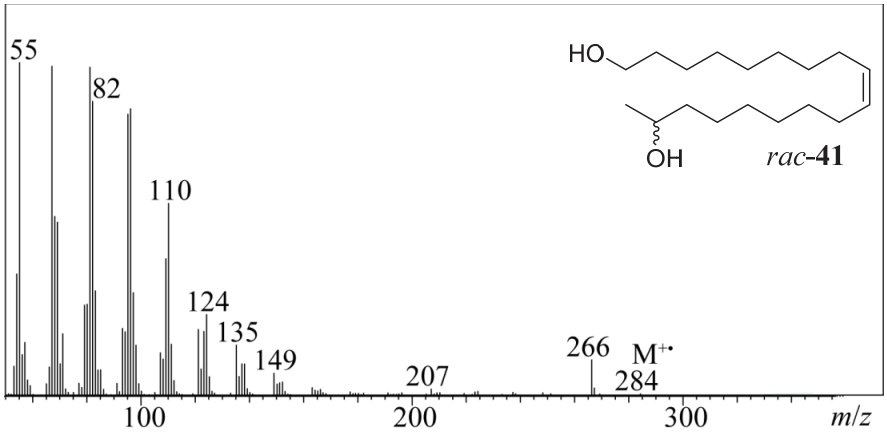

Figure A.7.5: MS (EI) spectrum of (9*Z*)-octadec-9-ene-1,17-diol (*rac*-**41**).

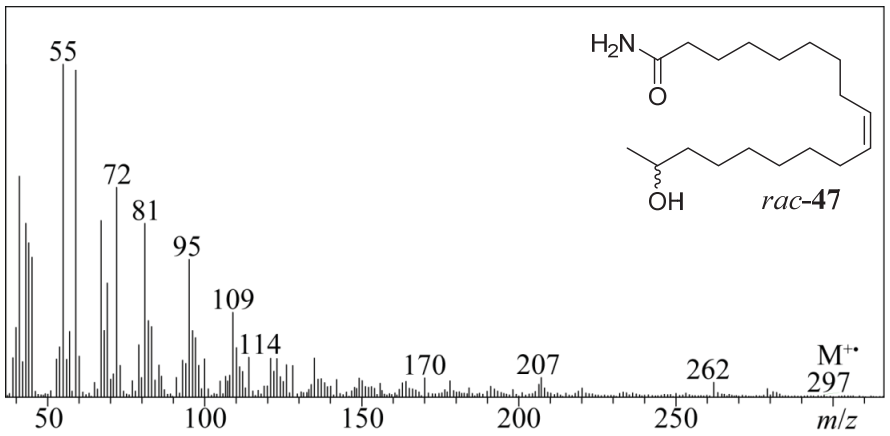

Figure A.7.6: MS (EI) spectrum of (9*Z*)-17-hydroxyoctadec-9-enamide (*rac*-**47**).

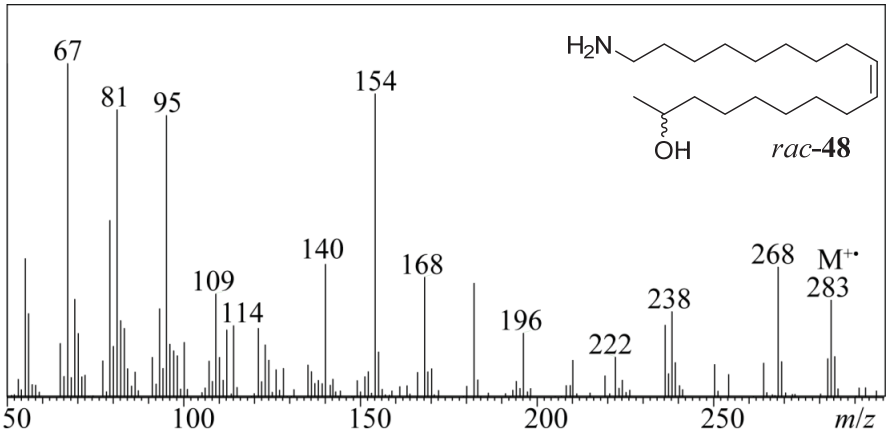

Figure A.7.7: MS (EI) spectrum of (9*Z*)-18-aminooctadec-9-en-2-ol (*rac*-**48**).

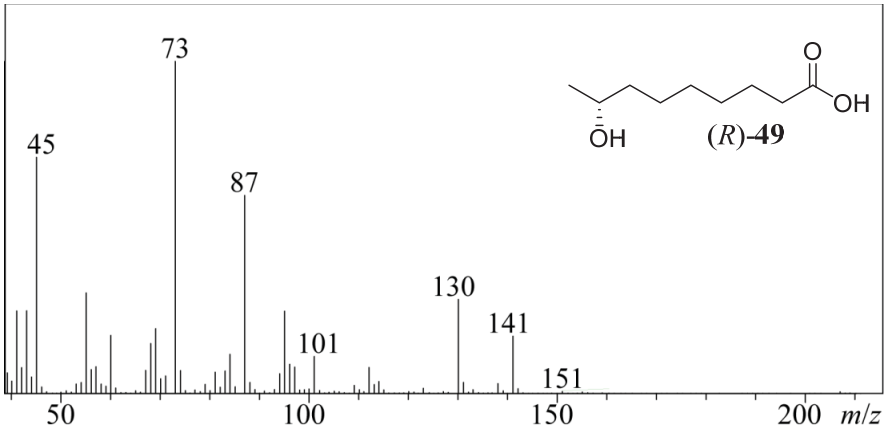

Figure A.7.8: MS (EI) spectrum of (8*R*)-8-hydroxynonanoic acid ((*R*)-**49**).

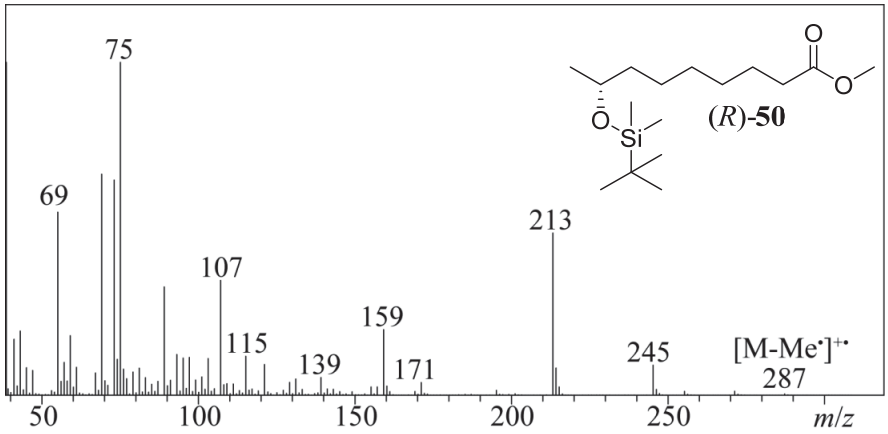

Figure A.7.9: MS (EI) spectrum of methyl (8*R*)-8-((*tert*-butyldimethylsilyl)oxy)nonanoate ((*R*)-**50**).

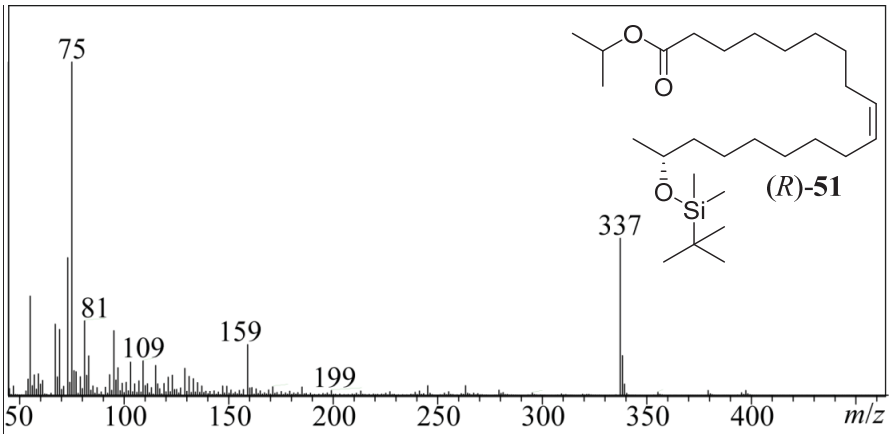

Figure A.7.10: MS (EI) spectrum of isopropyl (17*R*,9*Z*)-17-((*tert*-butyldimethylsilyl)oxy)-octadec-9-enoate ((*R*)-**51**).

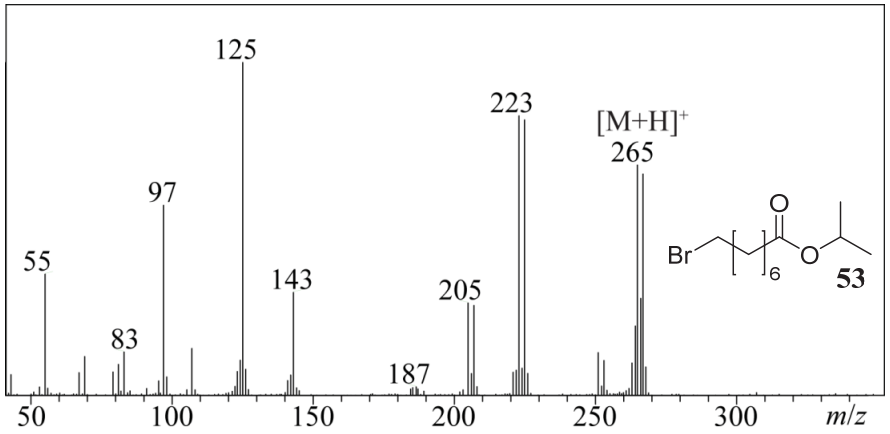

Figure A.7.11: MS (CI) spectrum of isopropyl 8-bromooctanoate (**53**).

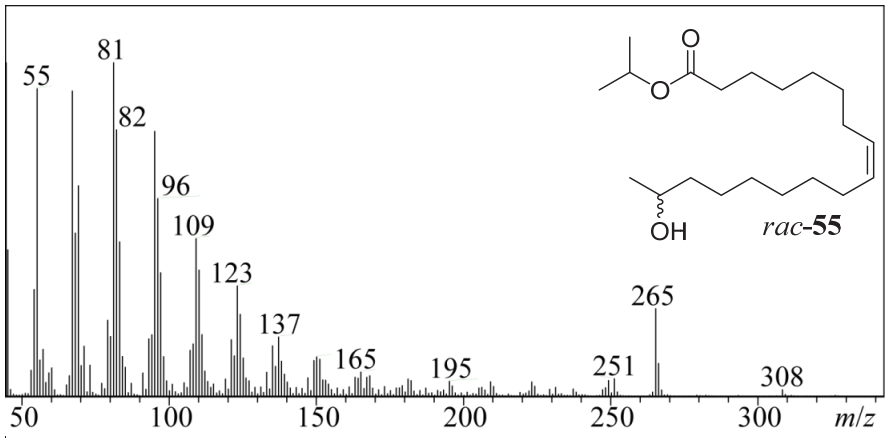

Figure A.7.12: MS (EI) spectrum of isopropyl (8*Z*)-16-hydroxyheptadec-8-enoate (*rac*-**55**).

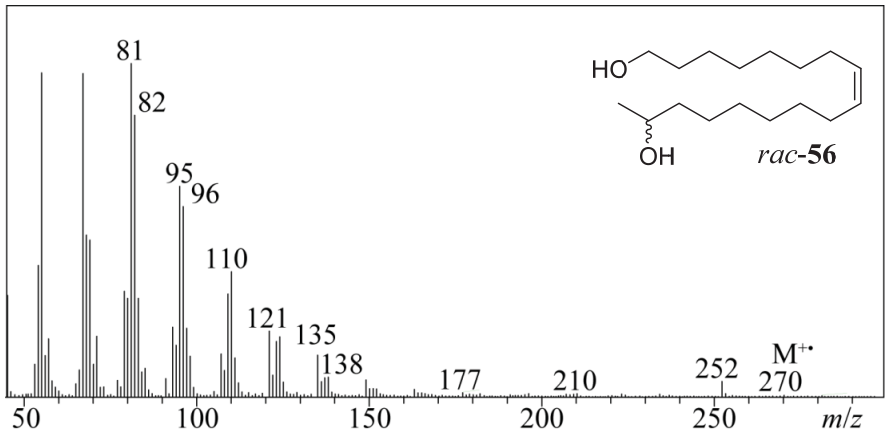

Figure A.7.13: MS (EI) spectrum of (8*Z*)-heptadec-8-ene-1,16-diol (*rac*-**56**).

A.8 AChE Inhibition Assays: Concentration-Dependency Curves for the Calculation of IC_{50} Values

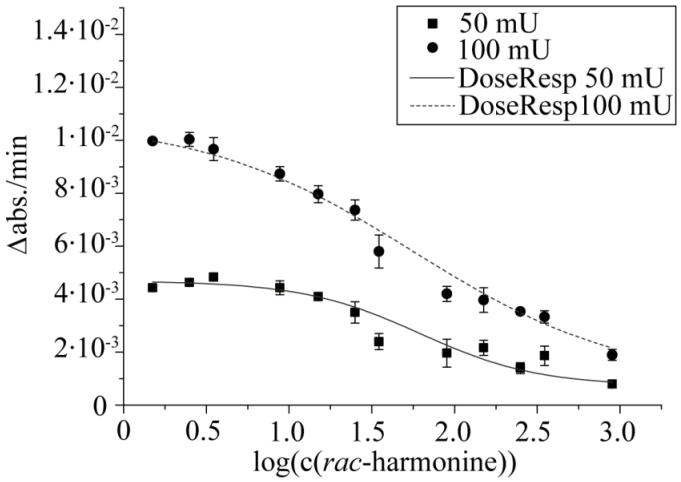

Figure A.8.1: Concentration-dependency curve of *rac*-harmonine *rac*-**5** with sigmoidal dose-response fitting (variable slope, n = 3, ± SEM). Concentration of *rac*-**5**: µM.

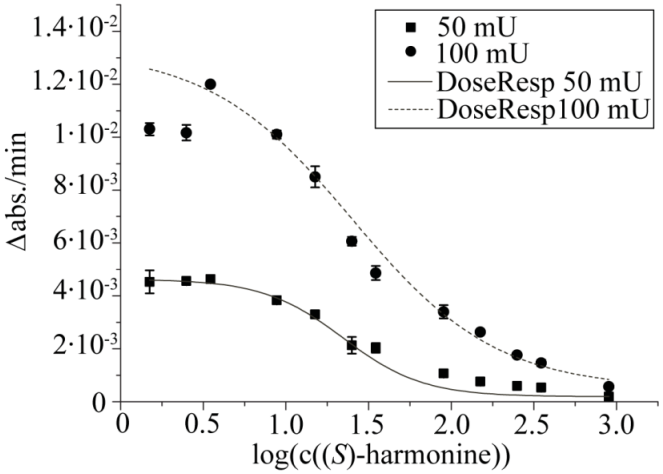

Figure A.8.2: Concentration-dependency curve of (*S*)-harmonine (*S*)-**5** with sigmoidal dose-response fitting (variable slope, n = 3, ± SEM). Concentration of (*S*)-**5**: µM.

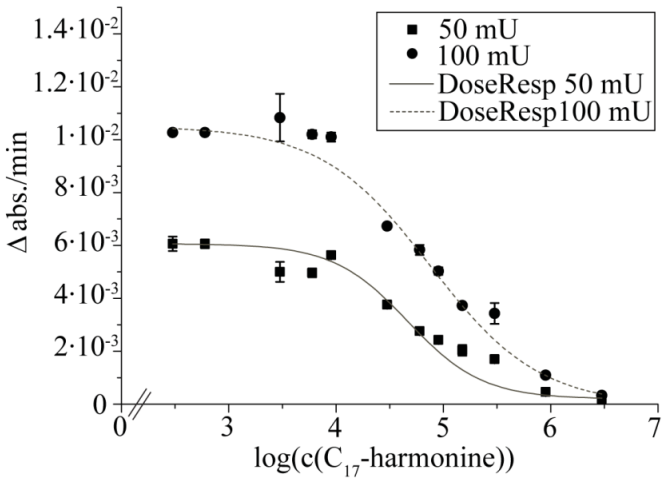

Figure A.8.3: Concentration-dependency curve of C_{17}-harmonine (*rac*-**58**) with sigmoidal dose-response fitting (variable slope, n = 3, ± SEM). Concentration of *rac*-**58**: nM.

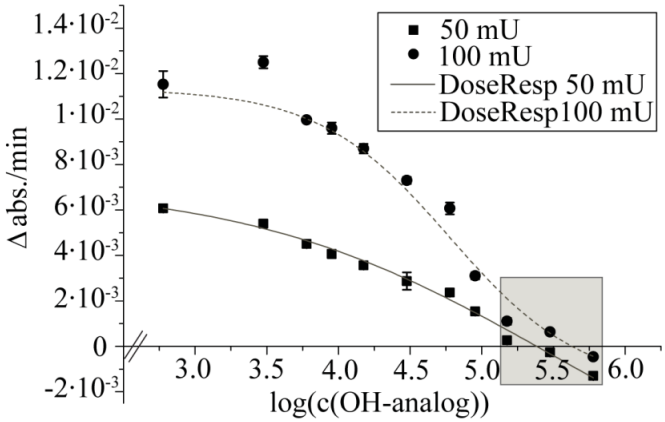

Figure A.8.4: Concentration-dependency curve of (*Z*)-18-aminooctadec-9-en-2-ol (*rac*-**48**) with sigmoidal dose-response fitting (variable slope, n = 3, ± SEM) used for calculation (11 data points). Concentration of *rac*-**48**: nM.

A.9 Modeling and Docking Studies: Additional Figures

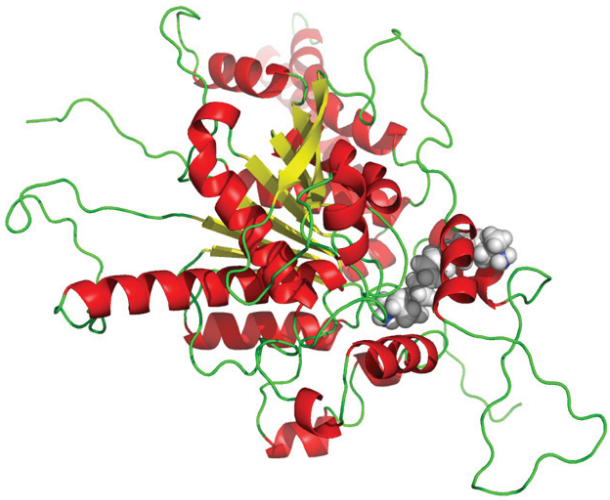

Figure A.9.1: Alternative view of the model of the sequence XP_001681951.1 with bond harmonine. The amino groups interact with E406 (surface; no specificity of the chiral carbon) and with D739 (bottom, probably near the active site).

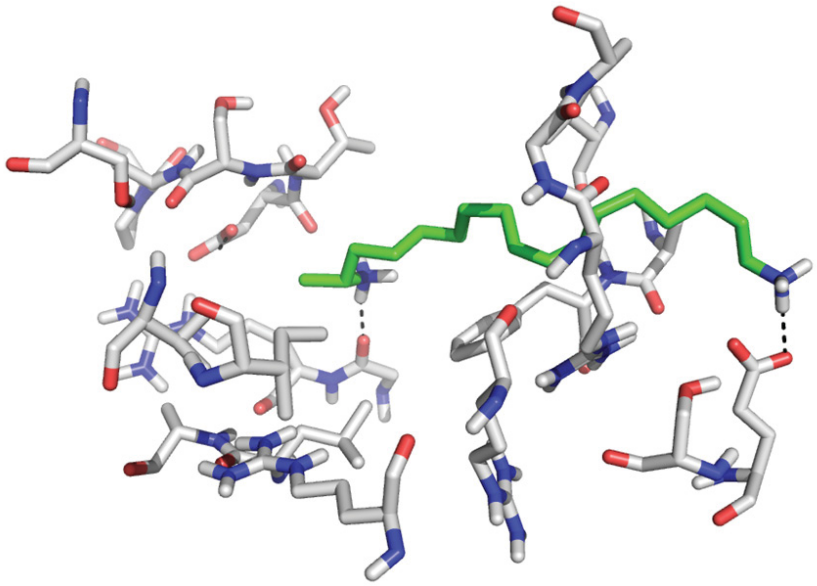

Figure A.9.2: Second most favored docking arrangement of the C_{17}-harmonine (*rac*-**58**) (interaction energy: -39.2 kcal mol^{-1}). Alternatively to **Fig. 3.19** (chapter 3.3.4.2) a salt bridge with E406 can be formed but not with D739.

B Acknowledgements

Special thanks go to my supervisor Prof. Dr. Wilhelm Boland. He did not only give me the opportunity to work in his department but he also gave me the chance to outgrow my former self. Through the topic I was working on and his continuous suggestions and ideas he introduced me to ecological, biochemical and also bioinformatical techniques and expanded thereby my horizon.

I would also like to thank Prof. Dr. Rainer Beckert (Institute of Organic Chemistry) as my second supervisor from the Friedrich Schiller University of Jena for his commitment and his input during the committee meetings and beyond and for his support throughout this thesis.

Financial support by the Max Planck Society is gratefully acknowledged. As a member of the IMPRS I would like to thank the IMPRS for financially supporting one conference visit.

I especially would like to thank my cooperation partners from the Institute for Molecular Infection Biology (Würzburg) Dr. Anita Masic, Martina Schultheis and Dr. Uta Schurigt for conducting the antileishmanial assays and for their help with the interpretation. Furthermore, I would like to thank PD Dr. Wolfgang Brandt (Leibniz Institute of Plant Biochemistry, Halle) for modeling of the inhibitor-enzyme-complexes and Ding Wang for her help with the sequence search and the BLAST.

I would like to thank Dr. Tobias Engl for the AcN-CI-MS/MS measurement and his help with the interpretation of the spectra. For HR-MS measurements I would like to thank Sybille Lorenz and Dr. Marco Kai, for technical support Dr. Maritta Kunert and Kerstin Ploß, and for NMR support Dr. Christian Paetz.

I would like to thank my office colleague Dr. Stephan von Reuß for proofreading of this thesis and for his help and ideas whenever I was stuck during my laboratory work. I would also like to tank Dr. Stefan Bartram for proofreading and for his ideas when derivatizing problems or complicated MS spectra occurred.

I am very thankful to Angelika Berg and Anja David for their help with the beetle rearing. I would also like to thank Dr. Ilka Vosteen and Dr. Grit Kunert for the regular aphid replenishment, Dr. Henrike Schmidtberg and Prof. Dr. Andreas Vilcinskas (Fraunhofer Institute for Molecular Biology and Applied Ecology, Giessen) for their introduction into “how to dissect and handle Asian lady beetles”, and Dr. Heiko Vogel for lending me space in his climate chamber and the opportunities to talk to him about entomology in general.

I would like to thank the whole (former) “beetle group” for showing me how to handle beetles, injections, and dissections. I would especially like to thank Dr. Peter Rahfeld for his introduction into enzyme biochemistry, GraphPad Prism and his initial help to set up the AChE inhibition assays. In this context, the help of Dr. Axel Schmidt is also acknowledged. Thank you to Gerhard Pauls for his help with analytical techniques (HP-LC and SPE) whenever problems occurred and for becoming a very good friend during the last four years. Thank you for providing laughter and/or new ideas on how to proceed whenever necessary.

I would like to thank the whole “EEE group” for letting me use their instruments, agar and bacteria. Thanks to Glen D’Souza for introduction to the Spectra MAX 190 and very special thanks to Anne-Kathrin Dietel for helping with the bacterial assays, for collecting beetles for me (together with Thomas and Kristin), for helping to take pictures of the restless beetles, and for being one of the best friends I made during the accomplishment of my thesis.

I thank Janine Hofmann for letting me use her microbial growth inhibition assay equipment and for her friendship and support. Furthermore, I would like to thank all BOL-members for their help and support. I would like to thank Grit Winnefeld for everything she did to help and support me during the past four years and her administrative work. Thanks to Angela Schneider for providing an occasional parking spot. I would like to thank the library team, the IT-team and the “Haustechnik” for their support.

Of course, I am grateful for my supporting office and lab colleagues and I would especially like to thank my friends Dr. Anne Morgenstern and Dr. Abith Vattekkatte for helpful discussions, helping hands, lots of fun inside and outside of the institute, evenings with tasty Indian food (Thank you so much Tulsi), and numerous more good times we had together.

I would like to thank Tony Pawlik for proofreading of this thesis, mental support, and for making the time in Jena at least double as good as it would have been without him. Thank you to my friends outside of the institute, especially to Caro, Miriam, Dana, Daniel, Julia, Kerstin, Jihye, Jonghwa and Jürgen. Without you my life would not have been the same and many funny and exceptional moments would have never happened.

Very last but not least I would like to thank my family for being the best family someone can dream of, for their continuous support, love and their help. You were not only there to support me psychologically but also physiologically by crawling through our garden in order to collect beetles for me. Special thanks go also to my sister for reading my thesis and for sending me the lovely care package when times were rough. Thank you so much.

C Selbständigkeitserklärung

Ich erkläre hiermit, dass ich die vorliegende Arbeit selbständig und unter Verwendung der angegebenen Hilfsmittel, persönlichen Mitteilungen und Quellen angefertigt habe.

_____ _____

(Ort, Datum) (Unterschrift)

Erklärung:

Ich erkläre,

dass mir die geltende Promotionsordnung der Fakultät bekannt ist;

dass ich die Dissertation selbst angefertigt, keine Textabschnitte eines Dritten oder eigener Prüfungsarbeiten ohne Kennzeichnung übernommen und alle von mir benutzten Hilfsmittel, persönlichen Mitteilungen und Quellen in meiner Arbeit angegeben habe;

dass mich folgende Personen bei der Auswahl und Auswertung des Materials sowie bei der Herstellung des Manuskripts unterstützt haben: siehe Danksagung;

dass die Hilfe eines Promotionsberaters nicht in Anspruch genommen wurde und dass Dritte weder unmittelbar noch mittelbar geldwerte Leistungen von mir für Arbeiten erhalten haben, die im Zusammenhang mit dem Inhalt der vorgelegten Dissertation stehen;

dass ich die Dissertation noch nicht als Prüfungsarbeit für eine staatliche oder andere wissenschaftliche Prüfung eingereicht habe;

dass ich nicht die gleiche, eine in wesentlichen Teilen ähnliche oder eine andere Abhandlung bei einer anderen Hochschule als Dissertation eingereicht habe.

_____ _____

(Ort, Datum) (Unterschrift)